Behavior of Inorganic Matters during Coal Gasification

By

Seyyedali Hosseini

A thesis submitted in partial fulfillment of the requirement for the degree of

Doctor of Philosophy

In

Chemical Engineering

Department of Chemical and Materials Engineering

University of Alberta

Abstract

Inorganic particle deposition and unsteady slag flow is one of the main issues in entrained-flow gasifiers causing several problems, especially, tap hole blockage and emergency shutdown.

For the first part of the experiments in this study, slag collector probe was used to take depositions and analyze blockage in terms of operating conditions and particle trajectories. Increasing the temperature resulted in higher total deposition. Although, by increasing the temperature the weight of slag droplets increased, but, it did not guarantee the safe operation by preventing blockage. The reason was understood to be related to different effects of temperature on ash deposition and slag flow rate. Increasing the temperature, increased stickiness of the particles and amount of the deposition, but, decreased the viscosity and caused higher slag flow rate which could remove more deposition from the plate. Using two coal types proved that ash composition has essential effect on the amount and thickness of the deposition. For fuel with higher ash viscosity, increasing the temperature resulted in higher blockage probability. Back-Scattered Electron (BSE) of this fuel showed that iron-bearing particles on the surface of slag made the surface sticky for other particles to stick. For this fuel, the effect of increase in the particle stickiness was higher than the decrease in slag viscosity. Computer Controlled Scanning Electron Microscopy (CCSEM) analysis of this fuel showed that the percentage of excluded minerals was higher than included ones and most of iron-bearing particles were in excluded condition. The coal with higher calcium content had lower ash viscosity and increasing the temperature resulted in higher slag flow and lower blockage

probability. CCSEM analysis of this fuel showed that most of calcium was in included nature which resulted in more particle coalescence making big agglomerations. The most important understanding of comparing the results of these two fuels was that inorganic matter loading (especially loading rate of iron and calcium) can be more effective than the viscosity in inorganic deposition. Increasing particle velocity mostly resulted in lower deposition. The reason is most probably related to the residence time, carbon conversion and kinetic energy. Large particles at low temperature and high gas flow had lowest deposition tendency. Two different types of feeder configurations were used to evaluate the effect of particle trajectory. The results showed that the particle injection pattern has significant effect on the deposition growth at different locations. The feeder leading the particles to collide with the wall in a narrow area resulted in severe deposition near the feeding spot. Other feeder with wider sticky surface resulted in more uniform deposition with lower thickness. Finally, it was understood that the traditional deposition models must be enhanced by considering new parameters such as iron loading, mineral association types and the deposit surface formed by aerodynamic of the feeder.

The difference of the iron concentration on the surface and bulk of depositions made a motivation to investigate the possibility of the surface reactions. Analyzing slag surface under reducing and inert atmosphere showed that iron can react with gaseous species and leave the surface which can lead to a decrease in the surface stickiness.

The second set of the experiments is performed based on controlled injection of the inorganic particles. The results showed higher deposition by increasing the temperature. Increasing the particle velocity slightly decreased the deposition at lower temperature and slightly increased the deposition at higher temperature. It was understood the effect of

velocity is related to the liquid fraction of particles. Increasing the impact angle of the particles slightly led to higher deposition. Effects of the impact angle and velocity were much lower than the effect of temperature.

A 2D-axisymetric model was developed to simulate inorganic deposition. Particle interaction with the wall was introduced to the model as User Defined Function (UDF). The operating condition parameters and the properties of the inorganic matters were considered in the sub-model and the results were saved in User Defined Memory (UDM). Comparison of the modeling and experimental results showed a reliable accuracy of location of deposition, but, the error of the amount of deposition was high which thought to be reasonable considering the simplifying assumptions. It was understood ignoring the mineral association with coal could be the main source of errors.

Preface

The main results and understandings of this work are presented in chapters 3 to 5 of this thesis in the form of research papers. In addition, some extra results and analysis are presented in appendices B, C and D. The ideas of all the experiments are mine. Data collection and analysis in chapter 3 to 5 and literature review in chapter 2 are my original work. I am the sole author of all the chapters. My supervisor, Dr. Rajender Gupta of the Department of Chemical and Materials Engineering supervised all my works including the experiments and modeling during my PhD program to bring my ideas into practice in the most efficient way and provided me required corrections and modifications to edit the chapters.

Chapter 3 of this thesis has been published as Hosseini S, and Gupta R, "Inorganic Matter Behavior during Coal Gasification: Effect of Operating Conditions and Particle Trajectory on Ash Deposition and Slag Formation," *Energy and Fuel* 2015, 29, 1503−15. This Chapter is reprinted (adapted) with permission form Energy and Fuel. Copyright (2015) American Chemical Society.

This work is dedicated to my parents and my sister for their immeasurable and unconditional help, support and love.

Acknowledgement

I wish to express my immeasurable love and gratitude to my wonderful father, mother and my lovely sister who supported me unconditionally during all the stages of my life.

I am very grateful to my supervisor Dr. Gupta. I highly appreciate all his help and support and his valuable guides during my PhD program.

I want to express my great love to my girlfriend Samira Sadeghi who was always beside me and was concerned about all my problems as hers and supported me to have motivation doing my research, especially, when I was disappointed facing problems in my researches.

I am highly thankful to my amazing friend Saeid Niknaddaf for all his unlimited supports and helps.

Special thanks to Dr. Farshid Vejahati for his helps and guides. He built the gasification setup which was used by many students from University of Alberta and other universities.

I appreciate the financial support of C^5MPT and Helmholtz-Alberta initiative (HAI), Faculty of Graduate Studies and Research and Faculty of Engineering of University of Alberta.

Table of Contents

List of Tables

List of Figures

List of Symbols

A_{eff}	Effective available surface for reaction
C_D	Drag coefficient
c_p	Specific heat capacity at constant pressure
d_p	Diameter of particle
d_{max}	Maximum spread diameter
E	Excess energy
E_k	Kinetic energy
ΔE_k	Loss of kinetic energy
E_s	Surface energy
F_a	Fluid-added mass force
F_c	Char particle flux rate on slag surface ($kg.m^{-2}.s^{-1}$)
F_d	Drag force
$F_{\sigma,z}$	Capillary force
F_s	Slagging index
h	Enthalpy
HT	Hemisphere temperature (K)
IT	Initial deformation temperature (K)
k	Thermal conductivity ($W.m^{-1}.K^{-1}$)
k	Turbulent kinetic energy
ls	Thickness of deposit layer
$\dot{m}_L$	Liquid slag flow rate
P	Pressure
PC	Particle capture probability
q_r	Heat flow through inorganic deposition layer ($W.m^{-2}$)
r, R_p	Radius of particle
r_{trans}	Transition radius
Re	Reynolds number
R_w	Radius of the tube of furnace

S	Penetration depth of the particle into slag layer
S_h	Energy source term
S_j, S_m	Momentum source term
S_p	Mass source term
t	Time
T	Temperature
T_c	Temperature of cold face of deposit layer
T_{cv}	Temperature of critical viscosity
T_e	Temperature of radiation source
T_f	Fluid temperature
T_s	Temperature of ash surface
$T_{(25\%)}$	Temperature of 25% shrinkage
$T_{(50\%)}$	Temperature of 50% shrinkage
u	Average velocity
u_s	Velocity of liquid slag
u_z	Slag velocity
U	Fluid velocity vector field
$U_{z,max}$	Maximum slag velocity
u'	Fluctuating velocity due to turbulence
v_p	Velocity of particle
v_g	Velocity of gas
Vs	Volume fraction of solid in slurry mixture
W	Work of deformation against viscosity
W_a	Work of adhesion
W_c	Work of cohesion
We	Weber number
X	Carbon conversion
X_{cr}	Critical carbon conversion
α	Angle of wall with horizontal line
α_Λ	Absorptivity

β	Contact angle
γ	Surface tension ($N.m^{-1}$)
δ	Thickness of slag layer
ε	Turbulent dissipation rate
ε_Λ	emissivity
ε_r	Emissivity of deposit surface
ζ	Maximum spread ratio
θ	Impact angle
λ	Thermal conductivity ($W.m^{-1}.K^{-1}$)
μ	Viscosity (Pa.s)
μ_g	Viscosity of gas (Pa.s)
μ_L	Viscosity of liquid (Pa.s)
μ_s	Viscosity of slurry (Pa.s)
μ_t	Turbulent viscosity (Pa.s)
ρ	Density
ρ_Λ	Reflectivity
ρ_p	Density of particle
ρ_s	Density of slag
σ	Stefan-Boltzmann constant (radiation heat transfer equation)
σ	Viscous stress (momentum balance equation)
τ	Stress tensor
ϕ	Viscous dissipation

Chapter 1. Introduction

1.1. Overview of coal and gasification process

Coal, the solid organic rock, is one of the most popular sources of energy because it is exuberantly, evenly, and widely distributed all around the world (not concentrated in few regions) and therefore is not affected by the geopolitical tensions. Coal is a cheap energy source which is very easy to transport and store [1]. It is proven that there is near 1000 billion tonnes of coal in the world. It is predicted that the global demand of this fossil fuel at the end of current decade reaches to 9 billion tonnes per year. As a matter of global energy production, coal is the second source of energy by producing about 30% of the required energy in the world (after oil which produces 31%) [1]. The most important application of coal is in power plant for electricity generation and today more than 40% of the electricity produced worldwide is coal-based and in many countries such as China, India and the United States this contribution is even higher [1].

Combustion is traditionally the major process for utilization of coal which is under huge global objections. This objection is mostly due to the severe environmental pollution

(nitrogen and sulfur oxides) and greenhouse gas emissions (carbon dioxide). Furthermore low efficiency of the plants working based on the coal combustion process leads to higher fuel consumption and finally more pollutants production. Governments and Industries are now more concerned about the issues of air pollution and global warming. Therefore, more innovative technologies adaptable with the stringent environmental regulations for utilization of coal seem to be necessary to consistently deal with the increasing demand for energy [1-3].

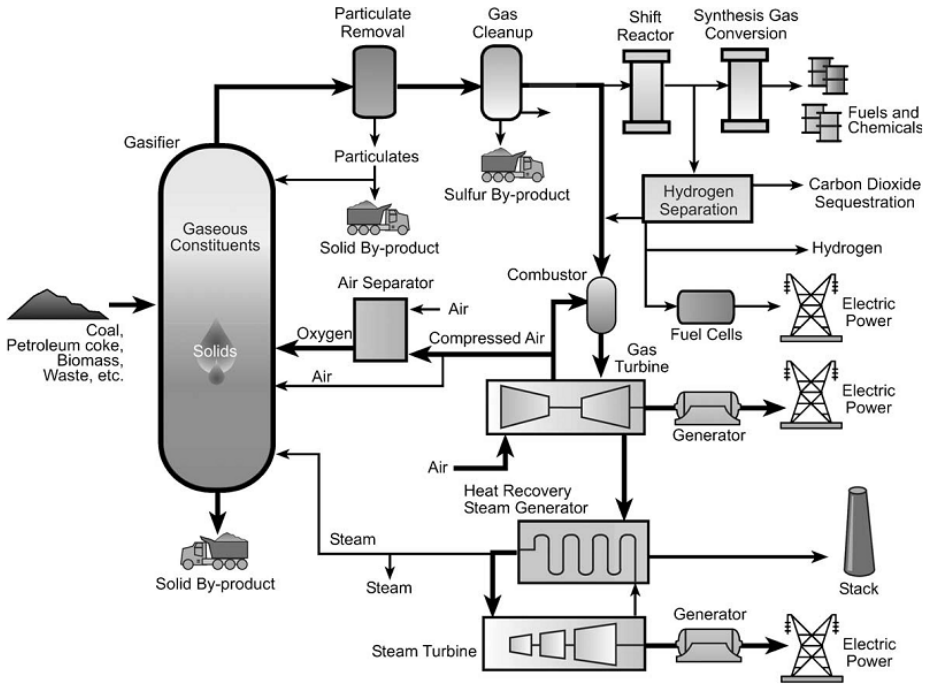

Figure 1.1: Gasification-based energy conversion options [4]

For clean and efficient utilization of coal, gasification can be a suitable option. Gasification is a process that converts any carbon containing fuel to the gaseous products with utilizable heating content [2,3]. In fact, gasification is a process to upgrade any solid fuels (such as coal, biomass, municipal wastes etc. which are hard to handle and operation) by converting it into a gas mixture that can be processed, purified and used

much easier [2-5]. Gasification is an endothermic process in which oxygen, steam and carbon dioxide can be used as gasifying agent. The main desired product of gasification is syngas which is a mixture of hydrogen and carbon monoxide. Syngas can be used for many purposes such as electricity generation (as the most important use), petrol production, methanol, dimethyl ether (DME) and ammonia synthesis, ore reduction and domestic uses [2-6].

Using gasification technology, the efficiency will be improved and the environmental impacts and greenhouse gas emissions will be significantly reduced [2]. The production and efficiency of the gasification process is affected by many parameters such as chemical composition of the fuel, types of the gasifying agents, operating conditions (i.e. temperature, pressure, particle size of the fuel, residence time of fuel particles in the furnace) and type of feeding or injection (burner configuration) which determines the contact pattern and consequently the extent of the reactions between fuel and gasifying agents [2,3]. The systems that work based on gasification technology are typically capable of utilizing all carbon containing feed stocks, such as coal, biomass, petroleum coke, heavy oil sand residue etc. [2]. The Integrated Gasification Combined Cycle (IGCC) is a technology which utilizes coal gasification process instead of the traditional combustion process. This process is widely reported to be more efficient (with higher thermal efficiency and lower fuel consumption) with lower environmental pollutants [3,4]. Separation of sulfur and nitrogen species (without production of SO_x and NO_x) and also CO_2 capture can be performed much easier in gasification process (in combination with Carbon Capture and Separation (CCS)) which leads to many economical (lower cost) and operational (lower volume) advantages especially in gas treatment units

compared with traditional combustion-based power plants [3]. Although higher efficiency of the gasification-based processes and wide applications of syngas (as the main desired product) make gasification a valuable and interesting technology to secure the existing sources of energy for future generations, but, gasification process (especially what is currently applied in power plants) is not as reliable as the combustion-based process. Availability, reliability and safety during the operation of the plants which use gasification process are the main concerns and issues for its wider application [2,3].

1.2. Details of gasification process

Containing many homogeneous and heterogeneous reactions makes gasification an extremely complex chemical process. Inside a gasifier, coal particles usually undergo three basic stages that take place at the same time because of the high temperature and high heating rate. These stages are pyrolysis (devolatilization), partial oxidation (combustion) and gasification [3-7].

During gasification process, firstly devolatilization starts by rapid increase in the temperature of the feed particles which leads to breakage of the weaker chemical bonds. As a result of this stage tars, oils, and hydrocarbon gases are produced which then might participate in other reactions to form H_2, CO, and CO_2. The carbon containing particle that remains from parent particle after devolatilization stage is called char and then reacts further with gasifying agents like steam, O_2 and CO_2 [4]. Char gasification involves heterogeneous (gas–solid) reactions in which carbon content of the char particle is converted into syngas. The gasification process reactions might be exothermic or endothermic [2]. The main endothermic reaction is CO_2 reduction and the main

exothermic reaction is burning of carbon with oxygen to produce CO_2. The main reactions that occur during gasification process can be summarized as below [2]:

Reaction of oxygen with carbon and hydrogen:

$$C + O_2 \rightarrow CO_2 \qquad \Delta H = -394\ KJ/mol \qquad (1-1)$$

$$2C + O_2 \rightarrow CO \qquad \Delta H = -111\ KJ/mol \qquad (1-2)$$

$$2H_2 + O_2 \rightarrow 2H_2O \qquad \Delta H = -242\ KJ/mol \qquad (1-3)$$

Water gas shift reaction:

$$H_2O + CO \leftrightarrow H_2 + CO_2 \qquad \Delta H = -41\ KJ/mol \qquad (1-4)$$

Gasification with CO_2 (Boudouard's reaction):

$$C + CO_2 \leftrightarrow 2CO \qquad \Delta H = +172\ KJ/mol \qquad (1-5)$$

Gasification with steam (Water gas reaction):

$$H_2O + C \leftrightarrow H_2 + CO \qquad \Delta H = +131\ KJ/mol \qquad (1-6)$$

Gasification with hydrogen (Methane reaction):

$$C + 2H_2 \leftrightarrow CH_4 \qquad \Delta H = -75\ KJ/mol \qquad (1-7)$$

Steam methane reforming reaction:

$$CH_4 + H_2O \leftrightarrow CO + 3H_2 \qquad \Delta H = +206\ KJ/mol \qquad (1-8)$$

Due to low oxygen concentration (Oxygen is fed at sub-stoichiometric amount based on the inlet feed carbon content) and highly reducing conditions during gasification process, most of the sulfur existing in the fuel will be converted to hydrogen sulfide which can be separated easily. Therefore, the amount of the environmental pollutants and harmful gases produced by gasification process are much lower in comparison with conventional combustion process [3,4].

1.3. Gasification Today

The revolution in gasification technology started during last 15-20 years. Great increase in the costs of energy is the main reason for this fact. During 1980 the price of oil was 20-30US$/bbl but in early 2000 the price increased to 55-70US$/bbl [2]. Sharp growth of industrialization lead to an increase in the energy demand and consequently people looked at coal as an alternative interesting source of energy especially because of its cheaper price and wider availability to be a substitute for energy sources with unstable prices [2].

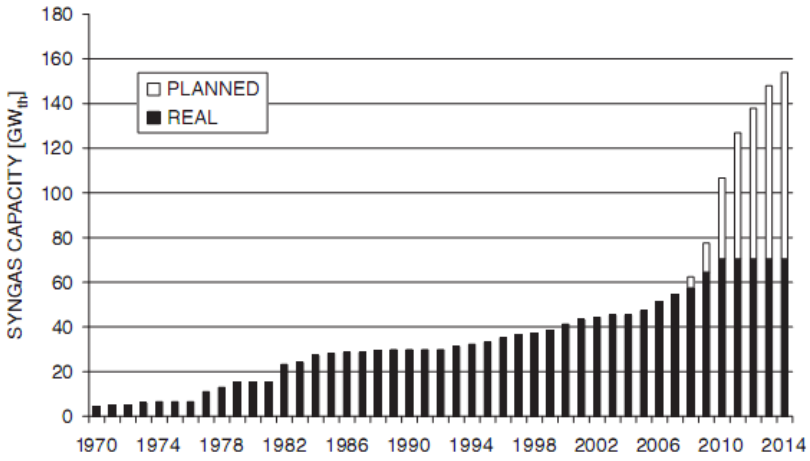

Figure 1.2: Cumulative worldwide gasification capacity [2]

Therefore, big companies aimed to participate in the gasification technology progress to be more involved in the worldwide energy production. Gasification technology of Texaco built an integrated coal power plant in 2004 in US and then corporation of GEE and Bechtel developed a 630 MW_e IGCC plant. In Italy gasification technology is applied for heavy oil desulfurization and power generation in three refineries with capacities in the range of 250-500 MW_e. Pernis refinery of Shell in Netherlands produces 285 t/d

hydrogen and generates 115 MWe. There are lots of gasification-based projects in the planning or design phase in various industries in other European countries. Another field which received increased attention is production of chemicals from coal. The Eastman plant in Kingsport, Ube in Japan and some of the other eminent gasification technologies (such as Lurgi, GE Energy and Shell) work in this area [2].

Attention to the Canadian oil sands has increased greatly due to the high price of crude oil. Based on the feasibility studies, gasification can be a key technology in development of oil sand utilization, especially, upgrading process residue is an interesting feed for gasification process. Long Lake project by Opti Canada is the first plant operating with gasification technology and many other plants are in the preliminary stage of design and construction [2]. Sherritt International designed some gasification plants based on the coal reservoirs in Alberta.

1.4. Types of gasification technologies

Gasification process can be performed in different type of reactors mainly based on the operating conditions and obligated requirements which are determined by the fuel properties. The principal groups of gasifier applied in different industries are: fluidized bed gasifier, fixed bed gasifier and entrained-flow gasifier [3,8]. Figure 1.3 shows brief information about the characteristics of each type of gasifiers [8].

1.4.1. Fluidized bed gasifier

Feed particles in a fluidized bed gasifier have moderate sizes typically in the range of 0.5-5mm which must be dried before suspension in the bed. The bed might be made of ash or sand and is fluidized by gas flow [8]. The operating temperature of this kind of gasifiers

must be kept very low (usually lower than 1000°C), because, at higher temperature ash particles coalesce and therefore agglomeration might occur, which results in non-uniform bed fluidization. Therefore, feed must be checked before using to ensure that the ash fusion temperature of coal is higher than operating temperature of the reactor [8]. Based on this fact, fluidized bed gasifiers do not operate at slagging condition. In addition, because of low operating temperature, this kind of gasifier is appropriate for reactive coal and also the fuels which contain poisonous, hazardous and troublemaker materials [3,8].

1.4.2. Fixed bed gasifier

In a fixed bed gasifier, the coal particles (usually with big sizes in the range of 5-80mm) and the gasifying agents are passed through reactor in counter-current pattern [8]. Due to working with large feed particles, the residence time in this kind of gasifier must be long. This kind of gasifier does not have the temperature restrictions and can operate either at low temperature (dry ash mode) or at high temperature (slagging mode). Because of working with large particles, it is recommended to use highly reactive fuels in this kind of gasifier [3,8].

1.4.3. Entrained-flow gasifier

Flow pattern of fuel and gasifying agents is concurrent in entrained-flow gasifier with very short residence time of fuel particles (usually in the range of 5-10s). With low residence time, acceptable conversion can be achieved only by recycling a part of the downstream un-reacted materials, increasing the temperature and using small size pulverized fuel [8]. Operating at high temperatures typically higher than the ash melting temperature range, the inorganic contents of fuel are melted and produce a slag layer

which flows down on the wall of gasifier by gravity and then is discharged through a taping system at the bottom. Operating under intense conditions, makes this kind of gasifier suitable for high fuel throughput and gives it flexibility of working with a wide range of less reactive fuels. This gasifier is also capable of working with dry or slurry feed [8].

Among various gasification technologies, application of the entrained-flow gasifiers has increased significantly because of its high efficiency, high capacity, relatively simple design and operation and also its lower environmental related issues. IGCC plants commonly utilize entrained-flow slagging gasifier, because, there is an essential requirement to have very low concentration of sticky particles in the exit gas flow to have appropriate performance with less possible troubles in the downstream equipment, turbines and in CO_2 sequestration and capture unit. For this reason, it is desired to design the gasifier in a way that most of the ash particles stick to the reactor wall and finally be removed as slag through the bottom of the gasifier [6, 9].

Most of the commercial entrained-flow gasifiers are operating in slagging condition. Slag can penetrate into the refractory and causes corrosion, erosion, refractory cracks and lead to material loss. In designing step of the entrained-flow gasifier, ash content (amount and composition) of the fuel is a crucial parameter which has minimum and maximum value [8]. Steady removal of slag depends highly on the flow behavior of slag which can be characterized by various parameters such as temperature and composition dependence of the viscosity of slag [8]. One of the main disadvantages of the entrained-flow gasifier results from the low concentration of the fuel in the gasifying reaction zone and the co-current flow pattern of the fuel and reactant which eliminates the possibility of the

internal heat exchange between the product gas and incoming steam [6]. Some other issues related to the entrained-flow gasifier are [8,10]:

- Issues related to the feeder system and very short lifetime of burners.
- Short lifetime of the refractory used for wall protection.
- Fouling, corrosion and erosion in down-stream equipment such as syngas cooler.
- Tap hole blockage due to unpredicted and unsteady flow of slag.

For most coal types, usually more than 50% of the ash flows down on the wall of furnace as molten slag and the rest is carried by the outlet gas as fly ash. The quench tank temperature must be precisely controlled, because, if uncontrolled flashing happens and steam generates in the tank and goes into the gasifier, it might cause an increase in the deposition thickness by heat consumption and increasing the solidification rate of the flowing slag [6].

As a matter of wall design, entrained-flow gasifiers are categorized into refractory wall and membrane wall. The first type is much simpler and cheaper but the lifetime of the second type is much higher. The reason is that the wall temperature of the membrane wall gasifier is usually lower due to the heat exchange with cooling fluid (usually water) and therefore there will be a solid layer which protects the wall [8,10]. Slag layer can act as a heat transfer medium but sometimes might also play a catalytic role. For example, ferric oxide in the slag can oxidize carbon [6]:

$$Fe_2O_3 + C \rightarrow 2FeO + CO \qquad (1-9)$$

Also carbon might be oxidized by oxygen containing species such as sodium sulfate [6]:

$$Na_2SO_4 + 4C \rightarrow Na_2S + 4CO \qquad (1-10)$$

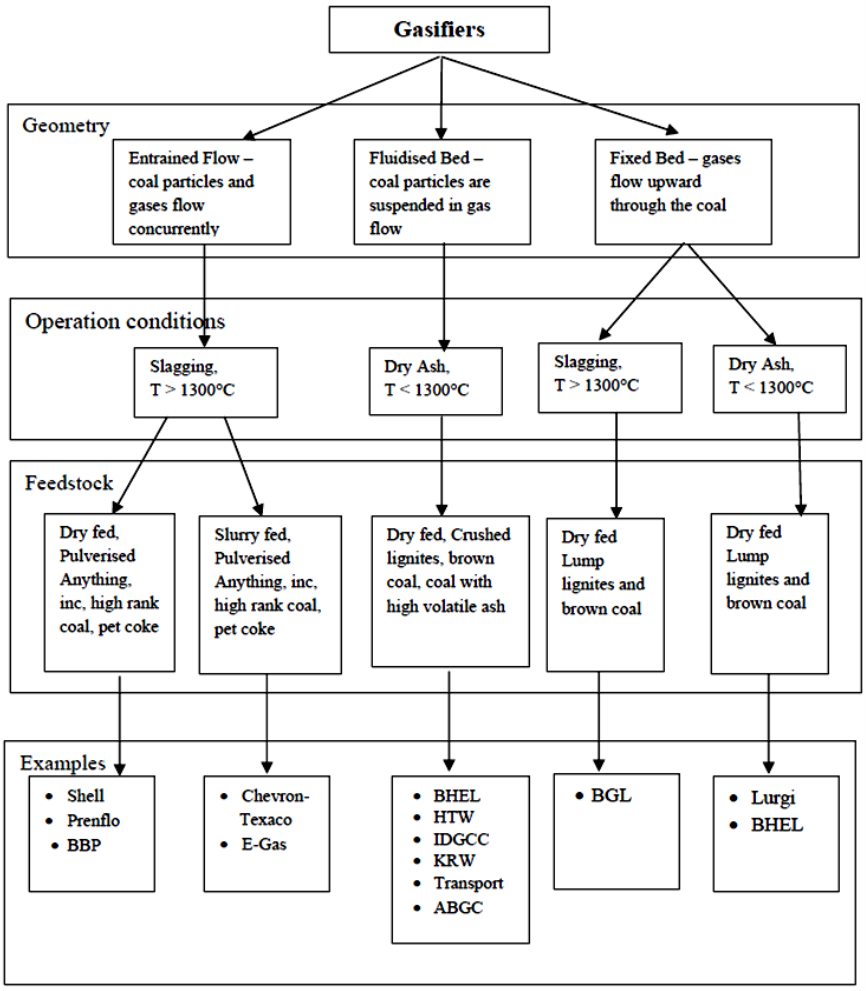

Figure 1.3: Different types of commercially available gasification technologies [8]

Blockage in the slag discharge hole at the bottom may lead to costly emergency shut-down and affect strongly the reliability of the gasifier. Although, it has been several decades since the entrained-flow gasifiers have been commercialized and widely received attentions, but, their reliability is still a bottleneck for wider uses especially in power production plants which are not supposed to operate based on risky processes [10].

1.5. Research objectives

As discussed earlier in this chapter, gasification is an environmental friendly process for utilizing of coal as a cheap and abundant source of energy. Especially, IGCC which is a promising technology for power generation uses gasification process as the main part of its combined cycle. Despite of the advantages of the gasification process, the safety and reliability of this process are still big obstacles for wider applications. One of the main issues affecting the reliability of the gasification process is unpredicted inorganic matters behavior in terms of ash deposition and slag formation. Uncontrolled slag flow which might lead to the bottom hole blockage is mentioned in lots of studies to be the main phenomenon reducing the reliability and availability of the entrained-flow gasifiers. Despite of the importance of this occasion, the slag flow blockage is not studied and characterized well as a function of operating conditions and fuel properties. Experimental analysis of the blockage probability is very difficult and costly in the industrial plants. In order to do the thickness measurement analysis and taking deposit samples at various conditions, gasifier must be shut down after each specific condition which is not economically acceptable in industrial scale. The type of the fuel is one of the main factors determining the inorganic behavior, ash deposition and slag flow, but there are little studies on Canadian coals regarding slag formation in gasification process. In addition, it is not economically reasonable to do experimental analysis for all the conditions to have a reliable prediction of the mineral behavior. Therefore, modeling the inorganic deposition and slag flow provides a good opportunity to have reliable predictions at any desired operating condition using various types of fuels. But, to be sure about the reliability of the model, it must be tuned based on the experimental results at the same conditions.

Considering all of above discussions, the main objectives of this research are fourfold as below:

1- Evaluation the inorganic deposition and slag formation especially considering the blockage probability in terms of the operating conditions, fuel characteristics and different feeding configuration (injection types). A cylindrical slag collector plate made of Kawool paper is used to take samples at different location inside the drop tube furnace. Temperature and particle velocity (by adjusting the gas flow rate) are studied as the operating conditions. Two types of Canadian coals with two different sizes of each fuel are used to investigate the effect of inorganic compositions on the mineral matter behavior. Two different fuel injection configurations were tested to evaluate the effect of the particle flow pattern on the inorganic deposition. Having all the results in a table provides a valuable data bank to have a reliable source of the mineral matters behavior and blockage probability. Image analysis such as Scanning Electron Microscopy (SEM) and BSE analysis are utilized to analyze the deposition samples at different locations produced under various operating conditions. Energy-dispersive X-ray spectroscopy (EDX) helps to analyze the composition of the samples.

2- According to the literature, one of the main steps in any CFD modeling of the inorganic particle deposition and slag formation is particle capture criterion which is introduced to the software as a predetermined rule to decide when a particle sticks to the wall and when a particle rebounds after collision with the wall. The second part of the experiments is performed based on the controlled particle injection. Particles are injected with specific temperature, velocity, carbon

conversion and impact angle on a ceramic plate. Based on the amount of the deposition and comparison of all the data, a particle capture criterion can be achieved. This part of the experiments needs to be continued in future to have an extended data base to reach a comprehensive reliable capture criterion.

3- Performing a CFD modeling for ash deposition and slag formation during gasification is the third and last step of this study. Commercial ANSYS-Fluent software is used. Discrete Particle Model (DPM) is used for particle tracking and Eulerian-Lagrangian frame work is applied for simulation of the gas-particle interaction to increase the accuracy of the model. Based on the particle capture criterion introduced to software by UDF, the inorganic deposition is determined based on the affecting parameters such operating conditions and properties of the particles and wall surface. The deposition results are saved in UDM. The model is developed based on an electrically heated drop tube furnace which was used in the experiments; therefore, the experimental results can be used to validate the modeling results.

Chapter 2. Literature review

2.1. Introduction to mineral matter behavior in coal gasification

The expression of ash is called to the inorganic material remaining after consumption of the combustible part of each fuel particle during high temperature utilization processes. Fly ash is a heterogeneous mixture of inorganic matters having a composition approximately close to the original mineral matters in coal. Ash residue is mainly composed of oxides and sulfates [6]. Due to the high temperature in entrained-flow gasifier (which is usually higher than ash fusion temperature), ash particles melt and produce molten slag layer on the wall of gasifier. It must be noticed that these is a difference between ash and mineral matters. Unchanged inorganic matters in the raw fuel are called mineral matters [6]. Some of the pure minerals in coal are kaolinite, calcite, pyrite, quartz, dolomite, illite and anorthite. After utilization process, these minerals will be in the form of various oxides such as SiO_2, Al_2O_3, FeO, Fe_2O_3, CaO etc. in the ash. Figure 2.1 shows ash and slag formation processes during coal gasification. Build-up of

slag on the wall of gasifier can cause erosion and corrosion of the refractory and also creates many other problems during the operation of gasifiers and down-stream equipment such as syngas cooler and lead to the extra maintenance cost and unscheduled emergency shut-down. Therefore, ash deposition related issues which essentially affect the operation of the entrained-flow coal gasifiers are usually a very big and highlighted concern of any designer. During char–slag transition, a particle can deposit on the wall of gasifier and consequently its burnout behavior might be affected by changing the residence time and available active surface area for reaction [7,10].

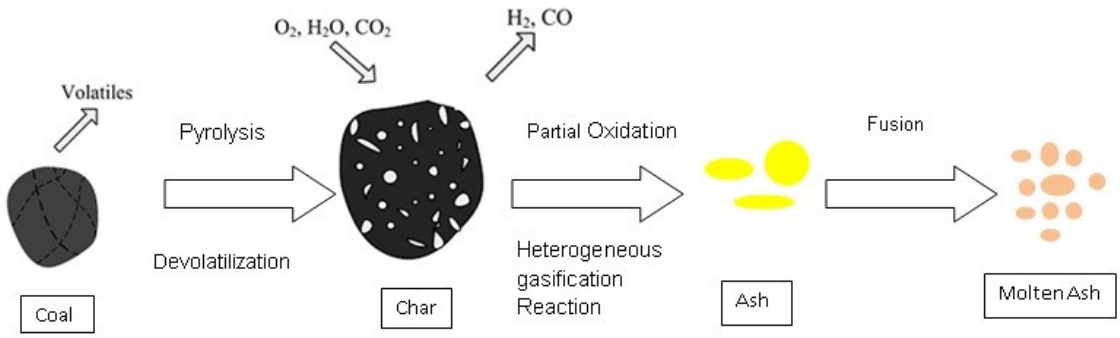

Figure 2.1: Conversion process of coal particles in an entrained-flow slagging gasifier [7]

Uncontrolled slag flow and slag-refractory interaction influence the reliability of the gasifier. Therefore, it is very important to study the inorganic matters behavior and slag flow at high temperature and have more accurate information about ash fusion temperature, viscosity, temperature of critical viscosity (T_{cv}), the influence of fluxing material etc [8]. Viscosity of slag is mentioned to be the most important property governing the slag flow behavior. The rate of slag discharge and the slag layer thickness on the wall of gasifier strongly depend on the viscosity. T_{cv} is the temperature at which the behavior of the slag flow starts to deviate from Newtonian fluid and with small

decrease in the temperature the viscosity increases rapidly [8]. Steady and continuous discharge of slag is one of the basic and vital requirements for normal operation of the entrained-flow slagging gasifiers. For slag to have continuous flow and appropriate layer thickness, its viscosity at the discharge temperature must be low enough (typically less than 25 Pa.s) [8,11]. In order to have low viscosity, one approach is to operate at very high temperature (for example by increasing oxygen which might reduce the heating value of syngas and also decrease the life time of the refractory walls) and another procedure is to add fluxing material such as limestone and dolomite [12]. In order to have a suitable slag flow, operating temperature of gasifier should be higher than T_{cv}. It must be noted that although operating at low temperature can result in very viscose slag flow with high thickness, but, operating at very high temperature can cause very fast refractory abrasion leading to unacceptable maintenance cost. Therefore, an optimization is required in this case. Preliminary studies might show the demand of the large amount of fluxing materials or very high operation temperatures which based on the cost analysis can result in extra operational expenses and consequently make a particular feedstock unreasonable for the utilization process. Therefore, it can be concluded that the viscosity of slag determines the suitability of a particular coal for a gasification process. In order to have a reliable assessment of the suitability of a particular coal for a specific gasifier, knowing the compositional and temperature dependence of the slag flow behavior is significantly important [8,11].

It must be noticed that there is usually distinguishable differences between the properties of the laboratory ash (produced in muffle furnace) and the ash generated under the conditions of the industrial gasifier. The reason is coal ash properties are highly

dependent to the conditions at which the ash is generated and the history that each particle experienced inside the furnace. Ashes produced under real gasification conditions usually undergo transformations suddenly and in a very short time, but, the rate of the changes in the laboratory ash is usually much slower. This signifies the great importance of taking and characterizing samples from real conditions rather than relying on the studies of the ash produced by muffle furnace [13,14].

2.2. Various types of mineral matter in coal

As a matter of size, distribution, type and degree of association within the coal matrix, the original minerals in the raw coal are categorized into two major groups of included and excluded minerals. Included mineral addresses to the inorganic materials that were a part of the plant from which the coal was derived. Excluded mineral mentions to the inorganic materials transported by wind and water and deposited in the peat during the process of the fuel generation [6]. Different degree and types of association of various minerals within the coal matrix result in different characteristics and behavior during any utilization processes. The degree and strength of different species association essentially affect the time after which each inorganic particle can be released from the char particle and then might be able to adhere to the surface of the wall or other particles. Therefore, characterization of the mineral association especially for low melting point inorganic matters such as iron, calcium and alkali containing minerals is of great importance. In this regard Rassk did valuable studies and categorized the association of many inorganic species [6]. As an example, for iron (as one of the main inorganic elements affecting the deposition behavior) the association with the inorganic deposition can be categorized as

oxide fumes came from the organically attached or included parts, sulfide and oxide from partially oxidized pyrite (which might be separate or inherent), large size residues form separate siderite and dissolved iron (usually from inherent source) in the melted deposit mainly containing silicate [6].

Reactions of the volatilized matters in the hot spot section of the flame and nearby area lead to the formation of the fume matters which mostly are composed of sodium and potassium sulfates and are the main cause of the fouling problems by condensation on the cold surfaces in the industrial boilers and furnaces [6]. Sticky film resulted by alkali condensation plays a precursor role to capture the transported residue particles by the gas phase and also may cause extra maintenance expenses due to the material loss by forming corrosive compounds. Sulfate form of sodium, potassium and calcium make up the majority of the submicron size particles in any utilization processes especially working with pulverized coal [6,14]. Rassk [14] reported that approximately half of the sodium in coal vaporizes to form salts during the high temperature processes. There are some evidences showing that sodium captures other silicacious inorganic matters in the ash residue or in the carried particles by flue gas [15]. In combustion (at both high and low temperatures), sulfur is the main reason of corrosion. Some alkali sulfate compounds can be melted at temperatures about 830°C. Having adequate concentration of sulfur in the form of sulfur trioxide (SO_3), alkali iron sulfates might form liquid film at temperatures as low as 540°C [6]. While cooling in the bottom section of the reactor or downstream equipment at temperature around 160°C, sulfur trioxide condenses to form sulfuric acid (as an extremely corrosive compound) if enough excess air is present in the process.

Under reducing conditions during gasification process most of sulfur will be converted to hydrogen sulfide (H_2S) or other sulfides species in the deposits [6].

Properties of coal are completely different form its mineral content. Specific gravity of the raw coal is in the range of 1.2-1.4 whereas the mineral contents have specific gravity in range of 2-5 or even higher [6]. It is hard to determine the mineral matter of the fuel from ash residue remained after the utilization process, because, during high temperature operations, inorganic content of the fuel experience many physical transformations and chemical reactions and only few minerals such as quartz may remain approximately unaltered during high temperature process. As a matter of composition, most of the minerals in coal can be categorized into one of the groups below [6]:

Aluminosilicates-Clay minerals

It can be said that minerals in this group are the most well-known inorganic matters in coal such as kaolinite and illite. Minerals of this group are usually categorized as excluded minerals because they are usually transported by wind or water. Crystalline types of the minerals of this group usually have water in their lattice structure [6].

Sulfide minerals

Iron disulfides pyrite and marcasite (which have the same composition and formula but different crystal structure and are called dimorphs) are the major sulfide minerals found in most coal types. These minerals are of crucial importance during any utilization process, because, they bring a significant share of the total amount of the sulfur into the process which can result in fouling, corrosion and also cause environmental problems by high SO_2 emission during combustion [6].

Sulfate minerals

The minerals of this group usually might not be observed considerably in the mineral content of fresh raw coal however, iron sulfide might be oxidized and produce sulfates during mining process. Gypsum and barite are the most famous sulfates found in the fresh coals [6].

Carbonate minerals

Carbonate minerals are reported to be related to the environment of the initial stages of fuel formation and usually are composed of iron, calcium and magnesium. Calcite ($CaCO_3$) and siderite ($FeCO_3$) are the major carbonates in most types of coal [6].

2.3. Types of slag layer

Slag layer can be typically classified into four categories: crystalline, glassy, plastic and alkalescent which are different in the structure and consequently have various properties. Measurements based on the experimental observations showed that the thickness of the flowing slag is minimum for crystal layer type and is maximum for glassy layer type. The slag film properties must be carefully studied as they affect the furnace temperatures, progress of the heterogeneous reaction and coal conversion by influencing the heat exchange rate between gas phase and the wall of gasifier. The slag film on the wall of furnace is divided into three layers [16]:

- The exterior section which is called the real liquid flowing layer and based on experimental analysis, this layer usually contains no solid crystals (usually with temperature higher than T_{cv}).

- Plastic flow layer located below the real liquid layer in which some solid crystals might be observed (usually in the temperature range of T_f to T_{cv}).
- The last layer which is located between plastic flow layer and the wall of furnace is the solid immobile layer. Based on the operating temperature of the process and type of the wall of gasifier (refractory or membrane wall), this layer might exist or not. Temperature of this layer is typically lower than T_{cv}.

Having the fixed rate of ash generation (constant amount of the inorganic matters which stick to the wall in specific operational time), the slag layer thickness on the wall of gasifier can be adjusted by the heat load and the process temperature while doing the operation or by adding fluxing material (to decrease the viscosity of slag) before doing the operation [16].

2.4. Effects of mineral matter composition on slag flow

Ash deposition and slag flow behavior significantly depends on the ash fusion temperature and viscosity which both depend on the mineral composition of the parent coal. Adding fluxing material or additives is a method to decrease the viscosity. One of the major components existing in the ash and slag is SiO_2. A famous proposed theory which can explain many aspects of the behavior of the viscosity of melted deposition (mostly including SiO_2) is network theory which is based on the effect of incoming oxides on the silicacious network. Oxides which lead to increase the viscosity are called network formers and oxides which cause decrease in the slag viscosity are called network modifiers [8]. Based on the network theory, larger viscosity happens when the net is bigger due to the more internal friction between the layers when liquid layer flows [17].

Silicon dioxide as the principal component in the ash, acts as a network former. The alkali oxides such as Na_2O, K_2O and Li_2O are categorized into network modifiers group. The role of alkaline earth oxides such as MgO, CaO depends on their composition in the deposition layer. By adding CaO and MgO (when their concentration is low), the microstructure becomes homogeneous and cause to break the big nets to smaller ones (by importing more negative oxygen ions) and consequently, viscosity decreases. Overall content of CaO and FeO could greatly affect the viscosity and T_{cv} [8,14,17]. Song et al. [13] reported that adding CaO leads to decrease in the melting point (ash fusion), viscosity and T_{cv} of the slag and the extent of the improving is different for each additive material. In this regard, Wei et al. [18] observed that MgO had better effect than CaO in improving the liquid content of slag. Adding 10% of MgO was found to be more efficient than 20% of CaO in the liquid formation. Figure 2.2 shows the effect of CaO on the flow temperature of ash and slag. Adding CaO until 35% reduces the flow temperature of ash and slag and above that increasing CaO shows network former effect [13]. Lingxue et al [17] evaluated the effect of CaO on the slag behavior and found the same trend. They reported that T_{cv} firstly decreases by increasing CaO, and then reaches a minimum value when the content of CaO is around 15%. Lu et al [19] studied the effect of inorganic matters composition on the fusion temperature and concluded that the formation of anorthite is the main reason for low ash fusion temperature. Based on their hypothesis, mullite ($3Al_2O_3 \cdot 2SiO_2$) reacts with the added CaO to form anorthite ($CaO \cdot Al_2O_3 \cdot 2SiO_2$) with low melting temperature, but, by adding more CaO, Gehlenite is formed, thus the liquidus temperature increases [19, 20]. Depending on the chemistry of slag, especially the concentration of alkali or alkaline earth elements, aluminum oxide (Al_2O_3) and ferric

oxide (Fe_2O_3) can be a network former or a network modifier [8]. Different states of iron exhibit various effects on the viscosity. The state of iron (Fe^{2+} or Fe^{3+}) generally depends on the operating conditions such as temperature, pressure and oxidizing or reducing environment [12]. Some elements may have more important role in slagging behavior and also may change the temperature at which slagging occurs. Iron is one the most important elements in slagging behavior and at very high concentrations, the slagging properties of the inorganic residue might be observed at temperatures as low as 700 °C. The dissolution of iron in the aluminosilicates and quartz decreases the melting point of the mixture. Another affecting component is sodium which has a highlighted role in slag formation at lower temperatures [21, 22].

To characterize the effect of the composition on ash deposition and slag behavior, defining parameters such as base to acid ratio or alkali index is very helpful. These indices are mostly relied on the ratio of basic components (FeO, CaO, MgO, Na_2O and K_2O) to acid compounds (SiO_2, Al_2O_3) in the ash multiplied by some other empirical factors [23].

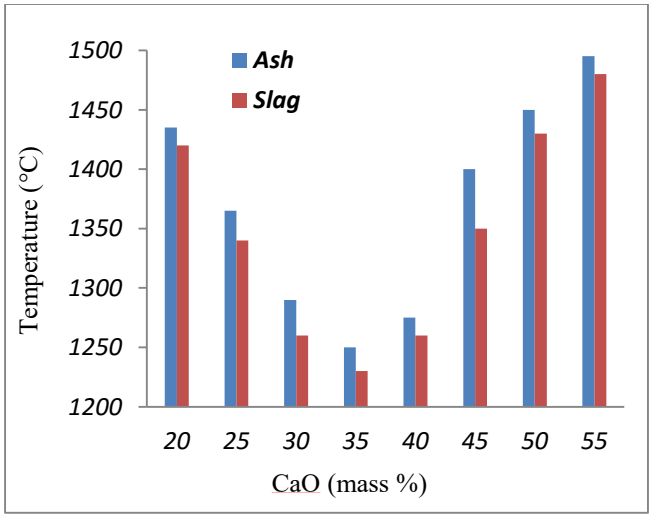

Figure 2.2: Flow temperature of ash and slag with the different CaO content [13]

2.5. Effect of atmosphere on ash deposition and slag flow

Atmosphere of the reactor surrounding the ash deposition and slag layer influences their behavior mainly by affecting the viscosity, especially, when the sample contains considerable amount of iron. It is widely observed that at a constant temperature the viscosity is usually lower under reducing conditions than the viscosity in oxidizing environment [18]. Based on the atmosphere characteristics, there are two types of entrained-flow gasifier. The first type is air-blown gasifier which produces syngas with concentration of about 10% H_2 and 30% CO and the other type is oxygen-blown gasifier used for producing higher concentration of syngas including approximately 30% H_2 and 60% CO. Inorganic deposition and slag layer characteristics within these two types of gasifiers are different. Experimental investigations show that the slag from air-blown gasifier is glassy and granular, but, in oxygen-blown gasifier iron oxide might be completely reduced to the elemental iron state with different shapes at solid condition which may cause problems with the slag handling after discharging [18]. Wei et al. [18] observed that for CO_2/H_2 ratio of 10/90, the liquid content in slag is higher than CO_2/H_2 of 50/50. Most of these kinds of observations are related to iron as the most plenteous heterovalent element in the inorganic deposition causing vital variation under different oxidizing and reducing atmospheres. In XRD pattern of the slag produced at CO_2/H_2 of 10/90, the characteristic peak of iron was detected which is because of the iron precipitation in strong reducing atmosphere. Therefore, it can be concluded that the precipitation of iron particles influences the characteristics of the slag for example by changing the liquid behavior from Newtonian to Plastic flow [12]. Gupta et al. [22] highlighted the existence of CO_2 in the atmosphere as a strongly affecting reason for the

mineral transformations in the char particles during gasification processes. Based on the experimental observations, they reported that pyrohotite and iron oxides are essential reactive phases showing the most transformations in the presence of CO_2.

2.6. Mineral matter transformation during gasification

Mineral matters in any fuel such as coal undergo many physical and chemical transformations while heating in any high temperature utilization process. The first change is losing water of hydration and moisture release [6]. In a normal coal, moisture might be in the form of surface moisture, inherent moisture and chemically-bounded moisture (which determines the rank of the coal). Surface-adsorbed and inter-lattice water existing in the clay minerals evolve through an endothermic transformation in the early stage of the heat-up process [6]. Then, release of CO_2 and sulfur oxides happens by calcite decomposition and pyrite oxidization. Liquid phase formation initiates sintering at about 650°C (might vary by formation of various eutectics) which finally leads melting and then reactions start to occur in the liquid phase at about 1000°C. At temperatures higher than 1100°C, volatilization of alkalis happens and at the same time, the endothermic lattice destruction might commence [6]. The processes mentioned above can be analyzed using Differential Thermal Analysis (DTA), but, the heating rate in this method is extremely lower than the actual heating rate a particle faces through real utilization processes inside the furnace. Based on this fact, many researchers reported that water release and structure changes usually will not be fully completed especially during the early stages of the process [6].

Bulk properties of the inorganic matters affect the process of transformation. The modification and alteration in the shape and structure of the inorganic matters are mainly governed and dominated by the properties such as surface tension and viscosity which are functions of the temperature, composition and atmosphere. In this regard Frenkel (1945) reported that the required time for an irregularly shaped particle to transform to sphere can be approximately calculated by the equation below [14]:

$$r = r_0 e^{-t/(4\pi\mu/\gamma)} \qquad (2-1)$$

In above equation, r is the distance of a point on the initial surface from the center of the sphere with the same volume with radius r_0, μ is viscosity and γ is surface tension [14]. This correlation might be useful to validate the spherical particle assumption in modeling based on the residence time of the particles. In this regard it is widely accepted that most of the inorganic particles passing around the flame with the temperature of 1430°C or higher have spherical shape; however, there are some exceptions such as quartz particles which have very high melting temperature and therefore might only be partially surface melted and hold their original non-spherical shape. The final shape depends on the composition, size, residence time and the flame temperature [6].

Inorganic constituents in coal during combustion or gasification can transform into vapors, aerosols and solid or liquid ash. After structural change followed by fusion at high temperatures, inorganic content in the ash might undergo many possible chemical reactions. Some of the reactions among the inorganic matters at high temperatures are listed below [24, 25]:

$$Al_2O_3.2SiO_2.2H_2O \rightarrow 2H_2O + 2SiO_2 + Al_2O_3 \qquad (2-2)$$

$$3CaO + Al_2O_3 \rightarrow Ca_3Al_2O_6 \qquad (2-3)$$

$$CaO + 2Al_2O_3 \rightarrow CaAl_4O_7 \quad (2-4)$$

$$4FeCO_3 + O_2 \rightarrow 2Fe_2O_3 + 4CO_2 \quad (2-5)$$

$$Al_2O_3 + SiO_2 \rightarrow Al_2O_3.SiO_2(sillimate) \quad (2-6)$$

$$Al_2O_3.SiO_2 + 2Al_2O_3 + SiO_2 \rightarrow 3Al_2O_3.2SiO_2(mullite) \quad (2-7)$$

Figure 2.3 shows the mineral transformation of coal ash. By increasing the temperature, the amount of mullite increases (as the main thermodynamically stable compound at high temperatures), the amount of SiO_2 decreases because of the reactions between SiO_2 and Al_2O_3, but, some inorganic compounds such as sillimate have maximum value (at about 1300°C). All these observations prove that reactions happen in solid or liquid phase between inorganic matters at high temperatures during gasification process [24]. On the base of XRD results, most of mullite and SiO_2 are in crystal phase. Some inorganic compounds might undergo through different pathways and structures changes. At high temperatures fayalite ($Fe_2(SiO_4)$) sometimes transforms to glassy phases but sometimes transform to ferrite phases (which is not stable because of strong polarization) and is not detectable by XRD analysis. Due to the lack of accurate and reliable method to study and analyze the generated amorphous phases, FTIR is potentially the best available method for determination the change of melts structure and the degree of polymerization of aluminosilicate networks (during any utilization process) because of its sensitivity to the short range order structure [16]. Different amorphous or crystalline phases have significant effects on the properties such as surface tension and polymerization degree of the molten deposit which finally determine the thickness of the flowing layer.

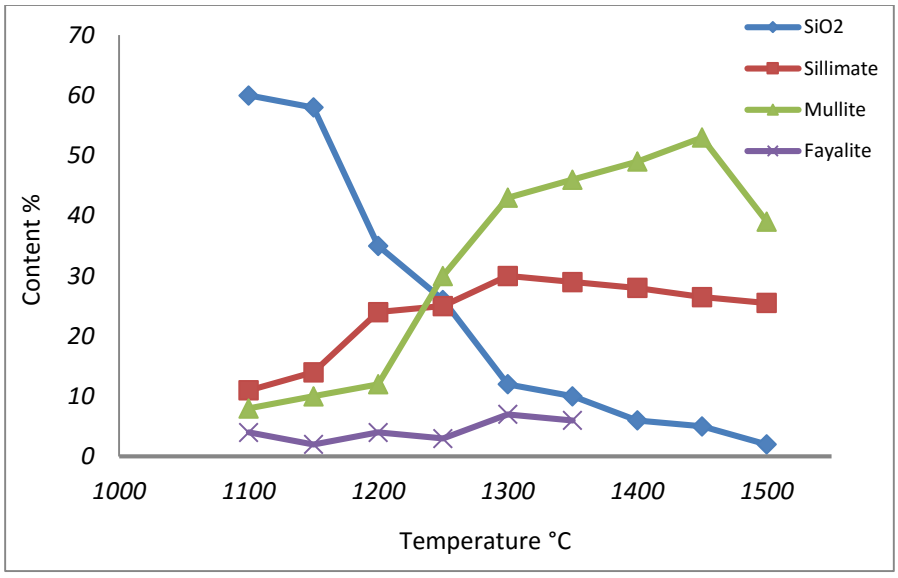

Figure 2.3: Minerals transformation for HN coal ash at different temperatures [24]

Iron-rich glass will be formed by decomposition of pyrite (which might have included or excluded origin) while heating. Type and degree of mineral association as a matter of being included or excluded affects the transformations and reactions. For example, some reactive minerals such as dolomite are mostly present with included nature and are highly associated with the carbon fraction; therefore, it can participate in many of mineralogical reactions just at the later stages of the gasification process near to the end of the reactor when most of the organic materials in coal have been consumed by gasification reactions. In mineralogical transformations studies during gasification process, existence state of different species, type and degree of association, bulk chemistry and mineralogy of coal must be taken into consideration to evaluate the possibility of the interactions as accurate as possible [26,27]. Matsuoka et al. [28] performed some experiments to analyze the ash forming reactions during gasification process using CCSEM. Their observations showed that the system of K–Al–Si and Fe–Al–Si are almost the same as their original state in the raw coal and they do not participate in the reactions with other species at temperatures

below 500 °C. Based on the low Na content in aluminosilicates and silicates in the raw coal and the significant amount of Na in aluminosilicates in the char at the temperature around 800 °C, they concluded that sodium containing species reacted with aluminosilicate, principally kaolinite at that specific temperature range [28].

Gupta et al. [29] reported that from the starting point of the partial melting till transformation to the completely melted homogeneous liquid, the deposit composition varies continuously. This observation is related to both reactions between various species and also the extent of the dissolution of different species in the melted deposits. Presence of some species affects the solubility of the others. If there is high iron content in the ash, solubility of SiO_2 increases and its level in the melt quickly reaches to that of the bulk ash whereas, for the ash with low iron content, this process is much slower due to the lower particle solubility in melt, and uniform composition (close to bulk ash) might be observed only at very high temperatures or in the later stages of the process [29].

Essential affecting interactions are not just between the inorganic matters, but, at the same time the interaction between aluminosilicate melts and the carbon content of the char particles affects the polymerization and surface tension [16]. Rassk (1966) reported that at the inorganic-carbon interface, iron carbide might form and react with other mineral species and finally cause the formation and release of carbon monoxide [14]:

$$2Fe_3C + SiO_2 \leftrightarrow Fe_3Si + 3Fe + 2CO \qquad (2-8)$$

Gas formation and release might also occur through other pathways which are less probable reactions (because of low solubility and diffusivity of carbon in the molten slag) as below [14]:

$$FeO + C \leftrightarrow Fe + CO \qquad (2-9)$$

$$SiO_2 + 3C \leftrightarrow SiC + 2CO \qquad (2-10)$$

Gas release process is a function of the rate of carbon dissolution in the molten deposit (in various forms such as pure carbon or iron carbide), surface tension and reaction rates. These reactions affect the surface characteristics of the molten slag and consequently influence the particle capturing ability of the slag layer which is crucially important in ash deposition phenomenon [14].

2.7. Influence of mineral matter on gasification process

Slag may participate in chemical and physical interactions with char and consequently affect gasification process. During high temperature processes, carbon conversion might be hindered due to the surface coverage and pores plugging of the char particles by molten aluminosilicates. Surface tension is the main affecting property in this regard which determines the degree of polymerization (of surface) and the extent of spread of molten phase on the char surface [24]. Lin et al. [30] reported a decrease in the char reaction rate at conversions more than 50% and at temperatures around ash melting point or higher temperatures and related this phenomenon to the pore blockage happened by spreading of molten slag, which finally resulted in the reduction of the available surface area for reactions. In an adverse phenomenon, formation of slag may significantly extend the residence time of the particles in the gasifier and consequently, affect the carbon conversion [31]. When the char particles adhere to the slag layer, their carbon content may remain segregated on the surface of the slag and continue to be gasified or it can be encapsulated into molten layer with no more chance of reaction and all these depend on the parameters such as ash-carbon interfacial tension, ash viscosity and overlying of

carbon particles by newly impacting ash material. In addition, in non-vertical section of the gasifier the buoyancy force can be effective [31]. Noda et al. [32] based on the experimental results reported that particles with combustible content reacts at lower rates when captured by the slag layer due to the lower surface area inside and on the surface of the particles. Zhao et al. [33] reported that reactivity of the trapped carbon in fine slag is lower in comparison with that of coarse slag. Usually the fine slag includes high content of un-reacted carbon which is economically desired to be mixed again with the feedstock and recycled to the gasifer [33]. Ash deformation and fusion affect the morphology development of the char particles. The reactivity of the pure organic carbons in the char and carbon produced from decomposition of SiC (inorganically bound carbon) are completely different [25].

Mineral matters in coal influence the reactivity especially, in low-ranked coal due to their catalytic effects on the gasification reactions which is a function of the chemical form, concentration and distribution in the coal matrix. Alkalis and alkaline-earth elements are famous inorganic matters with catalytic effects. Skodras and Sakellaropoulos [23] found that reactivity and the rate of gasification are linear functions of alkali index. They observed that in CO_2 and H_2 atmosphere, gasification reaction rates will be promoted proportionally to Ca concentration. There is no correlation for Fe catalytic effect on gasification, however, it is generally approved that Fe (not in oxide form) has catalysis effect [23].

Schmitt (1981) reported that the presence of included inorganic matters (as dispersed matters) within the coal matrix prepare channels which help the gasifying agents to diffuse into the char particles, react with the carbon content, and produced syngas release

from char particle and therefore, enhance the rate of gasification reactions. However, if the ash content is too high, it is possible that molten inorganic matters encapsulate unreacted carbon and reduce the process efficiency [14].

By forming a molten slag layer with different thicknesses on the wall of reactor, mineral matters influence the heat transfer inside the gasifier and affect the efficiency of the gasification process. Costen et al. [34] reported that even a very thin layer of the deposit can cause a substantial decrease in the heat exchange (between wall and gas phase). As a case study, they reported 35% reduction in the heat exchange as the result of the presence of a thin layer with thickness of 0.7 mm on the wall. The type and structure of the deposition are of great importance in this regard and there is a considerable difference between heat exchange behavior of sintered deposit and flowing liquid layer [14].

2.8. Coal and ash particle size distribution

Having many parameters involved in fly ash characterization such as inter-particle morphology changes, heterogeneous non-uniform chemical composition and size distribution make the study of ash deposition behavior very difficult [35]. Size of mineral matters strongly affects their behavior during pyrolysis, combustion and gasification. Size distribution is an important parameter for modeling ash deposition, slag generation and char-slag interaction during coal utilization processes. Particle size determines the mechanism of particle transfer especially particle movement toward the wall inside the reactor. When there is swirl/tangential flow the mass transfer from gas to wall is governed by the inertial mechanism resulted by centrifugal forces. This mechanism is more effective for larger particles and therefore most of big particles might collide with

wall while fine particles mainly follow the gas phase [36]. There is a great difference between deposition behavior of big and small particles. Colliding with the wall is the first required step for sticking. The large inorganic particles can easily collide with the wall because of large inertia, but, the fraction of these particles is relatively low. For small ash particles, it is less possible to reach and collide with the wall because they follow the gas path due to the low inertia. The fraction of small inorganic particles in ash is much larger than big particles and consequently, the probability of their inroad into the boundary layer by the turbulent effect is high. Therefore, most of the depositions is due to the presence of small particles [37].

The particles in a typical pulverized coal are generally in the range of 10-150μm and the inorganic mineral content are usually finer and unevenly dispersed within the coal particles weather as separate particles or associated with the coal particles [15]. Seggiani et al. [38] reported that the mass fraction of minerals in a typical pulverized coal is generally between 1 to 50%. These mineral matters may exist in the form of very small ionically bounded material to the carbon content or as big separate mineral particles (usually in the range of 1 to 15 μm). Size distribution in the ash products includes submicron particles which are produced by condensation of volatilized species (vaporized in the hot flame area and condensed in colder sections), big ash particles generated from heating and oxidation of excluded mineral matters (producing the particles in range of 10-20μm) and very big agglomerates formed by coalescence of the inorganic matters (might be bigger than 100μm) [15].

In gasification process considering the operating condition, there is a size distribution for coal, char and inorganic particles and therefore, the same degree of gasification cannot be

expected from all the particles. Having the coal particles in very small dimensions, promotes the heating up process and consequently improves the reaction of carbon with the gasifying agents as they flow through the gasifier. When the particle size increases, the overall gasification rate generally tend to decrease due to the decrease in the gas phase mass transfer and diffusion into porous structure of pyrolized char [6, 22, 39].

Regardless of the original size distribution of the feed before injection into the furnace, there are some phenomena affecting the size of the coal, char and inorganic particles inside the furnace such as fracture or agglomeration which is related to the type of each particle. In this regard, Raask (1984) reported that the silicasious inorganic matters such quartz did not fracture considerably due to the sudden heating in the reactor, but, non-silicate minerals such as pyrites or carbonates fracture fast and extensively when the particles are faced to rapid heating [14].

Some models for predicting the particle size distribution have been proposed. The first model is called full coalescence model. Based on this model, the char particle participates in all the reactions while shrinking but maintains its integrity and all of the different ash particles dispersed in the char particle coalesces and finally appear as a single particle. Using this assumption in any gasification modeling, there will be only one ash particle resulted from every coal particle [40]. The other model is called no-coalescence model. Based on this model, coalescence does not happen and therefore, each inorganic particle whether presented as excluded mineral or dispersed in char will form an ash particle [40]. In reality, the particles behave somewhere between the assumption of these two models. Barta et al. [41] developed the Random Coalescence (RC) model which is a combination of the two restricting cases of full coalescence and no-coalescence models. Based on this

model, inorganic particles are present on the exterior surface of the char particle and coalescence is only possible if the inorganic matters collision happens by progressing of the reactions and receding of the char surface. In this model, transition radius (r_{trans}) is defined as a value that if the char particle radius decrease to that, significant penetration of the gasifying agents into the char particles happens and internal burning occurs. At the end, if the char porosity reaches a critical value, disintegration happens that cause release of the rest of dispersed inorganic as separate ash particles [41]. Seggiani et al. [38] investigated the RC model in coal combustion and reported that r_{trans} is a function of the coal and inorganic particle size and also the fraction of the mineral matters. They introduced the ratio $2r_{trans}/D_{coal}$ as an index of the mineral matter coalescence. Another phenomenon which affects the particle size distribution is agglomeration. If enough amount of the low melting point eutectic is present within the coal matrix it would act as glue to force other particles to stick together and make big agglomerates. Considering many complicated phenomena involved in size distribution of the particles during any coal utilization process, there is still a lack of comprehensive model in this regard and more studies are required to be done.

2.9. Compositions of ash and slag at different locations

Wall et al. [42] reported that slag layer composition is not usually the same as bulk ash composition of the parent coal. Yu et al. [43] used a deposit probe placed parallel to the gasifier wall to take slag deposit inside the gasifier and found that included and excluded minerals have different deposition behaviors. Based on their results, leaving fly ash has composition close to the bulk ash, but, included minerals mostly deposit in the area near

the burner and excluded minerals are mostly deposited in the area above the burner. In addition, carbon content in their slag samples showed that even at low carbon conversion, the char particles might be trapped by slag. Therefore, it is more logical not to use the bulk ash viscosity to calculate slag flow and thickness in all the sections of the furnace during gasification process [43].

Based on the experimental observations of Costen et al. [34], deposition behavior is mostly related to the size and weight of the particles. The smaller particles are deposited near the burner inlet and heavier particles deposited far from the burner. This behavior is most likely related to their different inertia. Inorganic composition is another parameter affecting the location of the deposition. Aluminosilicates are mostly deposited in top section and their deposition is reduced as they move downward along the length of gasifier. This observation might also be related to the temperature. Because of high temperatures near the burner area, compounds with high melting temperatures can be sticky enough to deposit. However, in lower sections, endothermic gasification reactions reduce the temperature, therefore, the viscosity of aluminosilicate increases and their deposition tendency decreases [34].

2.10. Mineral matter and slag analysis tests

2.10.1. Ash Fusion Test (AFT)

AFT test is a traditional and the most accepted method of evaluating the tendency of coal ash transformation to slag. This method categorizes the temperatures related to different steps from ash softening to complete melting. Based on this method ash particles are assumed to be sticky when they start to soften at Initial Deformation Temperature (IDT).

This parameter is visually recorded when the tip of the ash cone is rounded. The main deficiency about AFT is its inaccuracy because it is based on the subjective visual characterization (however the accuracy of this method has been enhanced recently utilizing computer programs). This method deals with the average flow properties and do not specify the exact temperature at which melting starts [21, 29]. This method also gives no accurate information about the conditions at which the slagging or sintering might be observed during the operation. Van Dyk et al. [21] observed the IDT at 1300 °C for an ash sample, whereas slag formation already started to take place from 1000°C for that sample. An AFT analysis only gives some information about the temperatures at which the structure of a cone shaped ash material deforms and gives no information about the properties of the slag below that point. Various relationships between AFT and composition has been proposed based on acid to base ratio, silica ratio etc. [6].

2.10.2. X-ray diffraction (XRD)

XRD test reveals various crystalline phases present in the materials and when applied for coal or char, it can only specify the major phases. The deficiency of this method is that it provides little information about minor phases and cannot recognize amorphous phases [28]. Brachi et al. [36] performed XRD analysis on coarse slag and observed no distinct peaks due to the amorphous structure of slag. However the method detected two peaks of anhydrite and periclase in fine slags. A typical result of XRD analysis is shown in Figure 2.4.

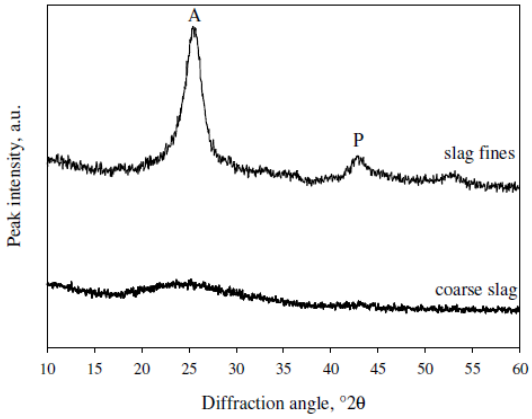

Figure 2.4: **XRD analysis for coarse slag and slag fines (A: anhydrite, $CaSO_4$, P: periclase, MgO) [36]**

2.10.3. Thermo-Mechanical Analysis (TMA)

TMA analysis can be used as a method for evaluation the viscosity and the change in the viscosity due to the flux addition. In metallurgical science, reliable methods to study the physical properties at very high temperature are mostly based on the shrinkage evaluation. In TMA technique, the penetration of a ram into a pellet of ash is recorded as the temperature of sample is increasing [44, 45]. Initially when the temperature is low, the melt formation is very slow and the ram does not penetrate that much, but, as the temperature increases gradually, melting and reaction happen and liquid phase starts to form which fills the open network or pores of the ash and consequently lead to the initial shrinkage. Various indices have been introduced based on TMA analysis. It is thought that essential sample deformation happens at $T_{(25\%)}$ which is the temperature corresponding to 25% shrinkage [29].

Bryant et al. [46] investigated the effect of adding fluxing agent (CaO) to coal ash on the shrinkage at high temperature using TMA in combination with viscosity measurement. It is widely reported that in typical coal utilization process for safe operation, the slag

viscosity must be in the range of 15-25 Pa.s. They reported that 10-95% shrinkage corresponds to this viscosity range. Increasing CaO content significantly reduces the viscosity and causes a great increase in the shrinkage. Figure 2.5 shows a typical Schematic of ash sample during TMA analysis [46].

It is possible to observe some peaks during TMA analysis which are corresponding to the rapid fusion events during heating. Gupta et al [29] reported that these peaks are related to the formation of eutectics which can be tracked and recognized on phase diagrams. They usually observed the first peak at ~10% shrinkage, but, the second peak depends on the iron and calcium contents. For most of the cases, the second peak happened at ~30% shrinkage, but, for cases containing high iron and high calcium contents, second peak happened at ~50% shrinkage.

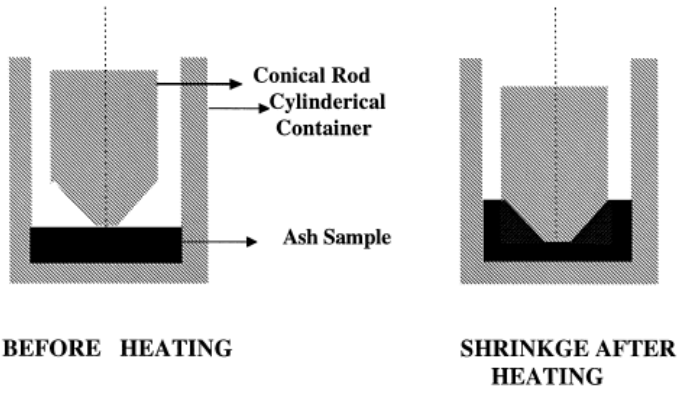

Figure 2.5: **Schematic diagram of the ash sample in the thermo-mechanical analysis technique [29]**

Based on the well-known assumption of the equality of the volume fraction of a phase to the cross-sectional area fraction of it [47], Gupta et al. [29] applied image analysis to estimate the porosity using the digitized images at different temperatures. They found that the bulk porosity decreases till the formation of closed pores which depends on the iron content. Most of their experiments showed a relation between T(50%) with closed

and spherical pore formation. Alkali and silicate composition affect the porosity of the samples which consequently influence the shrinking process. These results proved that, TMA analysis in combination with other techniques such as image analysis or viscosity measurement, helps in better understanding of the structural changes happened in ash depositions during heating process [29].

2.10.4. SEM/EDX

Developing SEM in combination with other techniques in 1965 essentially enhanced the ability to identify extremely fine minerals and inorganic matters in coal [14]. Using SEM/EDX technique, it is possible to analyze the structure and morphology of ash and slag together with the composition of each point of the sample which helps to find out about the fate of various particles. SEM/EDX analysis provides an accurate technique helping to observe various interactions between minerals at different stages of a process and gives valuable information about the size, morphology and composition of the minerals simultaneously making it possible to study the mechanisms of various phenomena [14]. In this regard, ash surface studies performed by Raask and Goetz (1981) showed large number of submicron-size particles on the surface of spherical or rounded aluminosilicates. EDX analysis revealed that carried particles are mainly sodium and potassium sulfates. Then they started to propose probable mechanisms and test them. A possible mechanism for their observation is adhesion of the vaporized alkali metal at the surface of melted silicate particles and then, the alkalis oxides were sulfated by different forms of sulfur oxide in the flue-gas [14].

Numerous studies and lots of valuable results have been achieved by SEM analysis. Based on SEM analysis, Ambrosino et al. [48] reported that carbon content in fine pieces

of slag was larger than the coarse slag particles. Their results showed that slag might have a significant carbon content as high as 54%. The importance of this method will be understood knowing that permanently encapsulated carbon by slag will not be disclosed by thermal analysis. In this case, cutting the sample and cross section analysis by SEM-EDX is able to reveal the presence of un-reacted carbon inside slag [36]. Zhao et al. [33] based on the SEM images found that the surfaces of the fine slag samples were covered with fine floccules and small spheres and using EDX analysis they observed that the carbon content of floccules is higher than the spheres. Then they reported that during melting of the minerals, inorganic matters had tendency to coalesce and form carbon-free spheres while carbon usually remains as floccules and does not participate in the formation of ash sphere [33].

2.10.5. CCSEM

CCSEM scans thousands of particles in order to produce statistical information on all the existing elements in a sample. CCSEM technique applies EDX analysis to measure the relative concentrations of each inorganic element and using relative concentration index classifies the processed particle into an appropriate mineral category. When based on the information of a particle it cannot be classified into a certain group, then, it will be categorized as unknown group. This technique records the dimensions of each particle at the same time of compositional analysis. Therefore, the area and finally the weight of each particle can be calculated. The main deficiency of CCSEM analysis is its uncertainty in processing finely dispersed minerals including cation-exchanged metals and fine mineral particles with sizes lower than 1 μm [28, 49].

Miller and Schobert [50, 51] observed 50% of the inorganic material in the unknown classification meaning that a large amount of the minerals have been transformed into complex phases after the process. When using CCSEM for weight calculation, it must be noticed that the value of density used for similar composition of the inorganic in the ash and minerals in the raw coal might be different. Ca-rich phase in coal is usually calcite with density of 2.7 g/cm^3 but Ca-rich phase in char or ash is CaO which has a density of 3.3 g/cm^3 [28]. Like other analysis, when interpreting the results of CCSEM, appropriate care must be taken to prevent from errors. Ghosal et al. [35] measured the size distributions resulted by CCSEM and also by multisizer. By comparing the results, they conclude that CCSEM over-predicts the size. The error might be related to the method used for preparation the samples for the test.

CCSEM allows determination of mineral association in coal and can determine the size distribution of both excluded and included minerals in raw coal. Utilizing this ability of CCSEM, Gupta et al. [52] analyzed coal gasification process and reported that big excluded minerals particles do not participate in the slag formation considerably. Zhang et al. [49] used CCSEM to investigate the effect of the included and excluded mineral particle size on the inorganic behavior and transformation during combustion. At high values of calcium to sulfur ratio, calcium aluminosilicate was able to capture sulfur dioxide, but, at lower values it was not able to do that. Matsuoka et al. [28] studied the ash forming reactions during gasification using CCSEM and concluded that at temperatures below 800 °C, excluded minerals do not interact with each other and included calcium containing species mostly participate in calcination and sulfuration reactions.

2.11. Models for slag viscosity

As the most important and governing parameter of the slag flow, viscosity depends mostly on the composition, operating conditions (such as temperature and atmosphere), experienced thermal history and solid fraction. The effect of solid fraction is essential at the fractions higher than 10% [53].

In order to have reliable estimation about the suitability of a particular coal for a gasifier, or to optimize the fluxing or blending procedure, it is essential to have valid knowledge of the temperature and composition dependence of the slag viscosity. This information could be gained from either experimental measurements or from estimations obtained using predictive models. The difficulty and high cost of the experimental measurement of the viscosity of slag generated from coals, has led to many predictive models which are mostly functions of the chemical composition and temperature [8,54]. Most of the developed models for predicting the slag viscosity are semi-empirical models such S^2 and Urbain which are theoretically based on Newtonian fluids and require regression of the experimental data for parameter tuning [12]. Urbain model is based on the fully molten mixture (pure liquid) assumption while in real conditions the slag is a heterogeneous mixture of liquid and solid crystals [21]. If the generated slag contains some solid particles, slag most likely do not exhibit the behavior similar to Newtonian fluid. Usually, non-Newtonian behavior may be due to the presence of solid crystals or presence of immiscible liquids [12]. Molten slag is a complicated mixture of various components containing complex phases. Therefore, each empirical viscosity models will be suitable for only a limited specific temperature and composition ranges. For choosing a model, it is suggested to consider the composition of the existing slag and select a model that

performs well for slags with similar composition [8]. Coals with high ash flow temperature, need fluxing material such as limestone to enable continuous slag tapping in entrained flow gasifiers. Therefore, finding proper model to predict reliable results for viscosity and temperature of critical viscosity at each specific value of added fluxing material is very beneficial [8]. Table 1.1 represents some of the well-known models.

Hurst et al. [54] presented a two parameter Arrhenius-type model for viscosity as below:

$$\ln(\mu) = A + {}^{B}/_{T} \qquad (2-11)$$

On the base of this model, Hurst et al. found that increasing FeO in the mixture of SiO_2, Al_2O_3, FeO and CaO (as an artificial slag) leads to lower viscosity value. Duchesne et al. [12] developed an artificial neural network model to calculate slag viscosity. They evaluated the effect of adding various amount of the fluxing materials on the ash viscosity and concluded that magnesium has better fluxing effect than calcium.

It must be noticed that usually there are some errors in the viscosity measurements which are mostly related to the measurement techniques. When comparing the results of experimental viscosity measurements with prediction of a model, the experimental procedure of measurement and type of the instrument must be considered. Rotational viscometers are mainly recommended for slag viscosity measurement due to their accuracy and wide range of application [12].

Crystallization and solid generation is a critical phenomenon affecting the viscosity of slag. Kondrative et al. [56] used Roscoe equation to consider the effect of solid particle suspensions and crystallization on the viscosity of partially crystallized slag systems.

$$\mu_s = \mu_L(1 - V_s)^{-2.5} \qquad (2-12)$$

Table 2:1: Major viscosity models for slag [55]

Theoretical basis	Model	Advantages	Limitations	Authors
Arrhenius $\eta_L = Aexp(B/T)$	S^2	Simple to use	Limited composition range, underestimate viscosity	Reid-Cohen
	Watt-feredy	Simple to use	Limited composition range, overestimate viscosity	Watt-feredy
	Shaw	Relatively simple to use	No physical justification Limited composition range, underestimate viscosity	Shaw
Frenkel-Weymann $\eta_L = ATexp(10^3\, B/T)$	Urbain and modified urbain	Larger compositional range	Harder to use, high discrepancies between predictions and experimental results	Urbain, Boiret Kondratiev, Jak
	Kalmanovitch-Frank	Larger compositional range	Harder to use, high discrepancies between predictions and experimental results	KalmanovitchFrank
	Riboud	Larger compositional range, easy to use	Inaccurate viscosity predictions over some compositional range	Riboud
	Structural model	Larger compositional range	Hard to use, requires thermodynamic package, underestimate viscosities	Zhang Jhanshahi
Eyring	UQ "quasi chemical"	Larger compositional range	Hard to use, excessively big amount of fitting parameters, requires thermodynamic package, underestimate viscosities	Kondratiev, Jak
Empirical correlation	CSIRO/CCSD	Simple to use	Very limited compositional range, poor predictions over boundaries	Hurst Browning Patterson

In equation 2-12, μ_s is the viscosity of slurry and V_s is the volume fraction of solids. This model works for both homogeneous and heterogeneous mixtures. The limit for application of heterogeneous models is 30% of solid fraction [56]. Semi-empirical model presented by Urbain is the basis of this model. Investigation of different combinations of fluxing agents of CaO and FeO by this model showed that the higher amount of FeO in

the mixture of CaO and FeO is more efficient in reducing the slag viscosity. This model also showed that with increasing SiO_2/Al_2O_3 ratio, the required amount of fluxing agents increases and at higher temperatures the required flux is lower [56].

2.12. Thermodynamic packages to study inorganic matter behavior

FACTSage is a thermodynamic software package which is able to calculate the inorganic multiphase equilibrium, liquid formation temperatures and the relative ratio of the liquid and solid phases under specified atmosphere based on the chemical composition. Lingxue et al. [17] used FACTsage in their study to predict the changes in the liquid formation temperature by adding different amount of CaO and also to calculate the liquid composition of slag at different T_{cv} (which can be obtained using tangent of viscosity-temperature curve). In addition, FactSage might have valuable application in calculating the phase fractions and compositions for the purpose of viscosity prediction [12]. Kondrative et al. [56] used FactSage to predict the fraction of solid and the composition of liquid in order to prepare a model to predict the slag viscosity as a function of the composition and temperature.

FactSage makes it practical to have access to Fact database (including slag, salt, ceramic and aqueous), alloy databases and ChemSage data files. User can import streams and mixtures from any desired sources and also is able to export them to other programs. FactSage is also able to handle simultaneously carbon reactions in combination with the minerals transformation under various atmospheres (gas composition) and this feature is one of the main advantages of this software [21].

Like any other characterization technique, using software package appropriate care must be taken in interpretation of the results and comparing them with experimental data. The liquid formation temperatures calculated by FACTsage are always higher than AFT results (about 150°C) because ash will not be fully melted during AFT test [17].

2.13. Thermal radiation and heat transfer properties of deposit

During the operation of a gasifier, slag layer receives heat by three mechanisms: radiation and convection heat transfer from hot species in the gas phase and energy brought through enthalpy of the deposited hot particles. Radiation is the dominant mechanism by transferring about 60% of the heat to the slag layer [57]. The equation of heat flow through a layer of deposit can be written as below [14]:

$$q_r = \epsilon_r \sigma (T_e^4 - T_s^4) = \frac{k}{ls}(T_s - T_c) \qquad (2-13)$$

Where ϵ_r= emittance of ash surface at temperature T_s

T_e= temperature of radiation source

T_c= temperature of cold face of the deposit layer

k= thermal conductivity

ls= thickness of deposit layer

σ= Stefan-Boltzmann constant

Absorptivity, emissivity and reflectivity are thermal properties essential in the heat transfer which are related as shown below [14]:

$$\epsilon_\Lambda = \alpha_\Lambda = 1 - \rho_\Lambda \qquad (2-14)$$

Where ϵ_Λ, α_Λ and ρ_Λ are the emissivity, absorptivity and reflectivity respectively which all depend on the radiation wave length. Because emittance measurement of the ash and deposits is usually easier to perform it is much more studied and analyzed than other parameters. Emissivity of the coal ash depends on the physical and chemical characteristics of the surface [6,14]. In this regard, Boow and Goard (1969) did investigations on the emittance of glass powders and artificial ashes of various sizes at 775K and proposed two expressions as below [14]:

$$\epsilon_r = 0.25 \log d + 0.13 \qquad (2-15)$$

$$\epsilon_r = 0.3 \log d + 0.16 \qquad (2-16)$$

In above equations ϵ_r is the emittance and d is the particle diameter in μm. The first equation can be applied for colorless glass powders and the second equation can be used for silicacious ash deposit (before sintering). They reported that these equations have acceptable accuracy when working with the particles in the size range of 7 to 420μm. Mulcahy (1966) reported that the emittance of ash particles decreases with increasing temperature. He also observed that emittance of slag is higher than sintered deposit and emittance of sintered deposit is higher than particulate ash and related this observation to the change of the reflective surface and variation of the existing state of species. The transformation from ferric to ferrous state of iron at high temperatures affects emittance of deposition [14]. Different levels of Fe_2O_3 and CaO in slag under different oxidizing and reducing environment result in the great changes in emittance of deposit [6,14].

Another important thermal property in heat transfer of deposit is thermal conductivity which determines the rate of the heat transfer from slag layer to the wall and affects the temperature and consequently the thickness of the slag layer. After sintering of ash there

is a noticeable increase in the thermal conductivity. Pore size of the deposit affects the conductivity. At low temperatures thermal conductivity decreases with increasing pore size [14]. Clements (1966) analyzed heat transfer of sintered deposit and reported a linear relationship between the thermal conductivity and bulk density. Boow and Goard (1969) proposed two equations for thermal conductivity based on the experimental analysis with acceptable accuracy for ash particles in the size range of 20-300μm at 975 K [14]:

$$\log k = (0.48 \log d) - 1.75 \qquad (2-17)$$

$$\log k = (0.56 \log d) - 1.63 \qquad (2-18)$$

The first equation is applicable for the colorless glass particles and the second equation is applicable for the iron-containing ash. In these equations, k is the thermal conductivity ($Wm^{-1}K^{-1}$) and d is the particle diameter (μm). Wall et al. (1979) mentioned that using thermal properties data of the ash obtained from laboratory prepared samples to estimate the actual heat transfer might result in the great errors. For example the emittance of the deposit collected from boiler tube is much higher than that of the artificial sample. Boow and Goard (1969) reported an order of magnitude difference between the thermal conductivity of the laboratory artificial inorganic samples and conductivity of the combustor deposits [14].

2.14. Inorganic matter depositions in coal utilization processes

2.14.1. Particle stickiness and sintering

Ash deposition process happens on the base of stickiness of the particles in which, many parameters and properties are involved. Boni et al. [58] assumed viscosity as the main affecting parameter and suggested that at viscosities bigger than 10^7 Pa.s particles are not

sticky. Stickiness may also be related to the condensed inorganic fumes and salts on the ash particles [52]. Composition and type of association of inorganic matters have great effects on their deposition behavior. Excluded inorganic particles can melt readily especially in reducing conditions of gasifier. Therefore, they might be deposited upon contacting with the wall in early stages of the process, but, char particles are not probable to stick due to low carbon conversion during early stages. Iron containing species and pyrite which have low melting point under reducing atmosphere mostly have excluded nature. Included minerals are only possible to stick when they are released from the coal matrix which happens gradually by carbon consumption as the char participates in the heterogeneous gasification reactions. The melting point of the included minerals is relatively high as most of SiO_2 and Al_2O_3 are distributed as included minerals and this makes the sticking process of included inorganic matters even harder. Char particles which are normally porous and therefore are less probable to stick (unless in contact with an extremely sticky slag layer) transform to sticky particles only at temperatures above the ash fusion temperature and at very high carbon conversion. Therefore, parameters such as residence time and mixing pattern which influence the carbon conversion consequently affect the stickiness of the particles [36, 43, 59-61].

By increasing the temperature of the particles, deformation happens (starting by partial surface fusion) and sintering gradually occurs by spreading a viscous liquid on each particle followed by pulling effect of the surface tension force. Initial bonding layer in the sintering deposit is usually composed of low-melting point eutectic especially sulfide compounds such as FeS, CaS and Na_2S. In this regard it has been reported that molten residue of pyrite can initiate sintering (by forming liquid bridge between particles) even

under inert condition [14]. Watt (1968) reported that alkali vapor transport has a crucial role in the sintering process. Alkalis condensation on the surface of ash particles or dissolution of alkalis in silicate (which reduces the viscosity strongly) promotes the sintering phenomenon. Based on the above discussions, viscosity and surface tension are two vital properties in sintering phenomenon. Increasing temperature reduces both viscosity and surface tension [14, 21].

2.14.2. The role of minor inorganic impurities in deposit formation

The role of minor species in deposit formation has been much less considered and investigated and phosphorous is one of the few exceptions in this regard. Crossley (1952) observed deposit material with phosphorus content of 20 percent in economizer resulted from a coal containing 0.4 percent of phosphorous. Crossley suggested that this big enrichment is mostly possible through volatilization/condensation mechanism similar to alkali salts. Phosphorus exist in coal as apatite, $CaF_2.3Ca(PO_3)_2$ and during heating will be volatilized as below [14]:

$$CaF_2.3Ca(PO_3)_2 + 10C \rightarrow CaF_2^{\uparrow} + 2P_2^{\uparrow} + 10CO^{\uparrow} + Ca_3(PO_4)_2 \qquad (2-19)$$

Huffman (1948) reported that about 67% of phosphorus in the apatite mineral can be vaporized. In presence of enough oxygen, the vaporized metal readily oxidizes [14]:

$$P_2 + 2\frac{1}{2}O_2 \rightarrow P_2O_5 \qquad (2-20)$$

Phosphorous oxide in combination with ash results in the formation of strongly adhered deposit which is very hard to remove from the surfaces. Other trace elements such as arsenic and lead are rarely observed with high concentration in the inorganic deposits,

but, there is a lack of experimental evidences regarding their effect on the deposit formation [14].

2.14.3. Char to slag transition

The structure of a char particle during carbon consumption by gasification reactions changes slightly and the density and porosity remain rather constant until high carbon conversion (up to 85%). This fact signifies that as the carbon conversion increases gradually, the char particle tends to maintain its initial porous structure and the size of char decreases by shrinkage mechanism. When most of the combustible content of char consumed (conversions about 89% or higher which mainly happens in later stages of gasification) and the char particle mostly consists of included minerals the transformation to slag might happen. Maloney et al. [62] observed gradual increase in the particle density as the particle size decreases by shrinkage while organic content being consumed by gasifying agents. They related this density increase to the size decrease of the particle and densification of the internal microporous structure [62,63].

Shrinkage and fragmentation are two mechanisms which explain the decrease in the size of char particles while being gasified. In shrinkage mechanism, char particle maintains its integrity during size reduction, but, in fragmentation a single char loses its integrity and breaks into many smaller particles. Shrinkage is believed to be important at initial stages of the process and fragmentation is governing at later stages [61, 63]. As mentioned before, knowing the size of particles is of great importance in modeling the process. Li et al. [61] used the equation below to relate the carbon conversion to char diameter.

$$d_P = d_0 \left[\left(1 - C_{coal}^{carbon} X\right) \frac{\rho_o}{\rho_P} \right]^{\frac{1}{3}} \qquad (2-21)$$

In this equation C_{coal}^{carbon} is the initial carbon content of the raw coal, d_0 and ρ_o are the diameter and density of the raw coal particle, respectively, and d_P and ρ_P are the diameter and density of char particles at carbon conversion of X, respectively. The experimental measured sizes have acceptable agreement with calculated values of this equation up to about 85% conversion. This proves that shrinkage is the dominant mechanism up to 85% conversion and after that fragmentation happens.

Particle size reduction and loss of microporous structure followed by melting of inorganic matters inside the char result in transformation from porous char (non-sticky particle) to molten slag (sticky particle). This phenomenon happens at the moment that ash fraction in the char reaches a threshold value (critical carbon conversion) at which surface area of the char decreases by about 91% or higher. The critical carbon conversion is higher for the coals with lower ash content or in another word transformation from char to slag happens later by consuming more organic content [63].

Only the mineral matters associated with the organic matrix inside the char particle (included dispersed inorganic inclusions) can participate in the phenomenon of char–slag transition. It must be noticed that, shrinkage and fragmentation are not the only mechanisms affecting the particle size change. If high concentrations of the low melting point compounds exist, many inorganic particles can coalesces to form big agglomerations rather than producing many small ash particles [63, 64].

2.14.4. Parameters affecting ash deposition and slagging

Most of the studies for ash deposition are performed based on the combustion process. In particle adhesion process, surface forces are of great importance such as Van der Waals

force which is accountable when submicron size particle is very close to the surface. Irregularities of the surfaces especially for oxidized metal can essentially promote the adhesion phenomenon. Physical properties such as viscosity and surface tension (both for particles and molten slag layer) affect the ash deposition. Work of adhesion (W_a) can be calculated by $\pi + \gamma(1 + cos\beta)$ and work of cohesion (W_c) can be calculated by 2γ in which, γ is the surface tension and β is the contact angle. For a system with contact angle of zero, the work of adhesion is maximum (bigger than W_c) and it is called perfect wetting [14]. Presence of the alkali metals especially in sulfates form improves the wetting characteristic of the liquid phase of ash to easily spread on the surface. If sulfates come in contact with carbon under reducing environment, they transform to sulfides which have better wetting characteristics. Analysis performed by Raask (1966) showed that the surface tension of the coal ash was about 0.32 Nm^{-1} which is approximately two times higher than that of sulfates [14]. Investigations and correlations to evaluate and predict the mineral surface tension is not well performed in comparison with viscosity. One of the few correlations for the inorganic surface tension is proposed by Hoy [65] introduced by the expression as below:

$$\gamma(1400°C) = 3.24SiO2 + 5.8Al2O3 + 4.4Fe2O3 + 4.92CaO + 5.49MgO + 1.12Na2O - 0.75K2O \qquad (2-22)$$

By performing experiments on three different coal types, Naruse et al. [37] reported that the deposition phenomenon is related to the particle size distribution and composition, degree of the inorganic association with coal matrix and the hydrodynamic and flow pattern of the gas phase. It is also accepted that the operating conditions and the properties and conditions of the target surface have essential effects on the deposition. Naruse et al. [37] observed that the ash with lower melting temperature had higher

deposition tendency and reported that the initial deposition fraction appears to be more related to the included minerals rather than the melting temperature. Li et al. [61] reported that the deposition can start only after significant changes in the density, size and surface area of the char particles which happens after critical carbon conversion.

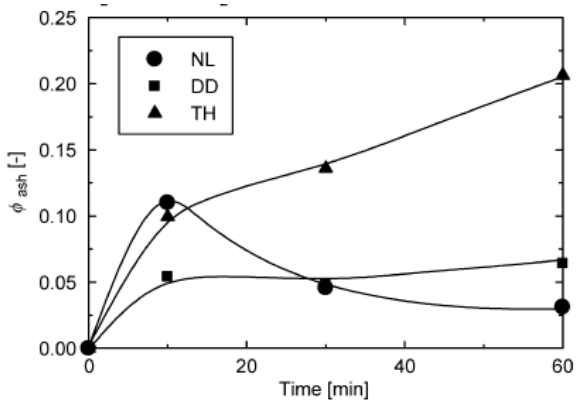

Figure 2.6: **Time dependence of deposition fraction for three coal types by Naruse et al. [37]**

Slagging indices traditionally and widely have been used in evaluation of slag formation and modeling. Various characteristics of the inorganic matters can be used for developing indices for ash deposition and slagging behavior. Iron oxide content, Fe_2O_3/CaO ratio, silica ratio, silica to alumina ratio, basic to acid oxides ratio and slag viscosity are the main factors used as criterion for the ash deposition by many researchers. Numerous indices have been proposed by many researchers, but, a reliable index must take into account the affecting parameters in inorganic deposition as many as possible. Utilizing ash fusion tests, Gray and Moore (1974) introduced a slagging index as a function of the initial deformation temperature (IT) and the hemisphere temperature (HT) [14]:

$$F_s = \frac{4IT + HT}{5} \qquad (2-23)$$

It was one of the first slagging indices considering only the physical properties of the inorganic matters. As discussed in previous sections, AFT is based on the visual subjective observations and not on the precise scientific measurements which has a large margin of error and within that margin viscosity might change by more than an order of magnitude. Considering only the ash fusion characteristics and ignoring other parameters leads to unreasonable results. For example, sticky slag layer on the boiler tubes approximately can capture 85% of the particles which collide with the wall due to the centrifugal force, whereas, by ignoring the effect of the transfer mechanism of particles the results of deposition modeling will be much lower than the real values [14]. Therefore, particle transfer mechanism is another essential parameter in the inorganic deposition which must be considered in a reliable index. Inertial effect dominates motion of the big particles whereas diffusion governs transfer of the small particles. Hedley et al. (1965) reported that vapor phase diffusion transport mechanism is more effective than particle diffusion in growth of the deposition. Thermal diffusion and thermophoresic are effective only for very small particles in the range of 0.5-5μm, especially at the locations with high temperature difference between the wall and gas [14].

In many studies the deposition tendency has been evaluated in terms of the different kinds of efficiency. Capture efficiency (CE) can be calculated by dividing the captured particle mass to the mass of the total injected particles. Energy-based growth rate (GRE) is the ratio of the deposited material to the low heat value of the fuel or consumed mass of the fuel and gives information about the deposition growth rate per unit of the energy production [66]. Hutchings et al. [67] developed a microstructure-based slagging index considering the quantified amount of CaO and Fe_2O_3. Rushdi et al. [68] proposed

slagging factor based on the TMA analysis considering the amount of the ram penetration and viscosity. Barroso et al. [66] modified the traditional expressions of slagging indices by considering aerodynamic diameter (related to the inertial impaction as the main particle transport mechanism) and inorganic matter loading based on the CCSEM analysis. However, the aerodynamic diameter of the ash particles, alone is not enough for predicting the inorganic deposition rate and the chemical composition must be taken into account. Scott [69] compared some proposed indices and reported that in case of the high calcium fuels, CCSEM-based index over-estimates the deposition tendency in comparison with base to acid ratio and concluded that the range of reliability of each index must be taken into consideration before application.

2.15. Modeling of mineral matter behavior

2.15.1. Char-slag interaction and particle capture criterion

Appropriate prediction of the fate of burning particles, especially in the regions close to the wall of furnace, has vital importance for the proper modeling, design and scale up of the gasifier. Char and mineral particles have various interactions with the slag layer on the wall which affect the particles fate and slag layer characteristics. Many researchers have studied various aspects of the particle-slag interactions. To have a reliable model of particle-slag interaction, all the important parameters such as dominant forces acting on particle (inertial, viscous and interfacial forces), particle and wall surface properties and operating conditions must be taken into account [39]. Montagnaro et al. [39] analyzed the effect of various transport mechanisms on the coverage of slag layer by refractory carbon particles. They developed a criterion for the ash particle deposition based on the

viscosities of the colliding particle and of the target slag layer and the probability of the collisions between un-fused particles. Li and Whitty [70] reported that char particles transform to sticky slag only at the temperatures higher than ash flow temperature and at carbon conversion higher than 90%. Different existence states of the particles (char or excluded inorganic) on the surface of slag layer depend on the particle kinetic energy, interfacial tension, viscosity and buoyancy [39].

In order to be captured by the slag layer, particles must first contact and then be wet by the molten slag film. The wetting characteristic of carbon on the slag layer is expected to be poor. Reactions between gas phase species such as CO with reducible material inside the deposit layer might affect the interfacial tension (if this phenomenon lowers the interfacial tension it is called reactive wetting). The wetting behavior of the slag depends on the composition mainly iron oxide content in the slag and operating conditions mainly temperature. In addition, wettability of char depends mostly on the ratio of the inorganic content to carbon [71]. Presence of iron in slag might cause formation of iron carbide at the surface which reduces the contact angle. Observations of Raask (1966) by heating microscope showed that alumina has a wetting surface but coke does not. In addition, the wetting behavior of slag is influenced by the atmosphere [14].

To evaluate the particle-slag interaction, it is crucial to have a reliable knowledge about the sizes and porosity of the particles interacting with molten slag layer. Particle size distribution can be obtained using optical microscope and image processing software and the internal surface area can be measured by gas adsorption [61].

The injection type of the fuel is another parameter affecting the particle-slag layer interaction. Tangential injection of the feed results in swirl flow and leads to higher

turbulence and better mixing and consequently the residence time and carbon conversion will be promoted [48]. Particle transfer mechanism affects the deposition behavior strongly. Inertial impaction is the most important mechanism for the particle behavior which is related to the size, velocity and density of the particles [72]. But, many particles carried by the inertial impaction escape from a non-captive and dry surface. A captive surface is a critical requirement for the rapid deposition. For very fine particles such as flame volatilized species (mainly sulfates) vapor diffusion is the dominant transfer mechanism. For particles in the size range of 0.1 to 5 μm, thermophoresic and electrophoresic mechanisms are applicable. For submicron size particles such as fume particles with size of lower than 0.1μm, Brownian motion is the governing transfer mechanism [14].

To analyze the fate of particle upon collision with a surface, it is beneficial to consider all the involved forces. At the moment of impaction, particle loses a part of its kinetic energy (due to the viscous resistance of the liquid on the surface or in the particle) [14,71]. Firstly, the particle must overcome the liquid surface tension to penetrate into it, but, after penetration (liquid surface rapture) the interfacial tension between particle and liquid might hold the particle. The surface tension force acting on a partially penetrated particle with radius of r and depth of s into a liquid with the surface tension of γ is given by [14]:

$$F = 2\pi(2sr)^{1/2}\gamma \qquad (2-24)$$

When this force is greater than other forces which might pull the particle back, particle can be held by slag. If the opponent force is gravitational force, the depth of penetration of a particle can be calculated by equality of equation 2-24 and gravitational force as given by the expression below [14]:

$$s = \frac{2r^5 \rho_p^2 g^2}{9\gamma^2} \qquad (2-25)$$

Montagnaro et al. [39] reported that only in the case that the colliding particles get embedded completely into the liquid slag; they can be assumed as permanently captured. For this case to happen, the inertia of the particle must be higher than the viscous and interfacial forces. This statement is equated as below [39]:

$$\frac{1}{2}\frac{\rho_{char}\pi d^3}{6}u^2 > 3\pi\mu u d^2 + \gamma\pi d^2 \qquad (2-26)$$

In above equation u is the particle velocity, d is the particle diameter, γ is the slag surface tension and μ is the slag viscosity. Assuming $3\mu u \gg \gamma$, they proposed the engulf criterion for particle by [39]:

$$du > \frac{36\mu}{\rho_{char}} \qquad (2-27)$$

Based on the common operating conditions during gasification process in the entrained-flow gasifiers and the typical properties of the liquid slag layer, Montagnaro et al. [39] concluded that the char particle engulfing is not probable to happen, unless for very big particles (>200 μm) colliding with very low viscosity layer (<1 kg m^{-1} s^{-1}). But, they did not mention about the role of the carbon conversion of char in their criterion which is a weak point of their study. Overlayering is another state of particle fate upon interaction with the slag layer. Extreme coverage of the slag with un-fused char particles (with considerable carbon fraction) prohibits additional char migration to the slag surface and lowers the deposition [39]. This state mostly depends on the rate of the char particle loading on the slag surface, liquid slag properties, removal of the trapped particles from impacted area (by convective mechanism) and the rate of reactions of the captured particles [39]. Based on the general properties of the inorganic matters, Montagnaro et al.

[39] concluded that overlayering is not that much possible to happen under typical conditions of gasifiers. They proposed three regimes for the char-slag interaction. Entrapped carbon regime (regime (E)) in that complete encapsulating of the particles happens and therefore, the combustible part of char cannot participate in the gasification reactions. Segregated carbon regime (regime (S)) in which the char particles will be captured by slag and remains on the surface and therefore, the combustible material of char might continue to be consumed by heterogeneous reactions. The third regime is segregated carbon regime with extensive carbon coverage (SC) in that incoming char particle covers almost the whole surface of the slag layer and therefore, newly incoming char particle cannot be captured. These regimes are shown in Figure 2.7.

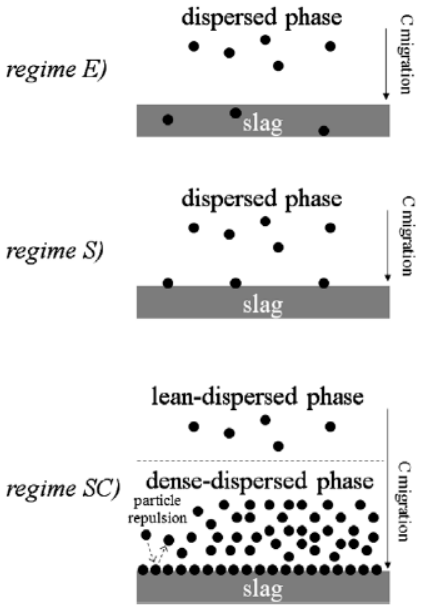

Figure 2.7: **Regimes of C-slag micromechanical interaction [39]**

Montagnaro et al. [39] assumed the slag layer as the only requirement for the sticking phenomenon. Therefore, viscosity and surface tension is only considered for slag layer.

But, carbon conversion and the extent of exposure of included minerals in the char particle must be considered to enhance the accuracy of this model.

Shimizu [59] proposed a simple model for char capture in which the char particles will be trapped if colliding with the slag covered surface and will be rebounded if hitting the dry wall or char covered sections. Therefore, the char flux rate per unit of the surface and the char consumption reaction rate are two essential parameters which determine the fate of the particles. The sticking chance of the char particle to the slag (molten layer) affects the concentration of the char particles in the gas phase, concentration of the char particles on slag and consequently, carbon content on the slag surface. They reported that the char capture rate essentially affects the temperature distribution in the furnace, because, consumption process of the carbon content of the trapped char through gasification reactions with H_2O and CO_2 (as endothermic reactions) and combustion reaction with O_2 (as exothermic reaction) can consume and release heat on the surface of the slag layer [59].

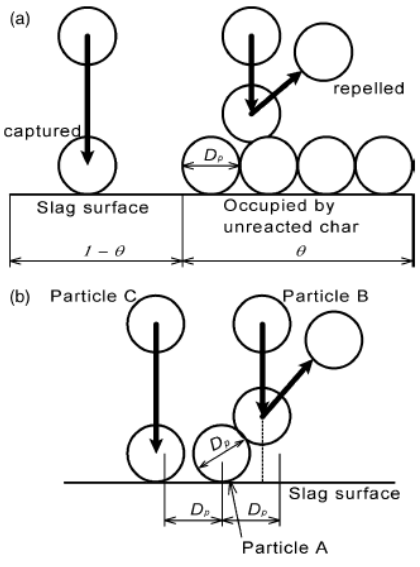

Figure 2.8: **(a) Concept of the model proposed by Shimizu [59] (side view); (b) Detail of the occupation of slag surface by one char particle (side view) [59].**

They hypothesized that due to the significant density difference between char and slag, char particle can only float on the slag surface. They introduced the probability of the char capture, PC, as a function of the char flux rate per unit area of the surface (F_c), particle density (ρ), particle diameter (d_p) and the rate constant of the char consumption (r) as follows [59]:

$$PC = \frac{1}{\frac{6F_c}{\rho d_p r} + 1} \qquad (2-28)$$

Based on this model, increasing the particle size and density increases the probability of the char particles to reach the slag surface which leads to the increase in the probability of the char particle capture by slag layer [59]. The first part is reasonable and accepted, because, bigger and heavier particles move by the inertial effect and can reach to the slag surface easier, but, the second part probably might not be correct for all the conditions. When heavy and big particles are not sticky the probability of rebounding is higher. Therefore, this kind of estimation of char capture by the slag surface can be applicable only if the char reactivity is very high and temperature is above T_{cv}. In this study the equations of modeling are not well explained. The logical explanation of the assumptions and calculation of the rate of increase in the covered surface fraction with un-reacted particles are not well explained. One of the deficiencies of this study is that the method for differentiation between the reacted and un-reacted char is not mentioned.

Shannon et al. [71] reported that it is the balance of the forces acting on the particles which determines the fate of the particles. These forces depend on the slag and particle properties, operating conditions of gasifier such as temperature and particle impact velocity. They presented a model based on the balance of three forces acting on the

particles: “drag force (F_d), capillary force ($F_{\sigma,Z}$), and fluid-added mass force (F_a)”, as schematically presented in Figure 2.9. In term of the drag force, they used the friction factor in the slag, cross section area of the contacted part of the particle, density, viscosity and velocity of the particle. In term of the fluid-added mass force, they considered the volume and also acceleration of the particles. In term of capillary force, they considered the surface tensions of the particle and slag. They concluded that two cases can be distinguished by using this model. Entrapment happens when the particle is fully encapsulated by slag and settling which happens when the particle is floated and stagnated on the surface of slag. This model could also predict the oscillation state which was observed only for few cases and rare conditions which was not that much probable to happen in real cases [71].

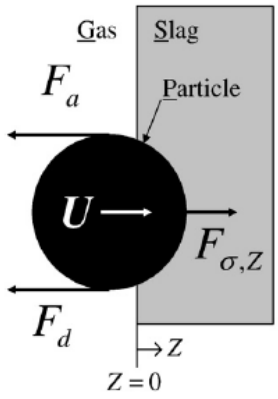

Figure 2.9: **Schematics of forces acting on a particle impacting a slag layer at a given velocity (U). [71]**

They introduced interfacial tension (contact angle) and slag viscosity as the most important parameters in the particle capture phenomenon. Viscosity as a sensitive function of temperature and composition (especially sensitive to CaO and FeO), significantly influences the drag force. Coverage of the surface of a particle or wall with carbon affects the contact angle and results in non-wetting behavior [71].

Mueller et al. [73] considered the kinetic energy and total surface energy to propose a model based on the mass and energy balances. They evaluated kinetic and surface energy in terms of the Reynolds number and Weber number and reached to an equation that calculates the ratio of the colliding particle diameter to the maximum particle diameter at the moment of impact as below [73]:

$$\zeta = \left((12 + We) / \left(3(1 - \cos\beta) + 4\left({We}/{Re^{0.5}} \right) \right) \right)^{0.5} \qquad (2-29)$$

They introduced excess energy, E, as the rebound criterion of this deposition model and evaluated the effects of velocity and impact angle by performing analysis at constant temperature and reported that if the excess energy of a particle is positive, then the particle will bounce off, otherwise it will be captured [73].

$$E = 0.25(d_{max}/d)^2(1 - \cos\beta) - 0.12(d_{max}/d)^{2.3}(1 - \cos\beta)^{0.63} + 2/3\,(d/d_{max}) - 1 \qquad (2-30)$$

Wall et al. [15] introduced the inertial mechanism as the most important mechanism of deposition for entrapment of the large sticky particles which are bigger than 15μm. As a mechanism for deposit initiation, it is assumed that sticky particles will be captured if the interfacial energy between the particle and wet surface is higher than the kinetic energy of impacting particle. As the second mechanism, they introduced the diffusion of the volatilized particles formed by vaporization of the included inorganic matters transported by thermophoresis. The third mechanism is condensation of alkalis, especially alkali sulfate which produce a sticky layer upon condensation and can capture fly ash particles. They reported that condensable submicron particles, fine silicates and large sticky particles usually form initial deposit layer [15].

Yong et al. [72] introduced a sub-model for the particle adhesion based on the slag and particle properties (as function of the temperature and composition) and considered the momentum transfer between the captured particles and surface. They also considered the possibility of the slag re-solidification. They reported that, high inertia particles mostly bounce off the surface while low inertial particles are captured and sometimes embodied in the slag layer. They assumed when both the particle and slag are in the liquid phase, the particle is always trapped regardless of the kinetic and surface tension energy. When there is solid–solid interaction, all the particles will be bounced off again regardless of the different energy comparisons. For other cases, the kinetic energy and interfacial energy must be compared. By applying Weber number, they made the comparison of the kinetic and interfacial tension energy of particle-slag at the moment of impact much easier and practical. Based on this model, a particle can be captured if the calculated Weber number is lower than a critical value. They assumed this critical value to be 1 [72]. Table 2.2 presents the criterion proposed by Yong et al. for particle capture.

Table 2:2: **Particle capture criteria proposed by Yong et al. [72]**

	Sticky particle		Non-sticky particle	
	$We < We_{cr}$	$We > We_{cr}$	$We < We_{cr}$	$We > We_{cr}$
Sticky wall	Slagging		Slagging	Reflect
Non-sticky wall	Fouling	Reflect	Reflect	

They reported that at higher values of the critical Weber number, the deposition will be higher [72]. The main problem of this model is related to the first assumption. The big melted particle in contact with the liquid slag might not stick due to the large force required for its retention. Another deficiency is ignoring the carbon conversion which is one of the most important parameters in the ash deposition.

Ni et al. [74] developed a sub-model based on the maximum spread diameter and excess rebound energy to evaluate the inorganic deposition. At the moment of collision, a fully melted particle starts to deform by spreading, and therefore its diameter increases. After the diameter of droplet reached to the maximum value, the droplet motion direction changes, but, it can continue to deform again back to its initial shape and move to reverse direction if its possessed energy after stretching is adequate. By comparing the surface energy, kinetic energy, and potential energy of the particle before collision and at the moment of impaction, the ratio of the particle diameter to its maximum diameter upon collision can be calculated. The energy balance is written as below [74]:

$$E_{s1} + E_{k1} = E_{s2} + E_{k2} + \Delta E_k + W \qquad (2-31)$$

In above equation ΔE_k is the loss of kinetic energy and W is the work of the particle deforming against viscosity. Based on above equation, they reached to the final formula for d_{max}/d_0 as below [74]:

$$\xi_{max} = \frac{d_{max}}{d_0} = \sqrt{\frac{1+We}{\frac{3\bar{s}}{8D_0}We + 3(1-\cos\beta) + \frac{4We}{\sqrt{Re}}}} \qquad (2-32)$$

Then they used this ratio in another equation for the excess energy to predict the fate of the particle at the moment of collision. Higher deposition at higher temperature can be explained by increasing the surface tension. Particles with bigger size and higher surface tension have higher maximum spread diameter [74]. Increasing maximum spread diameter reduces the excess rebound energy and consequently increases the deposition probability [74]. The parameters in the equations of this model are defined improperly and it is hard to investigate the validity of these calculations. They reported that the small particles have lower excess rebound energy, but, they also mentioned that for the large

molten slag particles, the deposition probability is higher due to the higher maximum spread ratio. These statements cannot be compatible findings.

2.15.2. Slag formation modeling

In order to develop a comprehensive model to have reliable predictions of the ash deposition and slag formation, it is necessary to combine the main stages of the inorganic matter variations and interactions (with other particles or with the wall surface) during the gasification processes into one model framework. Slag layer modeling started with very simple models decades ago (with assumptions like such as plug flow and constant rate of the captured ash) and reached to more reliable and accurate states in many recent models (for example by utilizing Eulerian–Lagrangian framework) [73].

Seggiani [75] developed a simple model to simulate the time varying phenomena of the slag formation on the wall of coal gasifier. 1D slag model of Seggiani was combined with a three-dimensional model of gasification which calculates the temperature and syngas composition profile inside the gasifier. Seggiani used T_{cv} as the solid-liquid phase transition, ignored the shear stress between the gas and slag, assumed linear temperature profile across the slag layer and assumed constant physical properties for deposition. Seggiani evaluated the effect of the operating conditions of gasifier on the slag behavior. He made some changes in operating conditions and calculated the response time of the model. He found out that, slag related variables have much slower response (about 2 h) compared with the gas phase variables (about 15 min). Although this model as an innovative and pioneer work in slag modeling has become the basis of many future studies, but, it had some serious defections. Seggiani did not consider the phenomena of the particle interaction and adhesion to the slag layer. The difference in the inorganic

compositions which affects the properties of the slag layer and may lead to the different behavior of slag is not considered. Assuming the fixed inlet mass from ash content to the slag layer is the main deficiency of this model.

Sheng et al. [76] developed a 2-D axisymmetric model for slag flow considering solidification phenomenon. They considered slag to be Newtonian fluid at the temperature above the T_{cv}, used VOF model to simulate the free surface between slag and gas phase and solved mass, energy and motion equations and finally calculated the temperature distribution and the thickness of the slag layer. They assumed that, in each control volume the summation of the liquid slag volume fraction and syngas volume fraction is 1 and ignored the volume of the solid slag in each control volume. They reported that, RNG k-ε model resulted in more accurate predictions than standard k-ε model. They used discrete transfer radiation model (DTRM) assuming single ray leaves the surface element in a specific range of solid angles [76]. The properties of slag are considered to be constant. The size and composition differences of the inorganic particles inside the gasifier is not considered and mass deposit of slag is assumed to be constant which is a weak point of this model.

Mueller et al. [73] developed a CFD-based ash deposition model. They considered various phenomena such as particle fusion, impaction and sticking or rebounding and gradual deposit layer growth. They assumed that fly ash particles smaller than 75 μm containing molten phase higher than 15% are sticky and will be trapped upon collision [73]. But, they did not mention how they measured the molten fraction of a particle. They reported that inertial impaction showed a significant contribution (>99%) for the transport of particles on the surface of the probe [73].

Costen et al. [34] developed a three-dimensional CFD model of the ash deposition in pulverized coal combustion. They applied Navier–Stokes equations and standard k-ε model in Eulerian framework for gas phase and Lagrangian framework for particles. Considering the effects of inorganic compositions and type of the mineral association within coal matrix, increased the accuracy of this model. They reported that, the alkali species are the main reason for the deposition in the convective heat transfer section because of the condensation of these species on cold surfaces. Therefore, they considered the evaporation of alkalis from the included and excluded minerals applying single Arrhenius type reaction [34]. They assumed that excluded mineral matters to be in equilibrium with the gas phase and included minerals to be in equilibrium with the char particle. Viscosity is the main parameter used to make the decision about the fraction of the captured particles by the surface. In order to have a criterion for arrival of the fly ash particles to the wall surface, they defined a critical velocity, which is the minimum velocity that a particle must have to pass an especial distance in a stagnant and viscose environment. They used Kalmanovitch model for calculating viscosity of the ash and assumed that all the inorganic particles are transformed to the fly ash as soon as entering the furnace. They reported that without application of the effect of thermophoresis, particles smaller than 10 μm did not deposit that much and followed the gas flow due to their lower momentum. But, applying thermophoresic caused an increase in the deposition of small particles [34]. Lack of a precise particle capture is the main weakness of this model.

CFD modeling usually leads to high computational expenses and especially for dynamic modes of the complicated process (in which many complex phenomena are involved) is

not recommended. For modeling in dynamic mode, space division approach is the best option, because, it is a compromise approach between one-dimensional models and CFD models which provides acceptable accuracy and prevents high computational costs [10,76]. Yang et al. [10] used a Reactor Network Model (RNM) based on space-division concept to model ash deposition and slag formation in gasifier in dynamic mode. Considering the flow pattern and gas flow hydrodynamic, they divided the furnace into several zones and performed the calculations in each zone based on either a plug-flow reactor or a continues well-stirred-tank reactor and by this concept, covered all the domain of the furnace except the slag layer on the wall. The concept of their model is shown in Figure 2.10 and Figure 2.11.

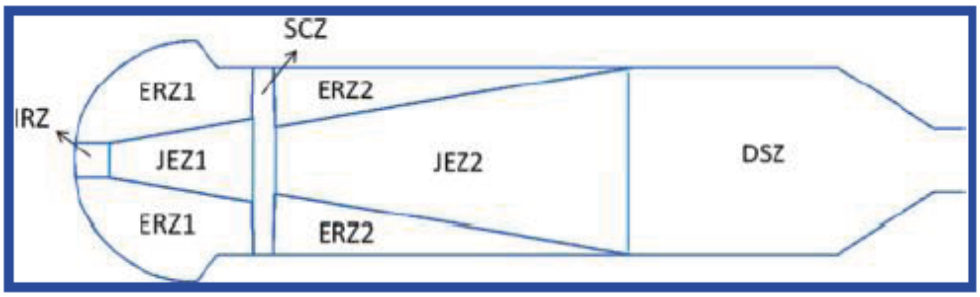

Figure 2.10: **Schematic diagram of space division in the oxygen-staged gasifier done by Yang et al. [10].**

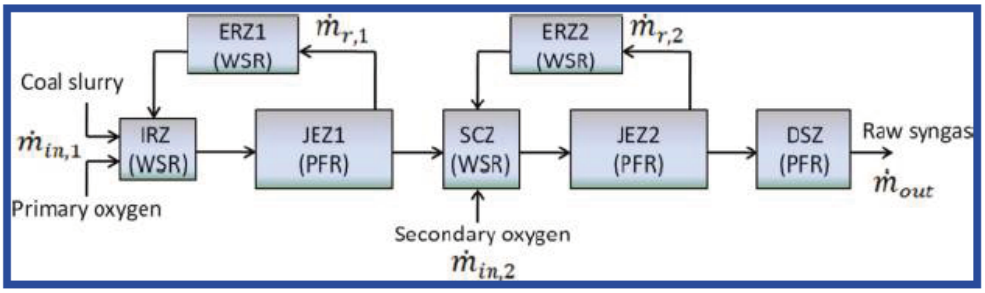

Figure 2.11: **RNM model for the oxygen-staged gasifier done by Yang et al. [10].**

Yang et al. [10] assumed constant pressure in the reactor, uniform size of the particles and ignored the diffusion transport mechanism (due to much higher effect of convection). They considered convection heat transfer terms for gas-to-particle and gas-to-wall and radiation heat transfer terms for particle-to-particle and particle-to-wall. But, they ignored the radiation for gas to wall and particles in the heat transfer sub-model. They assumed that for particles in the zones which are in contact with the wall, all the ash content will be transferred to the slag layer and the combustible part bounces off which is not a reliable assumption. This model predicts the temperature distribution in the near wall regions more accurate than one-dimensional models [10]. They reported that increasing the temperature reduces the thickness of the solid layer in membrane wall. They also evaluated the different effects of the operating conditions on slag layer in membrane and refractory wall gasifiers and reported that, refractory wall dynamic response to any operating change is much slower than membrane wall due to its higher storage capacity [10]. This model is not accurate enough in evaluating and monitoring flow turbulence, gas/solid reactions and particle-wall interaction which is a defection in comparison with the CFD models. In this study there is no mechanism for the mineral particles interaction with the slag layer or capture criterion. This model does not consider the effect of the particle size and composition on the deposition.

Li et al. [77] developed a 2D-axisymmetric model for simulation the slag flow in super heater tube section of a boiler and used Seggiani's model for the flow calculation. In the related CFD model they used DPM for particle trajectory tracking and assumed that all the colliding particles will be captured (which is not an acceptable assumption in the real

conditions of a gasifier). This model showed that at higher slag surface temperatures, the temperature of the slag and gas are closer [77].

Ni et al. [53] applied a combination of the continuum surface force (CSF), VOF and discrete-ordinate method (DOM) model to have more accurate predictions for gas/liquid surface tension, free surface of the liquid layer and radiation, respectively. They assumed that, above the T_{cv} slag behaves as Newtonian fluid, between T_{cv} and T_f behaves like plastic fluid and below T_f slag is solid. They assumed all the properties to be constant and ignored any possible reactions between the inorganic species in the slag layer. Based on the results of their case studies, they reported that, the slag throat is the critical part of the slagging entrained-flow gasifier. They also reported that, the assumption of the linear temperature profile across the liquid slag layer is not reliable. This model can predict the variation of the solid and liquid slag thickness as function of the operating parameters. Lack of a reliable particle capture criterion to calculate the rate of the particle adhesion (actual deposition value) more accurately is a weakness of this modeling. They did not mention the type of the feeding system, size of the inorganic particles and the association type.

Yong et al. [78] proposed a steady-state model for slag layer formation coupled with a CFD model of coal combustion, considering the momentum transfer between captured particles and wall and slag re-solidification probability. After being trapped by the liquid layer, the combustible part of the particle can undergo further reactions. Temperature across slag layer is assumed to be cubic and T_{cv} is phase transition temperature. The results showed that about 56% of the particles fed to the furnace can be captured. The ash particle capture criterion in this model is based on the probabilistic sub-model used by

Tominaga et al. [79]. This criterion uses ash viscosity as the key parameter for slagging. Based on the ash deposition model of Tominaga et al. the particles will deposit on the slag layer if either the ash and slag viscosities are below a critical value at the moment of impaction. Yong et al. [78] improved the particle capture sub-model by taking into consideration the stickiness of the wall of gasifier and particles. However, they improved the particle capture criterion, but, they did not consider the direction of the particle impaction in the sub-model which is one of the main affecting parameters in the particle entrapment. The wall consumption sub-model is used to calculate the reaction after particle adhesion. This sub-model calculates the sinking level of the trapped particles and by this method the real available surface of the particles which can participate in the reactions will be used in modeling [78]. They used the equation below for surface calculation and the related parameters are presented in Figure 2.12.

$$A_{eff} = 2\pi R_P \left(R_P + \sqrt{R_P^2 - a^2} \right) \qquad (2-33)$$

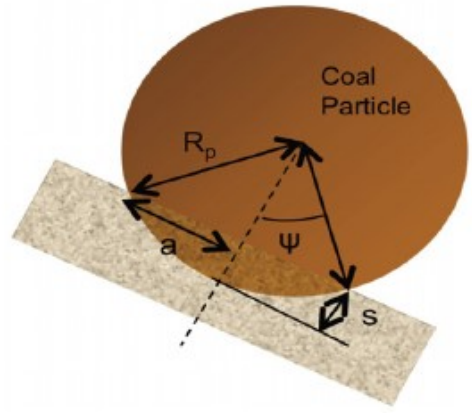

Figure 2.12: **Illustration of sink position, covered angle and contact radius proposed by Yong et al.[78].**

They assumed that, the reactions take place only at the outer surface area and ignored the porosity of the coal and internal surfaces reactions, however, it is generally accepted that

the gasification reactions primarily happen on the internal surface. This CFD model provides particle feeding rate per unit area of the target surface, particle temperature and particle velocity for slag model and these values are not presumed constant numbers which makes this model one of the most comprehensive proposed models. The results of this model showed that particles with high Weber number, low carbon conversion and high momentum mostly will be reflected. The trend of the results is reasonable but, comparison the results with experimental data is required to evaluate the accuracy.

Sun et al. [80] proposed a dynamic model of a gasifier used in IGCC considering the time-dependent deposition and slag flow. Dynamic models is of great importance as it can predict the effect of any kind of changes on the deposition and slag flow which are extremely useful for controlling the process. They assumed linear temperature profile across slag layers. The slag sub-model is one dimension which only depends on the axial direction. All the properties assumed to be constant. The dynamic behavior of the slag layer is assumed to be effected just by the thermal effect and the effects associated to the different compositions of slag are ignored. The worst part of the assumptions is constant flow rate of the liquid slag. Having this assumption, the effect of the particle capture efficiency and various slag compositions at different locations is ignored resulting in a slag layer which has the same composition of the original minerals which do not reflect the real conditions in the gasifier. They reported that, by 20% increase in the steam/coal ratio, liquid slag transforms into solid slag due to the decrease in the slag surface temperature. A step change of +1% in the oxygen/coal ratio results in the higher gas temperature and consequently more liquid slag will be formed by melting solid slag.

They observed that dynamic response of all the operational variables are more sensitive to oxygen/coal ratio rather than to steam/coal ratio.

Du et al. [81] proposed a mathematical model of the inorganic deposition in entrained flow gasifier. They considered the gas phase to be continuum and k-ε is used for the turbulence calculation. Coal particles trajectory is modeled based on Lagrangian framework. They used the Discrete Transfer Radiation Model (DTRM) as the dominant heat transfer mechanism in the gasifier. They assumed entrapment of all the colliding particles which is not an accurate and realistic assumption. This model predicts high amount of deposition in the first stage because the amount of pulverized coal injected in this stage was larger than the second stage and based on that they concluded that the ash deposition on the wall is a function of the particle concentration. The model could be more realistic by applying a more accurate and comprehensive capture criterion to evaluate the effect of the operational parameter on ash deposition. They did not present analytical calculations to evaluate if the walls of the first and second stages could practically receive and deposit that much particles or not.

Li et al. [16] developed a mathematical model of a slag layer inside a slagging entrained-flow gasifier based on the traditional mass and heat-transfer equations and considered the possibility of the presence of various layers of slag on the wall. Lin et al. [82] developed a mathematical model to predict quantitatively the thermal stress of slag layer caused by the temperature variation. They only considered the solid slag layer and reported that cracking in the slag layer is mainly related to the thermal stress. Based on this model, it is concluded that the porosity of the slag strongly affects the thermal and mechanical properties. Lower porosity leads to the higher thermal conductivity. Based on this model,

they reported that larger slag layer during cooling process are more probable to crack. They suggested the thickness of the slag layer must be adjusted to an optimized value by adjusting the operating conditions.

One of the best models presented for the ash deposition and slag flow is performed by Chen et al. [83]. This model includes a 2D slag model coupled with a 3D CFD model of the furnace for the gasification process. They applied char–slag interaction and wall burning sub-models. In the particle capture of this model, temperature of particle and wall, carbon conversion of the char particles and energy comparison were all considered to determine the fate of each particle at the moment of impaction. They reported that, T_{cv} has a great effect on the thickness of the slag layer on the wall, especially, in the formation of solid slag layer. To enhance the accuracy of this model, Chen et al. [84] proposed a three-dimensional slag model in dynamic mode including two multiphase flow models and considered well-characterized sub-models for the particle-wall interactions and particle behavior after sticking. Their work includes one of the most advanced and comprehensive models proposed for the ash deposition and slag formation so far.

References

[1] International energy Agency, http:// www.iea.org

[2] Higman C, Vander Burgt M, Gasification, Elsevier Sciences, 2003

[3] Vejahati F, Entrained-flow gasification of oil sand coke, PhD thesis, Department of Chemical and Materials Engineering, University of Alberta, Spring 2012

[4] Stiegel G J, Ramezan M, Hydrogen from coal gasification: An economical pathway to a sustainable energy future, International Journal of Coal Geology 65 (2006) 173– 190

[5] Crnomarkovic N, Repic B, Mladenovic R, Neskovic O, Veljkovic M, Experimental investigation of role of steam in entrained flow coal gasification, Fuel 86 (2007) 194–202

[6] Elliot M A, Chemistry of coal utilization, Secondary supplementary volume, NAS-NRC committee on chemistry of coal, 1981 by Wiley & Sons, Inc.

[7] Li S, Char–slag transition during pulverized coal gasification, PhD Thesis, Chemical Engineering Department, university of Utah, 2010

[8] Kinaef N, A review of mineral matter issue in coal gasification, CCSD (Cooperative research centrefor coal in sustainable development) research report 60, 2006, Australia

[9] Walsh P M, Sarofim A F, Beer J M, Fouling of Convection Heat Exchangers by Lignitic Coal Ash, Energy and Fuels 6:709-715 (1992).

[10] Yang Z, Wang Z, Wu Y, Wang J, Lu J, Li Z, Ni W, Dynamic model for an oxygen-staged slagging entrained-flow gasifier, Energy Fuels 2011, 25, 3646-3656

[11] Song W, Tang L, Flow properties and rheology of slag from coal gasification, engineering research center of large scale reactor engineering and technology, East China University of science and technology, 2010

[12] Duchesne M A, Macchi A, Lu D Y, Hughes R, Artificial neural network model to predict slag viscosity over a broad range of temperatures and slag compositions, Fuel Processing Technology 91 (2010) 831–836

[13] Song W, Tang L, Zhu X, Wu Y, Rong Y, Fusibility and flow properties of coal ash and slag, Fuel 88 (2009) 297–304

[14] Raask E, Mineral impurities in coal combustion, Behavior, Problems and Remedial Measures, Hemisphere Publishing Corporation, New York, 1985.

[15] Wall T F, Mineral matter transformation and ash deposition in pulverized coal combustion, The combustion coal institude, 1992/pp. 1119-1126

[16] Li X, Li G, Cao Z, Xu Sh, Research on Flow Characteristics of Slag Film in a Slag Tapping Gasifier, Energy fuels 2010, 24, 5109-5115

[17] Lingxue K, Jin B, Wen L, Zong-qing B, Zhen-xing G, Effect of lime addition on slag fluidity of coal ash, Journal of Fuel Chemistry and Technology, 2011, 39(6), 407-411

[18] Wei Y, Li H, Honma K, Tanoskai T, Ninomiya Y, Effect of additives on slag properties in an entrained bed gasifier, World of Coal Ash (WOCA) Conference, 2011, Denver, USA

[19] Lu T, Zhang L, Zhang Y, Feng Y, Li H X, Effect of mineral comosition on coal fusion temperature. Journal of Fuel Chemistry and Technology, 2010, 38(2): 23–28.

[20] Yu L J, Huang Z Y, Cheng J, Pan H Y, Zhou J H, Cen K F, Study on the coal ash fusibility during blending coal combustion. Journal of Fuel Chemistry and Technology, 2009, 37(2): 139–144.

[21] Van Dyk J C, Waanders F B, Benson S A, Laumb M L, Hack K, Viscosity predictions of the slag composition of gasified coal, utilizing FactSage equilibrium modeling, Fuel 88 (2009) 67–74

[22] Gupta S, Dubikova M, French D, Sahajwalla V, Effect of CO2 gasification on the transformations of coke minerals at high temperatures, Energy & Fuels 21 (2) (2007) 1052

[23] Skodras G, Sakellaropoulos G P, Mineral matter effects in lignite gasification, fuel process technology 77-78 (2002) 151-158

[24] Bai J, Li W, Li C, Bai Z, Li B, Influence of mineral matter on high temperature gasification of coal char, Journal of Fuel Chemistry and Technology, 2009, 37(2), 134-138

[25] Liu H, Luo C, Toyota M, Kato S, Uemiya S, Kojima T, Tominaga H, Mineral reaction and morphology change during gasification of coal in CO_2 at elevated temperatures, Fuel 82 (2003) 523-530

[26] Matjie R H, French D, Ward C R, Pistorius P C, Li Z, Behavior of coal mineral matter in sintering and slagging of ash during gasification process, Fuel Process Technol. (2011), doi:10.1016/j.fuproc.2011.03.002
[27] Couch G, Understanding of slagging and fouling in PF combustion. IEA Coal Res 1994.
[28] Matsuoka K, Suzuki Y, Eylands K E, Benson S A, Tomita A, CCSEM study of ash forming reactions during lignite gasification, Fuel 85 (2006) 2371–2376
[29] Gupta S K, Wall T F, Creelman R A, Gupta R P, Ash fusion temperatures and the transformations of coal ash particles to slag, Fuel Processing Technology 56 _1998. 33–43
[30] Lin S, Hirato M, Horio M, The characteristics of coal char gasification at around ash melting temperature, Energy & Fuels 8 (1994) 598–606
[31] Montagnaro F, Salatino P, The role of slag formation on late carbon conversion in entrained-flow gasification of coal, Dipartimento di Chimica, UniversitaStudi di Napoli Federico II, Napoli, Italy, 2009
[32] Noda R, Naruse I, Ohtake K, Fundamentals on combustion and gasification behavior of coal particle trapped on molten slag layer. J Chem Eng Jpn 1996;29:235–41.
[33] Zhao X, Zeng C, Mao Y, Li W, Peng Y, Wang T, Eiteneer B, Zamansky V, Fletcher T, The surface characteristics and reactivity of residual carbon in coal gasification slag, Energy Fuels, 2010, 24, 91-94
[34] Costen P G, Locwood F C, Siddique M M, mathematical modeling of ash deposition in pulverized fuel-fired combustors, Proceedings of the Combustion Institute, Volume 28, 2000/pp. 2243–2250
[35] Ghosal S, Ebert J L, Self S A, Chemical composition and size distributions for fly ashes, Fuel Processing Technology 44 (1995) 8 l-94
[36] Brachi P, Montagnaro F, Salatino P, Char-Wall Interaction and Properties of Slag Waste in Entrained-Flow Gasification of Coal, European Combustion Meeting 2011
[37] Naruse I, Kamihashira D, Miyauchi Y, Kato Y, Yamashita T, Tominaga H, Fundamental ash deposition characteristics in pulverized coal reaction under high temperature conditions, Fuel 84 (2005) 405–410

[38] Seggiani M, Bardi A, Vitolo S, Prediction of fly-ash size distribution: a correlation between the char transition radius and coal properties, Fuel 79 (2000) 999–1002

[39] Montagnaro F, Salatino P, Analysis of char–slag interaction and near-wall particle segregation in entrained-flow gasification of coal, Combustion and Flame 157 (2010) 874–883

[40] Wilemski G, Srinivasachar S, Sarofim A F, Modeling of mineral matter redistribution and ash formation in pulverized coal combustion. In: Benson SA, editor. Inorganic transformations and ash Deposition during combustion, New York: Engineering Foundation Press, ASME, 1992.

[41] Barta L E, Toqan M A, Beer J M, Sarofim A F, Prediction of fly-ash size and chemical composition distributions: the random coalescence model. 24th Symp.(Int) on Combustion, The Combustion Institute, 1992. p. 1135–44.

[42] Wall T F, Liu G S, Wu H W, Roberts D G, Benfell K E, Gupta S, Lucas J A, Harris D J, The effects of pressure on coal reactions during pulverised coal combustion and gasification, Progress in Energy and Combustion Science 28 (2002) 405–433.

[43] Yu G, Zhu Q, Chi G, Guo Q, Zhou Z, Study on slag composition and flow property in a bench-scale OMB gasifier, Fuel Processing Technology 2012

[44] Ellis G C, The thermomechanical, electrical conductance and chemical characteristics of coal ash deposits, NERDDP Project No. 1181, Final Report, Vol. 3, SECV R&D Department, Australia, 1989.

[45] Raask E, Sintering characteristics of coal ashes by simultaneous dilatometry–electrical conductance measurements, J. Thermal Anal. 16 _1979. 91.

[46] Bryant G W, Lucas J A, Gupta S K, Wall T F, Use of Thermomechanical Analysis To Quantify the Flux Additions Necessary for Slag Flow in Slagging Gasifiers Fired with Coal, Energy & Fuels 1998, 12, 257-261

[47] Hilliard J E, Quantitative microscopy, in: R.T. DeHoff, F.N. Rhines _Eds., McGraw-Hill, USA, 1968, pp. 45–76.

[48] Ambrosino F, Aprovitola A, Brachi P, Marra F S, Montagnaro F, Salatino P, Char-slag interaction in entrained flow gasifier: modeling of experimental evidences, XXXIV Meeting of the Italian Section of the Combustion Institute

[49] Zhang L, Sato A, Ninomiya Y, CCSEM analysis of ash from combustion of coal added with limestone, Fuel 81 (2002) 1499-1508

[50] Miller S F, Schobert H H, Effect of the Occurrence and Composition of Silicate and Aluminosilicate Compounds on Ash Formation in Pilot-Scale Combustion of Pulverized Coal and Coal-Water Slurry Fuels, Energy Fuels 1994;8:1197–207.

[51] Miller S F, Schobert H H, Effect of the Occurrence and Modes of Incorporation of Alkalis, Alkaline Earth Elements, and Sulfur on Ash Formation in Pilot-Scale Combustion of Beulah Pulverized Coal and Coal-Water Slurry Fuel, Energy Fuels 1994;8:1208–16.

[52] Gupta R, Wall T F, Kajigaya I, Miyamae S, Tsumita Y, Computer controlled scanning electron microscopy of minerals in coal- implications for ash deposition, Prog. Energy Combust.Sci, vol. 24.Pp 523-543, 1998

[53] Ni J, Zhou Z, Yu G, Liang Q, Wang F, Molten slag flow and phase transformation behaviors in a slagging entrained-flow gasifier, Ind. Eng. Chem. Res. 2010, 49, 12302-12310

[54] Hurst H J, Novak F, Patterson J H, Viscosity measurements and empirical predictions for some model gasifier slag, Fuel 78 (1999) 439-444

[55] Patterson J, Hurst H, Quintanar A, Boyd B, Tran H, Evaluation of the slag flow characterization of Australian coals in slagging gasifiers, CCSD (Cooperative research centre for coal in sustainable development) research report, 2001, Australia

[56] Kondrative A, Jak E, Predicting coal ash slag flow characteristics (viscosity model for the Al_2O_3-CaO-FeO-SiO_2 system), Fuel 80 (2011) 1989-2000

[57] Sheng L, Yingli H, Numerical study on slag flow in an entrained-flow gasifier, ASME international Mechanical Engineering Congress and Exposition, Seattle, USA, 2007

[58] Boni, Transformations of inorganic coal constituents in combustion system, DOE Report No. AC22-86PC 90751, 1990.

[59] Shimizu T, Tominaga H, A model of char capture by molten slag surface under high-temperature gasification conditions, Fuel 85 (2006) 170–178.

[60] Li S, Wu Y, Whitty K J, Ash deposition behavior during char-slag transition under simulated gasification condition, Energy & Fuels 24 (2010) 1868–1876.
[61] Li S, Whitty K J, Physical phenomena of char–slag transition in pulverized coal gasification, Fuel Processing Technology 95 (2012) 127–136
[62] Maloney D J, Monazam E R, Casleton K H, Shaddix C R, Evaluation of char combustion models: measurement and analysis of variability in char particle size and density, Proceedings of the Combustion Institute 30 (2005) 2197–2204.
[63] Hurt R H, Dudek D R, Longwell J P, Sarofim A F, The phenomenon of gasification-induced carbon densification and its influence on pore structure evolution, Carbon 26 (1988) 433–449.
[64] Wu H, Wall T, Liu G, Bryant G, Ash liberation from included minerals during combustion of pulverized coal: the relationship with char structure and burnout, Energy & Fuels 13 (1999) 1197–1202.
[65] Hoy H R, Robert A G, Wilkins D M, Behavior of mineral matter in slagging gasification process, J. Inst. Gas Eng., 1965, 5, 444-469
[66] Barroso J, Ballester J, Pina A, Study of coal ash deposition in an entrained flow reactor: Assessment of traditional and alternative slagging indices, Fuel Processing Technology 88 (2007) 865–876
[67] Hutchings I S, West S S, Williamson J, An assessment of coal-ash slagging propensity using an entrained-flow reactor, in: L. Baxter, R. DeSollar (Eds.), Applications of Advanced Technology to Ash-Related Problems in Boiler. Proceedings of the Engineering Foundation Conference. Waterville Valley, New Hampshire., July, 1621, 1995, pp. 201–222.
[68] Rushdi A, Sharma A, Gupta R, An experimental study of the effect of coal blending on ash deposition, Fuel 83 (2004) 495–506
[69] Scott D H, Ash Behavior during Combustion and Gasification, IEA Coal Research, London, 1999.
[70] Li S, Whitty K J, Investigation of Coal Char−Slag Transition during Oxidation: Effect of Temperature and Residual Carbon, Energy Fuels 23 (2009) 1998–2005

[71] Shannon G N, Rozelle P L, Pisupati S V, Sridhar S, Conditions for entrainment into a FeO_x containing slag for a carbon-containing particle in an entrained coal gasifier, Fuel Processing Technology 89 (2008) 1379–1385

[72] Yong S Z, Gazzino M, Ghoniem A, Modeling the slag layer in solid fuel gasification and combustion – Formulation and sensitivity analysis, Fuel 92 (2012) 162–170

[73] Mueller C, Selenius M, Theis M, Skrifvars B J, Backman R, Hupa M, Tran H, Deposition behavior of molten alkali-rich fly ashes—development of a sub-model for CFD applications, Proceedings of the Combustion Institute 30 (2005) 2991–2998

[74] Ni J, Yu G, Guo Q, Zhou Z, Wang F, Sub-model for Predicting Slag Deposition Formation in Slagging Gasification Systems, Energy Fuels 2011, 25, 1004–1009

[75] Seggiani M, Modeling and simulation of time varying slag flow in a Prenflo entrained-flow gasifier, Fuel 77 (1998) 1611-1621

[76] Sheng L, Yingli H, Numerical study on slag flow in an entrained-flow gasifier, ASME international Mechanical Engineering Congress and Exposition, Seattle, USA, 2007

[77] Li B, Brink A, Hupa M, CFD investigation of slagging on a super-heater tube in a kraft recovery boiler, Fuel Process. Technol. (2011), doi:10.1016/j.fuproc.2011.08.007

CFD applications, Proceedings of the Combustion Institute 30 (2005) 2991–2998

[78] Yong S Z, Ghoniem A, Modeling the slag layer in solid fuel gasification and combustion- Tow-way coupling with CFD, Fuel 97 (2012) 457-466

[79] Tominaga H, Tamashita T, Ando T, Asahiro N, Simulator development of entrained flow coal gasifiers at high temperature & high pressure atmosphere. IFRF Combust J 2000, Article No 200004

[80] Sun B, Liu Y, Chen X, Zhou Q, Su M, Dynamic modeling and simulation of shell gasifier in IGCC, Fuel Processing Technology 92 (2011) 1418-1425

[81] Du M, Hao Y, Numerical Simulation of Ash Deposition in Entrained-flow Gasifier, School of Energy and Environment Southeast University Nanjing, China, 2009 IEEE

[82] Lin W, Liang Q, Yu G, Liu H, Gong X, Numerical modeling for non-steady thermal stress analysis of slag layer in a membrane wall entrained-flow gasifier, Fuel 90 (2011) 2396–2403

[83] Chen L, Yong S Z, Ghoniem A F, Modeling the slag behavior in three dimensional CFD simulation of a vertically-oriented oxy-coal combustor, Fuel Processing Technology 112 (2013) 106–117
[84] Chen L, Ghoniem A F, Development of a three-dimensional computational slag flow model for coal combustion and gasification, Fuel 113 (2013) 357–366

Chapter 3. Inorganic matter behavior during coal gasification: Effect of operating conditions and particle trajectory on ash deposition and slag formation

3.1. Abstract

Ash particle deposition and uncontrolled slag flow which can lead to tap hole blockage is one of the main issues during coal gasification. In this work, a special collector probe was used to collect ash deposition and analyze slag formation and blockage probability in terms of the operating conditions and particle trajectories. Increasing the temperature led to increase in the total deposition. Although by increasing the temperature the weight of

the produced slag flow increased, but, it was observed that, increasing the temperature could not guarantee the safe operation by preventing from deposition blockage. Using two Canadian coal types proved that the ash composition of coal has a significant effect on the amount and thickness of the deposition on the wall. For fuel with low ash viscosity, increasing the temperature increased the slag flow and blockage never happened. But, for fuel with high bulk ash viscosity, by increasing the temperature, the blockage probability did not decrease. The reason might be related to the different effects of temperature on the particle stickiness and slag viscosity at specific range of temperature. CCSEM analysis showed that excluded iron bearing minerals of the first coal and included calcium bearing minerals of the second coal had substantial effects in the deposition tendency of these fuels. Increasing the velocity of the particles by gas flow rate mostly resulted in the reduction of the deposition. Fuel with larger particles at low temperature and high gas flow has the lowest deposition tendency. To evaluate the effect of the particle trajectory/aerodynamics, two different types of feeding configuration were used and the results showed that feeder type has significant effect on the deposition pattern and growth at different locations. One feeder by injecting the particles in a narrow area, led to the high inorganic accumulation near the feeding spot resulting in severe depositions with thickness of several centimeters. The other feeder resulted in more uniform deposition by producing wider sticky surface with lower deposition thickness on the wall of furnace.

Keywords: ash deposition, slag formation, CCSEM, BSE/EDX, particle trajectory, blockage

3.2. Introduction

Inorganic deposition during coal utilization processes such as combustion or gasification affects heat transfer inside the reactor and changes the performance, capacity and efficiency of the process [1-3]. Using entrained-flow coal gasifier it is desired to discharge the inorganic matters as liquid slag as much as possible to reduce the ash deposition problems in downstream equipment. But, uncontrolled and unsteady slag flow may cause blockage at the bottom of the reactor near the slag tapping hole and consequently lead to unscheduled emergency shut-down of the process which could be an economical disaster. Considering the growing interests and even after several decades of the commercial applications, the availability and reliability of the entrained-flow gasifiers are still the bottlenecks for its wide and safe utilization [4]. Therefore, it is crucially important to have a reliable evaluation of the inorganic matter behavior, ash deposition and slag flow inside the gasifier. Steady removal of the slag from tapping hole is of significant importance for the safe and proper operation of entrained-flow gasifier [5].

Mineral composition of the raw fuel, viscosity of the ash and slag, temperature of critical viscosity and ash fusion temperature (AFT) are the most common factors used for characterization the inorganic deposition and slagging behavior [6-11]. Numerous studies are focused on empirical indices such as alkali index, base to acid ratio and silica ratio to evaluate and characterize the slagging behavior of various fuels [12, 13]. Many researchers proposed correlations to predict the viscosity of ash mostly based on the temperature and composition [14, 15]. It is accepted that, the shape and structure of the deposits are related to the properties such as viscosity and surface tension and to the operating conditions such as temperature and atmosphere [16]. Therefore, the influence

of the inorganic compositions, additives and operating condition on viscosity, ash fusion temperature and temperature of critical viscosity as the main affecting factors on deposition tendency have been widely investigated [17-20]. In addition, the effect of the environment on the inorganic matters behavior has been the topic of a number of studies [21, 22].

The first step of slag formation in coal combustion or gasification is sticking of the ash particles to the wall of furnace. During gasification process, inorganic matters and char particles at various levels inside the furnace hit the wall with different properties; some of them stick and the rest rebound. Particle properties (temperature, composition, angle of impact and velocity) and impacted surface properties (surface roughness, temperature and composition of the existing deposit layer) are the main factors affecting the fate of the particles [23]. Particles capture by the wall determines the amount of the deposition and is of crucial importance especially for modeling purpose (sticking particles are the inlet mass of the slag layer). Traditionally this phenomenon is mostly related to the viscosity, ash fusion temperature and carbon conversion and is usually evaluated by empirical indices [24-26]. Most of the current models and correlations for ash deposition and slag formation are mainly based on the viscosity. Low viscosity of the inorganic particle at the moment of impact to the wall makes larger the loss of energy. Therefore, there is less energy for the low viscosity particles to rebound and consequently the probability of sticking to the surface is higher [1]. Mueller et al. [27] assumed the kinetic energy and total surface energy as the important factors and proposed a sticking model based on the mass and energy balances. Shannon et al. [28] concluded that the fate of the particles is related to the balance of forces acting on the particles and proposed a model based on the

balance of drag force, capillary force and a fluid-added mass force. Ni et al. [29] studied the slag droplet deposition in the slagging combustor and in order to define a criterion for particle rebound used maximum spread diameter and excess rebound energy. They considered viscosity, surface tension, particle impact angle, and impact velocity as the affecting parameter in their model. Montagnaro et al. [30, 31] studied the interactions between char and slag layer and coverage of the slag layer by the carbon containing char particles. They reported that, complete entrapment of the char particles into the slag layer only could occur if the colliding char particles encapsulated well within the slag layer which requires particle kinetic energy (inertia) to overcome viscous and interfacial energies. This condition is mostly possible for the high speed particles with large diameter and slag layer with low viscosity. In some studies Weber and Reynolds number are introduced as indicators of particle condition to be used as criterion for particle capture. We number is defined as the ratio of the particle kinetic energy to the surface tension energy and is calculated by equation below [32]:

$$We = \frac{\rho_P v_P^2 d_P}{\gamma} \qquad (3-1)$$

In this equation, ρ_p is the density of the particle, v_p is the velocity of the particle, dp is the diameter of the particle. Yong et al. [32] observed that the tendency of a particle to be captured by slag layer is higher at larger We_{cr}. They observed an inverse relation between the temperature of critical viscosity and the mass of deposition in slag layer. Shimizu and Tominaga [33] assumed that char particles will be rebounded if they hit the area covered by unreacted char particles and will be captured if they hit the molten slag surface. Luan et al. [1] investigated the deposition behavior of high viscosity ash and evaluated the

effects of impact velocity, deposition time and particle size using a probe inside a drop tube furnace. They concluded that high particle impact velocity and low temperature of surface of the probe reduce the ash deposition strongly.

Slag layer at each specific location on the wall of furnace may have different properties which are not the same as the properties of the bulk of ash. The reason is various char and inorganic (included and excluded) particles may stick to the different locations on the wall of furnace based on their properties (fusion temperature, viscosity, surface tension, type of association and carbon conversion) and operating conditions (particle velocity and injection pattern). This aspect has been investigated in some studies but still more works need to be done. Wall et al. [34] observed that, the inorganic deposition and slag layer flowing down the wall of furnace usually does not have the composition of the bulk ash of the fuel. Yu et al. [35] reported that bulk ash composition should not be used for all the areas covered with slag layer. They used a deposit collector installed parallel to the gasifier wall to take samples of the inorganic matter depositions and found that the deposition behavior of included and excluded minerals is different and slag viscosity at different locations varied based on the included and excluded mineral content. Costenet al. [36] reported that there is difference in the behavior and deposition tendency of the particles with different sizes and densities. Bigger particles with higher density mostly are captured by the molten slag layer far from the feeding spot or burner. The reason is related to the different transport mechanisms. Bigger particles with higher density are mostly affected by inertial forces while smaller particles are mostly carried with the gas flow [36].

Deposition rate of the various particles (char and ash) depends on the gas medium flow pattern and particle trajectories [37]. Ni et al. [38] reported that various gas flow field in different gasifiers, affect the particle flow behavior and their depositions. Li et al. [39] observed differences in the deposition behavior using different burner configuration. Barroso et al. [40] reported that complementing the indices with the parameters related to the amount and trajectories of the ash particles flowing inside the furnace is reasonable due to the strong dependence of the inorganic deposition to the flow pattern through the furnace and ash flux. Despite the highlighted importance of the effect of particle trajectory on the inorganic matter deposition, it is not widely studied and fully understood.

Although one of the most critical consequences of unpredicted inorganic behavior and uncontrolled slag flow in a coal gasifier is blockage at the tapping hole (which reduces the reliability and availability of the gasifier too much), but, this phenomenon is less investigated in the literature. Unlike viscosity and some other properties and indices which were the topic of several studies, blockage probability and particle trajectory are less investigated. In addition, there are only few studies about the ash particle interaction with the wall at different locations. In this work, a removable collector probe was used to take ash deposition at different locations inside the furnace during gasification process and the results of specific section were quantified. In addition, using two different feeders, the effect of the particles trajectory pattern on the ash deposition has been evaluated. The experimental results will be useful in validating the CFD modeling of ash deposition and slag formation in future studies.

3.3. Experiments

An electrically heated vertical drop tube furnace was used to perform coal gasification experiments. For temperatures up to 1500°C, Mullite tube was used and for higher temperatures alumina tube was used [46]. The dimension of the furnace is 63.5mm ID and 1530mm total height. The temperature of the furnace during gasification process was controlled by three PID controllers located at the top, middle and bottom sections of the furnace [46]. Based on the safety rules the maximum permitted operation temperature in this furnace is 1650°C. Nitrogen flow was used to carry the coal particles coming from a screw feeder (attached to a hopper) to entrain them inside the furnace. Vibrating walls of the hopper inhibited the bridging of fine particles to produce a uniform solid flow [46]. Nitrogen and air were preheated by passing around steam generator and an inline heater. The residence time of the particles inside the drop tube was adjusted by the total gas flow rate. Feeder was volumetrically calibrated for each fuel. Gasification products passed through an air cooled collection probe. After the collection probe a cyclone was used to collect large solid particles (including char, ash and slag droplets) from the flue gas. After cyclone a bag filter separates particles smaller than few macrons in size. Figure 3.1 shows the gasification setup [46].

The feeding probe consisted of two concentric tubes. The coal carrier tube was a quarter inch tube in which nitrogen carried the coal particles from feeding hopper into the furnace. This tube was located inside a half inch steel tube for carrying the gasifying agents. This simple feeding system (two open ended tubes) resulted in strong axial flow downward with very low mixing which led to the low carbon conversion. Due to the strong axial flow and low carbon conversion, the amount of the inorganic deposition in

the slag collector plates installed on the wall of furnace at different location was very low, especially, on the vertical section of the slag collector probe. The carbon conversion must be higher in order to be closer to the conditions of a real gasifier and get more deposition.

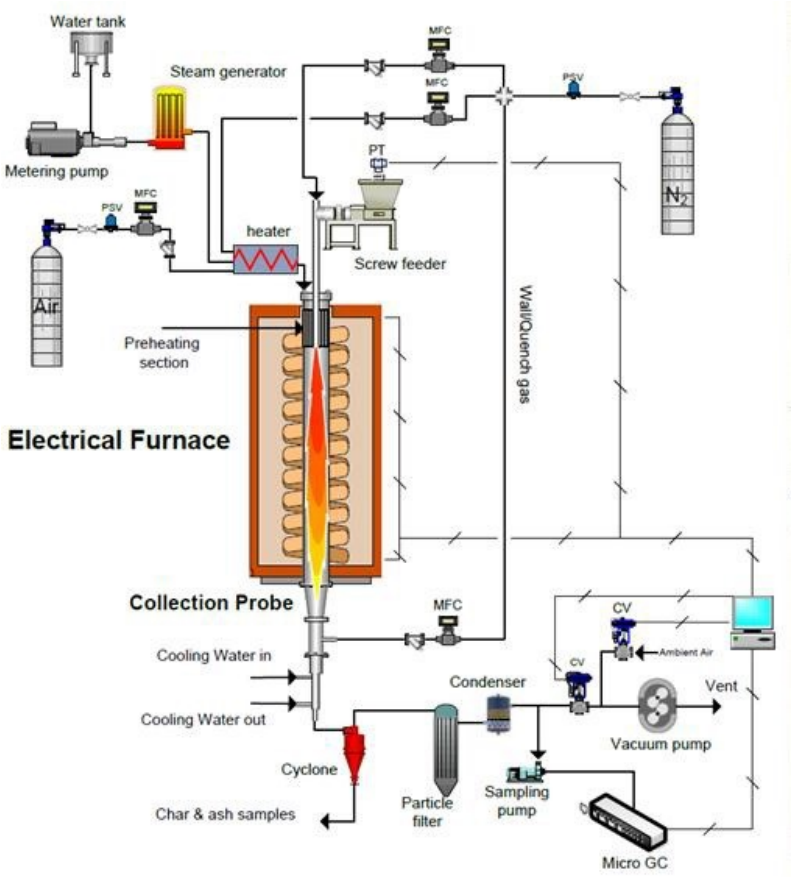

Figure 3.1: **Scheme of the gasification setup [46]**

Two designs for feeding configuration were tested to increase the turbulence and mixing and also to evaluate the different patterns of the particle trajectory. In the first feeder, the bigger tube which transported air was open-ended, and the tip of the fuel carrier tube was designed with four holes with diameter of 3mm. The results of this feeder are presented under the title of C4. In the second feeder, the coal carrier tube located inside the air tube

was open-ended and the tip of the air carrier tube was designed with eight holes at the edge with diameter of 2mm. The results of this feeder are presented under the title of A8. Figure 3.2 shows configuration of the feeders.

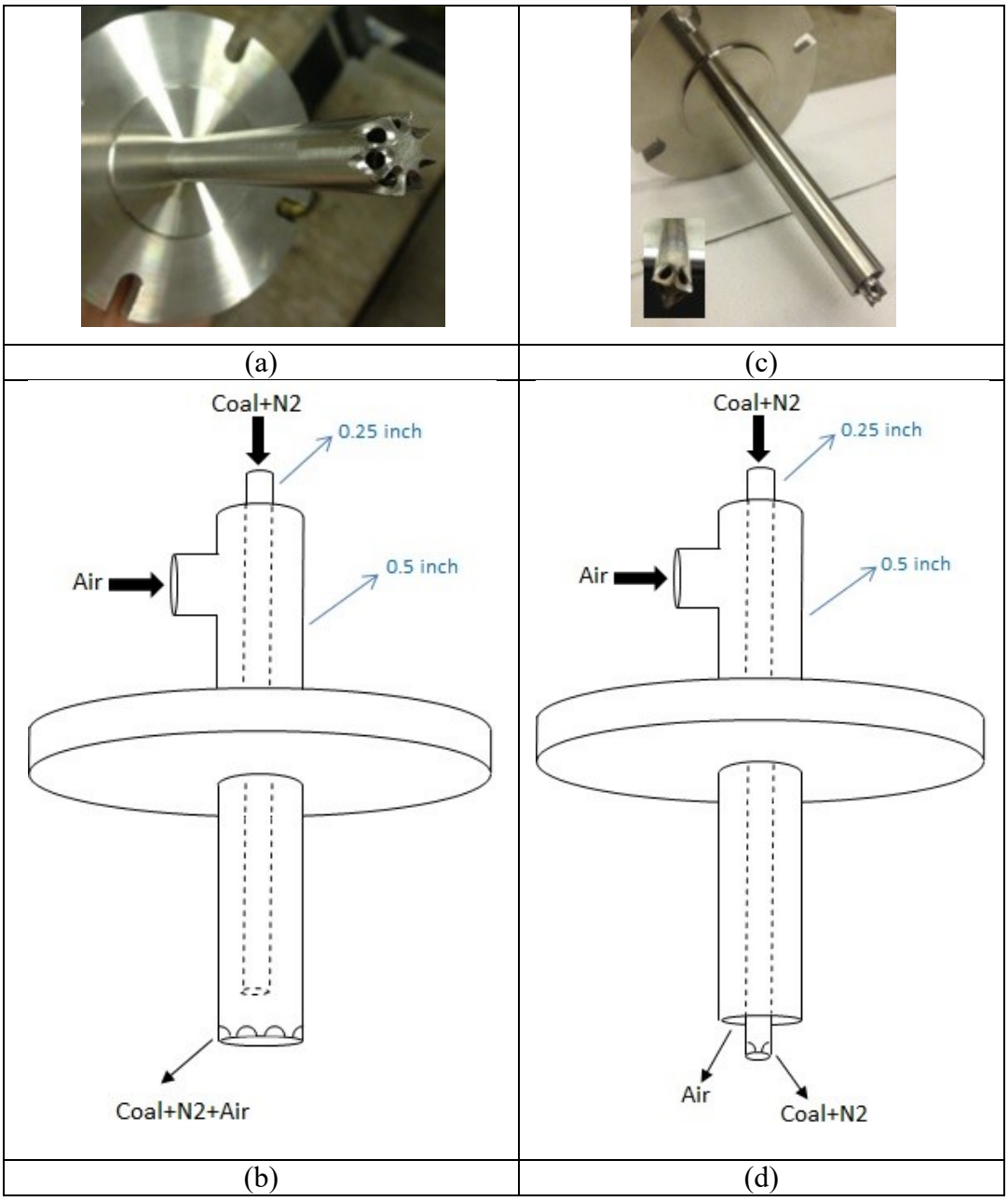

Figure 3.2: Feeder configurations (a,b) Feeder A8 (c.d) Feeder C4

Two types of Canadian coal (F1 and F2) were used in the experiments of this study. Two size ranges were used for each fuel. S1 contained fine particles with diameter in the range of 28- 53 microns and S2 included coarser particles in the range of 150-212µm. The proximate, ultimate and inorganic composition analysis of the coals is presented in Tables 3.1 to 3.3. The ultimate analysis is dry ash free basis and samples were prepared based on D3176 standard. For proximate analysis samples were dried based on D7582 standard.

Table 3:1: **Proximate analysis of the coal samples**

	F1-S1 Wt%	F1-S2Wt%	F2-S1 Wt%	F2-S2Wt%
Volatile matter	22.27	23.51	34.95	34.27
Fixed carbon	39.43	44.93	41.85	43.01
ash	29.27	21.22	12.39	10.50
moisture	9.03	10.34	10.81	12.22

Table 3:2: **Ultimate analysis of the coal samples (daf*)**

	F1-S1 Wt%	F1-S2Wt%	F2-S1 Wt%	F2-S2 Wt%
C	53.3	46.5	54.9	50.8
N	0.8	0.5	1	0.9
H	3.5	2.6	4.1	3.5
S	0.4	0.4	0.5	0.5
O	42	50	39.5	44.3
*daf: dry ash free				

Table 3:3: **Ash composition analysis (w%)**

	SiO_2	Al_2O_3	Fe_2O_3	CaO	Na_2O	MgO	K_2O	BaO	TiO_2	SO_3	P_2O_5
F1-S1	52.1	23.7	7.9	6.5	2.7	1.3	1.5	-	0.8	3.4	-
(STDEV)	(0.76)	(0.32)	(0.47)	(0.42)	(0.10)	(0.12)	(0.06)		(0.07)	(0.31)	
F1-S2	44.5	17.2	8.4	12.2	2.3	1.2	1.4	-	1.1	11.6	-
(STDEV)	(1.28)	(0.41)	(0.75)	(0.49)	(0.08)	(0.19)	(0.04)		(0.08)	(0.72)	
F2-S1	33.4	22.4	6.7	15.8	6.4	3.2	-	1.8	1.0	8.5	0.7
(STDEV)	(1.15)	(0.77)	(0.36)	(0.91)	(0.15)	(0.26)		(0.17)	(0.09)	(0.76)	(0.06)
F2-S2	26.5	16.9	8.1	22.6	5.1	3.9	-	1.5	0.9	13.8	0.6
(STDEV)	(0.74)	(0.39)	(0.52)	(0.51)	(0.17)	(0.18)		(0.16)	(0.05)	(0.49)	(0.06)
STDEV: Standard Deviation											

A special slag collector probe was installed inside the furnace to take inorganic deposition samples during coal gasification experiments, as shown in Figure 3.3. The probe was made of Kawool paper shaped by hardener solution to be strong enough to tolerate the high temperatures during gasification process. The hardening process of the probes was done by soaking them into the hardener solution and drying them several times (once a day during a week). The length of the probe is 20cm with the bottom hole diameter of 1cm. Samples were taken from the top, middle and bottom sections. For the top section, the probe was installed 10 cm inside the furnace from top. For the middle section the probe was installed exactly in the middle of the furnace and for the bottom section the plate was installed 10cm above the collection probe. Based on the information of inorganic content of each fuel, the operation was done until 60gr of the inorganic matters entered the furnace. To quantify the results, the weight of the slag collector plates were measured at the end of each experiment and the weight and percentage of the inorganic matter deposition were calculated. For plates installed at the top section of the furnace, the relative deposition was defined as the ratio of the mass of deposit inside the plate to the total mass of inorganic matters brought into the furnace by coal.

$$DP\% = \frac{mass\ of\ deposit\ inside\ collector\ plate}{total\ mass\ of\ inorganic\ entered\ by\ the\ fuel} \times 100 \qquad (3-2)$$

Collector plates for middle and bottom sections were only used to take samples for BSE, SEM and EDX analysis to study the morphology and composition, but, quantified deposit calculations were not possible to perform for these sections because of the uncertainty and inaccuracy of the results.

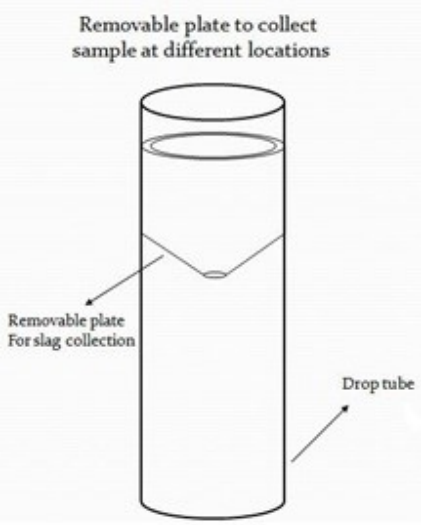

Figure 3.3: Slag collector plate inside the drop tube furnace

3.4. Results and discussion

3.4.1. Effect of Temperature

Temperature is one of the most important affecting parameters during gasification process. Temperature affects the process efficiency, product distribution, particles stickiness, slag layer flow (by affecting the viscosity) and consequently the amount of deposition. Increasing the temperature can result in higher deposition by increasing the stickiness of the particles, but, at the same time can lead to the decrease in the deposition thickness by reducing the slag layer viscosity. The results of the deposition on the collector plates installed at the top section are presented in Tables 3.4 and 3.5. The values for viscosity presented in these tables are experimentally measured by Duchesne et al. [41]. Based on the experimental viscosity measurement of F1, the temperature range of 1350°C-1650°C has been selected. Since for larger size of F1 (F1S2) the ash content is lower than smaller size (F1S1), the collector plate is in contact with corrosive inorganic

deposition for longer time. Therefore, the slag collector probe might be damaged by molten slag at 1650°C; hence the results for F1S2 at 1650°C could not be quantified. The ash content of F2 had lower fusion temperature and viscosity, therefore, the temperature range of 1250°C-1450°C has been selected for this fuel. Ash deposition and slag layer of this fuel at higher temperatures were extremely corrosive; therefore, quantified measurement for F2 at higher temperatures could not be performed. The images of the corroded probes for these fuels are shown in Figure 3.4. The reason for the corrosive behavior of F2 (which is much more corrosive than F1 at the same condition) is its lower viscosity. Low viscosity allows the liquid slag to spread fast and penetrate easily into the structure of the collector plate and react with its material and therefore lead to the high corrosion. Solid slag layer (which is immobile) not only is not corrosive but also is a protective layer for the membrane wall gasifiers. In addition, at low viscosities, the diffusion of various species inside the liquid slag will be promoted and increases the reaction rates between different species of the molten layer and the material of the wall which finally will be appeared as corrosion and material loss. This fact signifies the crucial role of the viscosity in corrosive characteristic of the liquid slag layer.

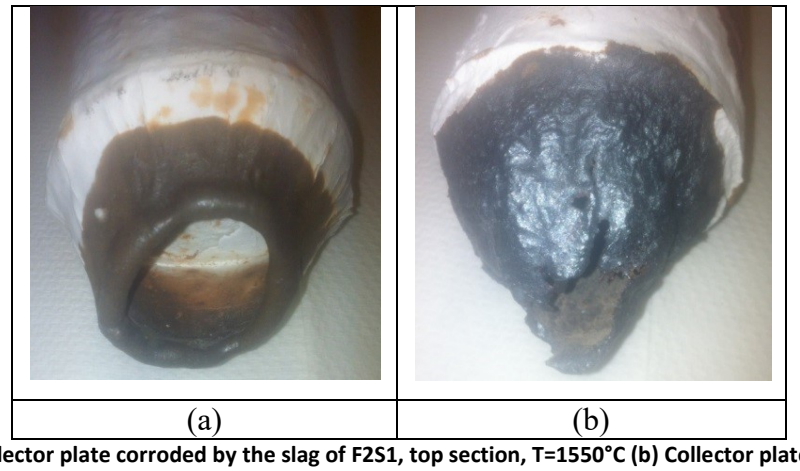

Figure 3.4: **(a) Collector plate corroded by the slag of F2S1, top section, T=1550°C (b) Collector plate corroded by the slag of F1S2, top section, T=1650°C**

Figures 3.5-3.8 show that for all the cases (different fuels, feeders and particle sizes) the amount of deposition increases with temperature. Yong et al. [32] and Luan et al. [1] observed the same trend of the increasing deposition at higher temperatures in their experiments.

One reason might be related to the behavior of inorganic matters with different association natures within the coal matrix. Based on the association with the coal matrix, the minerals are categorized as included and excluded minerals. By increasing the temperature, some excluded minerals with lower melting point such as pyrite might be partially or fully melted with low viscosity. Therefore, these particles are stickier at higher temperatures. Included minerals can form low melting point compound especially in reducing atmosphere of gasification process. At higher temperatures, due to the reduction of the carbon content of the char particles, more included minerals are exposed to the char particles surface making them stickier. These two factors work together to increase the total amount of the deposition in each case.

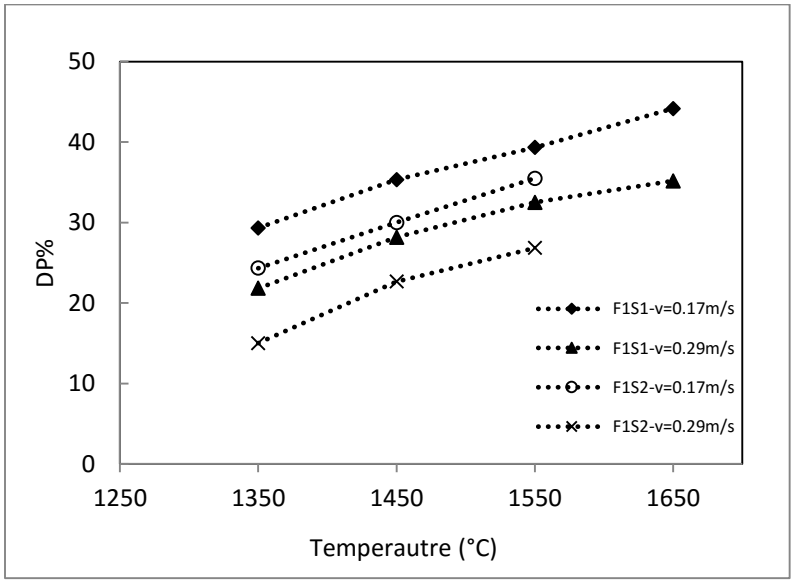

Figure 3.5: **Effect of temperature on the deposition of fuel F1, feeder C4**

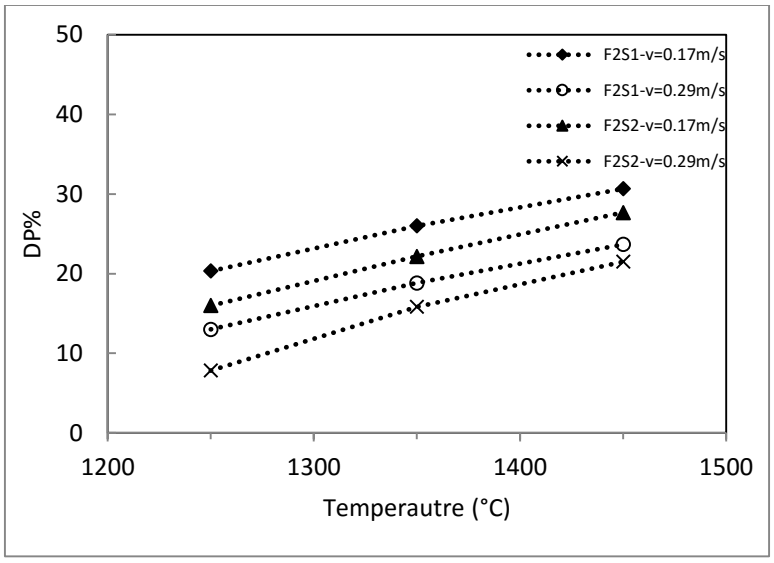

Figure 3.6: **Effect of temperature on the deposition of fuel F2, feeder C4**

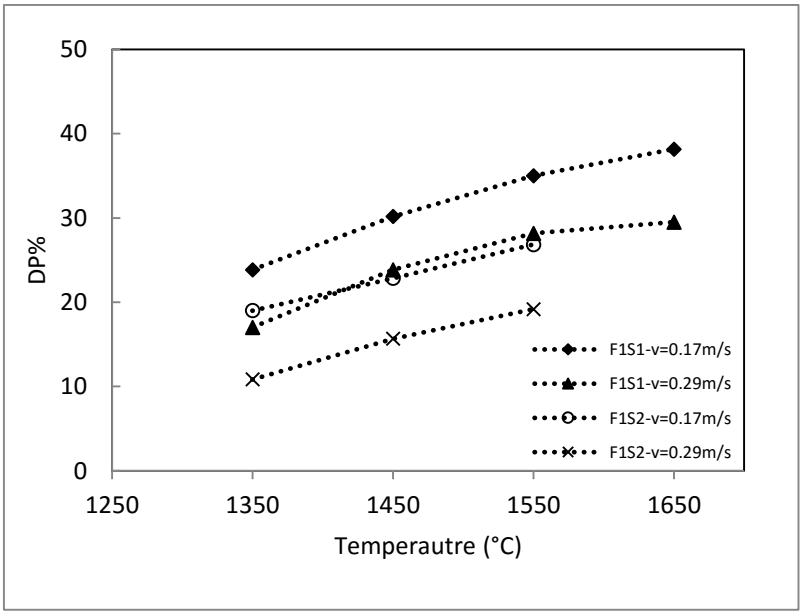

Figure 3.7: **Effect of temperature on the deposition of fuel F1, feeder A8**

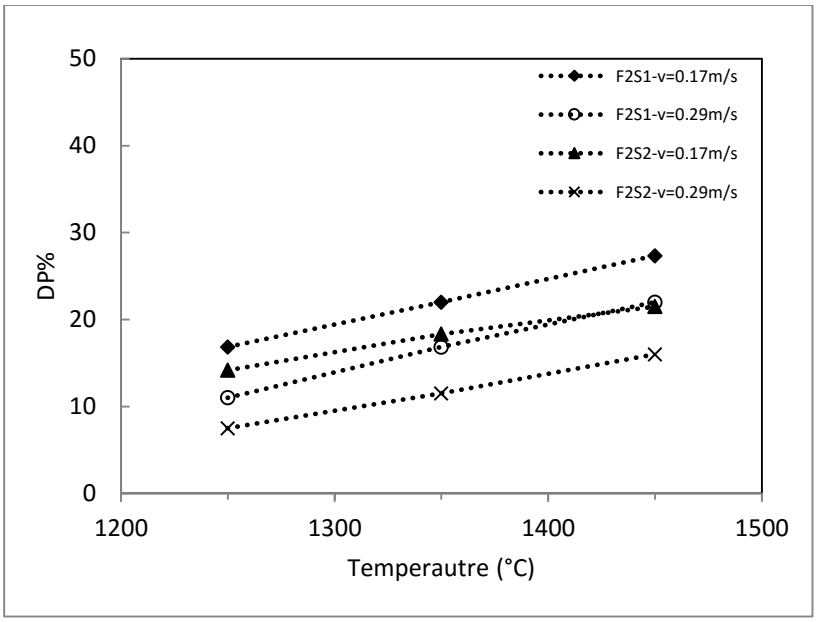

Figure 3.8: **Effect of temperature on the deposition of fuel F2, feeder A8**

For each fuel at higher temperatures, slag droplet falling down from the bottom hole of the collector plate might be observed. These droplets are collected in cyclone and their weights are added to the weight of the deposited material inside the collector plate to calculate the total deposition. Tables 3.4 and 3.5 demonstrate that by increasing the temperature, the weight of the slag droplet (if produced) increases in most of the cases which is due to the decrease in the slag viscosity.

Table 3:4: Experimental results of F1

Fuel: F1			T=1350°C	T=1450°C	T=1550°C	T=1650°C
Feeder: C4	S1:28-53µm	Air: 5L/min N_2: 1L/min $V^{in} = 3.16$	V_P: 0.163 µ:- TD: 17.6 SD: 0 Blockage: Y	V_P: 0.173 µ~139 TD:21.2 SD:2.9 Blockage: Y	V_P:0.183 µ~41.5 TD:23.6 SD:3.1 Blockage: Y	V_P:0.193 µ~14.6 TD:26.5 SD: 6.2 Blockage: Y
		Air: 5L/min N_2: 2L/min $V^{in} = 3.69$	V_P: 0.190 µ:- TD: 17.2 SD: 0 Blockage: Y	V_P: 0.202 µ~139 TD:21.5 SD: 1.6 Blockage: Y	V_P: 0.214 µ~41.5 TD:24.2 SD: 1.3 Blockage: Y	V_P:0.225 µ~14.6 TD:26.1 SD: 4.5 Blockage: N
		Air: 5L/min N_2: 5L/min $V^{in} = 5.27$	V_P: 0.272 µ:- TD:13.1 SD: 0 Blockage: N	V_P:0.289 µ~139 TD:16.9 SD: 0 Blockage: N	V_P: 0.305 µ~41.5 TD:19.5 SD: 0 Blockage: N	V_P:0.322 µ~14.6 TD:21.1 SD:1.7 Blockage: N
	S2:150-212 µm	Air: 5L/min N_2: 1lit/min $V^{in} = 3.16$	V_P: 0.163 µ:- TD: 14.6 SD: 0 Blockage: N	V_P: 0.173 µ~139 TD:18.0 SD: 0 Blockage: N	V_P:0.183 µ~41.5 TD:21.3 SD:1.2 Blockage: Y	
		Air: 5L/min N_2: 2lit/min $V^{in} = 3.69$	V_P: 0.190 µ:- TD:13.5 SD: 0 Blockage: N	V_P: 0.202 µ~139 TD:17.9 SD: 0 Blockage: N	V_P: 0.214 µ~41.5 TD:20.5 SD: 0 Blockage: Y	
		Air: 5L/min N_2: 5L/min $V^{in} = 5.27$	V_P: 0.272 µ:- TD:9.0 SD: 0 Blockage: N	V_P:0.289 µ~139 TD: 13.6 SD: 0 Blockage: N	V_P:0.305 µ~41.5 TD:16.1 SD: 0 Blockage: N	
Feeder: A8	S1:28-53µm	Air: 5L/min N_2: 1L/min $V^{in} = 6.32$	V_P: 0.163 µ:- TD: 14.3 SD: 0 Blockage: N	V_P: 0.173 µ~139 TD: 18.1 SD: 0 Blockage: N	V_P: 0.183 µ~41.5 TD:21.0 SD: 1.2 Blockage: Y	V_P:0.193 µ~14.6 TD:22.9 SD: 1.4 Blockage: N
		Air: 5L/min N_2: 2L/min $V^{in} = 7.37$	V_P: 0.190 µ:- TD:14.2 SD: 0 Blockage: N	V_P:0.202 µ~139 TD:18.4 SD: 0 Blockage: N	V_P: 0.214 µ~41.5 TD:20.7 SD: 0 Blockage: Y	V_P:0.225 µ~14.6 TD:22.4 SD: 2.5 Blockage: N
		Air: 5L/min N_2: 5L/min $V^{in} = 10.53$	V_P: 0.272 µ:- TD:10.2 SD: 0 Blockage: N	V_P: 0.289 µ~139 TD:14.3 SD: 0 Blockage: N	V_P:0.305 µ~41.5 TD:16.9 SD: 0 Blockage: N	V_P:0.322 µ~14.6 TD:17.7 SD: 0 Blockage: N
	S2:150-212 µm	Air: 5L/min N_2: 1L/min $V^{in} = 6.32$	V_P: 0.163 µ:- TD:11.4 SD: 0 Blockage: N	V_P: 0.173 µ~139 TD:13.7 SD: 0 Blockage: N	V_P: 0.183 µ~41.5 TD: 16.1 SD: 0 Blockage: N	
		Air: 5L/min N_2: 2lit/min $V^{in} = 7.37$	V_P: 0.190 µ:- TD:10.1 SD: 0 Blockage: N	V_P:0.202 µ~139 TD:13 SD: 0 Blockage: N	V_P: 0.214 µ~41.5 TD: 15.6 SD: 0 Blockage: N	
		Air: 5L/min N_2: 5L/min $V^{in} = 10.53$	V_P: 0.272 µ:- TD:6.5 SD: 0 Blockage: N	V_P: 0.289 µ~139 TD:9.4 SD: 0 Blockage: N	V_P:0.305 µ~41.5 TD:11.5 SD: 0 Blockage: N	

VP: particle velocity in furnace (m/s), V^{in}: particle initial velocity (m/s), µ: viscosity (Pa.s), TD: total deposition (g), SD: slag droplet (g)

Table 3:5: Experimental results of F2

Fuel: F2			T=1250°C	T=1350°C	T=1450°C
Feeder: C4	S1:28-53µm	Air: 5L/min N_2: 1L/min $V^{in} = 3.16$	V_P: 0.153 µ~29.05 TD:12.2 SD: 0 Blockage: Y	V_P: 0.163 µ~8.55 TD:15.6 SD: 1.6 Blockage: N	V_P: 0.173 µ~4.16 TD:18.4 SD: 2.2 Blockage: N
		Air: 5L/min N_2: 2L/min $V^{in} = 3.69$	V_P: 0.178 µ~29.05 TD:11.9 SD: 0 Blockage: N	V_P: 0.190 µ~8.55 TD:15.2 SD: 1 Blockage: N	V_P: 0.202 µ~4.16 TD:18.9 SD: 1.7 Blockage: N
		Air: 5L/min N_2: 5L/min $V^{in} = 5.27$	V_P: 0.255 µ~29.05 TD:7.8 SD: 0 Blockage: N	V_P: 0.272 µ~8.55 TD:11.3 SD: 0 Blockage: N	V_P: 0.289 µ~4.16 TD:14.2 SD: 0 Blockage: N
	S2:150-212 µm	Air: 5L/min N_2: 1L/min $V^{in} = 3.16$	V_P: 0.153 µ~29.05 TD:9.6 SD: 0 Blockage: N	V_P: 0.163 µ~8.55 TD:13.3 SD: 0 Blockage: N	V_P: 0.173 µ~4.16 TD:16.6 SD: 0.9 Blockage: N
		Air: 5L/min N_2: 2L/min $V^{in} = 3.69$	V_P: 0.178 µ~29.05 TD:8.2 SD: 0 Blockage: N	V_P: 0.190 µ~8.55 TD:12.6 SD: 0 Blockage: N	V_P: 0.202 µ~4.16 TD:16.0 SD: 0.6 Blockage: N
		Air: 5L/min N_2: 5L/min $V^{in} = 5.27$	V_P: 0.255 µ~29.05 TD:4.7 SD: 0 Blockage: N	V_P: 0.272 µ~8.55 TD:9.5 SD: 0 Blockage: N	V_P: 0.289 µ~4.16 TD:12.9 SD: 0 Blockage: N
Feeder: A8	S1:28-53µm	Air: 5L/min N_2: 1lit/min $V^{in} = 6.32$	V_P: 0.153 µ~29.05 TD:10.1 SD: 0 Blockage: N	V_P: 0.163 µ~8.55 TD:13.2 SD: 0 Blockage: N	V_P: 0.173 µ~4.16 TD:16.4 SD: 0.6 Blockage: N
		Air: 5L/min N_2: 2L/min $V^{in} = 7.37$	V_P: 0.178 µ~29.05 TD:9.5 SD: 0 Blockage: N	V_P: 0.190 µ~8.55 TD:13.7 SD: 0 Blockage: N	V_P: 0.202 µ~4.16 TD:16.1 SD: 0.7 Blockage: N
		Air: 5L/min N_2: 5L/min $V^{in} = 10.53$	V_P: 0.255 µ~29.05 TD:6.6 SD: 0 Blockage: N	V_P: 0.272 µ~8.55 TD:10.1 SD: 0 Blockage: N	V_P: 0.289 µ~4.16 TD:13.2 SD: 0 Blockage: N
	S2:150-212 µm	Air: 5L/min N_2: 1L/min $V^{in} = 6.32$	V_P: 0.153 µ~29.05 TD:8.5 SD: 0 Blockage: N	V_P: 0.163 µ~8.55 TD:11.0 SD: 0 Blockage: N	V_P: 0.173 µ~4.16 TD:12.9 SD: 0 Blockage: N
		Air: 5L/min N_2: 2L/min $V^{in} = 7.37$	V_P: 0.178 µ~29.05 TD:7.5 SD: 0 Blockage: N	V_P: 0.190 µ~8.55 TD:9.8 SD: 0 Blockage: N	V_P: 0.202 µ~4.16 TD:13.2 SD: 0 Blockage: N
		Air: 5L/min N_2: 5L/min $V^{in} = 10.53$	V_P: 0.255 µ~29.05 TD:4.5 SD: 0 Blockage: N	V_P: 0.272 µ~8.55 TD:6.9 SD: 0 Blockage: N	V_P: 0.289 µ~4.16 TD:9.6 SD: 0 Blockage: N
VP: particle velocity in furnace (m/s), V^{in}: particle initial velocity (m/s), µ: viscosity (Pa.s), TD: total deposition (g), SD: slag droplet (g)					

3.4.2. Effect of gas flow rate (particle velocity) and particle size

Nitrogen carries the coal particles into the furnace. To evaluate the effect of the velocity in this study, only nitrogen flow rate was varied and oxygen flow rate was kept constant. Increasing the gas flow rate has various effects on the process which most of them work to decrease the mineral deposition on the bare wall. Montagnaro et al. [31] reported that big particles with high impact velocity can break easier into the slag layer (with extremely low viscosity) and get embodied into the molten liquid which is very less probable based on the typical conditions of gasifiers. But, there is a difference between the behavior of the bare wall and slag covered wall. It is an accepted fact that the reactor wall which is covered by molten slag layer is more likely to capture and trap the incoming particles than the dry wall [32].

By increasing the gas flow rate, the velocity of the particles increases as presented in Tables 3.4 and 3.5. Therefore, the particles collide with the wall with higher kinetic energy by which, the probability of rebounding is higher in most cases [1, 27]. In addition, by increasing the gas flow rate the residence time of the particles inside the furnace decreases which leads to higher unburnt carbon content in the ash residue resulting in lower carbon conversion. When the carbon conversion is lower, there are lower amount of the inorganic matters exposed to the surface of chars making them sticky enough to be captured by the slag collector probe. Shimizu and Tominaga [33] reported the same observation in their studies.

Figures 3.9-3.12 show the deposition for different feeders, fuels and temperatures as function of velocity. In each specific condition usually the deposition decreases with increasing the velocity or gas flow. Luan et al. [1] observed the same trends in their

experimental results. In all the experiments, the deposition at the gas flow rate of 10 L/min is lower than the deposition at 6L/min. But, in some cases the deposition at the gas flow rate of 7 L/min is larger or approximately equal to the deposition at 6 L/min (the equivalent velocity of each gas flow rate (which depends to the temperature) is presented in Tables 3.4 and 3.5). This might be due to the effect of the turbulence and mixing at gas flow rate of 7L/min. At low temperatures, the effect of increase in the gas velocity is more noticeable. The reason is lower stickiness at lower temperature and higher kinetic energy at higher gas flow rate work together to prevent the char particles from sticking to the slag collector probe. By increasing the velocity or gas flow rate, the deposit on the bare wall in the vertical section of the collector plate decreases which can be seen in Figure 3.16. Influence of the velocity on bigger particle size is realizable even in low gas flow rate which can be explained by the higher kinetic energy. In addition, the small particles can reach to the thermal equilibrium sooner than bigger particles. Hence, small particles reach to the temperature of the furnace and melt sooner than bigger particle. Kreutzkam et al. [42] reported that smaller particles follow the streamlines of the gas phase better than the big particles (which usually follow their own paths), therefore, do not collide with the surface of the probe or wall and consequently do not tend to deposit that much. But, the results of this study showed higher deposition for smaller particles. In this work, it must be noticed that based on the configuration of the feeders most of the particles collide with the wall of the collector probe independent of their size and smaller particles are stickier and more probable to be captured. Chen et al. [37] and Yong et al. [32] observed the same trend as well. They reported that high inertia particles (big particles with high velocity and density) mostly tend to rebound. Chen et al. [37] reported

that even at low carbon conversion, particles with low velocity and small Weber number can be trapped. Based on the Weber number definition as the ratio of the kinetic energy to the interfacial surface tension energy, in case of the bare wall, particles with lower Weber number are more probable to stick. Weber et al. [43] reported that the particle can stick to the wall if all the kinetic energy possessed by the particle before collision dissipates by the target surface at the moment of impact which is usually probable due to the presence of the film with low viscosity. But, particles with higher kinetic energy than the lost energy at the moment of collision bounce off the surface (unless if they break into the liquid layer). At the same condition of the temperature and velocity, the kinetic energy of the bigger particles is higher than the smaller ones. Therefore, when the big particles hit the wall, because of higher energy the possibility of rebounding is higher unless the wall is covered by liquid slag with low viscosity. In case of the slag covered or wet wall, higher energy helps the particles to break into the slag layer and get encapsulated permanently (only if the viscosity of molten slag layer is low enough). Comparison of the depositions of different sizes at the same operating conditions in Figures 3.5-3.8 and Figures 3.9-3.12 shows that the fuel with bigger particle size has lower deposition tendency. According to Luan et al. [1] smaller particles lose their kinetic energy sooner. Therefore, smaller particles are more prone to stick (with higher deposition tendency) if they can invade into the boundary layer around the wall and reach to the surface of slag.

Carbon conversion is another affecting parameter in the deposition tendency. Usually at the same operating conditions, carbon conversion of the smaller particles is higher than the big ones. Particles with high carbon conversion (over 80%) have higher tendency to

be captured [37]. But, it must be noticed that there might be an unpredicted slowdown in the carbon consumption rate of the char particles under gasification process at conversions more than 50% and around the ash fusion temperature range [44]. The reason is that molten included inorganic matters cover and close the pores, holes and the channels inside the char particles and prevent the gasifying agents to penetrate into the char particles to react with carbon content at high temperatures [44].

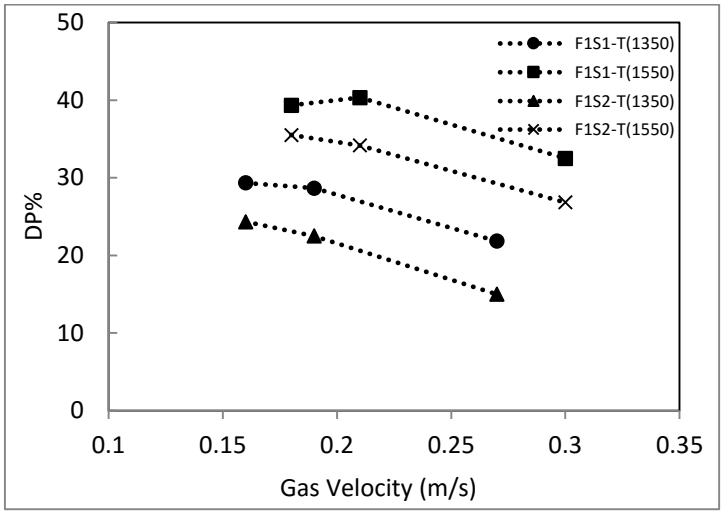

Figure 3.9: **Effect of gas flow rate on the deposition of fuel F1, feeder C4**

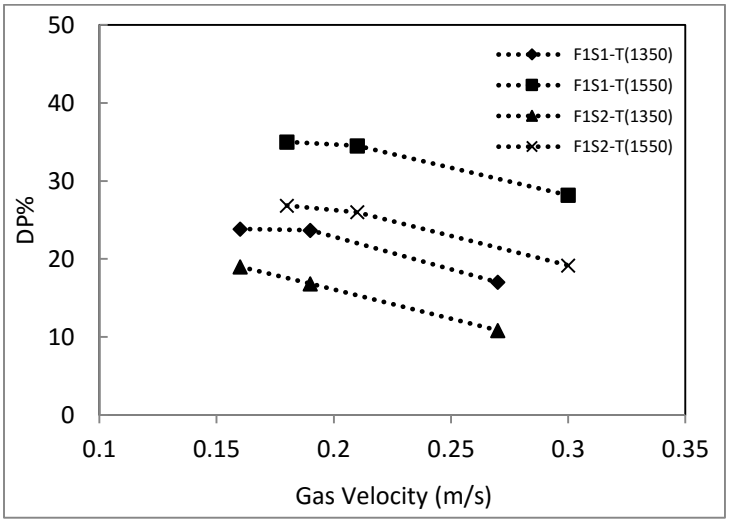

Figure 3.10: **Effect of gas flow rate on the deposition of fuel F1, feeder A8**

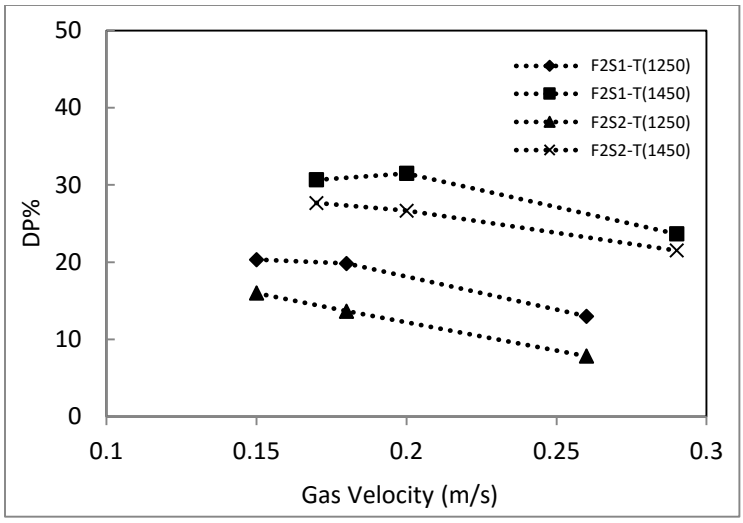

Figure 3.11: **Effect of gas flow rate on the deposition of fuel F2, feeder C4**

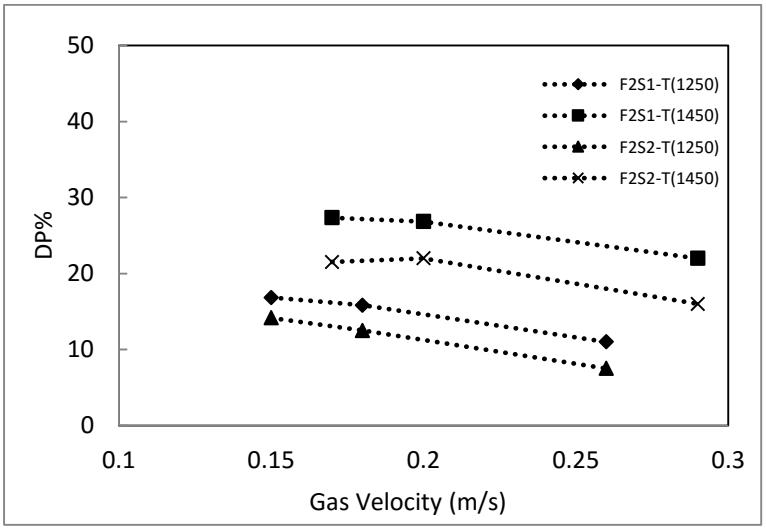

Figure 3.12: **Effect of gas flow rate on the deposition of fuel F2, feeder A8**

3.4.3. Effect of ash composition

Fuels F1 and F2 have different inorganic contents which are presented in Table 3.3. The experimental measurement presented in Table 3.4 and 3.5 demonstrate that at the same condition the bulk ash viscosity of F2 is lower than F1. Therefore, it seems that the deposition tendency of the inorganic matters of F2 must be higher than F1. The reason is

that, usually ash particles with lower fusion temperature and lower viscosity are melted sooner and have higher liquid fraction [41]. Therefore, ash particles with lower viscosity are more probable to stick. Also lower viscosity causes the slag layer to move and spread faster and make the wall surface a very sticky place for other incoming particles to be captured.

Comparison the results presented in Figure 3.5 to 3.12 or Tables 3.4 and 3.5 shows that in most of the experiments, the inorganic content of F1 had higher deposition tendency in slag collector plate. Only in few cases, especially for bigger particles, the ash deposition of F2 is higher than F1. It must be noticed that, all of the quantified results presented in this study are regarding collector plates installed at the top section. For both coals, most of the depositions happen at the top section of the furnace near the feeding spot and the deposition tendency for F1 is usually higher in this section. Rushdiet al. [26] performed ash deposition experiments in a pilot-scale setup and compared the amount of the deposition on the panels installed at different locations. They reported that more deposition was formed on the panel 1 which was the top section in their experiments. They related this observation to the higher temperature near the flame in the top section.

The depositions of both coals have been analyzed with BSE/EDX. BSE images of the depositions for top section show that the deposit layer is highly covered with iron as presented in Figure 3.13 and 3.14. In this regard, Rushdi et al. [26] reported that high ash loading with high iron oxide content caused a coal to show enhanced ash deposition. Therefore, it can be concluded that the reason of high deposition tendency of F1 at the top section is most likely related to the small iron particles. At reducing conditions of the gasification process, iron is mostly present in reduced states which has low melting point.

These low melting point particles are very liable to be captured by the wall of surface. Therefore, these particles act as precursors to make the wall sticky to capture other impacting particles including char and ash.

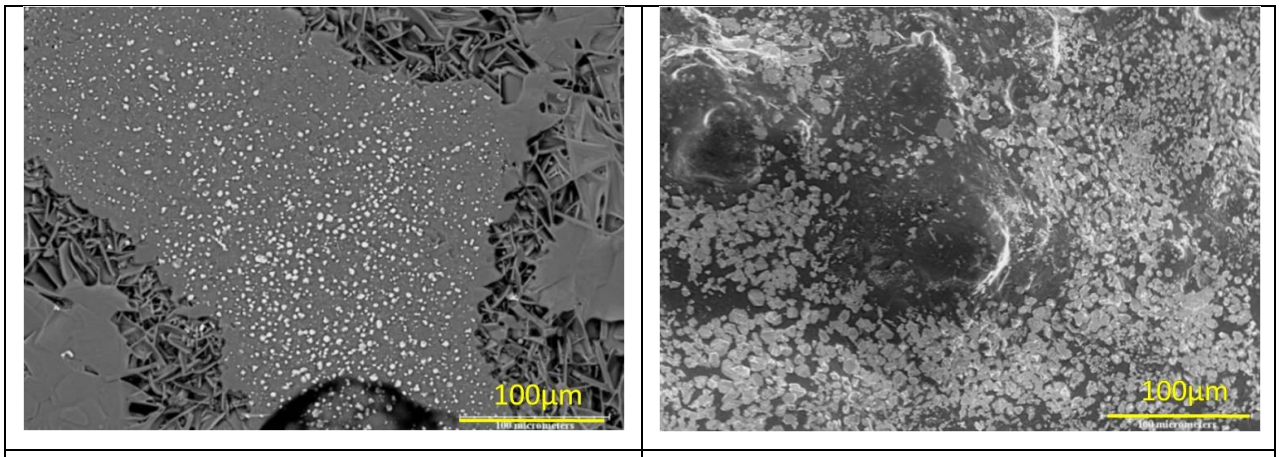

(a) (b)

Figure 3.13: **BSE images of iron deposition on the slag layer surface at top section (a) F2S1 1450°C (b) F1S1 1450°C**

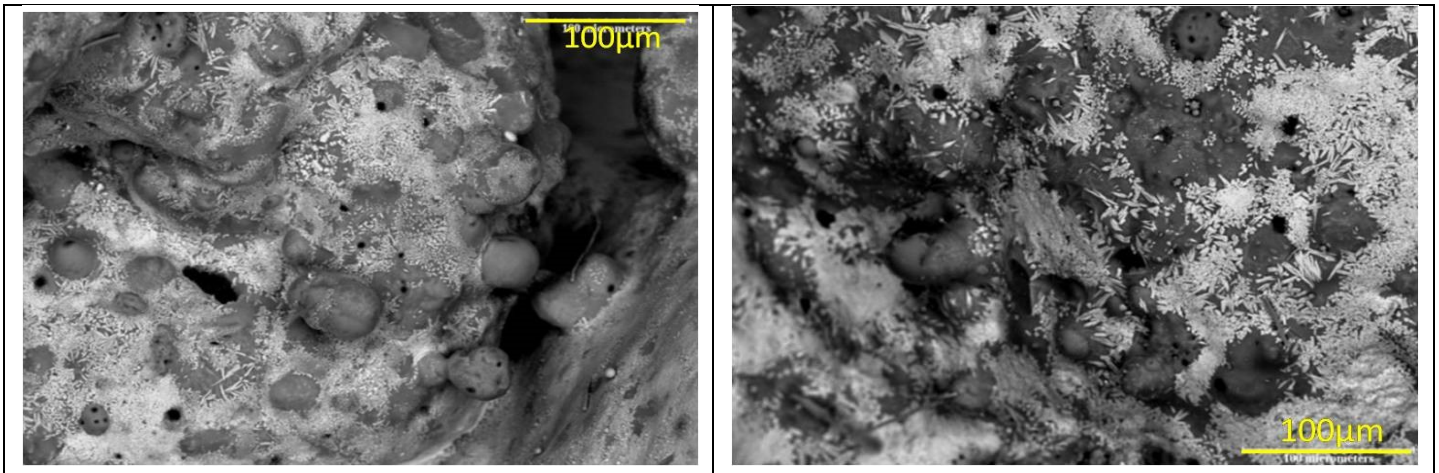

(a) (b)

Figure 3.14: **BSE images of the particles captured by iron covered surface (a) F1S1 1550°C (b) F1S1 1450°C**

BSE images and EDX analysis of the samples at different locations in Figure 3.15 and Table 3.6 show that there is lower iron concentration on the surface of the deposit in lower sections. Based on Rushdi et al. [26] and Barroso et al. [40], the sticking particles

(with high deposition tendency) are mostly rich in basic oxides, particularly iron and calcium-bearing species. These oxides lower the viscosity of the molten slag by formation of the low melting point compounds (which can be identified on the phase diagram) and therefore enhance ash deposition. In this regard, Degereji et al. [45] reported high deposition tendency for high iron content coal ash and very low slagging tendency for coal ash with iron content lower than 6%.

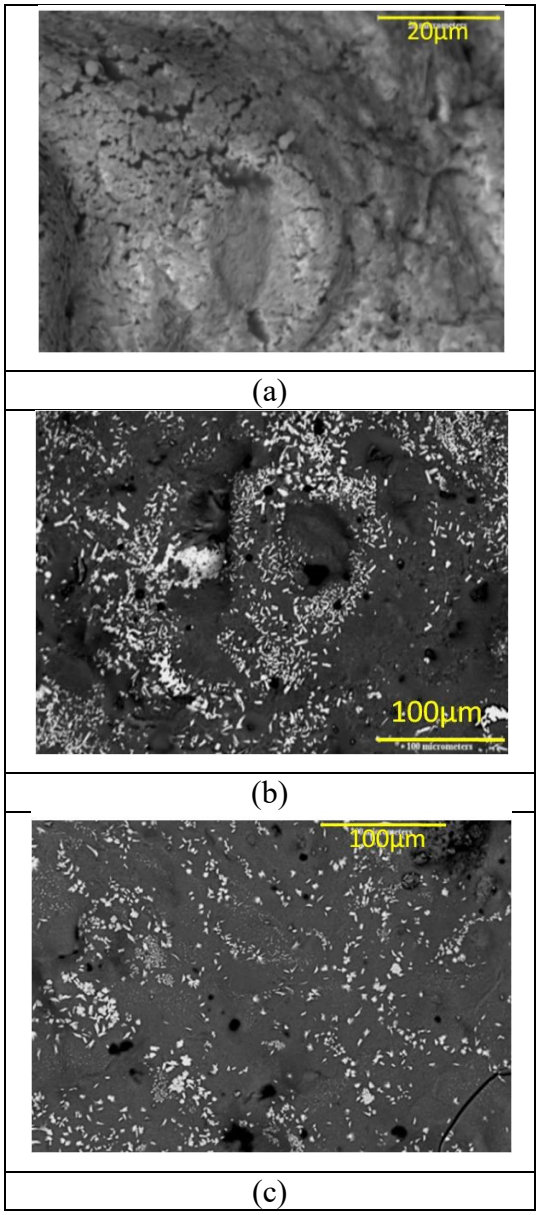

Figure 3.15: **Different iron concentration of the surface of deposition, F1S1, 1550°C (a) top (b) middle (c) bottom**

Table 3:6: **Average iron composition in the depositions of F1 at different locations determined by EDX**

	F1-Raw	F1-Top	F1-Middle	F1-Bottom	F1-Cyclone
Fe (%)	7.9	20.3	8.5	9	7.1

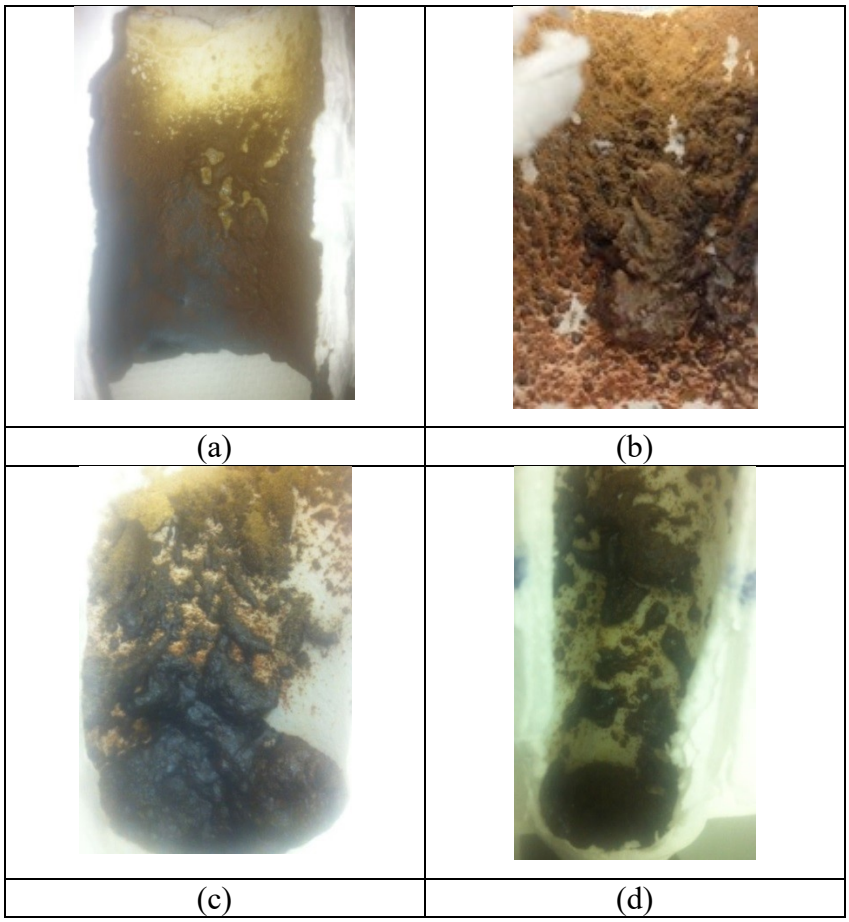

Figure 3.16: **Deposition on the wall of collector plate at the top section, Feeder: C4 (a) F2S1 T: 1450°C, N: 2L/min (b) F1S1 T: 1450°C, N: 1L/min (c) F1S1 T: 1450, N: 2L/min (d) F1S1, T: 1550, N: 2L/min**

Statistical calculations were performed based on the CCSEM analysis and the results are presented in Table 3.7. These results help to better understand the different deposition behaviors of the inorganic matters of F1 and F2. For F1, iron is mostly present as excluded particles. In addition, most of the inorganic matters of this coal exist separately as excluded minerals. Unlike included minerals, the stickiness of the excluded iron particles in reducing conditions is independent of the carbon conversion. This can explain

high iron concentration and high deposition tendency of F1 in the top section. The lower deposition tendency of F1S2 in comparison with F2S2 might be explained by the fact that the stickiness of the iron particles is not strong enough to hold the big particles. In this case, the ash particles of F2 because of the lower fusion temperature and bulk ash viscosity have higher deposition tendency. The same behavior for such particles has been also predicted by Montagnaro et al. [31].

Table 3:7: Statistical results of CCSEM analysis of F1 and F2

	F1					F2				
	Weight%	Number of particles	Area %	Fe	Ca	Weight%	Number of particles	Area%	Fe	Ca
Total		3340		8.06	1.74		3355		8.38	13.48
Included	33.1	1217(36.4%)	33.9	3.06	1.83	46.9	2087(62.2%)	48.9	4.48	22.65
Excluded	66.9	2123(63.6%)	66.1	10.53	1.69	53.1	1268 (37.8%)	51.1	11.83	5.37

Because of higher calcium content, ash of F2 has lower fusion temperature and viscosity in comparison with F1. Therefore, resulted slag layer of F1 flows down on the wall with a very slow rate and consequently the slag thickness grows fast. Figure 3.17 shows the slag layer from F1 and F2 at the top section. It is obvious that at the same condition, the slag generated from F1 is thicker than F2. Experimental results of F1 showed very small amount of deposition at the middle and bottom sections. Although for F2 the deposition in the middle and bottom sections is lower than the top section, but, the deposition is higher than F1 in these sections. This observation signifies the different behavior of the inorganic matters of these two fuels. Excluded iron-bearing particles of F1, stick to the wall of the furnace at reducing condition of the gasification process mostly as soon as they collide with the wall and make it a sticky surface for other particles to be trapped. CCSEM analysis presented in Table 3.7 shows that F2 has lower amount of excluded

mineral matters. In addition, most of the calcium-bearing minerals of F2 are present as included particles which require high carbon conversion to make the char particle sticky. Therefore, although F1 has higher fusion temperature and higher viscosity, but, its deposition at the top section is usually higher. The slag layer thickness of F1 grows fast due to its high viscosity. Because most of the irons stick to the top section, there is not enough iron to do the same role in the middle and bottom sections. Also, strong axial gas flow in combination with high slag viscosity of F1 might be other reasons for the low deposition in the lower sections inside the furnace. Due to the lower amount of excluded iron particles in F2, this fuel had more uniform deposition and severe deposition growth was not observed at all.

Working with F2, some depositions were observed even near the collection probe (where the temperature is around 1000°C). Some reasons can be introduced to explain these observations. Firstly, the melting point and viscosity of the bulk of ash of F2 is lower than F1. Therefore, the bulk of the inorganic matters of F2 are stickier than F1 at the same condition. But, the included mineral content of F2 is higher than F1. Especially most of the calcium contents are present as included minerals. Included minerals can make a particle sticky if they are exposed to the char surface which happens at higher carbon conversion in later stages of the gasification process. Therefore, in the lower sections of the furnace, by increasing the carbon conversion inorganic matters of F2 are able to stick to the wall. Lower ash content of F2, in comparison with F1, might be another reason for its lower deposition in top section. Because when the ash content is lower, higher carbon conversion is needed to make enough inorganic particles exposed to the char surface. Another reason is that the inorganic depositions of F2 usually form a

liquid slag layer quickly. Due to the low viscosity, this slag layer flows and spreads on the wall of the furnace from top to the bottom section (Figure 3.20 (a)). Consequently, a large area of the wall of the furnace will be a wet sticky target for other particles. For F1, the flowing slag layer is formed only at very high temperatures, and due to the high viscosity it can just flow a few centimeters down the wall with much higher thickness than slag layer of F2.

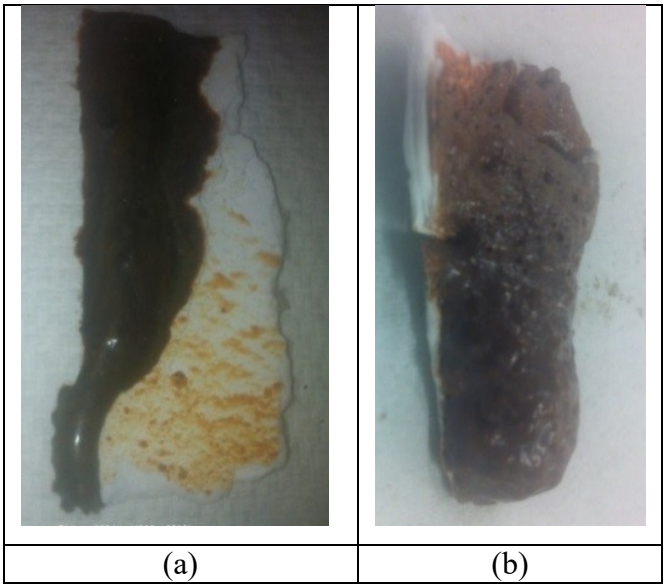

Figure 3.17: **Slag layer on the wall of collector plate at the top section T: 1450°C, N: 1L/min (a) F2S1 (b) F1S1**

BSE/EDX analysis of the ash residue of F2 showed lots of particles sticking together and making big agglomerations. In many of these agglomerations, it has been observed that calcium-bearing inorganic matters acted as glue and made other particles to stick together and form big agglomerations with size of more than hundred microns. Formation of the big agglomerations might be another reason of the lower deposition tendency of F2. Agglomeration is observed in F2S2 more than F2S1. This could be due to the higher included mineral content existed in the bigger particle. Particle agglomeration in case of

F1 happened much lower than F2. Figure 3.18 shows agglomerations of F2 at different conditions. Table 3.8 presents the EDX results regarding the composition of the specified points in Figure 3.18.

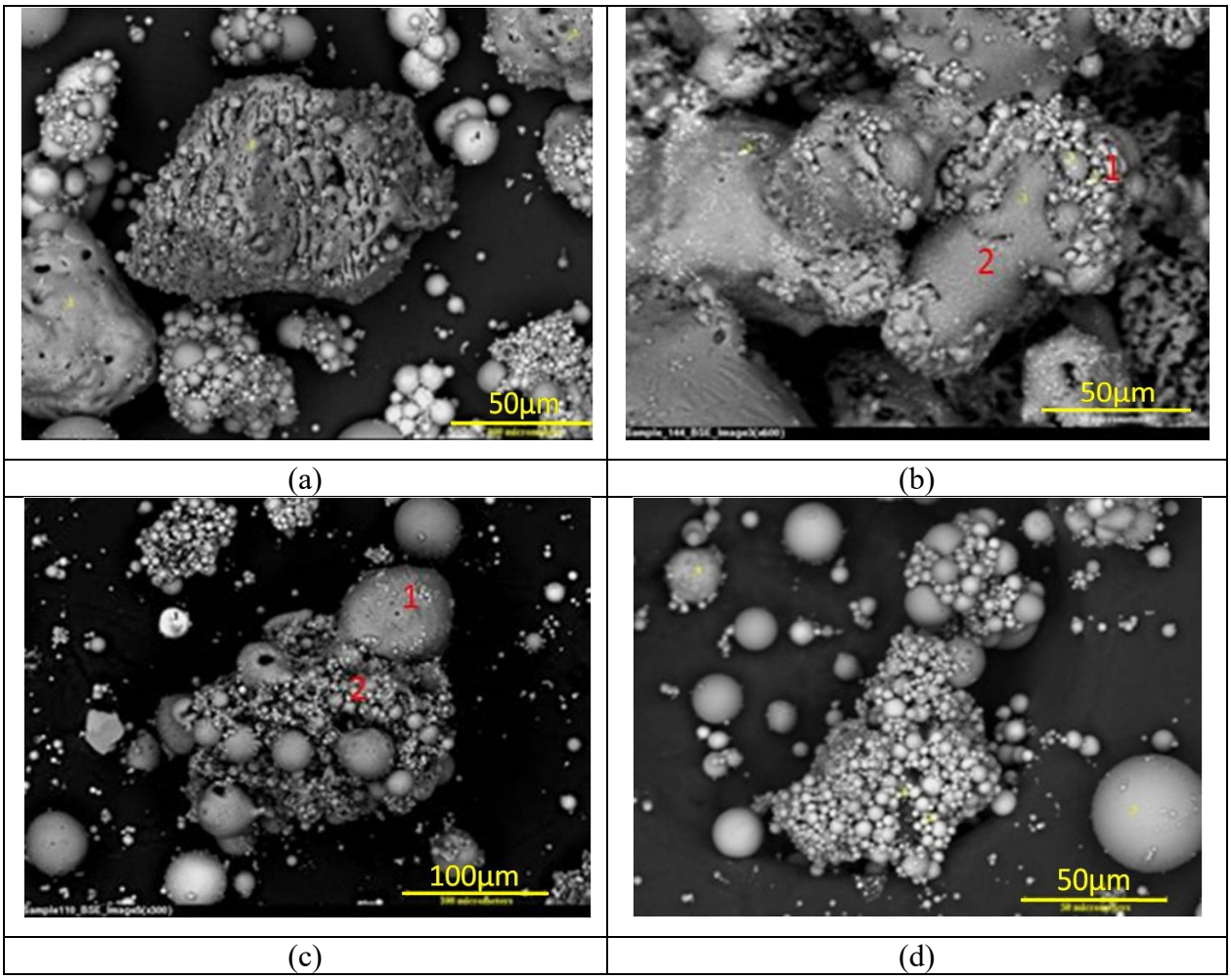

Figure 3.18: **BSE images of agglomerations of the minerals of F2 collected in cyclone (a) F2S2, T:1450°C ,N:1L/min, Feeder:C4 (b) F2S2, T:1450°C ,N:5L/min, Feeder:C4 (c) F2S2, T:1350°C, N:5L/min, Feeder:A8 (d) F2S1, T:1350°C ,N:1L/min, Feeder:C4**

Table 3:8: **EDX analysis of the specified points in figure 3.18**

	Si	Al	Fe	Ca	Na	Mg	K	Ba	Ti	S	P
(b) point 1	35.5	27.3	3.6	18.4	14	1.5	-	-	-	-	-
(b) point 2	15.3	13.2	3.6	51.3	4.6	5.3	-	-	-	1.5	5.3
(c) point 1	57.6	38.2	0.9	1.4	1.3	-	0.6	-	-	-	-
(c) point 2	30	32	4.8	25.1	-	1.7	-	-	5.7	-	0.8

BSE/EDX analysis of the ash residue of F2 showed lots of small iron-containing particle on the surface of other ash particles. But working with F1, very small amount of iron as separate particles were observed in the ash residue collected in cyclone. As presented in Figure 3.19, layer of iron sulfide is observed on some particles in the ash residue of F2 which was observed much lower in case of F1. Table 3.9 presents the EDX results for composition of the specified areas in Figure 3.19. Based on all of these observations, it can be concluded that working with F1 under reducing conditions of the gasification process, most of the iron particles can stick to the wall of furnace upon collision. But, iron-bearing minerals of F2 undergo various processes and can be seen at different states at various locations from top to the bottom section of the furnace and also in the ash residue collected in cyclone.

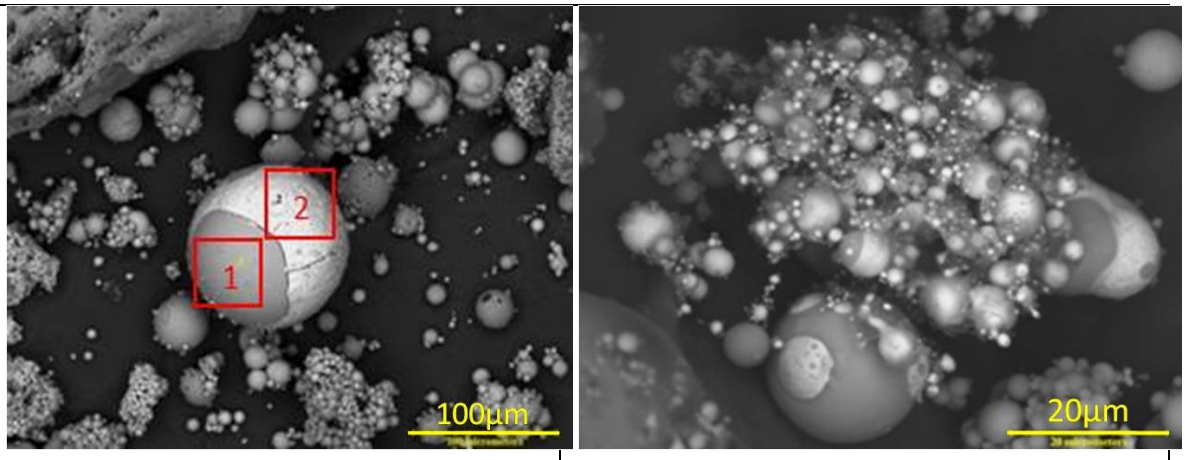

(a) (b)

Figure 3.19: **Iron sulfide layer on the ash particles, Feeder: A8 (a) F2S2, N: 1L/min, T:1350°C (b) F2S1, N: 1L/min, T:1350°C**

Table 3:9: **EDX analysis of the specified points in figure 3.19**

	Si	Al	Fe	Ca	Na	Mg	K	Ba	Ti	S	P
Area 1	27.6	22.5	19.1	19.7	6.4	1.3	0.4	2	0.3	0.9	-
Area 2	4.1	3.9	60	2	2.9	-	-	-	-	27.3	-

Figure 3.20 shows the slag layer of F2 on the wall of furnace. Most of the experimental results of F2 showed that the slag layer forms fast and flows down on the wall of furnace with a very thin thickness. Only at the bottom section near the collection probe where the temperature is very low, the slag layer might be very thick (as shown in Fig. 3.20(b)).

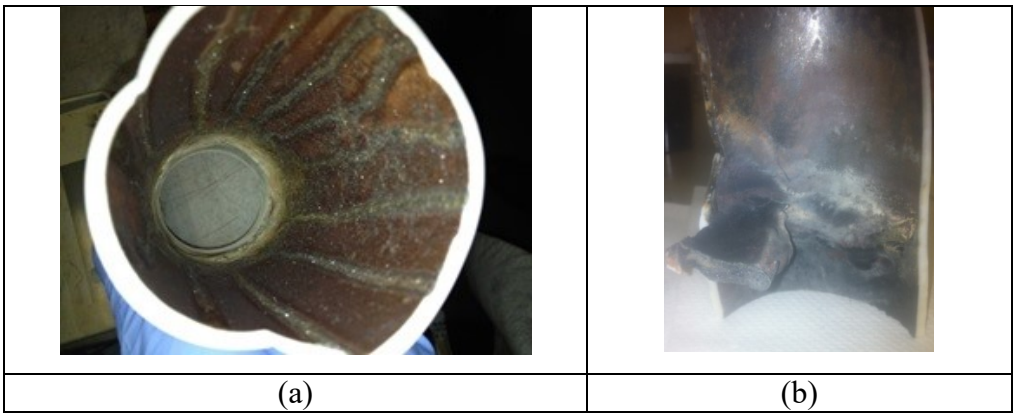

Figure 3.20: **Deposition at different locations on the wall of furnace for F2 (a) Feeder A8, middle section (b) Feeder C4, bottom section**

3.4.4. Effect of the particle trajectory (different feeding configurations)

Based on the quantified results of the ash deposition presented in Tables 3.4 and 3.5, using C4 feeding configuration, inorganic matters have higher deposition tendency in comparison with feeder A8. The reason is most likely related to the wet and sticky area produced by each feeder. A8 injects the particles in a way that they collide with the wall close to normal direction in a concentrated small area. In this case, stickier particles (especially iron-bearing inorganic matters which act as precursors) make that narrow section of collision very sticky. In this regard, Li et al. [39] analyzed different burners and reported that the feeder with higher number of the colliding particles with the wall results in higher particles sticking which consequently increases the total amount of the deposition. Ni et al. [38] reported that the highest particle concentration (which increases the particle capture probability) was observed at the impinging or feeding area.

Continuing the process with this condition makes the deposition in a narrow area to grow fast. The thickness in some cases might reach to several centimeters. In addition, Ni et al. [38] reported that the morphological structure of the deposit surface strongly depends on the temperature which may change from a particulate sintered porous surface to a non-porous molten surface. Molten surface provides a sticky capturing place on which other particles can adhere. High particle capture rate may result in the sintering of the deposit depending on the extent of melting of the incoming particles. Because of working with the electrically heated wall in this study, the temperature is higher on the wall of the furnace and is lower on the deposit surface (inverse temperature gradient in comparison with self-heated gasifier). Hence, when there is a severe growth of the deposition on the wall of furnace, the temperature of the deposit surface in that area will be lower which causes the surface to be less sticky. This fact could be another reason for the lower deposition resulted by A8 in comparison with C4.

Figure 3.21 shows contours of the velocity resulted by CFD modeling of both feeders with comparison of the initial contact area of the particles. The CFD modeling is performed by ANSYS-Fluent based on 2D-axisymetric geometry in Eulerian-Lagrangian frame-work. Discrete Particle Model (DPM) is used for the particle tracking and Realizable k-ε is applied to model the turbulence inside the furnace. Rosin-Rammler is used for the particle size distribution in the range of 28-53μm. Inlet velocity is used as the boundary condition for the air and carrier nitrogen inlet flow and outlet pressure is applied as the boundary condition of the exit stream. More detailed information about the modeling of this gasification setup is presented in chapter 5. The initial contact area is assumed to be the location that the gas flow carries the particles toward the wall of the

furnace. However, the bigger particles tend to follow their own paths based on their inertia and they usually do not follow the gas phase stream lines. The difference between the trajectories of the small and big particles is presented in chapter 5.

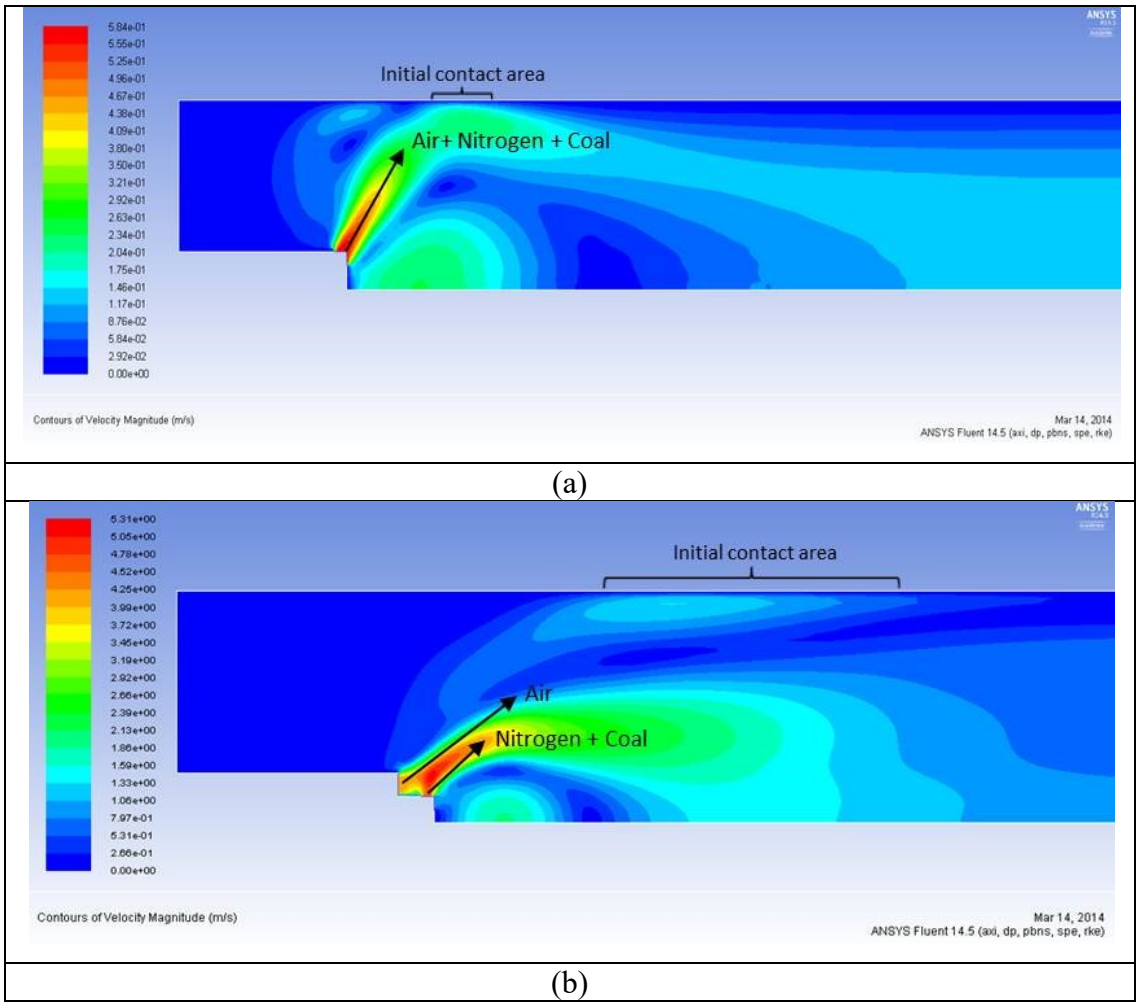

Figure 3.21: **Contours of velocity magnitude (a) Feeder A8 (b) Feeder C4**

Figure 3.22 shows the deposition on the wall of furnace resulted from A8. Using A8 and working with F1S1, the thickness of the deposition can reach to 25mm in the top section and makes the operation very risky due to the high probability of the blockage near the feeding spot. In this case the deposition is not uniform. Most of the particles hit the wall and deposit on the first 10 cm of the collector plate or the wall of furnace as shown in Figure 3.21 and Figure 3.22. This uneven particle distribution causes a concentrated thick

layer of deposition at the top section. Deposition thickness can be controlled by the gas flow rate and temperature. Increasing the gas flow rate from 6L/min to 10L/min (or increasing the average velocity of the particles from 0.178m/s to 0.297m/s) reduces the thickness of the deposition (more realizable for F1) and reduces the blockage probability. Figure 3.23 shows the deposition and BSE images of Figure 3.22 (a). Based on this image, it can be seen that the deposition is growing from the top and the slag flow is formed from the bottom. Because of the high viscosity of the ash content of F1, the flow of slag is not enough to reduce the deposit thickness. Figure 3.24 shows the deposition resulted from C4 at the same condition. For this feeder, the deposition is distributed over a wider area and the thickness of the deposit layer is lower in comparison with the deposition of A8. BSE images of Figure 3.23 and 3.24 shows that, regardless of the feeding configuration, the depositions resulted from F1 at the top section are highly covered with iron.

Using F1 and working with simple feeder (two concentric open ended tubes), a small amount of the deposition on the wall was observed only at the top section which is due to the presence of the sticky iron particles. But, because of the strong axial gas flow, some sticky particles were pushed downward and deposited on the cone-shape part of the collector probe in lower sections. Using C4 and A8, due to the higher turbulence and radial velocity of the particles, most of the iron-bearing particles hit the wall in the top section areas. Due to their low melting point at reducing conditions, iron-bearing particles are sticky and can adhere to the surface upon collision. Therefore, small amount of iron (and consequently other inorganic matters) can go and adhere to the bottom sections. This fact caused larger depositions on the wall while working with C4 and A8 as shown in

Figure 3.25. Figure 3.25 shows that the thickness of the deposit materials resulted from A8 is much higher in comparison with C4 and simple feeder.

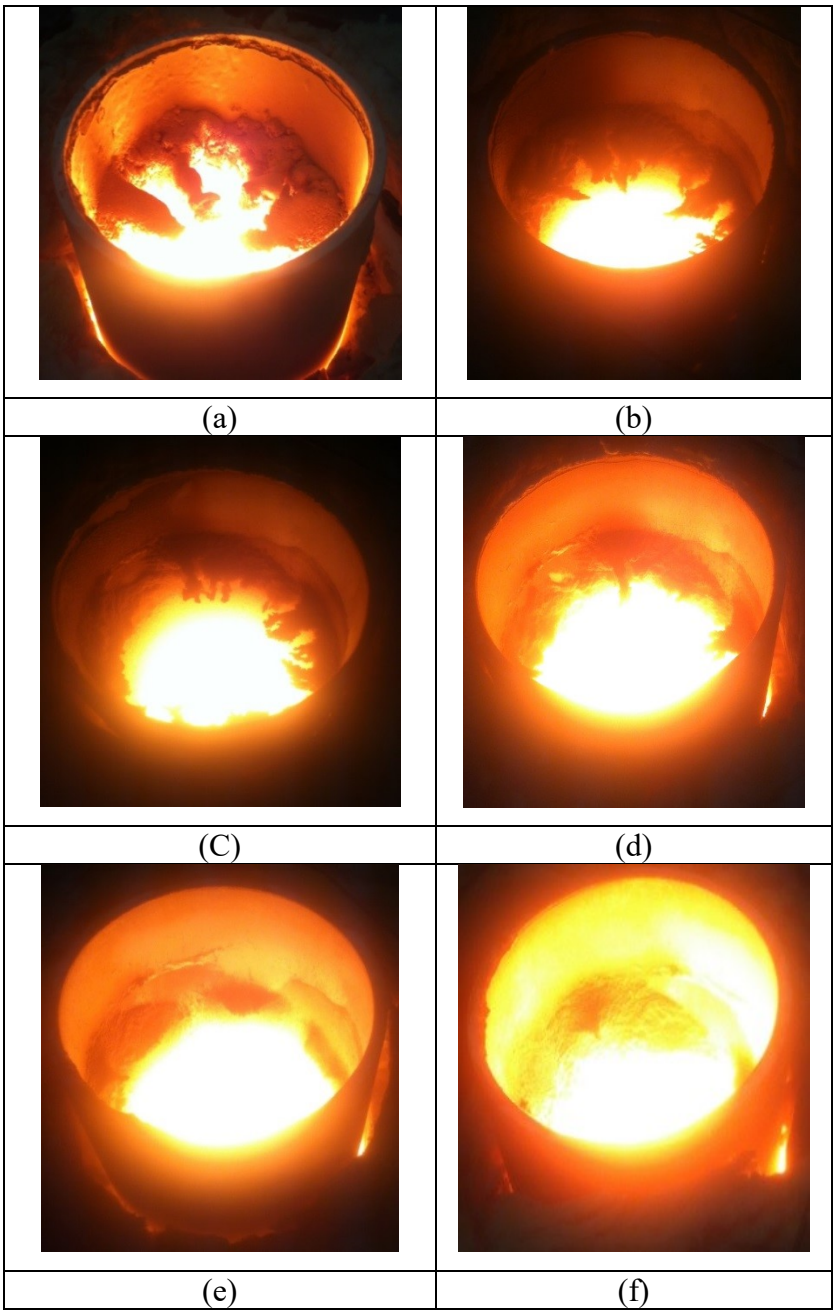

Figure 3.22: **Mineral deposition of Feeder A8, 5cm from top (a) F1S1, T=1450°C, N2:1L/min (b) F1S1, T=1450°C, N2:5L/min,(c) F1S2, T=1450°C, N2:1L/min (d) F1S2, T=1450°C, N2:5L/min (e) F2S1, T=1450°C, N2:1L/min (f) F2S1, T=1450°C, N2:5L/min**

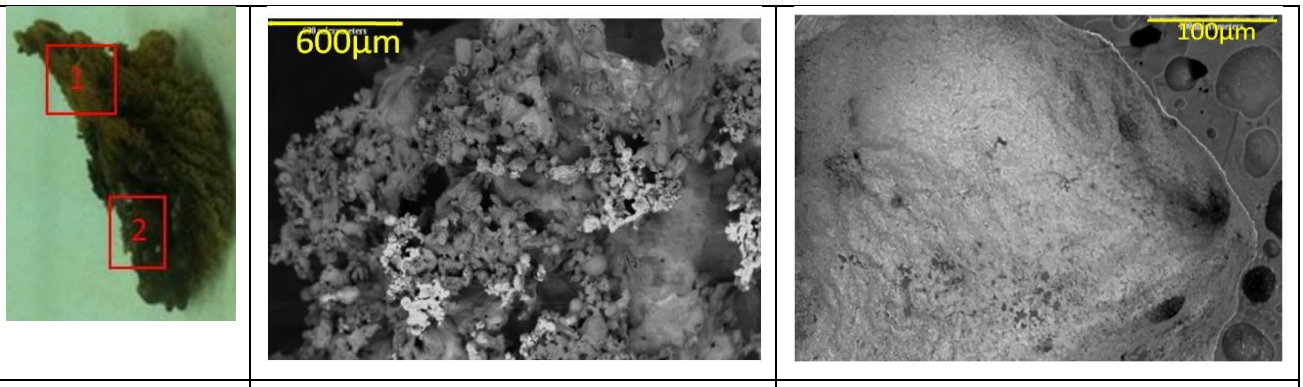

(a) (b) Area 1 (c) Area 2

Figure 3.23: **F1S1, T: 1450°C, Feeder: A8 (a) deposition at top section (b) BSE image of area 1 (c) BSE image of area 2**

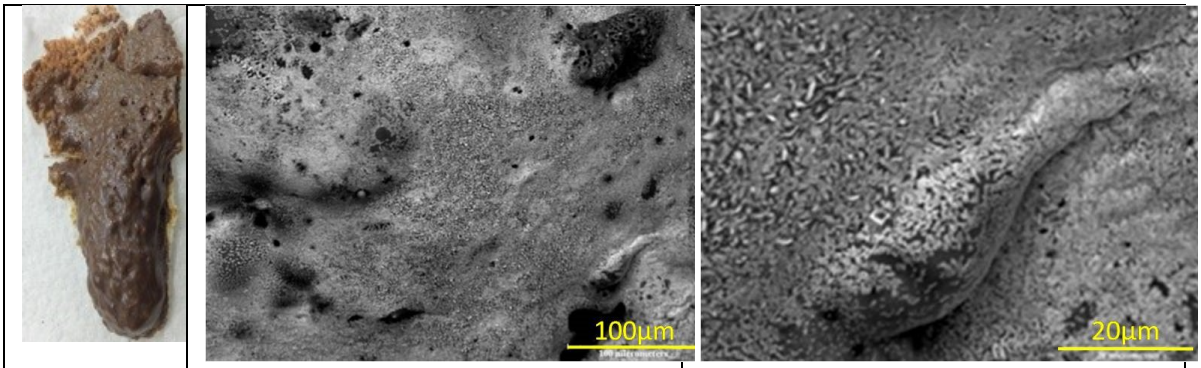

(a) (b) (c)

Figure 3.24: **F1S1, T: 1450°C, Feeder: C4 (a) Deposition at top section (b,c) BSE image of the deposition**

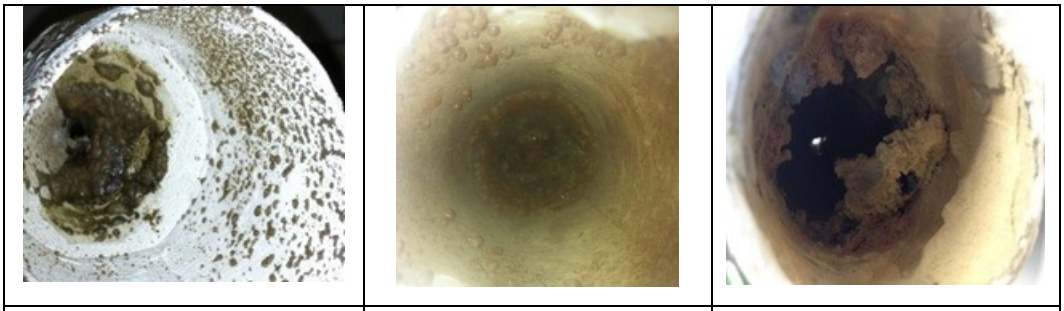

(a) (b) (c)

Figure 3.25: **Deposition resulted by different feeders at top section, T: 1350°C, N: 2L/min (a) simple feeder (b) feeder C4 (c) feeder A8**

3.4.5. Deposition blockage

It must be noticed that there are two kinds of the deposition growth in this study which may lead to the blockage. The first one is the growth of deposition of the sticky inorganic

particles at the place of the feed particles impaction to the wall (feeding zone) which is mostly occurred at the low carrier gas flow rate using A8 feeder. In this case, the top part of the deposit contains sintered sticky particles which start to melt from the bottom to generate slag flow as shown in Figure 3.23. If there is a small flow of slag (which cannot remove enough inorganic deposition out of the area), the deposition growth can be very high leading to the blockage inside a 63.5mm diameter tube. The second type of the blockage is slag flow blockage at the bottom hole of the slag collector plate which is similar to the tapping hole of a gasifier. In this case, when the slag flow rate is not high enough to remove the required amount of the molten slag, gradually the thickness of the deposition will be that much high to cause blockage at the bottom hole of the collector probe. Inadequate slag flow can be the result of two facts. Firstly, the incoming materials to the deposit layer (captured particles) might be too high which is due to the presence of high amount of the sticky particles. The second reason is the high viscosity of the liquid slag which is related to the inorganic composition of the ash content of coal and operating temperature (and also atmosphere inside the furnace). Experimental viscosity measurements for F1 showed that the viscosity of the slag generated from this fuel is too high. Therefore, working with F1, the slag flow must be managed by adding some fluxing material or by increasing the temperature of the furnace to reduce the viscosity.

Table 3.4 shows that for F1, blockage is possible even at very high temperatures. By increasing the temperature from 1350°C to 1450°C and 1550°C, the blockage probability does not decrease, especially at low gas flow rate. It can be concluded that for this coal, increasing the temperature to 1450°C and 1550°C, will not decrease the viscosity that much to increase the slag flow enough to prevent from blockage. At the same time the

stickiness of the particles increases at higher temperatures. This leads to the increase in the inlet mass to the slag layer and finally results in the blockage. For F1, due to the high viscosity of the ash content, working at temperatures up to 1550°C with C4 feeder, resulted in the blockage at the bottom of the slag collector plate. Depending on the operating conditions such as velocity of the particles and temperature (which can be considered in terms of Re and We for modeling purpose), the time after which the blockage occurs might be different. Tables 3.4 and 3.5 show that in some cases the blockage can be prevented by increasing the gas flow rate. The reason is the reduction of the amount of the sticking particles at the higher gas flow rate or higher particle velocity. The results of the experiments show that by increasing the temperature to very high value (1650°C), the slag flow can be fast enough to reduce the blockage probability. Working with F2, blockage might occur only at the low temperatures and low gas flow rates. In case of F2, by increasing the temperature the blockage can be prohibited well. Figure 3.26 shows the tip of the collector plate for F1S1 at different conditions. In order to reduce the blockage probability, three solutions can be proposed. Using fluxing material (or blending with other fuels) in order to reduce the slag viscosity to increase the flow rate of the liquid slag is the first option. Second option is to increase the operating temperature of the furnace. But, increasing the temperature might reduce the cold gas efficiency and also reduce the lifetime of the refractory materials in contact with highly corrosive depositions. The third solution is to increase the velocity of the particles by increasing the carrier gas flow rate to reduce the amount of the sticking particles as the inlet material to the slag layer. This can lead to the reduction in the coal carbon conversion and economically affect the process; therefore, an optimization study is

required. In addition, changing the trajectory of the particles during the gasification process to distribute the inorganic depositions over a wide surface and consequently decrease the deposition thickness can be considered as another management method of the inorganic matters.

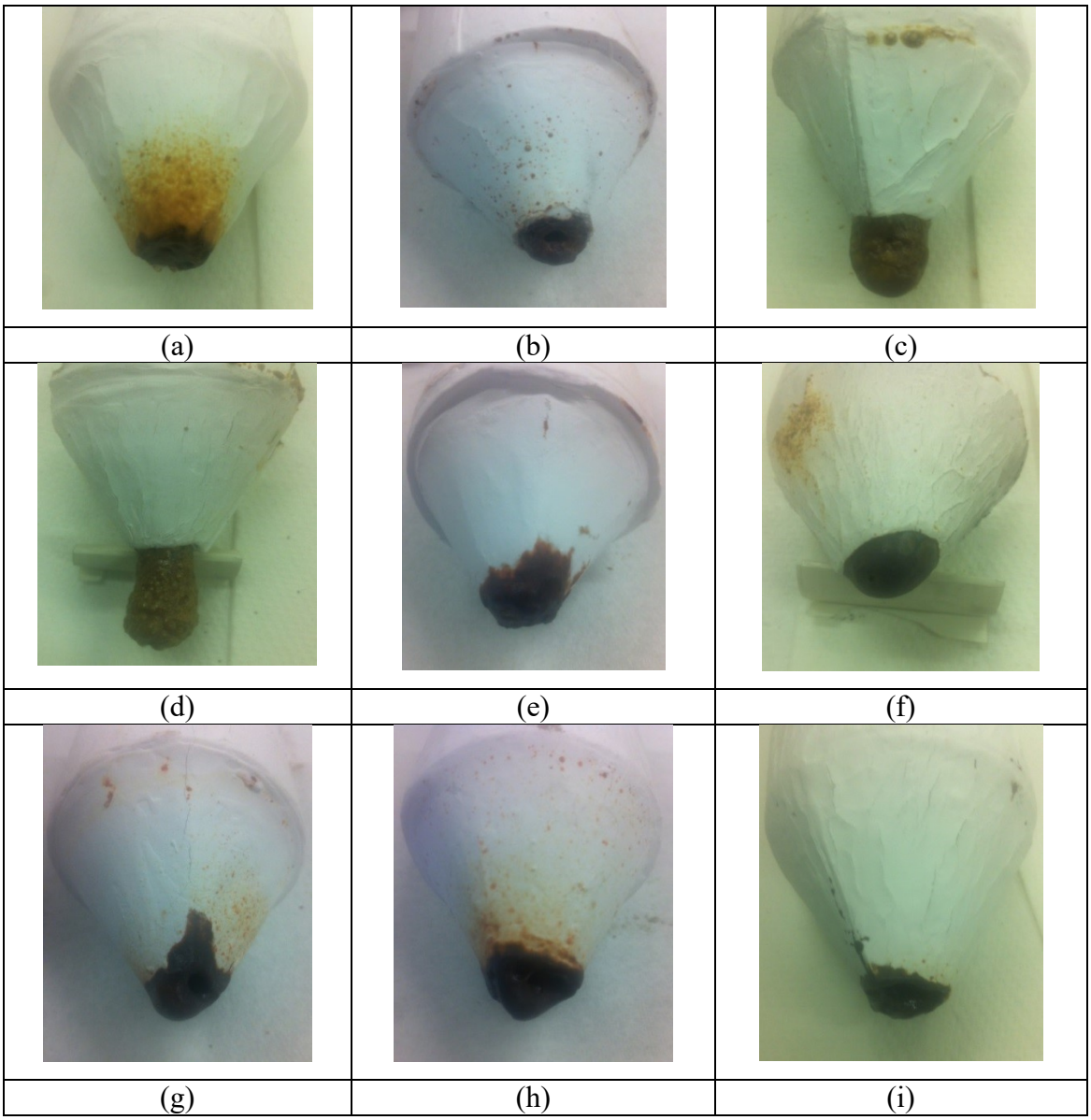

Figure 3.26: **Blockage at the bottom hole of the collector plate at the top section F1S1, Feeder:C4, (a) N: 1L/min, T: 1350°C (b) N: 2L/min, T: 1350°C (c) N: 1L/min, T: 1450°C (d) N: 2L/min, T: 1450°C (e) N: 1L/min, T: 1550°C (f) N: 2L/min, T: 1550°C (g) N: 1L/min, T: 1650°C (h) N:2 L/min, T: 1650°C (i) N: 5L/min, T: 1650°C**

One of the interesting experimental observations in this study is the slag droplet falling from the tap hole of the slag collector probe. The EDX analysis on the surface of the slag droplets showed that their composition is approximately close to the bulk ash composition of the coal. Figure 3.27 shows the slag droplets of F1 and F2. Slag droplets of F1 are larger than the droplets of F2 due to the higher viscosity.

Figure 3.27: **Slag droplets N: 1L/min, 3 droplets at left F2S1 1450°C, 3 droplets at right F1S1 1450°C**

3.5. Conclusion

In this study, gasification experiments with two types of Canadian coal and two different feeder configurations were performed. Two size ranges (coarser and finer) were used for each coal type. Temperature and gas flow rate were varied to evaluate the effect of operating conditions on the ash deposition.

Temperature

In all the experiments, increasing the temperature made the ash particles stickier and led to higher deposition. But, at the same time increasing the temperature reduced the slag viscosity which caused an increase in the flow rate of the molten slag layer. Therefore, by increasing the temperature, the slag flow usually increases. For each coal type, a

minimum value for the temperature might exist at which there is a controllable amount of the inorganic deposition and slag flow to prevent from blockage. But, considering two opposing results of the higher amount of the sticky particles and higher slag flow rate at higher temperatures, it was concluded that increasing the temperature cannot guarantee the safe operation by reducing the deposit thickness.

Gas flow rate (velocity of particles)/particle size

Increasing the gas flow rate in most cases reduced the amount of the deposition for both coals. The reason is most likely related to the kinetic energy of the particles at the moment of impact to the bare wall. In addition, increasing the gas flow rate reduced the residence time of the particles which resulted in the decrease in the carbon conversion of the char particles. Particles with lower carbon conversion are less sticky. Big particles because of higher kinetic energy showed lower deposition tendency than smaller particles at the same condition. Another reason for the higher deposition tendency of the smaller particles is that these particles usually have higher carbon conversion and in addition reach to the environment temperature sooner than the big particles. Therefore, smaller particles start to melt sooner.

Ash composition

For F1, iron showed an important role in the inorganic deposition behavior. CCSEM analysis of this fuel showed that most of the iron-bearing minerals were existed as excluded particles. Under reducing conditions of the gasification process, iron is presented in reduced state which has low melting point. These low melting point particles can be readily captured upon collision with the wall and make it a sticky surface for other particles to stick. Average EDX analysis of the deposition of F1 at different locations

showed that the iron concentration at the top section is much higher than the other sections.

Regarding the deposition tendency of F2, calcium had a significant role. Calcium made the viscosity of the bulk of ash and slag low enough which usually led to the smooth slag flow. In most of the experiments with F2, there was a thin layer of the slag flowing down the wall of the furnace. CCSEM analysis of this fuel showed that excluded minerals of F2 were lower than F1. In addition, most of the calcium-bearing minerals existed as included particles. At high temperatures, the inorganic particles of F2 adhered together and made big agglomeration. The reason is related to the melting of the included calcium-bearing inorganic matters which acted as glue to force other inorganic matters to stick together and make big agglomerations. The size of these agglomerations could reach to more than hundred microns which is hard to stick to the wall at the top section. In lower sections by increasing the carbon conversion and also by increasing the number of times that the particles collide with the wall, the probability of their sticking would increase. Working with F2 lots of inorganic agglomerates were observed in cyclone, but, in case of F1 ash agglomerates in cyclone were much lower.

Feeder configuration/particle trajectory

The deposition was affected by the feeding configuration for both fuels. Feeder A8 resulted in very thick depositions by injecting the coal particles on a narrow area. The severe growth of the deposition resulted by feeder A8 was more observable for F1 due to the high iron concentration on the surface of the deposit. Feeder C4 injected the particles on a wider area than A8, therefore, the deposition resulted by C4 was more uniform with lower deposition thickness.

Blockage probability

The blockage analysis of the collector probes showed that for F1 increasing the temperature form 1350°C to 1550°C did not decrease the blockage probability. In this case, increase in the stickiness of the particles (as the inlet mass to the slag layer) was more effective than the reduction of the slag viscosity at high temperature. Working with F1, even very high operating temperature could not guarantee the safe operation.

Blockage never happened in the slag collector probes during the gasification process of F2 at the temperatures higher than 1250°C. However, there was a very thick layer of the slag near to the bottom of the furnace where the temperature was very low. Using F2 and performing the process at the temperatures higher than 1250°C could assure the safe operation of the gasifier far from blockage. Therefore, the most important required precaution during the gasification process of F2 is adjusting the temperature to be in a specific range (1250°C-1450°C). Lower temperatures lead to the high slag layer thickness and higher temperatures lead to the extra maintenance cost due to the material loss and corrosion.

Acknowledgement

This study is financially supported by C^5MPT and Helmholtz- Alberta initiative (HAI) center. The authors thank to Dr. Farshid Vejahati for his great job of building the entrained-flow drop tube furnace used as the gasification setup in this study and also for all his guides and supports during the experiments.

Reference

[1] Luan C, You C, Zhang D, An experimental investigation into the characteristics and deposition mechanism of high-viscosity coal ash. Fuel 119 (2014) 14–20

[2] Zbogar A, Frandsen F, Jensen P A, Glarborg P, Shedding of ash deposits. Prog Energy Combust Sci 2009;35:31–56.

[3] Gupta S, Gupta R, Bryant G, Wall T, Watanabe S, Kiga T, Characterization of ash deposition and heat transfer behavior of coals during combustion in a pilot-scale facility and full-scale utility. Energy Fuels 2009; 23:2570–5.

[4] Yang Z, Wang Z, Wu Y, Wang J, Lu J, Li Z, Ni W, Dynamic model for an oxygen-staged slagging entrained-flow gasifier, Energy Fuels 2011, 25, 3646-3656

[5] Song W, Tang L, Zhu X, Wu Y, Zhu Z, Koyama S, Flow properties and rheology of slag from coal gasification, Fuel 89 (2010) 1709–1715

[6] Richards G H, Slater P N, Harb J N, Simulation of ash deposit growth in a pulverized coal-fired pilot scale reactor. Energy Fuels 1993;7:774–81.

[7] Arvelakis S, Folkedahl B, Dam-Johansen K, Hurley J, Studying the melting behavior of coal, biomass, and coal/biomass ash using viscosity and heated stage XRD data. Energy Fuels 2006;20:1329–40.

[8] Liu Y, Wu M, Qian J, Predicting coal ash fusion temperature based on its chemical composition using ACO-BP neural network. ThermochimActa 2007;454:64–8.

[9] Yin C, Luo Z, Ni M, Cen K, Predicting coal ash fusion temperature with a back-propagation neural network model. Fuel 1998;77:1777–82.

[10] Wall T, Creelman R, Gupta R, Gupta S, Coin C, Lowe A, Coal ash fusion temperatures-new characterization techniques, and implications for slagging and fouling. Prog Energy Combust Sci 1998;24:345–53.

[11] Winegartner E, Rhodes B, An empirical study of the relation of chemical properties to ash fusion temperatures. J Eng Power 1975;97:395.

[12] Skodras G, Sakellaropoulos G P, Mineral matter effects in lignite gasification, fuel process technology 77-78 (2002) 151-158

[13] Winegartner E, Coal fouling and slagging parameters. New York: American Society of Mechanical Engineers; 1974.

[14] Browning G, Bryant G, Hurst H, Lucas J, Wall T, An empirical method for the prediction of coal ash slag viscosity. Energy Fuels 2003;17:731–7.
[15] Jung B, Schobert H H, Improved prediction of coal ash slag viscosity by thermodynamic modeling of liquid-phase composition. Energy Fuels 1992;6:387–98.
[16] Raask E, Mineral impurities in coal combustion, Behavior, Problems and Remedial Measures, Hemisphere Publishing Corporation, New York, 1985.
[17] Song W, Tang L, Zhu X, Wu Y, Rong Y, Fusibility and flow properties of coal ash and slag, Fuel 88 (2009) 297–304
[18] Wei Y, Li H, Honma K, Tanoskai T, Ninomiya Y, Effect of additives on slag properties in an entrained bed gasifier, World of Coal Ash (WOCA) Conference, 2011, Denver, USA
[19] Ling-xue K, Jin B, Wen L, Zong-qing B, Zhen-xing G, Effect of lime addition on slag fluidity of coal ash, J Fuel ChemTechnol, 2011, 39(6), 407-411
[20] Lu T, Zhang L, Zhang Y, Feng Y, Li H X, Effect of mineral composition on coal fusion temperature. Journal of Fuel Chemistry and Technology, 2010, 38(2): 23–28.
[21] Duchesne M, Macchi A, Lu D, Hughes R, Artificial neural network model to predict slag viscosity over a broad range of temperatures and slag compositions, Fuel Processing Technology 91 (2010) 831–836
[22] Gupta S, Dubikova M, French D, Sahajwalla V, Effect of CO_2 gasification on the transformations of coke minerals at high temperatures, Energy & Fuels 21 (2) (2007) 1052
[23] Losurdo M, Spliethoff H, Kiel J, Ash deposition modeling using a visco-elastic approach, Fuel 102 (2012) 145–155
[24] Brachi P, Montagnaro F, Salatino P, Char-Wall Interaction and Properties of Slag Waste in Entrained-Flow Gasification of Coal, European Combustion Meeting 2011
[25] Li S, Whitty K J, Investigation of Coal Char−Slag Transition during Oxidation: Effect of Temperature and Residual Carbon, Energy Fuels 23 (2009) 1998–2005
[26] Rushdi A, Gupta R, Sharma A, Holcombe D, Mechanistic prediction of ash deposition in a pilot-scale test facility, Fuel 84 (2005) 1246–1258

[27] Mueller C, Selenius M, Theis M, Skrifvars B J, Backman R, Hupa M, Tran H, Deposition behavior of molten alkali-rich fly ashes—development of a submodel for CFD applications, Proceedings of the Combustion Institute 30 (2005) 2991–2998
[28] Shannon G N, Rozelle P L, Pisupati V, Sridhar S, Conditions for entrainment into a FeOx containing slag for a carbon-containing particle in an entrained coal gasifier, Fuel Processing Technology 89 (2008) 1379–1385
[29] Ni J, Yu G, Guo Q, Zhou Z, Wang F, Sub-model for predicting slag deposition formation in slagging gasification systems, Energy Fuels 2011, 25, 1004–1009
[30] Montagnaro F, Salatino P, The role of slag formation on late carbon conversion in entrained-flow gasification of coal, Dipartimento di Chimica, Universita Studi di Napoli Federico II, Napoli, Italy, 2009
[31] Montagnaro F, Salatino P, Analysis of char–slag interaction and near-wall particle segregation in entrained-flow gasification of coal, Combustion and Flame 157 (2010) 874–883
[32] Yong S Z, Gazzino M, Ghoniem A, Modeling the slag layer in solid fuel gasification and combustion – Formulation and sensitivity analysis, Fuel 92 (2012) 162–170
[33] Shimizu T, Tominag H, A model of char capture by molten slag surface under high temperature gasification conditions, Fuel 85 (2006) 170–178
[34] Wall T F, Liu G S, Wu H W, Roberts D G, Benfell K E, Gupta S, Lucas J A, Harris D J, The effects of pressure on coal reactions during pulverized coal combustion and gasification, Progress in Energy and Combustion Science 28 (2002) 405–433.
[35] Yu G, Zhu Q, Chi G, Guo Q, Zhou Z, Study on slag composition and flow property in a bench-scale OMB gasifier, Fuel Processing Technology 2012
[36] Costen P G, Locwood F C, Siddique M.M, Mathematical modeling of ash deposition in pulverized fuel-fired combustors, Proceedings of the Combustion Institute, Volume 28, 2000/pp. 2243–2250
[37] Chen L, Yong S Z, Ghoniem A F, Modeling the slag behavior in three dimensional CFD simulation of a vertically-oriented oxy-coal combustor, Fuel Processing Technology 112 (2013) 106–117

[38] Ni J, Liang Q, Zhou Z, Dai Z, Yu G, Numerical and experimental investigations on gas–particle flow behaviors of the Opposed Multi-Burner Gasifier. Energy Conversion and Management 50 (2009) 3035–3044
[39] Li Z, Zeng L, Zhao G, Shen S, Zhang F, Particle sticking behavior near the throat of a low-NOx axial-swirl coal burner. Applied Energy 88 (2011) 650–658
[40] Barroso J, Ballester J, Pina A, Study of coal ash deposition in an entrained flow reactor: Assessment of traditional and alternative slagging indices. Fuel Processing Technology 88 (2007) 865–876
[41] Duchesne M, Hall A, Hughes R, McCalden D, Anthony E, Macchi A, Fate of inorganic matter in entrained-flow slagging gasifiers: Fuel characterization. Fuel Processing Technology 118 (2014) 208–217
[42] Kreutzkam B, Wieland C, Spliethoff H, Improved numerical prediction of ash formation and deposition using a novel developed char fragmentation model. Fuel 98 (2012) 103–110
[43] Weber R, Mancini M, Schaffel-Mancini N, Kupka T, On predicting the ash behavior using Computational Fluid Dynamics. Fuel Processing Technology 105 (2013) 113–128
[44] Lin S, Hirato M, Horio M, The characteristics of coal char gasification at around ash melting temperature. Energy & Fuels 8 (1994) 598–606
[45] Degereji M U, Ingham D B, Ma L, Pourkashanian M, Williams A, Prediction of ash slagging propensity in a pulverized coal combustion furnace, Fuel 101 (2012) 171–178
[46] Vejahati F, Entrained-flow gasification of oil sand coke, PhD thesis, Department of Chemical and Materials Engineering, University of Alberta, Spring 2012

Chapter 4. Inorganic particles deposition based on controlled injection

4.1. Abstract

Considering the high cost of performing gasification experiments, predicting the inorganic deposition and slag layer formation using CFD models have been the topic of many researches. An accurate evaluation of the fate of the particles at the moment of collision with the wall is a critical step for a reliable model. In this work, inorganic content of a Canadian coal were injected under controlled conditions such as temperature, velocity and impact angle on the surface of half-cylindrical ceramic plates to evaluate the particle deposition behavior at different conditions. Percentage of the weight increase of the plates is presented for each specific condition.

Increasing the temperature resulted in increase in the amount of the deposition for all the experiments. At higher temperature, the effect of the temperature increase is lower. By

increasing the impact angle, the amount of the deposition increases slightly, however, impact angle is not the only affecting angle and at the same time, the orientation of the wall must be considered. Increasing the particle velocity slightly led to the higher deposition at high temperature and reduced the deposition at lower temperature. The dependence of the particle deposition to temperature is higher than the velocity and impact angle.

Keywords: Inorganic deposition, operating condition, particle impact angle

4.2. Introduction

Performance, reliability and efficiency of the coal gasification or combustion process are strongly influenced by the inorganic behavior. Fusion of the inorganic matters in the char particles at high temperature might hinder further reactions and lower carbon conversion. Molten and solid slag layers on the wall can affect the heat transfer drastically. Unsteady and uncontrolled flow might cause blockage at the bottom of the reactor. Reliability of the process which is strongly affected by the inorganic behavior is one of the main issues for plenteous industrial application of the gasification process [1-5].

Upon impaction of the ash particle to the bare wall or to the surface of the deposit, the viscosity and surface tension are thought to be the controlling factors [6]. Traditional sticking coefficients are mostly based on the viscosity (by comparison of the viscosity with a threshold value) to decide if a particle is captured or bounced off the surface [7]. Tominaga et al. [8] and Walsh et al. [9] related the char capture probability to the viscosity of the char particle and slag layer and assumed that when the viscosity is lower than a certain value then the particles will be captured. Many studies have been

performed to investigate the inorganic matter behavior focusing mostly on the viscosity, temperature of critical viscosity and ash fusion temperature in terms of the empirical and semi-empirical indices such as alkali index and base to acid ratio to characterize the inorganic deposition behavior of different fuels. Several correlations have been proposed to predict the viscosity mostly based on the temperature and composition [10-24]. It is also proved that atmosphere influences the state of the existence of some components such as iron which results in the great changes in viscosity [25-26]. Therefore, the dependency of the viscosity and ash fusion temperature has been widely investigated in terms of mineral compositions, additives, atmosphere and operating conditions.

Today due to the increasing interest toward wider application of the coal gasification process and inaccuracy of the empirical viscosity-based slagging indices, more accurate method for prediction ash deposition and slag formation is desired. Comprehensive CFD modeling of gasification including inorganic deposition and slag formation has been the topic of numerous researches in this regard. Based on the requirement for more accuracy, relying only on the viscosity and fusion temperature is not satisfying as the only criterion for prediction of the inorganic behavior in CFD modeling. Ash particles behavior at the moment of collision with the wall at different locations depends on their properties, operating condition of the furnace and the conditions of the wall. This phenomenon is of crucial importance in CFD modeling, because, it determines the inlet materials which form the slag layer. Temperature, composition, velocity and impact angle of the incoming particle in combination with the target surface properties such as composition of the current deposit layer are the main factors determining the fate of particles [27-30].

Luan et al. [4] analyzed the influence of the temperature, impact velocity, deposition time and fuel particle size on the mineral deposition behavior using a probe and found inverse relation between particle impact velocity and ash deposition. They observed that high inertia particle in contact with low temperature surface had lowest deposition tendency. Particle capture efficiency increases by increasing the carbon conversion and there is a sharp increase in the capture efficiency above a certain conversion value which is called critical conversion [7]. Li and Whitty [30] observed that operating at temperatures higher than ash flow temperature is not enough to make the char particles sticky and only at carbon conversions more than 90% the transformation from porous carbonacious char which is non-sticky to molten and sticky slag happens. Degereji [31] studied the surface properties and contact angle of the particles upon impact and proposed a slagging index based on viscosity, ash fusion and ash loading and reported a good agreement with experimental data. Mueller et al. [32] introduced a particle capture criterion based on the kinetic energy of the particles and total surface energy. The size of the particles must be considered as an affecting parameter as Costen et al. [33] observed the different behavior of inorganic matters based on their sizes. Yong et al. [34] proposed a capture criterion considering the relation between the particle velocity (v_p), particle diameter (d_p), particle density (ρ_p) and surface tension (γ) in term of Weber number.

$$We = \frac{Particle\ kinetic\ energy}{surface\ tension\ energy} = \frac{\rho_P v_P^2 d_P}{\gamma} \qquad (4-1)$$

They reported that, if the Weber is lower than the critical Weber number (We_{cr}), then the particle is probable to stick and assumed this critical number to be 1.

In most of the proposed criterions, the properties of the bulk of ash was used for all the interactions, but, Yu et al. [35] reported that using overall ash composition is not a good approach to analyze the interactions on all the surfaces covered with molten layer, because, particle are deposited based on their composition and this fact lead to the different local compositions and properties at different locations. The same observation is reported by Wall et al. [37]. In addition, the difference between bare wall and slag covered wall must be considered in an accurate criterion, because, particles may be captured easier upon colliding with the sections which is covered by liquid slag layer than in the case of the dry walls [34]. Shimizu and Tominaga [36] performed experimental analysis to investigate the char-slag interaction using a ceramic tube in an electric furnace. Having assumption for the formation of only a single layer of the char particles on the slag surface, they proposed a criterion for char-slag interaction based on that, if a char particle hit the surface of the slag it will be captured otherwise it will bounce off the surface. Based on this model, by increasing the char feed rate, the char capture rate decreases. Therefore, the phenomena of the char capture by slag layer plays a vital role, specially, when the char particles are not that much reactive. The main issue in their experiments was that the type of injection was not identical to the real situation, because, feeding was not implemented on the vertically flowing layer and also, the impact angle was not controlled as an affecting parameter. Montagnaro et al. [38, 39] studied the influence of the carbon loading on the surface of slag brought by the colliding char particles. They characterized the situation at which incoming particles get encapsulated by slag or trapped at the surface by comparing inertial, viscous and interfacial forces. They reported that, in non-vertical walls the buoyancy force must be taken into

consideration. They found out that only the high inertia particles (big particles with high velocity) interacting with molten liquid layer with low viscosity can plunge completely into the molten slag layer. Shannon et al. [40] based on the force balance formulation acting on the particles, proposed a capture model in terms of viscosity, surface tension and impact velocity as the main affecting factors. Mao et al. [41] studied the ash deposition in kraft recovery and in order to derive a capture criterion, applied energy balance while stretching and recoiling of the molten particle at the moment of impact. They defined excess energy in relation with the maximum value of the diameter that a particle might have after spreading. This diameter is called maximum spreading diameter. When the excess energy is positive, the particle will rebound otherwise it sticks to the surface. The particle spread can also be simulated with numerical modeling by solving Navier-Stokes equations which is very time consuming [42-43]. Assuming the inertia of the particles as the main affecting parameter, Ni et al. [44] used the model of Mao et al. [41] to apply it for gasification process. They reported that the maximum spread diameter of the particles at the moment of impact is a vital factor for particle sticking and introduced a model in terms of excess impact energy as a function of Reynolds and Weber number.

Particle trajectory and impact direction, affect the deposition behavior of the particles including chars and ash. Although, some studies reported the different behavior of the inorganic deposition based on the particle trajectories and feeding configuration [45-48], but, it is not well investigated.

In this work, the ash particles of a Canadian coal were used for injection on the surface of the half-cylindrical ceramic plates, installed on the wall of a drop tube furnace, under the

controlled condition. In each experiment the temperature, velocity and impact angle of the particles at the moment of impact was adjusted and the deposition results were quantified.

4.3. Experiments

The objective of the experiments in this study is to implement the controlled injection of the ash content of coal on a ceramic plate in order to evaluate the effect of the operating conditions on the inorganic matter deposition to be used as the particle capture criterion. The inorganic residue of coal is used to be injected through a 3/8" stainless steel tube on a removable ceramic plate inside a drop tube furnace. The ceramic plate is half-cylindrical with the diameter of 5.5cm and the length of 10 cm. By using the tubes with different tips the particles can be injected with specific angle. Figure 4.1 shows the tubes used for the injection with different impact angles.

Figure 4.1: Tubes with different tips to produce different impact angles

The ceramic plate was installed on a half cylindrical metal sheet which can be removed after each experiment at high temperatures. The injection point is located 25cm inside the furnace. After doing the experiment with specific impact angle (θ), the tube was changed

to repeat the experiment with a different impact angle. The injection setup shown in Figure 4.2, was placed inside an electrically heated drop tube furnace which is shown in Figure 4.3. The ceramic tube of the furnace with 6.35cm ID and 153cm total height can be used for temperatures up to 1500°C [52]. The feeder consists of a screw feeder including a hopper and stirring rod. Uniform feed injection was achieved by vibrating walls of the hopper to prevent bridging of the fine particles [52]. Nitrogen is used as carrier gas and by controlling the nitrogen flow rate the velocity of the particle was adjusted. A 3/8 inch tube transferred ash particles and nitrogen from feeding hopper into the furnace.

Figure 4.2: Injection set up including injector tube, removable ceramic plate and holder metal sheet

In order to prepare the ash particles for injection, a Canadian coal is grinded, sieved and the size range of 150-212 micron is separated and burned in a muffle furnace with carbon

conversion of 94%. The analysis of the coal and its inorganic content are shown in Tables 4.1 and 4.2. The ash fusion temperature analysis and the viscosity measurement for inorganic content of this fuel performed by Duchesne et al [49] are presented in Table 4.3 and Table 4.4.

Table 4:1: Proximate and ultimate analysis of the coal

Proximate analysis	w%	Ultimate analysis	w%
Volatile matter	34.27	C	50.8
Fixed carbon	43.01	H	3.5
ash	10.50	N	0.9
moisture	12.22	S	0.5
		O	44.3

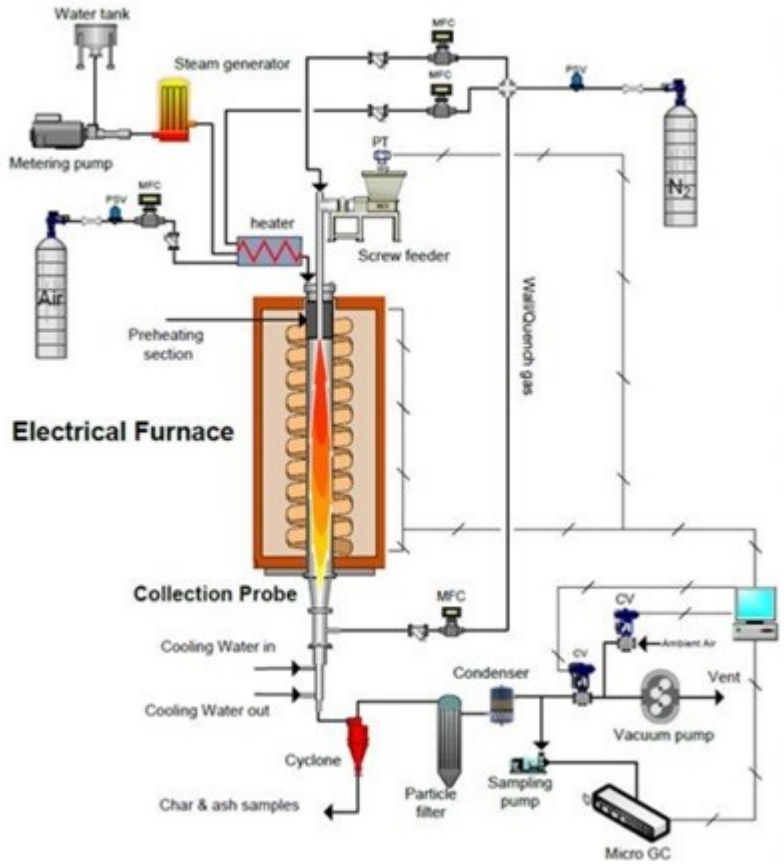

Figure 4.3: Atmospheric electrically heated drop tube furnace [52]

During each experiment 20g of the inorganic matters is injected on the ceramic plate. To quantify the results, the weight of the receiving ceramic plates is recorded before and at after each experiment and the percentage of the particles deposition is measured. During the experiments, the tubes must be cleaned several times by high pressure air. Fluctuation of the manometer of carrier gas helps to know when cleaning is required.

Table 4:2: Ash composition analysis

Inorganic composition	W%	STDEV
SiO2	26.5	0.74
Al2O3	16.9	0.39
Fe2O3	8.1	0.52
CaO	22.6	0.51
Na2O	5.1	0.17
MgO	3.9	0.18
BaO	1.5	0.16
TiO2	0.9	0.05
SO3	13.8	0.49
P2O5	0.6	0.06
STDEV: Standard Deviation		

Table 4:3: Ash fusion temperature analysis in °C [41]

	Oxidizing	Reducing
Initial	1191	1096
Spherical	1268	1107
Hemispherical	1299	1118
Fluid	1332	1177

Table 4:4: Viscosity measurement of ash [41]

Temperature (°C)	Viscosity (Pa.s)
1150	298.77
1200	91.7
1250	29.1
1300	14.3

The ash deposition rate in any coal utilization process can be analyzed as a function of the adhesion efficiency. Adhesion efficiency is defined as the ratio of the particle capture efficiency to the particle collision probability. Capture efficiency is expressed as the ratio of the particle mass captured by the surface to the total particle mass in the projected area [50]. Based on the configuration of the injection setup, it can be assumed that all the particles collide with the surface of the receiver plate; therefore, the collision probability can be assumed to be 1. Therefore, the capture efficiency equals to the adhesion efficiency and is introduced as the ratio of the mass of deposit collected on the ceramic plate to the total mass of the injected ash.

$$DP(\%) = \frac{mass\ of\ deposit\ on\ the\ ceramic\ plate}{total\ mass\ of\ injected\ ash} \times 100\% \qquad (4-2)$$

Figure 4.4 shows the deposition on the ceramic plate.

Figure 4.4: Particle deposition on the ceramic plate (T=1200°C, θ=60°)

4.4. Results and discussion

4.4.1. Effect of Temperature

During each coal utilization process, both ash deposition and slag flow are affected strongly by the temperature. Based on the mineral composition and atmosphere in the furnace, inorganic particles can be melted and sticky. Based on the literatures, stickiness of the particles is mostly related to the viscosity which decreases by increasing the temperature. In Table 4.4, the experimentally measured viscosity of the ash content of the coal is presented which shows a decrease rate by increasing the temperature. Carbon conversion as another parameter affecting the stickiness of the particle increases with temperature. In this study, ash particles with constant conversion are injected under an inert atmosphere. Therefore, temperature does not change stickiness in term of carbon conversion and only affects the inorganic properties.

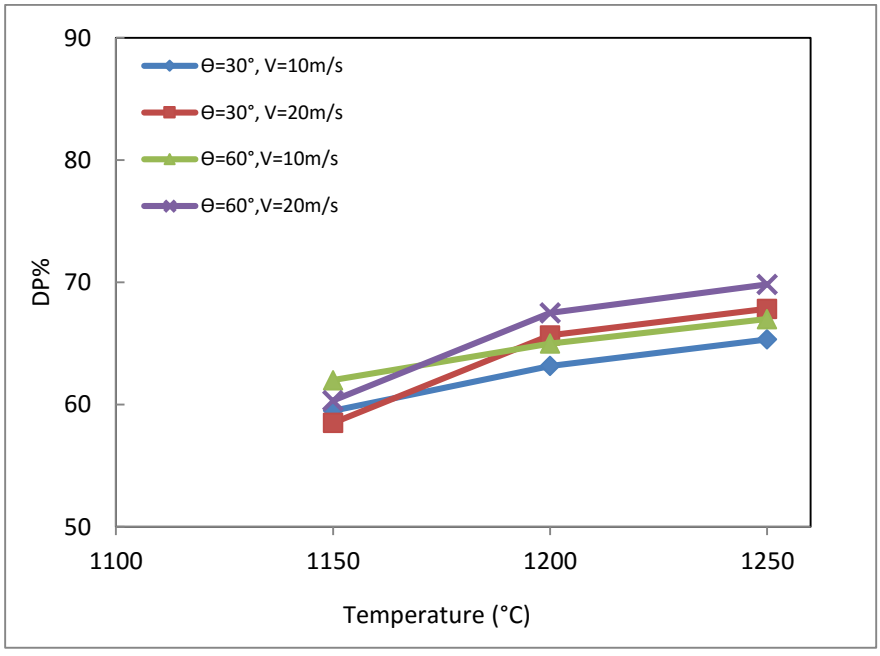

Figure 4.5: Effect of temperature on the particle deposition

The result of the ash deposition as a function of the temperature is shown in Figure 4.5. As it can be seen in this figure, for all the conditions of the impact angle and velocity by increasing the temperature the amount of deposition increases. Increasing the deposition at higher temperatures, was observed in experimental analysis performed by Yong et al. [34] and Luan et al. [4]. If the particles have lower viscosity at the colliding time with the surface, the energy loss will be larger. Therefore, the particles with lower viscosity will not have enough energy to rebound after collision and consequently are highly probable to stick to the surface [4]. Based on the studies of Ni et al [44], surface tension rises up at the higher temperatures and that might be the reason of the less rebound tendency at higher particle temperatures. The rate of increase in DP% for the first fifty degree rise in the temperature is usually higher than the second fifty degree. The reason might be related to the amount of the decrease in the viscosity from 1150°C to 1200°C which is 207.07 Pa.s and from 1200°C to 1250°C which is 62.6 Pa.s.

Analyzing the morphology of the ash using SEM images is very beneficial to understand the ash deposition behavior in term of the structural change at different temperatures. Figure 4.6 shows SEM images of the ash at different temperatures. Based on this figure, at temperature of 1200°C and higher the morphology of the melted ash does not change that much and the liquid fraction of the ash seems to be high, but, at lower temperatures, the deposition is mostly composed of the partially melted agglomerated spherical particles which is similar to sintered deposition. Performing thermodynamic calculations using FactSage can be very useful in this regard to calculate the liquid fraction of the ash particles at each specific temperature.

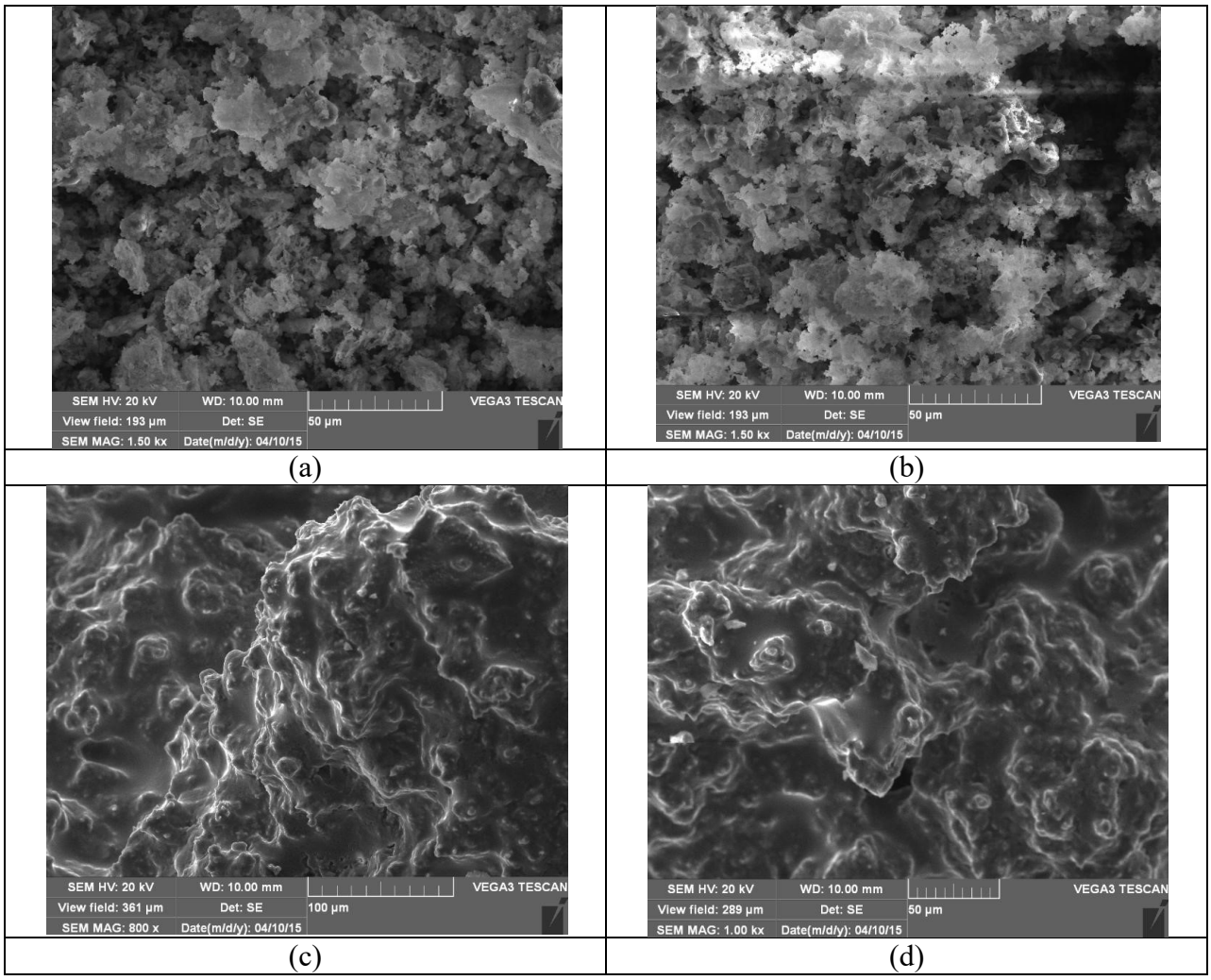

Figure 4.6: SEM images of ash (a) 1100°C (b) 1150°C (c) 1200°C (d) 1250°C

4.4.2. Effect of particle velocity

As the ash particles are transferred into furnace by nitrogen, the velocity of the particles at the moment of impact can be adjusted by the nitrogen flow rate. Depending on the existing condition, increasing the particle velocity might result in various behaviors of the particles and inorganic deposition. If the particle collides with a wet or slag covered walls the capture probability is higher [34]. Big particles with high impact velocity in contact with very low viscosity slag can penetrate into it and get engulfed completely into the

molten liquid layer [39]. If the particles hit the dry target, by increasing the velocity the probability of the rebounding is mostly higher, because, at higher velocity the particles have higher kinetic energy at the moment of impaction and due to the low dissipation of the initial energy on dry wall, the particles possess enough energy to bounce off [4,32].

Figure 4.7 shows the deposition in term of the particle velocity. The dependence of the deposition to the velocity is very low especially in comparison with the temperature. But, it can be seen that at lower temperature increasing the velocity slightly reduces the deposition and in higher temperature slightly increases the deposition.

Although, material properties and operating conditions are very important in the inorganic deposition behavior, but, the state of the impacting particle such as spherical or deformed is another affecting parameter in ash deposition. In this regard, it should be noticed that when a particle which is partially or fully melted impacts a surface, the cases presented in Figure 4.8 might be resulted. The particle can stick to the surface if all the possessed energy of that is dissipated by the target surface and if the dissipated energy at the moment of collision is lower than initial kinetic energy, then the particle will rebound [51]. When a molten particle with specific kinetic energy (based on its size, density and velocity) collide with a surface, the kinetic energy will be consumed while the particle is stretching out in radial direction [50]. By gradual conversion of the firstly possessed kinetic energy to the surface energy (a part of the energy will be lost as well), the particle deformation through stretching continues until the particle reaches to a state having highest possible diameter which is called splat state [50]. The highest possible diameter is introduced as a parameter called maximum spread, which is a diameter higher than that, more increase in the molten droplet diameter is not possible. The reason is that viscosity

and surface tension prohibit more deformation in the particle structure beyond maximum spread diameter. At the end of the spreading phenomenon, the initial spherical molten ash particle will be like a disk in splat condition as shown in Figure 4.8(a). Then the particle starts to recede (to go back to its initial shape) because the splat condition is non-equilibrium. Based on the wetability, particle impact condition and the operation condition at the moment of impact, the stretched particle might stick to the surface or recoil [50]. While recoiling, the amount of the remained energy possessed by the particle, determines if the particle sticks or not. The ratio of the maximum spread diameter to the initial diameter of the particle is a function of the Weber and Reynolds number [7,50].

Several numerical and analytical models have been developed to the predict the maximum spread diameter of droplet [7,50]. Mao et al. [41] developed a semi-empirical model for isothermal condition, which predicts the maximum spread in terms of the Weber number, Reynolds number, and contact angle as below:

$$\left[\frac{1}{4}(1-\cos\beta)+0.2\frac{We^{0.83}}{Re^{0.33}}\right]\left(\frac{d_m}{d_p}\right)^3-\left(\frac{We}{12}+1\right)\left(\frac{d_m}{d_p}\right)+\frac{2}{3}=0 \qquad (4-3)$$

In above equation d_m is the maximum spread diameter and d_p is the initial diameter. Based on this equation, the maximum spread increases at higher values of the Reynolds and the Weber number. Larger maximum spread upon impact causes to increase in the adhesion efficiency. In this regard higher kinetic energy is a crucial parameter which can lead to the higher spread [50]. Considering the particles to be fully melted at high temperatures, the concept and models of the spread diameter can explain the increase in the ash deposition with increasing the particle velocity at high temperatures. Based on the excess energy model by Mao et al. [41] and Ni et al. [44], for a molten particle at higher

temperature and higher kinetic energy, the capture probability is higher. Having higher velocity helps the particles to penetrate into the molten layer easier and this could be another reason for the increased in the deposition with high velocity and at high temperatures.

The reduction in the deposition by increasing the velocity at low temperatures is observed in some researches such as the works done by Chen et al. [47] and Yong et al. [34] who reported that particles with high kinetic energy usually tend to bounce off. Chen et al. [47] observed that when the velocity is low, even particles with low carbon conversion could be trapped. They reported that for the high carbon content char particles which are not completely melted, if the Weber number (the ratio of the kinetic energy to the interfacial surface tension energy) is low, even in contact with dry wall the particles might be captured.

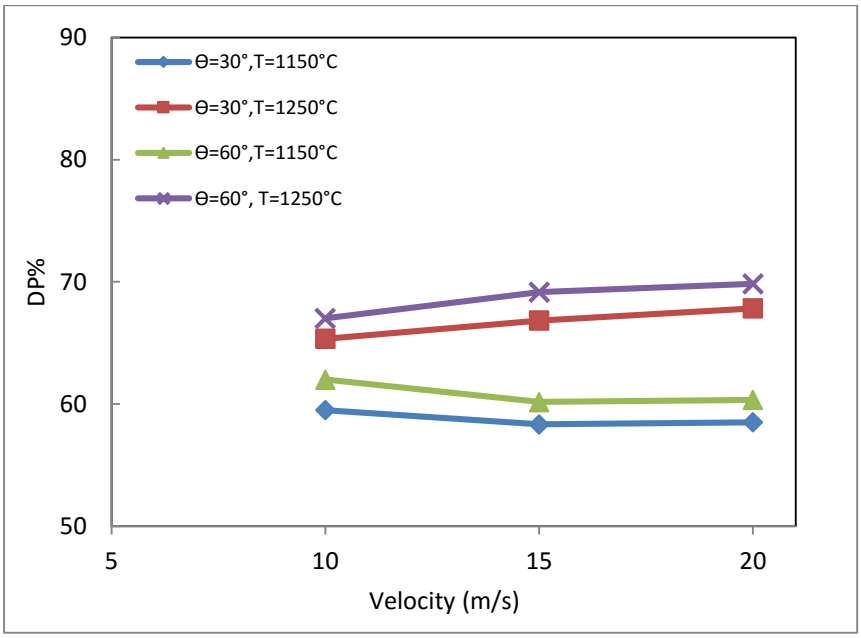

Figure 4.7: Effect of velocity on the particle deposition

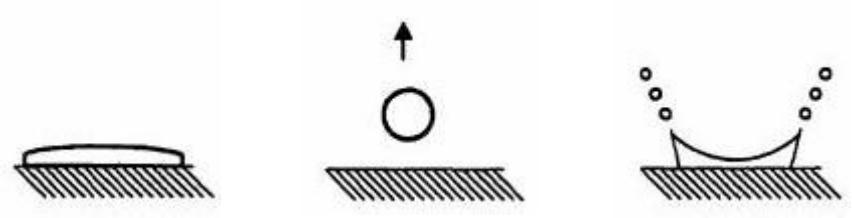

(a) (b) (C)

Figure 4.8: Behaviours of a drop falling impact (a) spread (b) rebound (c) splash [50]

4.4.3. Effect of particle impact angle

Injection experiments were performed for impact angles (θ) of 30° and 60° and the results can be compared in Figures 4.5 and 4.6. It was planned to do the experiments for impact in normal direction (θ=90°), but, too much sticking of the ash particle to the tube at the bending point near the tip, affected the weight measurement and accuracy of the results. Based on Figures 4.5 and 4.6, the deposition for impact angle of 60° is usually higher compared with 30°, however, the difference is very low. Based on Figure 4.9, when a particle hits the wall with impact angle of θ, the velocity of the particle (V_p) can be decomposed into the normal velocity (V_n) and tangential velocity (V_t). Increasing the normal velocity at low temperatures raises the rebounding probability by increasing the kinetic energy [34,47]. But, at higher temperatures when the liquid fraction of the particles is higher, increasing the velocity raises the We number which lead to increase in the maximum spread and consequently results in the higher deposition. Tangential component of the velocity always reduces the deposition, because, it pushes the particle downward on the wall, reduces the retention time and prevents the particles to stick. The effect of the tangential component of the velocity is similar to the effect of the gravity in the vertical sections which must be defeated by the sticking forces for a particle to be

captured. By increasing the impact angle, the tangential component of the velocity decreases and this can explain the higher deposition of θ=60°. The reason of the small difference between the depositions might be related to the high stickiness of the ash particles (burned coal particles with very high carbon conversion) which minimizes the effect of the other parameters to be observable.

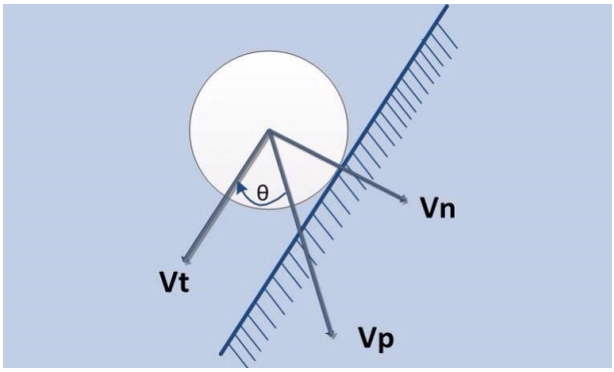

Figure 4.9: Decomposition of the velocity of particle into the normal and tangential components

$V_t = V_P \cos\theta \qquad (4-4)$

$V_n = V_P \sin\theta \qquad (4-5)$

The approximate depth of penetration of a particle in the molten liquid layer (for the surface of fused silicate) can be calculated by the equation below [13]:

$$s = \frac{2vd_p^2\rho_P sin\theta}{36\mu} \qquad (4-6)$$

In this equation v, r, ρ_P are velocity, diameter and density of the impacting particle respectively. θ is the angle of impaction and μ is the viscosity of the surface. This equation shows that by increasing the normal component of the velocity (V_n), the particles can penetrate more which increase their capture probability. The same behavior was predicted by Montagnaro et al. [38, 39]. Higher temperature by reducing the viscosity increases the effect of the high velocity in particle capture on the molten layer.

As a case study, the particles were injected vertically downward on a plate which had angle of 30° with horizontal line (α=30), therefore the impact angle is 60°. The results are compared with the impact angle of 60° on the vertically installed plates. The difference between the angles of these two cases is shown in Figure 4.10.

The deposition results presented in Figure 4.11 shows a high increase in the deposition for α=30 in comparison with α=90 at the same impact angle of θ=60°. Higher deposition for α=30 is probably related to the more retention time (the time that a particle is in contact with the plate). At α=30, if a particle does not stick to the plate, it usually moves on the plate until it reaches to the end of the plate to be carried out of the projection area and during this time it still has the probability of sticking. But, for the vertical plate, if the particle does not stick to the plate, it will be carried out of the projection area by the gas stream and there is no chance for another contact. The effect of the gravity is another parameter which helps the particles to stick in case of α=30, but, pulls the particles down and consequently acts against sticking phenomenon at α=90.

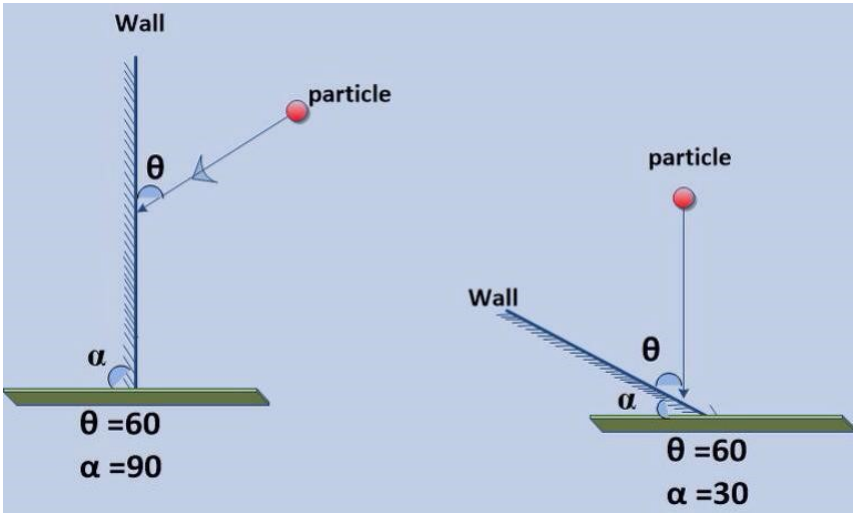

Figure 4.10: Different particle impact configurations with the same impact angle

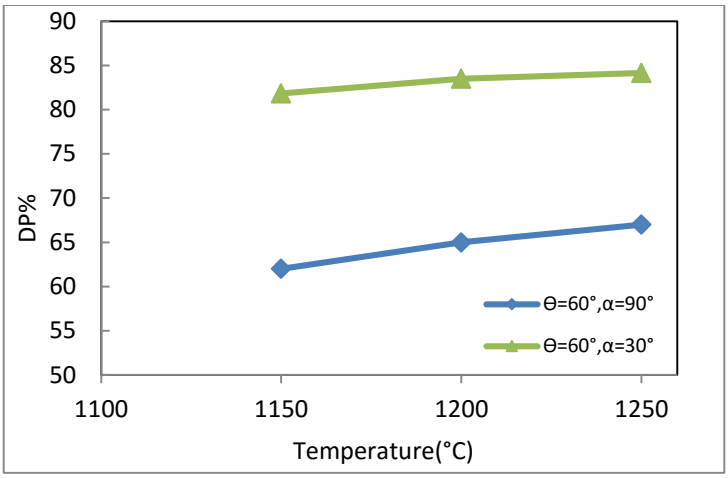

Figure 4.11: Deposition behaviour of different impinging configuration (V=10m/s)

4.5. Conclusion

In this study, the inorganic deposition behavior was studied by controlled injection in terms of the operation conditions such as temperature, velocity and impact angle.

In all the cases, increasing the temperature led to higher deposition, because, the ash particles are stickier at higher temperatures mostly due to the reduction in the viscosity. In addition, molten layer formed after sticking of the initial particles (which could be precursor to improve the capture efficiency), has lower viscosity as the temperature increases and captures more particles.

Increasing the velocity at low temperature had small effect and a slight decrease in the deposition was observed. The reason is related to the kinetic energy of the particles which is hard to dissipate at the moment of impact for the particles with higher velocity. Also, the existing layer on the plate has higher viscosity and penetrating into the high viscosity layer is hard and rebounding is more probable as the kinetic energy of the particle increases. At high temperature, increasing the velocity caused a slight increase in the deposition. The reason is thought to be related to the lower viscosity of the ash particles

and molten layer on the ceramic plate. High velocity particle can penetrate into the molten layer easier than the lower one. In addition, at higher temperature due to the higher liquid fraction, the maximum spread diameter is larger at higher velocity which finally increases the capture probability.

Changing the impact angle from 30° to 60° led to the higher deposition slightly. The reason is related to the change in the components of the particle velocity by variation in the impact angle. By decreasing the impact angle, the tangential component of the velocity of the particle increases which pushes the particle downward and will not let the particle to spread out on the surface or penetrate into the molten layer.

It was understood that the reason for not observing more distinguishable differences in the inorganic deposition behavior, especially, for the velocity and impact angle might be related to using ash (burned coal particles with high conversion). Coal particle with high carbon conversion is very sticky. Therefore, the probability of sticking to the surface is very high which minimizes the effect of other parameters. Using the char particles with lower carbon conversion probably will lead to the more distinguishable differences between various impact angles and velocities.

Acknowledgement

This study is financially supported by C^5MPT and Helmholtz- Alberta initiative (HAI) center. The authors thank to Herb Green for all his helps to make the required parts of the injection setup during the experiments. Special thanks to Dr. De Klerk, Dr. Liu and Dr. Prasad for the guidance which motivated us to think about controlled injection.

Reference

[1] Yang Z, Wang Z, Wu Y, Wang J, Lu J, Li Z, Ni W, Dynamic model for an oxygen-staged slagging entrained-flow gasifier, Energy Fuels 2011, 25, 3646-3656

[2] Song W, Tang L, Zhu X, Wu Y, Zhu Z, Koyama S, Flow properties and rheology of slag from coal gasification, Fuel 89 (2010) 1709–1715

[3] Zbogar A, Frandsen F, Jensen P A, Glarborg P, Shedding of ash deposits. Prog Energy Combust Sci 2009;35:31–56.

[4] Luan C, You C, Zhang D, An experimental investigation into the characteristics and deposition mechanism of high-viscosity coal ash. Fuel 119 (2014) 14–20

[5] Gupta S, Gupta R, Bryant G, Wall T, Watanabe S, Kiga T, Characterization of ash deposition and heat transfer behavior of coals during combustion in a pilot-scale facility and full-scale utility. Energy Fuels 2009; 23:2570–5.

[6] Erickson T A, Allan S E, Mccollor D P, Hurley J P, Kangb S G, Bakerb J E, Modeling of fouling and slagging in coal fired utility boilers. Fuel Process Technol 1995;44:155-71

[7] Balakrishnan S, Modeling and simulation of fly ash deposition on boiler heat-transfer surfaces and its mitigation strategies for Indian coals, Doctor of Philosophy thesis, Indian institute of technology-Madras, 2014

[8] Tominaga H, Yamashita T, Ando T, Asahiro N, IFRF combustion journal, article number 200004 2000.

[9] Walsh P M, Styre A N, Loehden D O, Monroe L S, Beer J M, Sarofim A F, Deposition of bituminous coal ash on an isolated heat exchanger tube: Effects of coal properties on deposit growth. Prog Energy Comb Sci 1990; 16:327–46.

[10] Winegartner E, Coal fouling and slagging parameters. New York: American Society of Mechanical Engineers; 1974.

[11] Ling-xue K, Jin B, Wen L, Zong-qing B, Zhen-xing G, Effect of lime addition on slag fluidity of coal ash, J Fuel ChemTechnol, 2011, 39(6), 407-411

[12] Browning G, Bryant G, Hurst H, Lucas J, Wall T, An empirical method for the prediction of coal ash slag viscosity. Energy Fuels 2003;17:731–7.

[13] Raask E, Mineral impurities in coal combustion, Behavior, Problems and Remedial Measures, Hemisphere Publishing Corporation, New York, 1985.
[14] Richards G H, Slater P N, Harb J N, Simulation of ash deposit growth in a pulverized coal-fired pilot scale reactor. Energy Fuels 1993;7:774–81.
[15] Yin C, Luo Z, Ni M, Cen K, Predicting coal ash fusion temperature with a back-propagation neural network model. Fuel 1998;77:1777–82.
[16] Skodras G, Sakellaropoulos G P, Mineral matter effects in lignite gasification, fuel process technology 77-78 (2002) 151-158
[17] Lu T, Zhang L, Zhang Y, Feng Y, Li H.X, Effect of mineral composition on coal fusion temperature. Journal of Fuel Chemistry and Technology, 2010, 38(2): 23–28.
[18]Wei Y, Li H, Honma K, Tanoskai T, Ninomiya Y, Effect of additives on slag properties in an entrained bed gasifier, World of Coal Ash (WOCA) Conference, 2011, Denver, USA
[19] Winegartner E, Rhodes B, An empirical study of the relation of chemical properties to ash fusion temperatures. J Eng Power 1975;97:395.
[20] Arvelakis S, Folkedahl B, Dam-Johansen K, Hurley J, Studying the melting behavior of coal, biomass, and coal/biomass ash using viscosity and heated stage XRD data. Energy Fuels 2006;20:1329–40.
[21] Wall T, Creelman R, Gupta R, Gupta S, Coin C, Lowe A, Coal ash fusion temperatures—new characterization techniques, and implications for slagging and fouling. Prog Energy Combust Sci 1998;24:345–53.
[22] Jung B, Schobert H H, Improved prediction of coal ash slag viscosity by thermodynamic modeling of liquid-phase composition. Energy Fuels 1992;6:387–98.
[23] Liu Y, Wu M, Qian J, Predicting coal ash fusion temperature based on its chemical composition using ACO-BP neural network. ThermochimActa 2007;454:64–8.
[24] Song W, Tang L, Zhu X, Wu Y, Rong Y, Fusibility and flow properties of coal ash and slag, Fuel 88 (2009) 297–304
[25] Gupta S, Dubikova M, French D, Sahajwalla V, Effect of CO_2 gasification on the transformations of coke minerals at high temperatures, Energy & Fuels 21 (2) (2007) 1052

[26] Duchesne M, Macchi A, Lu D, Hughes R, Artificial neural network model to predict slag viscosity over a broad range of temperatures and slag compositions, Fuel Processing Technology 91 (2010) 831–836
[27] Brachi P, Montagnaro F, Salatino P, Char-Wall Interaction and Properties of Slag Waste in Entrained-Flow Gasification of Coal, European Combustion Meeting 2011
[28] Losurdo M, Spliethoff H, Kiel J, Ash deposition modeling using a visco-elastic approach, Fuel 102 (2012) 145–155
[29] Rushdi A, Gupta R, Sharma A, Holcombe D, Mechanistic prediction of ash deposition in a pilot-scale test facility, Fuel 84 (2005) 1246–1258
[30] Li S, Whitty K J, Investigation of Coal Char−Slag Transition during Oxidation: Effect of Temperature and Residual Carbon, Energy Fuels 23 (2009) 1998–2005
[31] Degereji M U, Ingham D B, Ma L, Pourkashanian M, Williams A, Prediction of ash slagging propensity in a pulverized coal combustion furnace, Fuel 101 (2012) 171–178
[32] Mueller C, Selenius M, Theis M, Skrifvars B J, Backman R, Hupa M, Tran H, Deposition behavior of molten alkali-rich fly ashes—development of a sub-model for CFD applications, Proceedings of the Combustion Institute 30 (2005) 2991–2998
[33] Costen P G, Locwood F C, Siddique M M, Mathematical modeling of ash deposition in pulverized fuel-fired combustors, Proceedings of the Combustion Institute, Volume 28, 2000/pp. 2243–2250
[34] Yong S Z, Gazzino M, Ghoniem A, Modeling the slag layer in solid fuel gasification and combustion – Formulation and sensitivity analysis, Fuel 92 (2012) 162–170
[35] Yu G, Zhu Q, Chi G, Guo Q, Zhou Z, Study on slag composition and flow property in a bench-scale OMB gasifier, Fuel Processing Technology 2012
[36] Shimizu T, Tominag H, A model of char capture by molten slag surface under high temperature gasification conditions, Fuel 85 (2006) 170–178
[37] Wall T F, Liu G S, Wu H W, Roberts D G, Benfell K E, Gupta S, Lucas J A, Harris D J, The effects of pressure on coal reactions during pulverized coal combustion and gasification, Progress in Energy and Combustion Science 28 (2002) 405–433.

[38] Montagnaro F, Salatino P, The role of slag formation on late carbon conversion in entrained-flow gasification of coal, Dipartimento di Chimica, UniversitaStudi di Napoli Federico II, Napoli, Italy, 2009
[39] Montagnaro F, Salatino P, Analysis of char–slag interaction and near-wall particle segregation in entrained-flow gasification of coal, Combustion and Flame 157 (2010) 874–883
[40] Shannon G N, Rozelle P L, Pisupati V, Sridhar S, Conditions for entrainment into a FeOx containing slag for a carbon-containing particle in an entrained coal gasifier, Fuel Processing Technology 89 (2008) 1379–1385
[41] Mao T, Kuhn DSC, Tran H, Laboratory study of carryover deposition in Kraft recovery boilers. J Pulp Pap Sci 1997;23:565-70
[42] Kim H Y, Chun J H, The recoiling of liquid droplets upon collision with the solid surfaces. Phys Fluids 2001;13:643-59
[43] Fukaj J, Shiiba Y, Yamamoto T, Miyatake O, Poulikakos D, Megaridis CM, Wetting effects on the spreading of a liquid droplet colliding with a flat surface: Experiment and modeling. Phys Fluids 1995;7:236.
[44] Ni J, Yu G, Guo Q, Zhou Z, Wang F, Sub-model for predicting slag deposition formation in slagging gasification systems, Energy Fuels 2011, 25, 1004–1009
[45] Barroso J, Ballester J, Pina A, Study of coal ash deposition in an entrained flow reactor: Assessment of traditional and alternative slagging indices, Fuel Processing Technology 88 (2007) 865–876
[46] Li Z, Zeng L, Zhao G, Shen S, Zhang F, Particle sticking behavior near the throat of a low-NOx axial-swirl coal burner, Applied Energy 88 (2011) 650–658
[47] Chen L, Yong S Z, Ghoniem A F, Modeling the slag behavior in three dimensional CFD simulation of a vertically-oriented oxy-coal combustor, Fuel Processing Technology 112 (2013) 106–117
[48] Ni J, Liang Q, Zhou Z, Dai Z, Yu G, Numerical and experimental investigations on gas–particle flow behaviors of the Opposed Multi-Burner Gasifier, Energy Conversion and Management 50 (2009) 3035–3044

[49] Duchesne M, Hall A, Hughes R, McCalden D, Anthony E , Macchi A, Fate of inorganic matter in entrained-flow slagging gasifiers: Fuel characterization, Fuel Processing Technology 118 (2014) 208–217
[50] Naseri M, Effect of Particle Impact Velocity on Carryover Deposition, Master of Applied Science Thesis, University of Toronto 2000
[51] Weber R, Mancini M, Schaffel-Mancini N, Kupka T, On predicting the ash behavior using Computational Fluid Dynamics, Fuel Processing Technology 105 (2013) 113–128
[52] Vejahati F, Entrained-flow gasification of oil sand coke, PhD thesis, Department of Chemical and Materials Engineering, University of Alberta, Spring 2012

Chapter 5. CFD modeling of ash deposition and slag formation during coal gasification

5.1. Abstract

Inorganic matter deposition and slag formation are critical issues during coal combustion and gasification as they significantly affect the reliability and availability of the process. CFD modeling is a promising tool to reduce the high cost of the experimental prediction of the inorganic behavior and to evaluate the effects of the operating conditions on slag flow. A 2D-axisymetric model has been developed in ANSYS Fluent commercial software in steady state condition to simulate the ash particle deposition during coal gasification. Slag layer formation is calculated using Navier-Stokes equation. The phenomena of the char and ash particle deposition and their interaction with the wall of the furnace, has been introduced to the model as a user defined function (UDF). In the sub-model, the operating parameters such as wall temperature, particle temperature,

particle velocity, carbon conversion of the char particles and the physical properties of the inorganic matters such as temperature of critical viscosity (T_{cv}) and density have been considered. Navier-Stokes equation in combination with the continuity equation was used to calculate the slag layer thickness, based on the ash deposition as the inlet material forming the slag layer. The results of the ash deposition sub-model, in combination with the gasification model are saved in user defined memory (UDM) and it is possible to be passed to other models for further processing. The comparison of the contours of the inorganic particle deposition with the experimental results of ash deposition in an electrically heated drop tube furnace showed that the model predicts well the location of the particle deposition. Due to neglecting some affecting parameters, the error of the deposition values is high.

Keywords: CFD modeling, Coal gasification, Mineral deposition, Slag layer

5.2. Introduction

Entrained-flow coal gasifiers are of great interest especially in IGCC plants due to their higher energy efficiency and fuel conversion, high feed throughput and adaptability of working with an extensive range of fuels. Due to the low residence time of the coal particles and in order to have reasonable carbon conversion, the temperature in entrained-flow reactor must be very high causing fusion of the inorganic content of the fuel. Melted ash particles stick to the wall and form a slag layer flowing down to the bottom of the furnace. In IGCC systems, due to the strong swirl flow and intense pressure, ash particles are more concentrated near the wall and this characteristic cause further increase in the deposition tendency. In entrained-flow gasifier, up to 90% of the inorganic matters can be

discharged as molten slag. However, this layer can protect the wall of the furnace by acting as a thermal barrier and also help to better manage the disposal of the inorganic content of the fuel instead of having fly ash (which might cause problems in downstream equipment), but, steady removal of the molten inorganic matters is a great issue strongly affecting the reliability and safe operation of the gasification process [1-11].

Implementing the experimental analysis in the industrial combustion or gasification plants is very costly; because, to investigate the effect of each parameter, large number of experiments must be done requiring shut-down the process after each condition [19]. In order to increase the reliability and insure the safe operation of slagging entrained-flow coal gasifiers and considering the high cost of the experimental analysis of the process, it is very important to predict the inorganic deposition behavior and slag flow by modeling the process. Performing a comprehensive model which can simulate all the phenomena involved in the process is not feasible due to the extremely high computational costs. Therefore, the model must be implemented based on the reasonable simplifying assumptions. The studies regarding simulation of the gasification process started with very simple models with extremely simplifying assumptions such as plug flow of the gas and particles [12,13]. As the models gradually improved, researchers focused more on CFD modeling as a precious tool in this regard which reduces the high cost of the experimental evaluation of the inorganic behavior at various conditions. Seggiani [6] was a pioneer in slag formation modeling for coal gasification. He developed a three dimensional analytical time varying model of gasification, combined with a one dimensional slag layer model. This model could calculate both the solid and molten liquid layer thicknesses and evaluate the effect of various operating condition on the slag

layer in transient mode. However, the model proposed by Seggiani was a valuable guidance for many future studies, but, the simplifying assumptions of his model must be improved to be closer to the real situations and achieve more accurate and reliable results. Considering the fixed ash deposition rate without any particle capture sub-model is the most important defection of Seggiani's model. Particle capture sub-model is an important part of the slag layer modeling because, sticking particles are inlet materials of the slag model and determines the amount of the depositions which in molten sate build the slag layer. Despite the importance of the particle-wall interaction, in some studies a constant rate for the ash deposition was assumed. Liu and Hao [14] and Ni et al. [15] proposed 2D multiphase models for the inorganic deposition and slag flow without using a reliable particle capture sub-model.

The particle capture by the slag layer not only affects the amount of the deposition and slag flow, but also influences the gasification rate of the char particles. Depending on the type of entrapment, the particle residence time in the gasifier might be extended (which increase the gasification rate) or if a particle get embodied in the liquid slag layer completely, then any further reactions with that particle will not occur [16]. Unburnt combustible content of the captured char particles will react at slower rate due to the loss of surface area required for reactions [17]. Wang et al. [18] improved seggiani's model by considering the change in the momentum of slag flow by incoming particles. They proposed a wall burning model by introducing an effective surface area for the captured particles. By this method, they considered the decrease in the reaction rate caused by the blocked pores of the char particles which makes hard or prevents the diffusion of the gasifying agents into the char structure. At the moment of interaction of the particle with

slag layer, the fusible inorganic fraction of the coal particle might stick to the wall (or existing slag layer) and enable slag build-up. At the same time, unconverted carbon content of the char particle may remain segregated at the surface of the slag layer or get engulfed into it, depending on the parameters such as particle inertia, particle-slag interfacial tension and ash viscosity [19].

It is obvious that in order to have a reliable and accurate model, an accurate rule for the particle-wall interaction is necessary instead of assuming a constant particle deposition. This criterion must take into consideration as many affecting parameters as possible. There are some factors determining the particle fate while interacting with the wall. Some of these factors are related to the particles such as particle temperature, composition, angle of impact, velocity and kinetic energy. In addition, there are some factors which are dependant to the properties of the target surface such as surface roughness, temperature, viscosity, surface tension and composition of the existing deposited materials [20,21]. Montagnaro et al. [16, 22] analyzed the particle-slag interactions considering the effects of turbulence, centrifugal force caused by swirl flow, interaction of the incoming particles with existing layer, coating of the deposit surface by un-reacted carbon and proposed a simple 1D model considering the carbon particle segregation. They reported that coating of the slag layer by carbonacious material strongly affects the particle-wall interaction and concluded that, only high inertia particles can overcome viscous and interfacial forces and penetrate well into the slag layer (which is mostly possible for large particles having high kinetic energy interacting with slag layer with very low viscosity). Shimizu and Tominaga [24] proposed a simple model for the char capture under high-temperature gasification conditions. They reported that, the fate of the particles depends on the

properties of the colliding area and assumed that char particles will be rebounded if they collide with the wall in the area coated by the unburnt char particles and will stick if they collide with the slag covered surface. Therefore, based on this model the balance of the char arrival flux on the slag surface and the carbon removal flux caused by the rate of the char consumption by the gasification reactions, determines the fate of the char particles. Based on this theory, the char capture prediction is more important in case of utilizing the char with lower reactivity. Shannon et al. [25] considered the balance of the forces to evaluate the fate of the particles and used drag force, capillary force and a fluid-added mass force as the main acting forces on the particles. Mueller et al. [26] applied mass and energy balances and proposed a sticking model based on the kinetic and surface energies. Ni et al. [27] proposed a model based on slap diameter and excess energy. They introduced physical properties (like viscosity), particle impact angle and velocity as the affecting parameter and applied them in terms of Weber and Reynolds number. Young et al. [7] combined the models of Seggiani [6] and Wang et al. [18] and assumed a cubic temperature distribution profile inside the deposition and used a criterion for particle capture based on the stickiness of the wall and the colliding particles. Yong et al [8] performed a steady state two-way coupled model and proposed a sub-model to consider new rate of the porous char consumption trapped by the slag by calculating more accurate available surface for the reaction. Chen et al. [9] proposed a 2D slag model integrated with a 3-D CFD model of combustor utilizing char–slag interaction and wall burning sub-models and finally calculated the slag thickness. They reported that T_{cv} has a great effect on the thickness of slag the layer flowing down on the wall, especially by affecting the formation of the solid slag layer. In continue of this model, Chen et al. [10] performed a

time dependant fully three-dimensional slag model including particles deposition and slag by integrating two multiphase flow models. They did not model the solid slag layer because; the operating temperature in their study was higher than the solidification temperature of the inorganic content. They used the Volume of Fluid (VOF) model to simulate the gas and slag phase and used the Discrete Phase Model (DPM) to track solid particles. Models proposed by Chen et al. [9,10], are the most comprehensive models proposed for the ash deposition and slag formation due to using comprehensive sub-models for particle capture and other sub-models to evaluate the affecting phenomena.

In this study a 2D-axisymetric CFD model of ash deposition and slag formation during coal gasification has been performed based on an electrically heated drop tube furnace. The model is integrated with a sub-model for the ash particle sticking and deposition. The model is developed in commercial ANSYS Fluent software and sub-model is introduced to the main model as a UDF which is written code in C++ language. The results of the particle capture sub-model (including the amount and conditions of the trapped particles) and other required information are saved in UDM. Due to the high value of the viscosity of the liquid slag layer, the VOF two-phase flow model for slag flow formation developed in FLUENT failed to converge and give reasonable results for the slag layer thickness. Therefore, Navier-Stokes equation was solved analytically to calculate the thickness of the falling liquid slag layer on the wall of furnace.

5.3. Model description

5.3.1. Test facility and general gasification model

A steady state 2D-axisymetric model is implemented in ANSYS Fluent based on an atmospheric electrically heated drop tube furnace. The experimental setup is shown in Figure 5.1. The length of the furnace is 150 cm with inner diameter of 6.35 cm. The geometry of the furnace (considering some assumptions) is shown in Figure 5.2. 2D-axisymetric geometry used in the modeling is shown in Figure 5.3. ANSYS Design Modeler is used to create the geometry of the furnace. The ceramic material of the furnace tube for moderate temperatures is mullite and for temperatures higher than 1500°C alumina tube can be used. In order to take ash deposition samples, cylindrical plates made of hardened Kawool paper are used to cover the inner surface of the furnace.

The feeding part of the gasification setup consists of two tubes. The inner tube in which nitrogen carries coal particles is a quarter inch tube with 4 holes at the tip with diameter of 3mm. The other tube which carries the gasifying agents is an open ended half inch tube [35]. The feeding configuration is shown in Figure 5.4.

In the experimental part of the study (to get data for comparison with the modeling results) a Canadian coal is used. The ultimate and proximate analysis of the coal is presented in Table 5.1 and the inorganic composition analysis of the coal ash is presented in Table 5.2.

ANSYS Mesh software was used to create a multi-block structure containing square meshes for the 2D-axisymetric geometry of this model as shown in Figure 5.5. The total cell number of the model is 81078 with aspect ratio of 2.7 and orthogonal quality of 1. In this regard, models with different number of cells were tested starting with about 20000

cells which were gradually increased to about 100000 cells. This approach is called grid independency test. By this approach, the maximum number of cells which beyond that increasing the cell numbers does not affect the accuracy or stability of the results can be found. In the simple models, by increasing the cell numbers usually the results change until to reach a maximum cell number beyond that increasing the cell numbers does not change the results. In this study for models with different cell numbers, various results such as temperature distribution, contours of gaseous species concentration and particle deposition contours were analyzed. Although, due to the many involved phenomena, a simple straight-forward trend was not observed by increasing the number of cells, but, based on the comparison of the various results of different models, it was concluded that the model with about 80000 cells gives the best results and increasing the cell numbers beyond that is not reasonable.

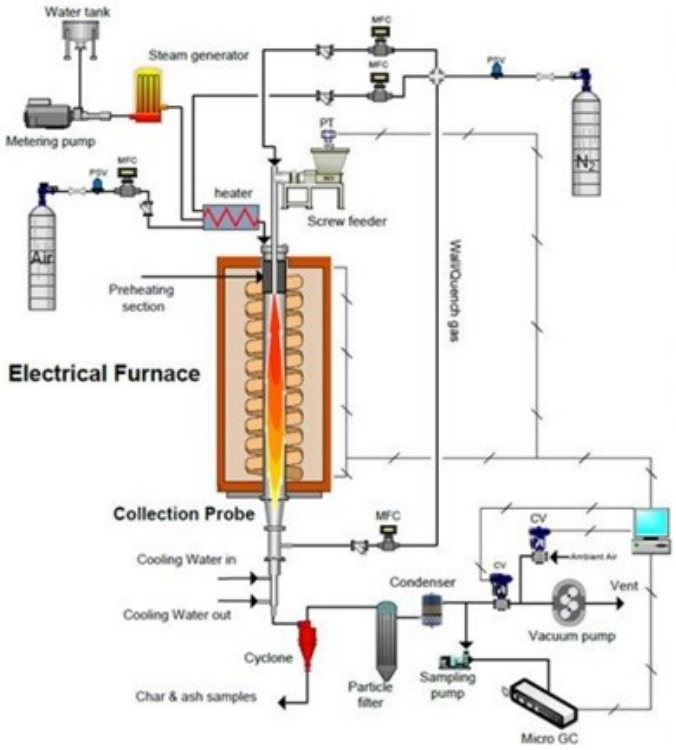

Figure 5.1: Schematic diagram of electrically heated drop tube furnace used for coal gasification [34]

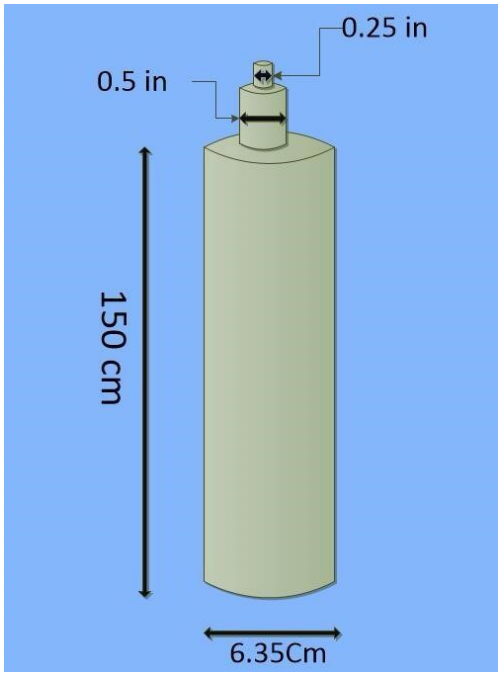

Figure 5.2: Geometry of drop tube furnace

Figure 5.3: 2D-axisymetric geometry of the furnace used in modeling

Table 5:1: Proximate and ultimate analysis of coal

Proximate analysis	w%	Ultimate analysis	w%		
Volatile matter	34.95	C	54.9		
Fixed carbon	41.85	H	4.1	Size	28-53µm
ash	12.39	N	1		
moisture	10.81	S	0.5		
		O	39.5		

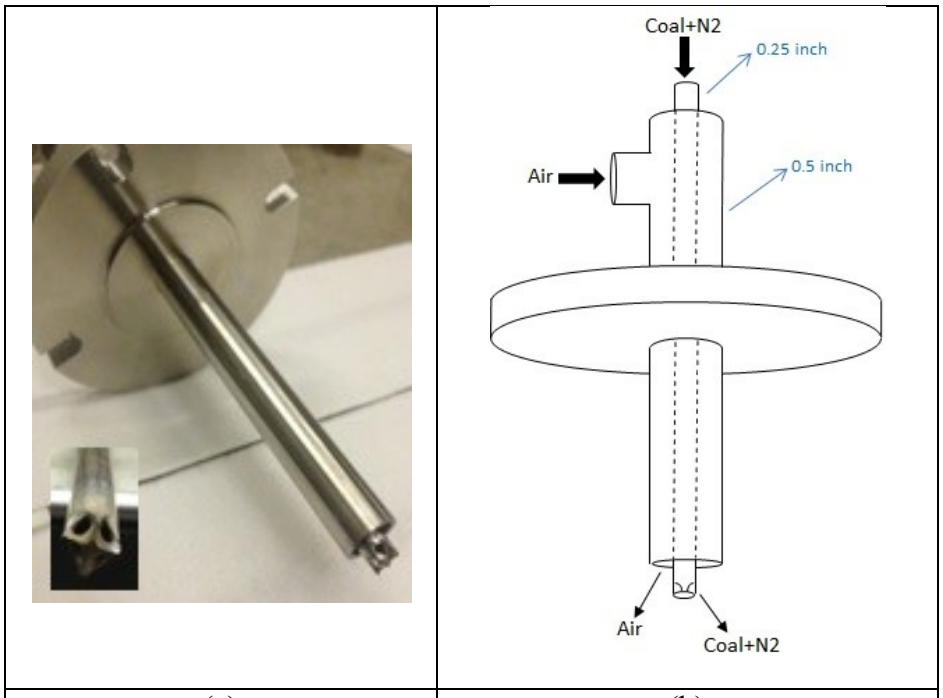

Figure 5.4: Feeding configuration of the gasification setup [35]

Table 5:2: Ash composition analysis

Inorganic composition	W%	STDEV
SiO_2	33.4	1.15
Al_2O_3	22.4	0.77
Fe_2O_3	6.7	0.36
CaO	15.8	0.91
Na_2O	6.4	0.15
MgO	3.2	0.26
BaO	1.8	0.17
TiO_2	1.0	0.09
SO_3	8.5	0.76
P_2O_5	0.7	0.06
STDEV: Standard Deviation		

Discretization performed by the mesh produces control volumes and FLUENT uses finite volume approach to solve numerically conservation equations of mass, momentum and

energy which are partial differential equations. The mass conservation or continuity equation is presented as below [19, 35,36]:

$$\frac{\partial \rho}{\partial t} + \nabla . \rho U = S_p \qquad (5-1)$$

This equation is applicable for both laminar and turbulent flow. In above equations, U is the fluid velocity vector field, ρ is the gas density and S_p is the mass source term transferred between continues phase and dispersed phase. The conservation equations for momentum and energy are as below, respectively [19]:

$$\frac{\partial}{\partial t}\rho U + \nabla . (\rho U U) = -\nabla P + \nabla . \sigma + S_m \qquad (5-2)$$

$$\frac{\partial}{\partial t}\rho h + \nabla . (\rho U h) = \frac{DP}{Dt} + \nabla . \lambda \nabla T + \sigma . \nabla U \qquad (5-3)$$

In above equations, P is the pressure of the gas phase, σ is the viscous stress, S is the momentum sources, T is the temperature of the fluid, λ is the thermal conductivity and h is the enthalpy. When the secondary dispersed phase affects the continuous fluid flow (as happens in two-way coupling) the term S considers this effect [19]. In one-way coupling if the gravity is considered, that would be the only body force acting on the fluid and the momentum source term is:

$$S_m = \rho g \qquad (5-4)$$

Conservation equations 5-2 and 5-3 are based on the laminar flow. In case of the turbulent flow the forms of the momentum and energy conservation equations in steady state condition will be as below, respectively [37]:

$$\frac{\partial}{\partial x_i}\left(\rho u_i u_j\right) = \rho g_j - \frac{\partial P}{\partial x_j} + \frac{\partial}{\partial x_i}\left(\tau_{ij} - \rho\overline{u_i' u_j'}\right) + S_j \qquad (5-5)$$

$$\frac{\partial}{\partial x_i}\left(\rho c_p u_i T\right) = \frac{\partial}{\partial x_i}\left(\lambda \frac{\partial T}{\partial x_i} - \rho c_p \overline{u_i' T'}\right) + \mu \emptyset + S_h \qquad (5-6)$$

In above equations $\emptyset$ is the viscous dissipation, u_i is the average velocity, u_i' is the velocity fluctuation, S_j is the momentum exchange source term and S_h is the energy exchange source term [37]. To involve the effect of the turbulence, turbulent viscosity or eddy viscosity is considered as a new parameter which is a function of the state of the turbulence. The term $\rho\overline{u_i'u_j'}$ in equation 5-5 is Reynolds stress which is related to the turbulent viscosity. There are various models to calculate the turbulent viscosity such as zero equation models, one equation models, two equation models, Reynolds stress model etc. [36]. Among various turbulence models, k-ε and k-ω which are the most famous two equation models are widely used in the CFD modeling of coal combustion and gasification. Based on Chen et al. [11], reliability of the turbulence models (especially in case of strong swirl flow in the gasifier), is still a bottle-neck to have accurate modeling results. Realizable k-ε and eddy dissipation model is used in this study to simulate the turbulence. In k-ε model, the turbulent viscosity is related to k (turbulence kinetic energy) and ε (turbulence dissipation rate) based on the equation below [36,37]:

$$\mu_t = \rho C_\mu \frac{k^2}{\varepsilon} \qquad (5-7)$$

The transport equations for Realizable k-ε model are [36]:

$$\frac{\partial}{\partial t}(\rho k) + \frac{\partial}{\partial x_j}(\rho k u_j) = \frac{\partial}{\partial x_j}\left[\left(\mu + \frac{\mu_t}{\sigma_k}\right)\frac{\partial k}{\partial x_j}\right] + G_k + G_b - \rho\varepsilon - Y_M + S_k \qquad (5-8)$$

$$\frac{\partial}{\partial t}(\rho \varepsilon) + \frac{\partial}{\partial x_j}(\rho \varepsilon u_j) = \frac{\partial}{\partial x_j}\left[\left(\mu + \frac{\mu_t}{\sigma_\varepsilon}\right)\frac{\partial k}{\partial x_j}\right] + \rho C_1 S_\varepsilon - \rho C_2 \frac{\varepsilon^2}{k + \sqrt{\nu\varepsilon}} + C_{1\varepsilon}\frac{\varepsilon}{k} C_{3\varepsilon} G_b + S_\varepsilon \qquad (5-9)$$

The definitions and equations for calculation the parameters of the equations 5-8 and 5-9 are presented in FLUENT user guide [36]. Parameters of the model that can be manipulated by user through Realizable k-ε model panel in FLUENT are C2 Epsilon (default value: 1.9), TKE Prandtl number (default value: 1), TDR Prandtl number (default

value: 1.2) and energy Prandtl number (default value: 0.85). All the default values of these parameters remained unchanged in this study.

Utilizing discrete particle model (DPM), particles are tracked in Lagrangian frame work and gas phase is modeled in Eulerian frame work. The particle dispersion due to the turbulence in DPM is modeled based on Stochastic Random Walk model which is believed to be an accurate model for dilute suspension modeling. P1 model is used as the radiation model inside the furnace.

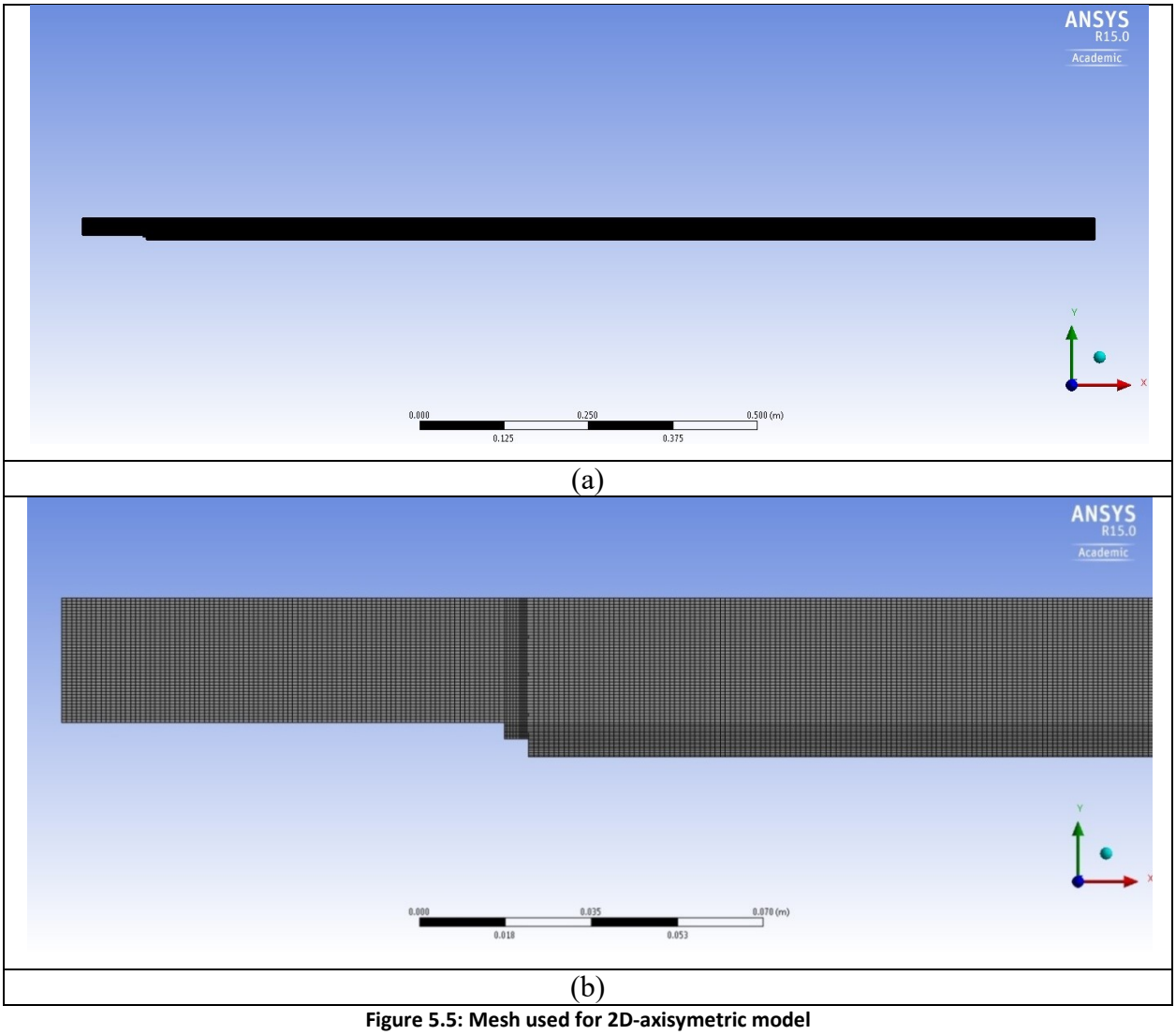

Figure 5.5: Mesh used for 2D-axisymetric model

The particles are mainly transported by the drag force and the turbulence (produced by fluid) in the dilute multiphase systems. In these systems, usually the spacing between particles is more than 100 particle diameters which is quite a big distance. Therefore, particles collision is not frequent and consequently particle-particle interactions can be neglected and particle motion tracking can be performed only based on the fluid dynamic forces [19]. When the free distance between particles is about 10 particle diameters or lower, the system is dense dispersed and the collision between particles cannot be neglected. Therefore, to track the motion of the particles, the interactions of the particles and their collisions must be considered in combination with the fluid dynamic forces [19]. Depending on the dispersion level of the particles, different degree of coupling between the continuous phase and the suspended phase can be applied. In one-way coupling, only the continuous phase affects the dispersed phase motion. In two-way coupling both continuous phase and dispersed phase affect each other. In four-way coupling both phases affect each other and in addition to that, the transport of the particles is affected by the particle-particle interactions as well. In modeling the systems including dense flows, four-way coupling is required. Based on the typical conditions of the entrained-flow coal gasifier proposed by Montagnaro and Salatino [22], the two-way coupling between particle and fluid phases is the best coupling option [19].

The interaction of the gas phase and particles in this study is implemented in a two-way coupling. Based on Lagrangian particle tracking model, the particle volume is ignored and the particles do not interact with each other in two-way coupling [21]. By solving the equations of motion for particles and assuming spherical, rigid and non-rotating particles, the trajectory of the particles is determined [10]. In DPM model all the transfer

phenomena between the gas phase and particles are characterized based on the ‘‘particle-source-in-cell’’ method and the motion of the particle is simulated by the balance of the drag force and gravity force as shown below [10]:

$$\frac{dx_p}{dt} = \vec{v}_p \qquad (5-10)$$

$$\frac{d\vec{v}_p}{dt} = \frac{18\mu_g}{\rho_p d_p^2}\frac{C_D Re}{24}\left(\vec{v}_g - \vec{v}_p\right) + \frac{\vec{g}\left(\rho_p - \rho_g\right)}{\rho_p} + \vec{F} \qquad (5-11)$$

In above equations, $\vec{v}_p$ and $\vec{v}_g$ are the particle and gas velocity respectively, μ_g is the gas viscosity, d_p is the particle diameter, C_D is the drag coefficient, and $\vec{F}$ can be replaced by any body forces acting on the particles which might be important depending on the conditions based on which the simulation is going to be implemented. All the parameters required for particle capture and slag sub-model such as particle feed rate per unit area, particles temperature, particles velocity and heat flux to the slag layer can be calculated and saved in UDM to be assigned by appropriate sub-model when required. Conservation equation for mass, momentum and energy for gas phase and particles are performed by FLUENT software. The mathematical models and equations used by FLUENT in Eulerian multiphase and also Eulerian-Lagrangian frame work applied in DPM can be found in the numerous references such as 3D modeling of Chen et al. [10].

In the main part of the modeling, the gasification reactions including heterogeneous solid surface reactions of carbon with the gasifying agents which mainly produce synthesis gas (mixture of CO and H_2), H_2O and CO_2 and homogenous gas phase reactions are considered to calculate the product gas compositions and the temperature distribution inside the furnace. In this regard multi-surface reaction model was applied based on the kinetic parameters of the gasification reactions presented in Table 5.3.

Table 5:3: Kinetic parameters of the reactions involved in coal gasification [23]

Reaction	A	E (J/kmol)	N1	N2	N3
Vol→CO+CH_4+H_2S+H_2+N_2+H_2O+O_2+Tar	2.119e11	2.027e8	1.5	-	-
CO oxidation reaction	2.239e11	1.700e8	1	0.25	0.5
CO+0.5O_2→CO_2					(H_2O)
Forward water-gas shift reaction (FWGS)	2.35e10	2.880e8	0.5	1	-
CO+H_2O→CO_2+H_2					
Reverse water-gas shift reaction (RWGS)	1.785e12	3.260e8	1	0.5	-
CO_2+H_2→ CO+H_2O					
Hydrogen oxidation	9.87e8	0.310e8	1	1	-
H_2+0.5O_2→ H_2O					
Reverse hydrogen oxidation	2.06e11	2.728e8	1	-	-
H_2O→ H_2+0.5O_2					
Char combustion	300	1.3e8	0.65	-	-
C<S>+0.5O_2→CO			(O_2)		
CO_2 gasification	2224	2.2e8	0.6	-	-
C<S>+CO_2→2CO			(CO_2)		
H_2O gasification	42.5	1.42e8	0.4	-	-
C<S>+H_2O→CO+H2			(H_2O)		

After each 40 iterations of the gas phase calculation in the main gasification model (to obtain a specific convergence), the solution results is used by DPM model to solve the particle momentum (in Lagrangian frame-work), reactions and energy equations and the interaction between gas phase and particles. The trajectory, velocity, temperature and composition of the particles are calculated by integrating the equations of continuity, momentum and energy for the particles in the gas flow field. Then the source term for gas phase equations will be updated based on the result of DPM calculation and then, all the equations for gas phase will be calculated again for another 40 iterations. This procedure

will go on until the desired convergence is obtained which usually happens when the gas phase variables do not change (based on the adjusted acceptable errors). The particle sticking sub-model is performed with every particle phase calculation and calculates the amount and location of the particle sticking and save them in UDM (to be used by slag model as mass source). Then, slag model can use the amount of the deposited particles and temperature of each point of the furnace to calculate the slag flow characteristics including the thickness, temperature profile and velocity. These integrated calculations will go on until steady state conditions is satisfied in both gas and particle phases.

Convergence of the model for each specific condition was accepted when the residual of each specific parameter reduces to a value lower than the adjusted orders of magnitude, as listed in Table 5.4.

Table 5:4: Adjusted error values for residuals

parameter	Adjusted error value	parameter	Adjusted error value
Continuity	10e-3	k	10e-3
x-velocity	10e-3	epsilon	10e-3
y-velocity	10e-3	Species fraction	10e-3
energy	10e-6	P1	10e-6

Specification of the boundary conditions is an important part of the CFD modeling while using software like FLUENT, because for each boundary, various options are available choosing them might affect the convergence of the calculations and accuracy of the results.

During the experiments, the mass flow rates of air stream and nitrogen stream (as coal particle carrier) was adjusted using mass flow controller, but in the modeling, the velocity inlet condition was the best option for these boundaries. Inlet temperature of the air and

nitrogen flow is 500 K as they were preheated. The surface from which nitrogen enter to the geometry was also activated via DPM injection setup as the entrance of the combustible coal particles with adjusted mass flow rate. In DPM injection rosin-rammler particle size distribution was applied. A summary of the boundary conditions are presented in Table 5.5. In order to differentiate between the excluded mineral particles and char, different particles with different type, density and size distribution could be defined.

Table 5:5: Boundary conditions of 2D-axisymetric model

Boundary Name	Condition	Value	Hydraulic diameter	Intensity
Air inlet	Velocity inlet	0.9m/s	0.00635m	10%
Coal + Nitrogen inlet	Velocity inlet	1.32m/s	0.003m	10%
Top Wall	Adiabatic	-	-	-
Side wall	Constant temperature	1250°C-1450°C	-	-
Outlet	Pressure outlet	-	0.0635m	5%

As mentioned earlier, the CFD model is based on an electrically heated drop tube furnace in which the temperature of the wall is kept constant using thermocouples and 3 PID controllers. Therefore the boundary condition of the wall is constant temperature which is introduced through DEFINE-PROFILE macro in UDF.

Generally, the gas phase could be considered to behave as incompressible flow when $M < 0.3$ and compressible when $M > 0.3$ [19]. In this study, the gas phase is modeled as the perfect incompressible gas.

5.3.2. Particle sticking sub-model

Many researchers have used the particle capture criterion based on only the viscosities of the colliding particles and slag at the moment of collision. But, in order to have an accurate model reliable for design and scale up, a proper prediction of the fate of the

inorganic and char particles is crucial [6]. The interactions of the particles and the wall (bare wall or slag layer), depend on the physical and chemical properties of the gas phase, particles and receiving surface. Stickiness capability of the particles depends essentially on unconsumed organic fraction and therefore, is dependant to the conversion degree and other parameters such as particle diameter, density, impact velocity, impact angle and also interfacial tension of the particle and wall [19].

To have an accurate slag flow prediction, an accurate particle capture criterion is required, because, sticking particles are constructive materials of the slag layer and are introduced as inlet source mass to the slag flow sub-model. To achieve reliable results for the particle-wall interaction phenomena, the particles trajectory inside the domain must be well predicted using stochastic random-walk in DPM, reliable resolution of the mesh integrated with a suitable turbulence model [10]. It must be noticed that char-wall interactions not only affect the amount of the deposition and its thickness, but also influence the temperature profile in the gas phase and also inside the slag layer. The reason is that the trapped char particles usually have some un-reacted organic fractions which might react further and by consuming or releasing energy (depending on the type of the reaction), affect the temperature distribution. This phenomenon affects the overall efficiency of the process depending on the amount and state (surface entrapment or fully encapsulation) of the trapped carbonaceous materials [19].

Particle sticking criterion must predict if a particle at the moment of the collision to the wall sticks or rebounds. In this study, the particle capture criterion proposed by Chen et al. [9] is used which considers the stickiness of the wall of the furnace and the properties

of the particles. This capture criterion presented in Table 5.6 is one of the most comprehensive capture criterions proposed in the literature.

Table 5:6: particle sticking criterion [9]

		Char/ash particle							
		TP>Tcv				TP<Tcv			
		X>Xcr		X<Xcr		X>Xcr		X<Xcr	
		We>Wecr	We<Wecr	We>Wecr	We<Wecr	We>Wecr	We<Wecr	We>Wecr	We<Wecr
wall	Tw>Tcv	trap	trap	reflect	trap	reflect	trap	reflect	trap
	Tw<Tcv	reflect	trap	reflect	trap	reflect	reflect	reflect	reflect

The criterion proposed in Table 5.6 is written in C++ language to be introduced to FLUENT as UDF. Interpret and compile are two options to introduce the UDF to FLUENT. This UDF is compiled with FLUENT due to the type of the instructions used in the code. X_{cr} in Table 5.6 is critical carbon conversion and is set to 0.88.

Li et al. [28] reported that the type and degree of the inorganic–carbon associations in the chars and their gradual transformation while being reacted, has a great effect on the particle behavior upon collision. This physical structural change is clearly observable with a drastic effect on the capture efficiency, when the carbon conversion of the char particle is higher than a critical value. Regarding carbon conversion as a key factor, Li and Whitty [29] observed that only at carbon conversion higher than 90%, there will be a recognizable transformation from non-adhesive porous char to the sticky droplet working at temperatures higher than the ash fusion ranges. Based on the criterion used in this study, the stickiness of the particles is assumed to be related to its temperature and carbon conversion and physical properties such as surface tension (γ) and temperature of critical viscosity (T_{cv}). The stickiness of the wall is related to its temperature. If temperature of the wall is higher than temperature of critical viscosity (T_{cv}) wall is assumed to be sticky.

For the particles, temperature must be higher than T_{cv} and carbon conversion must be higher than critical carbon conversion then the particle can be assumed sticky. If the wall surface and particles are not sticky, then the particle can stick only if the Weber number is lower than critical Weber number (We_{cr}) which is set to be 1 [9]. Weber number is the ratio between kinetic energy and surface tension energy and is calculated by UDF for each particle at the moment of colliding with the wall, according to the equation below:

$$We = \frac{Particle\ kinetic\ energy}{Surface\ tension} = \frac{\rho_P v_P^2 d_P}{\gamma} \qquad (5-12)$$

In above equation of Weber number, ρ_P is particle density, v_p is the velocity of the particle, d_P is the diameter of the particle and γ is the surface tension of molten particle or interfacial surface tension of the particle and target surface. In the particle capture sub-model of this study, the density of the inorganic matters is assumed to be 3.24 g/cm3, surface tension of the liquid slag layer is 0.382 N/m and temperature of critical viscosity is 1242°C. If the particle is trapped on the wall, its mass and energy will be saved in UDM (can be used by slag phase sub-model through the source terms) and the path of that particle will be deactivated, otherwise, the path of the particle will be calculated based on its energy and the particle continues its motion in the furnace. Some studies have been performed to determine the fate of the particles as a matter of being kept at the surface or getting embodied completely into the slag layer and some criteria in this regard have been propose. Montagnaro et al. [16,22] assumed that to be completely encapsulated into the slag layer, particle inertia must overcome interfacial and viscous forces of the slag as presented in equations below:

$$kinetic\ energy > viscous\ energy + interfacial\ energy \qquad (5-13)$$

$$\frac{1}{2}\frac{\rho_{char}\pi d^3}{6}u^2 > 3\pi\mu u d^2 + \gamma\pi d^2 \qquad (5-14)$$

In above equation ρ_{char} is the density of the char particle, u is the velocity of the particle, μ is the viscosity of the slag layer and γ is the surface tension of the liquid slag. By comparing the order of magnitude of the different terms of above equation, they proposed the equation below as the criterion for the complete entrapment of the particles inside the slag layer:

$$du > \frac{36\mu}{\rho_{char}} \qquad (5-15)$$

The entrapment phenomena and related calculations are not considered in the particle sticking sub-model of this study to reduce the required amount of the calculations and complexity of the model and to reduce the running time. If the incoming char particles stick to the surface of molten liquid layer without being completely embodied, the progress of any possible reaction is still allowed which results in the higher rate of coal conversion [19]. Various options regarding the fate of the unconverted carbon fraction of the trapped char particle might be applied in the modeling. One option is to allow all the residual carbon fraction of the char particle to participate in the heterogeneous gasification reaction (with the same rate of the non-captured particle) by sending it back to the gas phase in the same way as if the particle was not captured [19]. Second option is to ignore further reactions of the trapped carbon content. The most accurate option is to calculate the depth of the particle penetration into molten layer and based on that the available surface area of the char particle for further reactions can be calculated. A simplifying assumption in this regard, is to assume that all the trapped particles penetrate into the slag layer a quarter of the diameter of the particle. Based on the calculated active

surface of the char particle trapped on the slag layer surface a new kinetic rate for carbon consumption of the trapped char particle on the surface of slag layer can be used [9].

Two different approaches of hard-sphere model and soft-sphere model can be used to simulate the collision of the particle with the wall. In hard-sphere model, the collision is described with no particle deformation and in soft-sphere approach, based on the active forces and particle properties, the deformation of the particles is determined. The particle-wall interaction in this study is based on the hard-sphere model.

5.3.3. Slag flow model

In order to calculate the slag layer thickness, two approaches can be used. Analytical method based on Navier-Stokes equation for momentum balance and continuity equation for mass balance. The details of this method are presented in Appendix B. Based on this method the velocity of the slag layer on the wall can be calculated by the equation below:

$$u_z = \frac{\rho g_z}{2\mu}\left((R_w-\delta)^2 \ln\frac{r}{R_w} + \left(\frac{R_w^2 - r^2}{2}\right)\right) \qquad (5-16)$$

In this equation, μ and ρ are viscosity and density of the liquid slag layer, δ is the thickness of the layer and R_w is the radius of the furnace. By integrating velocity over the cross section area of the liquid slag layer, the mass flow can be calculated as below:

$$\dot{m}_l = \int_{\delta}^{R_w} 2\rho\pi r u_z dr \qquad (5-17)$$

$$\dot{m}_l = \frac{\pi\rho^2 g_z}{8\mu}\left[-4R_w^2(R_w-\delta)^2 + R_w^4 - 4(R_w-\delta)^4 \ln\left(\frac{R_w-\delta}{R_w}\right) + 3(R_w-\delta)^4\right] \qquad (5-18)$$

Having the experimental results of the ash deposition as the inlet mass of the slag flow and all the properties, the thickness related to specific condition can be calculated.

Another approach is to use VOF two-phase model in Eulerian-Eulerian frame work in FLUENT. The calculated results of the main gasification model and the particle sticking sub-model which are saved in UDM can be assigned by the slag model when required. The sub-model receives the temperature of the furnace and the heat flux of the gas phase from the main gasification model and also receives the amount of the captured particles from particle sticking sub-model. Then the amount of the captured particles can be introduced to the slag model as the source mass term. The source term will be used in continuity equation as below:

$$\frac{\partial}{\partial t}(\alpha_s \rho_s) + \nabla.(\alpha_s \rho_s \vec{v}_s) = S_p \qquad (5-19)$$

In this equation, ρ_s is the density of slag, $\overrightarrow{v_s}$ is the velocity of the liquid slag, S_p is the source term regarding ash particle deposition which is calculated and saved by particle sticking sub-model. Using this approach, a model for viscosity must be introduced to the software as UDF. Based on viscosity toolbox of slag proposed by Duchesne et al. [30], the Urbain model might be an appropriate model for the ash and slag viscosity for the coal type which was used in this study. BCURA S2 equation used by Seggiani [6] can be used as another option to calculate slag layer viscosity as below:

$$log\mu = 4.468S^2 + 1.265(10^4/T) - 7.44 \qquad (5-20)$$

$$S = \frac{SiO_2}{(SiO_2 + Fe_2O_3 + CaO + MgO)} \qquad (5-21)$$

Where, μ is slag viscosity in poise and T is temperature in K and S is silica ratio in which slag components are presented as weight percentage. The correlations proposed by Mills and Rhine [31,32] are good references for calculation the inorganic properties such as specific heat, thermal conductivity, density and surface tension to be used in the

modeling. The equations and values for all these properties can be defined in UDF to be assigned by the solver at appropriate time.

As discussed before, it is not possible to consider all the phenomena involved in gasification process due to the high computation cost. In addition, validated understandings about some phenomena are still lacking and some of the current criteria must be improved. In a reliable model reasonable assumptions must be applied to simplify the desired system in a logical way. The assumptions applied in this modeling are as below:

- Particles will be assumed to be fully melted as soon as they are captured by the wall. In real conditions, depending on the properties such as slag viscosity, char particle density, diameter and impact velocity and also interfacial particle-slag tension, char particle entrapment inside the slag layer might happen. This phenomenon is not considered in this modeling.
- Due to the much higher density of the molten slag compared with the gas phase, the shear stress by gas phase is ignored [6].
- The physical and chemical interactions between the slag layer and the ceramic wall of the gasifier are neglected in the modeling. Based on the composition of the refractory wall in real gasifiers, there might be physical and chemical interactions between the falling slag layer and the wall (at high temperatures) and liquid slag can penetrate deeply into the refractory material. This phenomenon alters the slag chemistry and consequently changes the slag viscosity. The penetration of the liquid slag into the porous structure of the refractory might

cause an essential decrease in the slag volume which is more probable in case of new walls [10].

- All the inorganic particles are assumed to have the property of the bulk of ash. The effect of local concentration of different inorganic species is ignored.
- The coverage of the ash deposition and slag with char particle including un-reacted carbon (which can result in rebounding incoming particles) is ignored. This can cause an increase in char particle rebounding from slag surface at the moment of collision with the wall which is covered with un-reacted carbon particles. In this regard Shimizu and Tominag [24] observed a decrease in char capture by increasing the char feeding rate which was the result of unroasted particle coverage at the slag surface. Montagnaro and Salatino [23] performed some studies about the possibility of overlayering of carbon particles deposited on the slag layer by newly impacting ash material and found that, it is not likely to happen in typical operating conditions of the entrained-flow gasifiers. Therefore, this assumption seems to be logical in this modeling.
- Due to the two-way coupling approach, coalescence of the ash particles, adhesion of flame volatilized species on the surface of fly ash and other particle-particle related interactions are not considered.

The effects of either electrostatic or thermophoretic forces are not considered in the current model. These forces could have significant effects on the very small ash particles especially for the particles with size range of 1 μm or lower [21]. The ash deposition layer collected on the Fiberfrax isolation under the feeder, presented in Figure 5.6, shows that some small particles were lifted up and deposited underneath the feeder.

Figure 5.6: Deposition layer under the feeder

5.4. Results and Discussion

The purpose of this modeling is to predict the inorganic matter behavior during coal gasification in terms of the amount and location of the ash particle deposition and slag layer thickness. The results of the particle deposition are compared with the experimental results of coal gasification in an electrically heated drop tube furnace.

In order to model the inorganic matter deposition during gasification process, the first step is to model the heterogeneous reactions between carbon content of the char particles and homogeneous reactions between different species in the gas phase. The main results of this step are gas product concentration contours and temperature contours. Other steps for particle deposition and slag formation might not be accurate and reliable, unless, the first step is proved to be reasonable and validated. The contours of temperature, CO_2 and CO production for the constant wall temperature of 1723K are shown in Figures 5.7 to 5.9 respectively.

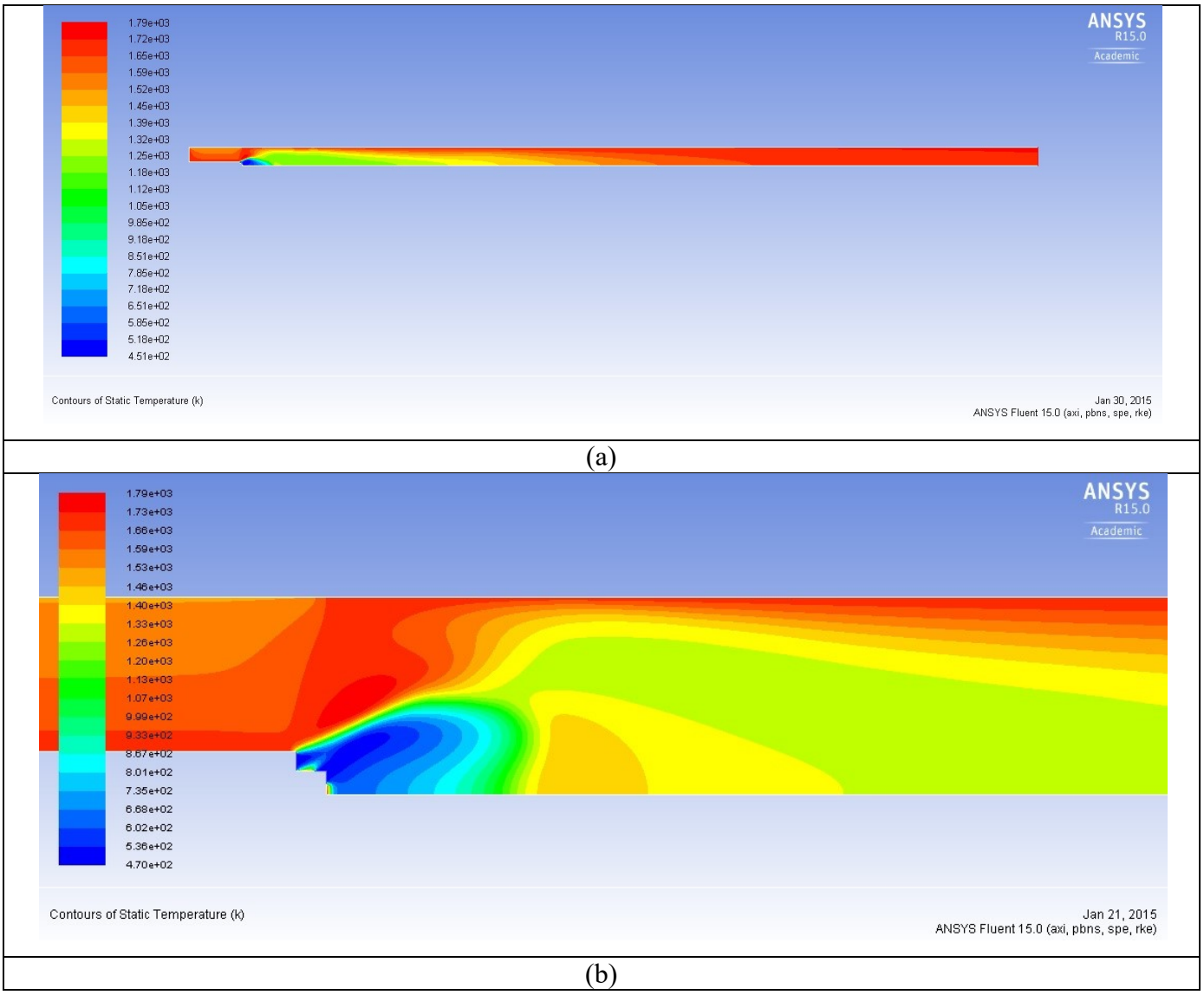

Figure 5.7: contours of temperature for constant wall temperature of 1723K (a) entire furnace (b) feeding spot area

The experimental measurement of the gas phase temperature during gasification process was not possible to perform to do comparison with the modeling results, but, the temperature distribution contour in Figure 5.7 is reasonable based on the understanding of the gasification process in an electrically heated furnace with constant wall temperature. There is a temperature peak around the feeding spot with the maximum value about 1790 K due to the existence of the flame resulted by the combustion of the

char particles as an exothermic process. The contour of CO_2 production in Figure 5.8 shows a high concentration of CO_2 (as the main product of the combustion of the carbon content of char particles) in the high temperature or flame area around the feeding spot which proves the existence of the combustion zone in the initial section of the furnace. In the combustion zone, most of the produced CO further reacts with oxygen to produce CO_2. Therefore, concentration of CO in this area is very low. Then due to the progress in the gasification reactions (which are slower in comparison with the combustion reactions), concentration of CO gradually increases and concentration of CO_2 decreases. Due to the very low feeding rate of this system, the generated heat from combustion is not enough to supply the required heat for gasification reactions and the needed energy is supplied by the electrically heated hot walls. Gasification reactions are endothermic and due to this reason the gas temperature should decrease after the combustion zone (as it decrease in self-heated gasifiers), but, due to the constant wall temperature, the gaseous mixture gradually reach the wall temperature as the mixture goes toward the end of the furnace. Based on the temperature contour, in most part of the furnace, the temperature near the wall is higher than the centre line (which is because of heated wall) and contours of CO_2 and CO production shows higher concentration of CO and lower concentration of CO_2 in that high temperature area near the wall. These results are in agreement with the current understanding of the gasification process in which by supplying the required heat at high temperature, the endothermic gasification reaction between carbon and CO_2 is promoted to produces more CO from CO_2.

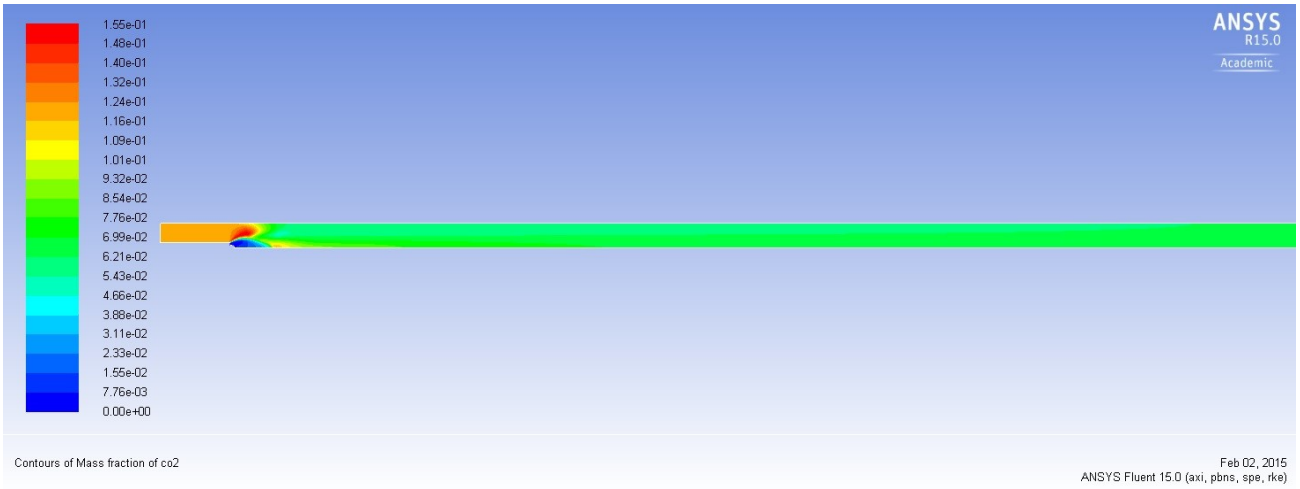

Figure 5.8: Contour of CO_2 production

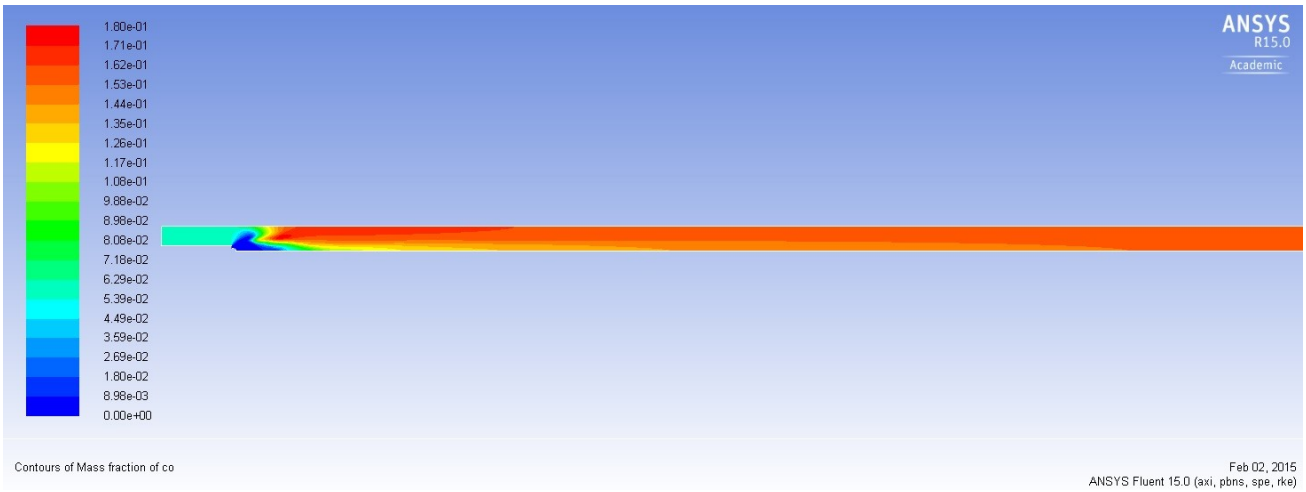

Figure 5.9: Contour of CO production

5.4.1. Particle deposition

As mentioned earlier in the particle sticking section, inorganic particle deposition is of vital importance due to its crucial role as slag builder, which is introduced as inlet mass source to the slag layer model. The amount of the particle capture by the wall highly depends on the stickiness of the particles and wall which is a function of the particle temperature, velocity (determined by gas flow rate), physical properties and carbon

conversion of char particles, temperature of the wall and properties of existing layer on the wall.

At higher temperatures, the particles are stickier due to the lower viscosity and higher carbon conversion. At higher carbon conversion, the char particles are stickier because more included inorganic matters are exposed to the surface of the char particle making it sticky enough to be captured. At higher particle velocity (especially in contact with bare wall), the particles are less probable to stick, because, the loss of the kinetic energy at high velocity is not enough to dissipate all the initial energy of the particles. Figure 5.10 shows the contour of particle deposition as the main results of this modeling.

The modeling result of the location of the particle deposition compared with the experimental result of the particle deposition is presented in Figure 5.11. This figure shows that the model predicts the main particle deposition location quite acceptable. However, comparison between experimental and modeling result for the amount of the deposition in Figure 5.12 shows noticeable differences. The error in deposition value increases from 27.1 % at temperature of 1250°C to 36.6% at temperature of 1450°C. Although, this model predicts well the deposition location, but, the amount of the deposition must be more accurate to consider it as a reliable model.

The error might be related to some of the assumptions of the modeling:

- The particle fragmentation is not considered. Importance of the fragmentation is that this phenomenon changes the particle size distribution by reducing the size of the particles and lowering the Weber number. Therefore, by fragmentation the possibility of the particle stickiness increases. In this regard Ai and Kuhlman [21]

reported that an accurate and reliable model for particle size is an essential part of the deposition and slagging modeling.

- Some sticky particles such as iron containing inorganic matters in reducing condition can easily stick to the wall and make the wall a sticky place for other particles. This fact is not considered in present modeling.
- The difference between included and excluded inorganic content of the coal is not considered.
- Gasification reaction rates might be another source of the errors. The reaction rates affect the amount of the carbon consumption in the char particles and consequently determine the carbon conversion of each particle. Carbon conversion is an applied parameter in the capture criterion and determines when a char particle is sticky enough to be captured by the wall.

In our previous experimental study [35] it was proved that in presence of the low melting point compounds with low viscosity and at high temperatures, coalescence of the inorganic particles happen leading to the big agglomerates formation. Calcium-bearing inorganic matters, act as glue in making this kind of agglomerations. As the inter-particle collisions are not considered in this modeling, formation of the agglomerates could not be predicted and evaluated.

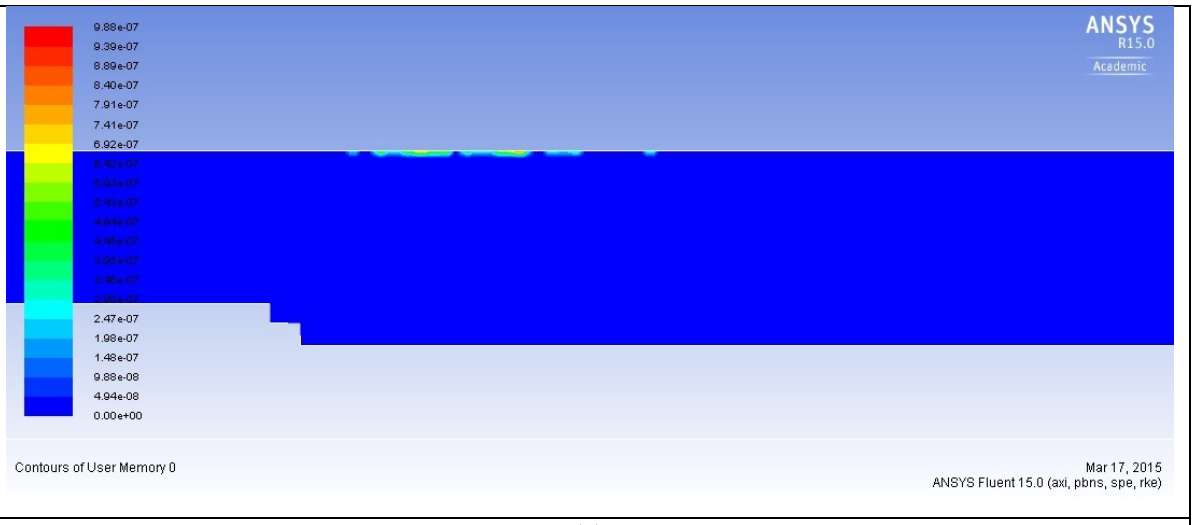

(a)

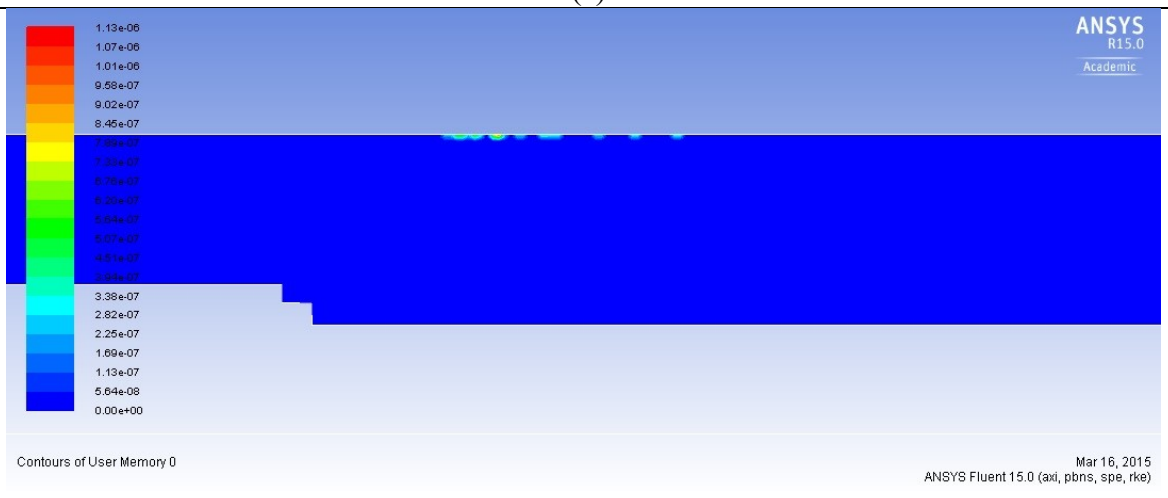

(b)

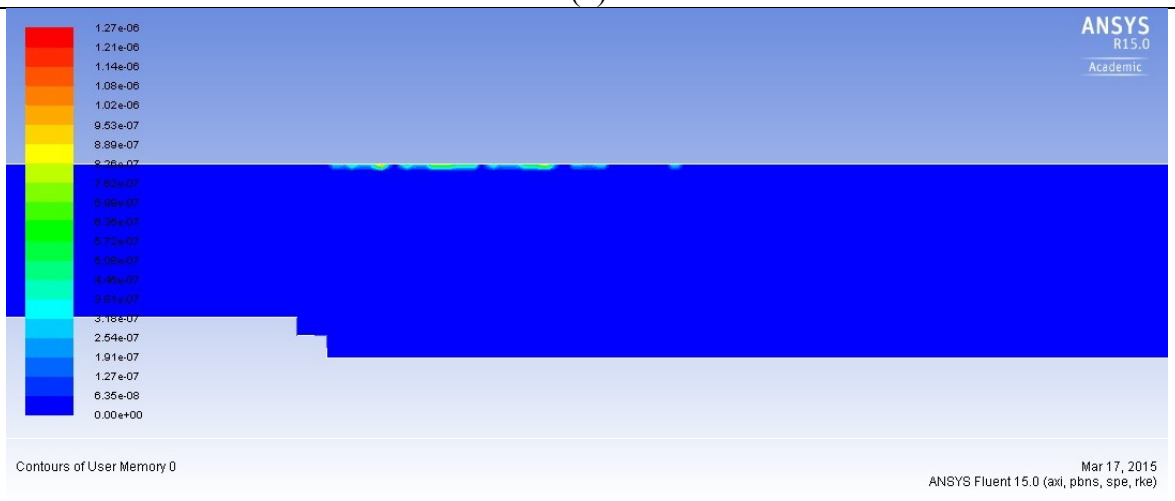

(c)

Figure 5.10: Contours of the particle deposition (a) Tw=1250°C (b) Tw=1350°C (c) Tw=1450°C

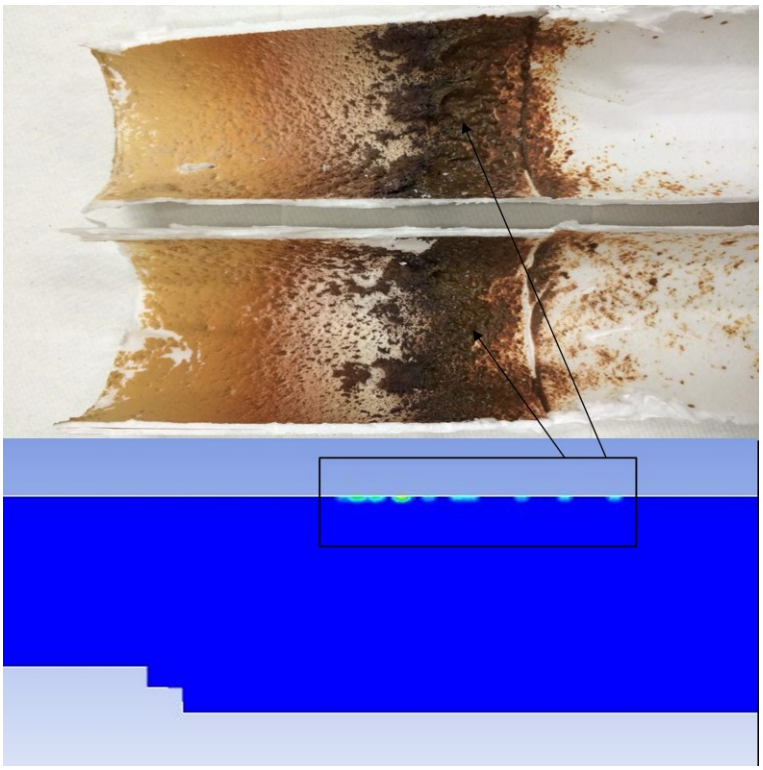

Figure 5.11: Comparison between experimental and modeling results of inorganic deposition

The slope of the increase in the particle deposition as a function of temperature is not well predicted as shown in Figure 5.12. The main reason might be that the decrease in the ash particle viscosity as a function of temperature (which affects the stickiness of the particles and capturing ability of the slag layer) is not introduced to the model by the particle capture criterion. Table 5.7 shows the experimentally measured values of the viscosity of the ash content of the coal. The amount of the deposition depends also on the temperature of critical viscosity (T_{cv}). In this regard Chen et al. [9] reported that the amount of the ash deposited on the wall of furnace increased from 23.5% to 44.1% when T_{cv} decreases from 1780 K to 1580 K. If a viscosity dependant index as a function of the temperature could be introduced to the particle stickiness sub-model, the slope of the

particle deposition as a function of temperature might be closer to the experimental results and consequently the modeling results would be more accurate and reliable.

Table 5:7: Viscosity measurement of ash [33]

Temperature (°C)	Viscosity (Pa.s)
1150	298.8
1200	91.7
1250	29.1
1300	14.3
1350	8.6
1400	5.7
1450	4.2

Temperature is not the only affecting parameter in particle deposition. The kinetic energy of the particle is another important parameter involved in the particle deposition. In this regard, Chen et al. [9] reported that usually the velocity magnitude of the trapped particles is lower than 4 m/s and near to the bottom of furnace the particles with lower carbon conversion and low velocity, can be trapped due to their lower velocity and smaller Weber number. Regarding the velocity magnitude, the direction components of the velocity must be taken into account. In the experimental part of current study, the particle deposition in the areas near to the bottom of the furnace is negligible due to the strong axial flow which pushes particles to move parallel to the wall of the furnace (the normal component of the velocity is negligible) and most of the depositions in the modeling are predicted near to the feeding area. By increasing the gas flow rate (or gas velocity), the flow inside the furnace will be more turbulent which results in more collisions of the carried particles with the wall, but, due to the higher kinetic energy lower amount of the particles can be captured.

Two main mechanisms are involved in migration of the particles toward the wall of furnace. The first one is the inertial mechanism which is more important in case of the coarser or high density particles. In this mechanism, the forces induced by the continuous phase such as drag force or centrifugal force (resulted by swirled flow), dominates the motion of the particles [19]. The other mechanism is turbulence-promoted dispersive motion which is mostly the result of the concentration gradients of the particle phase and is mainly determined by the turbulence inherent of the gas phase [19]. Working with very small coal particles, increases the heating up process and consequently promotes the reaction of the carbon fraction with the hot oxidant medium as they pass through the gasifier. But, these small particles mostly follow the gas stream lines which reduces their ability to continue their own path-line toward the wall [19].

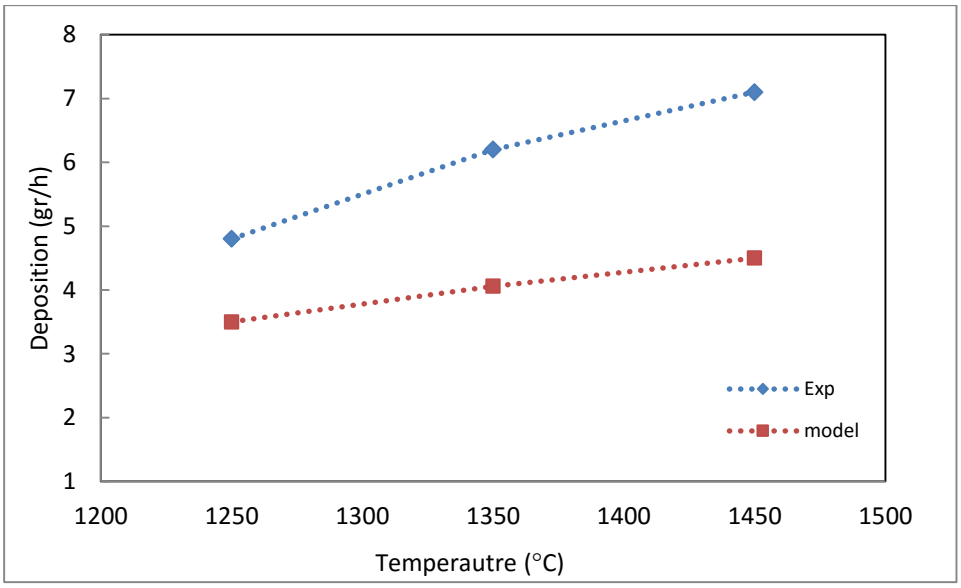

Figure 5.12: Experimental and modeling results for particle deposition

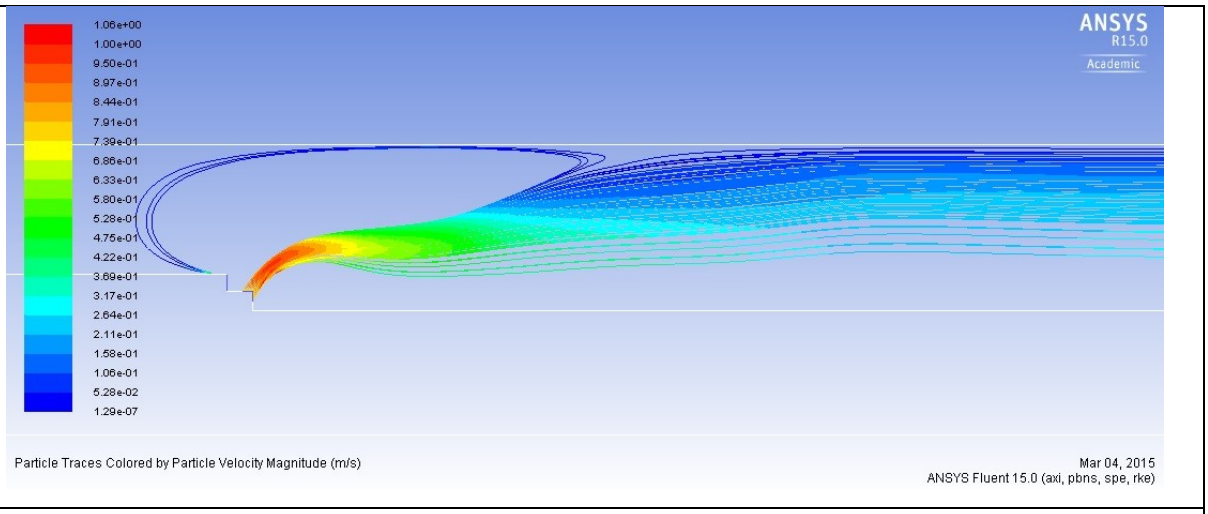

(a)

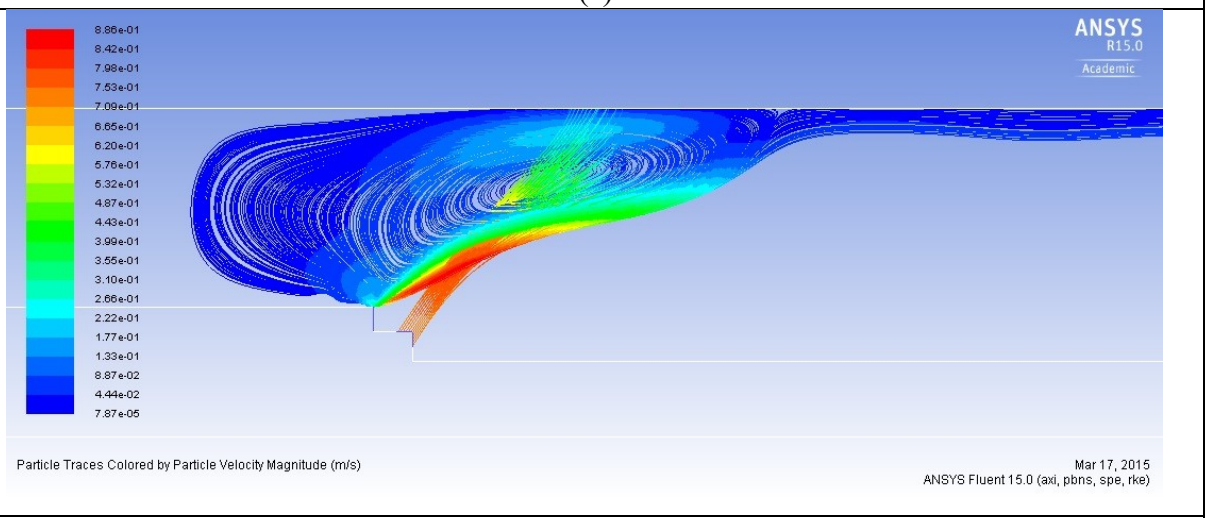

(b)

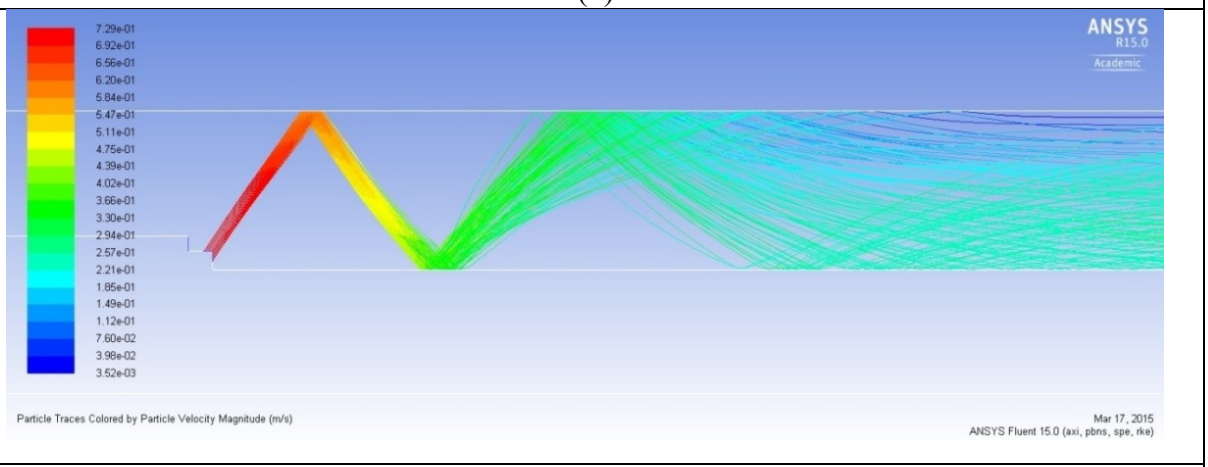

(c)

Figure 5.13: Contours of particle path-line (a) size range of 28-53µm (b) size range of50-100 µm (c) size range of 200-300µm

There is a difference between the behavior of the big and small particles. Small particles after the first impact usually are transported parallel to the wall and do not hit the wall again, but, the bigger particles due to the inertial effect might hit the wall several times. For both big and small sizes, the effect of the radial motion is reduced in the areas far from the feeding spot and therefore, most of the particles move parallel to the wall of the furnace. This fact is shown in Figure 5.13 which presents the contours of the path-line for the particles with different sizes. Contour of particle path-line is of great importance in order to evaluate the parameters related to behavior of the particles such as capture efficiency and sticking efficiency. These parameters are helpful to find the areas on the wall of furnace which are more probable to receive deposition and predict the possible locations of erosion and corrosion.

5.4.2. Slag layer thickness

The flow of slag on the wall of gasifier, especially its thickness is the main desired result of any inorganic deposition modeling. The main purpose of the modeling is to achieve a reliable prediction of the slag layer thickness to perform the gasification operation at the safe conditions to prevent from emergency shutdown resulted by the slag flow blockage. Experimental results of the coal gasification show that the slag layer starts to form and flow below the initial point of the particle deposition which is near the feeding spot at the top section of the furnace [35].

Figure 5.14 shows slag layer thickness for various amount of the deposition resulted by different operating temperatures. These thicknesses are calculated by solving Navier-Stokes equation for momentum balance and continuity equation for mass balance. Due to the low T_{cv} of the inorganic content of the coal, it has been assumed that there is no solid

slag layer. Also the temperature gradient inside the liquid falling slag layer (which affects the viscosity) is not taken into account. In this regard, Chen et al. [9] reported that when there is a thin thickness of the slag layer on the wall, temperature gradient inside the molten slag layer is less than 10 K and could be neglected.

However, by increasing the temperature the amount of deposition increases (as shown in Figure 5.12), but, based on Figure 5.14 the slag layer thickness decreases from 2.2mm at temperature of 1250°C to 1.3mm at temperature of 1450°C. This finding shows that the decrease in the viscosity at higher temperature is more effective than the increase in the amount of the particle deposition due to higher particle stickiness.

Table 5.8 presents the slag layer information such as slag layer thickness (δ[mm]) and maximum velocity of the slag (Uz,max[mm/s]) which happens at the surface of the slag. This table shows that by increasing the temperature, the velocity of the falling slag layer increases because of the decrease in the viscosity. The low slag velocity is in good agreement with the results of Chen et al. [10] who reported that the slag velocity is generally very low (especially in comparison with gas), because, the viscosity of the molten slag is in the range of 4-30 Pa.s which is approximately 6 order of magnitude higher than the gas viscosity. Because of the high density of the molten slag, gravity is the dominant cause of the slag flow which drives slag to flow in axial direction along the wall to the bottom of the furnace.

The calculated thicknesses in Figure 5.14, is based on the uniform particle distribution and deposition (based on the axisymetric assumption in modeling), but, the experimental results showed uneven deposition and slag flow as shown in Figure 5.15. This figure shows that slag layer does not cover all the surface of the wall of furnace evenly and

might have different paths with deviation from straight vertical line. Figure 5.16 shows the BSE image of the cross section of the slag layer on the wall which proves that the thickness of the falling slag layer on the wall is not uniform.

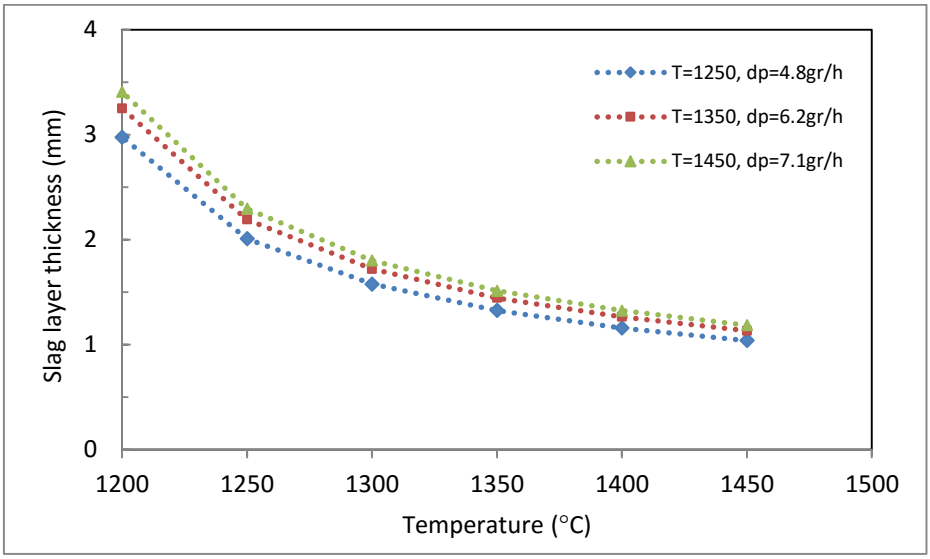

Figure 5.14: Slag layer thickness at different temperatures

Table 5:8: Slag layer characteristics at different temperatures

T[°C]	δ[mm]	μ[Pa.s]	Uz,max (at r=Rw-σ) [mm/s]
1250	2.204	29.1	2.3
1350	1.562	8.55	3.9
1450	1.275	4.16	5.4

Figure 5.15: Experimental results of slag flow on the wall of gasifier

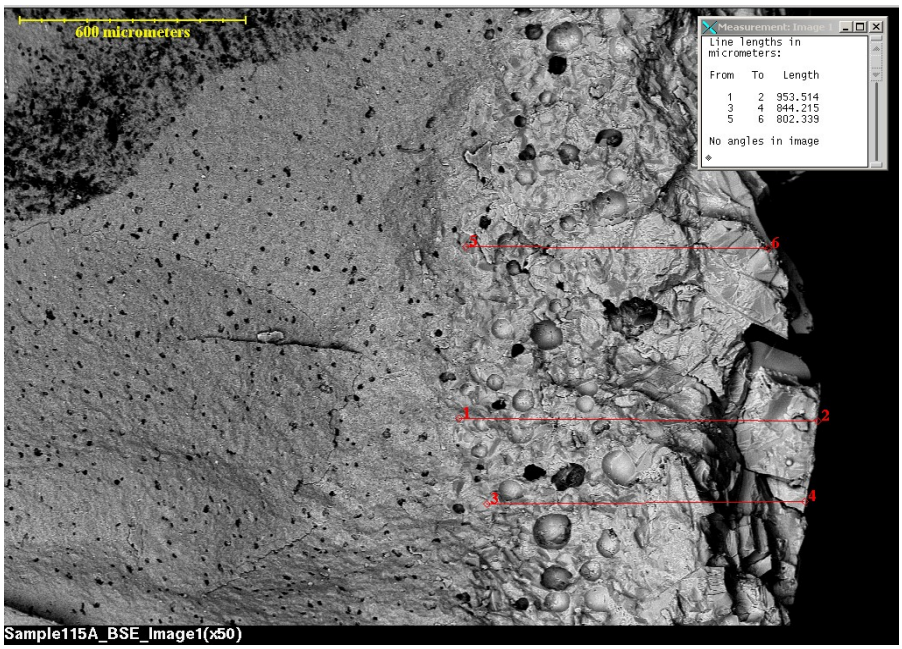

Figure 5.16: BSE image of the cross section of flowing slag layer on the wall of furnace

5.5. Conclusion

A 2D-axisymetric CFD model of the inorganic deposition is implemented in ANSYS Fluent based on an electrically heated drop tube furnace. A particle capture sub-model is integrated with the coal gasification model. Particle capture sub-model is written code in C++ language and is introduced to the software as UDF and the results are saved in UDM.

The particle deposition contours showed that the amount of the deposition increases with increasing the temperature, which is in agreement with the experimental deposition results. The reason is due to the higher stickiness of the particles at higher temperatures. Although, the location of the particle deposition is well predicted, but, there are noticeable differences between the predicted amounts of the deposition and the experimental values which is thought to be related to the simplifying assumptions of the

model and can be improved in future modeling by enhancing the assumptions and using more accurate sub-models. The most important improvement can be performed by considering the different types of association of the inorganic matters with coal particles (included and excluded mineral matters). CCSEM results can be used in this regard.

Although the amount of the deposition increases by increasing the temperature, but, the calculated slag layer thickness showed that the layer thickness at temperature of 1450°C is lower in comparison with the thickness at temperature of 1250°C. This shows that, the decrease in the viscosity of the molten slag layer is more effective than the increase in the amount of the particle deposition at higher temperatures.

The path-line of the particles with different sizes showed that the small particles would follow the gas stream-lines and usually move parallel to the wall after the initial impact with the wall, but, the big particles might hit the wall several times. Both big and small particles would move parallel to the wall when they are far from the feeding zone area.

Acknowledgement

This study is financially supported by C^5MPT and Helmholtz- Alberta initiative (HAI) center. The authors would express their special thanks to Dr. Esmaeil Safaee and Dr. Shayan Karimipour for all their guides and supports.

References

[1] Gupta S, Gupta R, Bryant G, Wall T, Watanabe S, Kiga T, Characterization of ash deposition and heat transfer behavior of coals during combustion in a pilot-scale facility and full-scale utility. Energy Fuels 2009; 23:2570–5.

[2] Song W, Tang L, Zhu X, Wu Y, Zhu Z, Koyama S, Flow properties and rheology of slag from coal gasification, Fuel 89 (2010) 1709–1715

[3] Luan C, You C, Zhang D, An experimental investigation into the characteristics and deposition mechanism of high-viscosity coal ash. Fuel 119 (2014) 14–20

[4] Zbogar A, Frandsen F, Jensen P A, Glarborg P, Shedding of ash deposits. Prog Energy Combust Sci 2009;35:31–56.

[5] Yang Z, Wang Z, Wu Y, Wang J, Lu J, Li Z, Ni W, Dynamic model for an oxygen-staged slagging entrained-flow gasifier, Energy Fuels 2011, 25, 3646-3656

[6] Seggiani M, Modeling and simulation of time varying slag flow in a Prenflo entrained-flow gasifier, PII: S0016-2361(98)00075-1

[7] Yong S Z, Gazzino M, Ghoniem A, Modeling the slag layer in solid fuel gasification and combustion – Formulation and sensitivity analysis, Fuel 92 (2012) 162–170

[8] Yong S Z, Ghoniem A, Modeling the slag layer in solid fuel gasification and combustion – Two-way coupling with CFD, Fuel 97 (2012) 457–466

[9] Chen. L, Yong S Z, Ghoniem A F, Modeling the slag behavior in three dimensional CFD simulation of a vertically-oriented oxy-coal combustor, Fuel Processing Technology 112 (2013) 106–117

[10] Chen L, Ghoniem A F, Development of a three-dimensional computational slag flow model for coal combustion and gasification, Fuel 113 (2013) 357–366

[11] Chen C, Horio M, Kojima T, Use of numerical modeling in design and scale up of entrained flow coal gasifier, Fuel 80 (20010 1513-1523

[12] Wen C Y, Chaung T Z, Entrainment Coal Gasification Modeling, Ind. Eng. Chem. Process Des. Dev., 1979, 18 (4), pp 684–695

[13] Govind R, Shah J, Modeling and simulation of an entrained flow coal gasifier, AIChE J., 30 (1), 79-92 (1984).

[14] Liu S, Hao Y, Numerical study on slag flow in an entrained-flow gasifier, ASME Conf Proc 2007;2007:793–800.

[15] Ni J, Zhou Z, Yu G, Liang Q, Wang F, Molten slag flow and phase transformation behaviors in a slagging entrained-flow coal gasifier. Ind Eng Chem Res 2010;49:12302–10.

[16] Montagnaro F, Salatino P, Analysis of char–slag interaction and near-wall particle segregation in entrained-flow gasification of coal, Combustion and Flame 157 (2010) 874–883

[17] Noda R, Naruse I, Ohtake K, Fundamentals on combustion and gasification behavior of coal particle trapped on molten slag layer. J Chem Eng Jpn 1996;29:235–41.

[18] Wang X H, Zhao D Q, He L B, Jiang L Q, He Q, Chen Y, Modeling of a coal-fired slagging combustor: development of a slag sub-model. Combustion and Flame 2007;149:249–260.

[19] Ambrosino F, Wall effects in particle-laden flows, PhD thesis in Chemical Engineering, Universita' Degli Studi Di Napoli "FEDERICO II", November 2011

[20] Losurdo M, Spliethoff H, Kiel J, Ash deposition modeling using a visco-elastic approach, Fuel 102 (2012) 145–155

[21] Ai W, Kuhlman J.M, Simulation of Coal Ash Particle Deposition Experiments, Energy Fuels 2011, 25, 708-718.

[22] Montagnaro F, Salatino P, The role of slag formation on late carbon conversion in entrained-flow gasification of coal, Dipartimento di Chimica, UniversitaStudi di Napoli Federico II, Napoli, Italy, 2009

[23] Nakod P, Orsino S, Walavalkar A, Sami M, Development and validation of a volatile break-up approach for gasification simulations, 38th International Technical Conference on Clean Coal and Fuel Systems, June 2-6, 2013

[24] Shimizu T, Tominag H, A model of char capture by molten slag surface under high temperature gasification conditions, Fuel 85 (2006) 170–178

[25] Shannon G N, Rozelle P L, Pisupati V, Sridhar S, Conditions for entrainment into a FeOx containing slag for a carbon-containing particle in an entrained coal gasifier, Fuel Processing Technology 89 (2008) 1379–1385

[26] Mueller C, Selenius M, Theis M, Skrifvars B J, Backman R, Hupa M, Tran H, Deposition behavior of molten alkali-rich fly ashes—development of a sub-model for CFD applications, Proceedings of the Combustion Institute 30 (2005) 2991–2998

[27] Ni J, Yu G, Guo Q, Zhou Z, Wang F, Sub-model for predicting slag deposition formation in slagging gasification systems, Energy Fuels 2011, 25, 1004–1009

[28] Li S, Wu Y, Whitty K J, Ash deposition behaviour during char–slag transition under simulated gasification conditions, Energy & Fuels 24 (2010) 1868–1876.

[29] Li S, Whitty K J, Investigation of Coal Char−Slag Transition during Oxidation: Effect of Temperature and Residual Carbon, Energy Fuels 23 (2009) 1998-2005

[30] Duchesne M A, Bronschb A M, Hughes R W, Masset P J, Slag viscosity modeling toolbox, fuel.2012.03.010

[31] Mills K C, Rhine J M, The measurement and estimation of the physical properties of slags formed during coal gasification: 1. Properties relevant to fluid flow. Fuel 1989;68:193–200.

[32] Mills K C, Rhine J M, The measurement and estimation of the physical properties of slags formed during coal gasification: 2. Properties relevant to heat transfer. Fuel 1989;68:904–10.

[33] Duchesne M, Hall A, Hughes R, McCalden D, Anthony E, Macchi A, Fate of inorganic matter in entrained-flow slagging gasifiers: Fuel characterization. Fuel Processing Technology 118 (2014) 208–217

[34] Vejahati F, Entrained-flow gasification of oil sand coke, PhD thesis, Department of Chemical and Materials Engineering, University of Alberta, Spring 2012

[35] Hosseini S, Gupta R, Inorganic Matter Behavior during Coal Gasification: Effect of Operating Conditions and Particle Trajectory on Ash Deposition and Slag Formation, Energy Fuels 2015, 29, 1503−1519

[36] ANSYS Fluent User's Guide, Release 15.0, November 13

[37] Silaen A, Wang T, Effect of turbulence and devolatilization models on coal gasification simulation in an entrained-flow gasifier, International Journal of Heat and Mass Transfer 53 (2010) 2074–2091

Chapter 6. Conclusion and Recommendations for future works

6.1. Conclusion

In the first part of experiments of this study, evaluation of the effects of the operating conditions and trajectory of the particles on the inorganic deposition and slag formation were done. In this regard, gasification experiments with two types of Canadian coal were performed to analyze the effect of the inorganic compositions on the particle deposition and slag flow. Two size ranges of particles were used for each coal type. Two different feeder configurations were tested. Temperature and gas flow rate were varied to evaluate the effect of operating conditions on ash deposition.

In all the experiments, increasing the temperature made the particles stickier (excluded inorganic particles and char particles containing included inorganic matters) and led to higher depositions regardless of the fuel type and feeding configuration. But, at the same time, increasing the temperature reduced the slag viscosity which caused the flow rate of the molten slag layer to increase. Therefore, by increasing the temperature, the slag flow

rate usually increases. It was understood that for each coal type, a minimum value of the temperature might exist at which the amount of the inorganic matters deposition and slag flow are controllable to prevent from blockage. But, considering two opposing results of the higher amount of the sticky particles and higher slag flow rate at higher temperatures, it was understood that increasing the temperature cannot guarantee the safe operation by reducing the deposit thickness.

Increasing the gas flow rate (or gas phase velocity), in most cases reduced the amount of the deposition for both fuels regardless of the type of the feeder. The reason is most likely related to the kinetic energy of the particles at the moment of impact to the bare wall. In addition, increasing the gas flow rate reduces the residence time of the particles which results in the decrease in carbon conversion of the char particles. Particles with lower carbon conversion are less sticky. Bigger particles, due to the higher kinetic energy showed lower deposition tendency than the smaller particles at the same condition. Another reason for the higher deposition tendency of the small particles is that these particles usually have higher carbon conversion and also reach to the environment temperature sooner than the big particles. Therefore, smaller particles start to melt sooner.

For F1, iron had an important role in the inorganic deposition behavior. CCSEM analysis of this fuel showed that most of the iron-bearing minerals existed as excluded particles. In reducing conditions during gasification experiments, most of the iron species exist in reduced states which have low melting point. These low melting point particles can be readily captured upon collision with the wall and make it a sticky surface for other particles to be trapped. Average EDX analysis of the deposition of F1 at different

locations showed that the iron concentration at the top section is much higher than other sections.

In deposition tendency of F2, calcium had a significant role. Calcium made the viscosity of the bulk of ash and slag low enough which usually led to the smooth slag flow. In most of the experiments with F2, there was a thin layer of the slag flowing down on the wall of the furnace. CCSEM analysis of this fuel showed that the excluded minerals of F2 were lower than F1. In addition, most of the calcium-bearing minerals existed as included particles. At high temperatures, the inorganic particles of F2 coalesced and adhered together and made big agglomerations. The reason was understood to be related to the melting of the included calcium-bearing inorganic matters which acted as glue to force other inorganic matters to stick together and make big agglomerations. The size of these agglomerations could reach to more than hundred microns which is hard to stick to the wall at the top section. In lower sections, by increasing the carbon conversion of the char particles and also by increasing the number of times that each particle collides with the wall, the probability of their sticking would increase. Lots of the inorganic agglomerates were found in cyclone for F2, but, in case of F1 ash agglomerates in cyclone were much lower.

Based on the comparison of the depositions of these fuels and CCSEM analysis of them, it was understood that using viscosity to predict the amount of the deposition might results in the wrong predictions of the inorganic matters behavior. Inorganic loading, especially iron and calcium loading is a very crucial parameter which might cause a coal with very high ash viscosity to result in very high deposition. High amount of the particle depositions in combination with low viscosity increases the blockage probability.

The deposition was affected by the feeding configuration for both fuels. Feeder A8 resulted in very thick deposition by injecting the coal particles on a narrow area. The severe growth of the deposition for feeder A8 was more observable for F1 due to the high iron concentration on the surface of deposit. Feeder C4 injected the particles on a wider area than A8, therefore, the deposition for C4 was more uniform with lower thickness.

Blockage analysis of the collector probes showed that for F1 increasing the temperature form 1350°C to 1550°C did not decrease the blockage probability. In this case, increase in the amount of the sticky particles (as the inlet mass to the slag layer) is more effective than the reduction of the slag viscosity at high temperatures. Working with F1, even very high operating temperature could not guarantee the safe operation.

Blockage never happened in slag collector probes during the gasification process of F2 at temperature higher than 1250°C. However, there was a very thick layer of the slag near to the bottom of the furnace where the temperature was very low. Therefore, the most important required precaution during the gasification process of F2 is controlling the operating temperature to be adjusted in a specific range. Using F2 and performing the process at the temperature higher than 1250°C could assure the safe operation.

Different concentrations of iron in the deposit layer in axial and radial directions, especially working with F1, signified a gas-inorganic interaction on the surface of slag. Analyzing slag pieces under different atmospheres proved the possibility of the reactions between iron and syngas species. It was understood that iron might react with the gaseous species, produce unstable gaseous compound and leave the surface. Also due to the solubility limitation, all the iron on the slag surface could not be dissolved into the deposit layer.

In the second part of the experiments in this study, ash deposition was studied by controlled injections in terms of operation conditions such as temperature, velocity and impact angle. The purpose of this set of experiments was to obtain experimentally validated criterion for ash particle stickiness.

In all the cases, increasing the temperature led to higher deposition, because, inorganic particles are stickier at higher temperatures. The reason is most likely related to the higher liquid fraction of the particles with lower viscosity at higher temperature. In addition, a molten layer forms after sticking of the initial particles which has lower viscosity as the temperature increases and captures more particles.

Increasing the velocity at low temperature slightly decreased the deposition. The reason is related to the kinetic energy of the particles which is hard to dissipate at the moment of impact for particles with higher velocity. Because at lower temperature the liquid fraction of the particle is lower and the particles might be rigid. Also the existing deposit layer on the plate had higher viscosity and penetration into the high viscosity layer was harder and rebounding was more probable as the kinetic energy of the particle increased. At high temperature, increasing the velocity slightly increased the deposition. The reason is thought to be related to the lower viscosity of the ash particles and molten layer on the ceramic plate. At higher temperature the liquid fraction of the particles is higher. Therefore the particles might deform to splat shape at the moment of collision. At higher velocity the spread diameter of the particles is higher which increases the sticking probability. In addition, high velocity particle can penetrate into the molten layer easier than the lower one.

Changing the impact angle from 30° to 60° slightly led to the higher deposition. The reason is related to the change in the components of the particle velocity by variation in the impact angle. By decreasing impact angle, the tangential component of the particle velocity increases which pushes the particle down and does not let the particle to spread out on the surface or penetrate into the molten layer.

It was understood that the reason for the small differences between the depositions at various velocities and impact angles might be related to the stickiness of ash (burned coal with very high carbon conversion). Ash particles are very sticky; therefore, the sticking probability to the surface is very high which minimizes the effect of the other parameters. Using the char particles with lower carbon conversion will probably lead to the more distinguishable differences between the deposition of the various impact angle and velocities.

The last part of this study was to perform a modeling for the inorganic matters deposition during coal gasification. A 2D-axisymetric CFD model was implemented in ANSYS Fluent based on an electrically heated drop tube furnace. A particle capture sub-model was integrated with the gasification model. Particle capture sub-model is written code in C++ language and is introduced to FLUENT as UDF and the results were saved in UDM.

The particle deposition contours showed that the amount of the deposition increases with increasing the temperature which was in agreement with the trend of the experimental results. The reason is increase in the stickiness of the particles and wall of the furnace at higher temperatures. The location of the particles deposition was well predicted. But, there was noticeable difference between the predicted amounts of the deposition compared with the experimental deposition values. These big errors are thought to be

related to the simplifying assumptions of the model and can be improved in future modeling by applying other sub-models to consider more affecting phenomena. Considering the temperature dependence of the viscosity in particle capture sub-model might improve the deposition results. In addition, considering the type of association of the inorganic matters with coal particles (included and excluded inorganic matters) enhances the accuracy of the deposition results. CCSEM analysis of the raw coal can be useful in this regard.

Calculated slag layer thickness showed that although the amount of the deposition increases at higher temperatures, but, the slag layer thickness at temperature of 1450°C is lower in comparison with the slag layer thickness at temperature of 1250°C. This result shows that the decrease in the viscosity of the molten slag layer is more effective than the increase in the amount of the particle deposition at higher temperature for this specific coal type.

The path-lines of the particles with different sizes showed that small particles would follow the gas stream-lines and usually move parallel to the wall after the initial impact, but, bigg particles would collide with the wall several times. Both big and small particles move parallel to the wall of the furnace when they are far from the feeding zone.

6.2. Recommendations for future work

1- The difference between included and excluded mineral matters can be considered to increase the accuracy of the particle interaction with the wall. Included minerals can be considered as a fraction of the combustible particles in DPM and for excluded minerals, a separate injection can be added considering only inert

particles. In UDF the properties of the included minerals must be entered as combustible captured and the properties of excluded must be entered as inert captured particles. Utilization of the results of CCSEM technique in modeling would be beneficial to get closer to the real gasification conditions.

2- It is very valuable to differentiate between the different compositions of the inorganic matters during gasification process. For example iron-bearing minerals in reducing conditions have low melting point and their behavior is different form alumina silicate minerals. Due to the low melting point, iron can stick sooner to the wall of furnace and then make the wall a sticky place for other particles to be captured. This fact was observed in experiments, but, was not considered in any CFD modeling till now. To take it into account, more than one type of combustible particles and more than one type of inert particles must be defined in injection panel in FLUENT.

3- The interaction between molten inorganic matters in the slag flow and the wall of furnace can be considered in CFD modeling. One of the main issues of inorganic matter is reducing the life time of the wall of the furnace by reacting and dissolving the wall material. Also, due to the reactions between the slag layer and the wall of furnace, the viscosity of the slag flow might change which affect the slag thickness on the wall.

4- Evaporation and condensation of the alkali metal oxide which might affect the capture efficiency of the surface is worthwhile to be considered in CFD modeling.

5- Considering the differences between the particles floated at the surface of the slag and the particles completely embodied into the slag (which affects the carbon

content in the slag layer, total fuel conversion and process efficiency) can promote the reliability of the model. Some criterions are proposed in this regard which can be used in the particle capture sub-model in UDF.

6- The four-way coupling in CFD modeling can be useful to consider the effect of the inter-particle collisions to evaluate the amount of the particle coalescence and agglomeration. This can enhance the accuracy of the model for particle deposition.

7- Considering the temperature dependence of the viscosity in the particle capture sub-model can be a good approach to improve the accuracy and reliability of the modeling results.

8- Performing controlled injection experiments with char particles with different carbon conversions.

9- Performing controlled injection experiments with particles with specific size and composition. Then it is possible to calculate the We and Re number for each particle to obtain more accurate criterion.

10- The effect of the slag layer coverage by carbon particles on the fate of incoming inorganic matters can be investigated in controlled injection. It is possible to cover the surface of slag layer by low converted char particle and then inject inorganic matters or char particles and analyze the behavior. This finally can be useful in modeling.

11- It is very beneficial to design a setup to inject the particles tangentially (swirl flow injection) to simulate the conditions of the industrial gasification plants and then evaluate the deposition based on the operating conditions.

Full References

Chapter 1 and 2

[1] International energy Agency, http:// www.iea.org

[2] Higman C, Vander Burgt M, Gasification, Elsevier Sciences, 2003

[3] Vejahati F, Entrained-flow gasification of oil sand coke, PhD thesis, Department of Chemical and Materials Engineering, University of Alberta, Spring 2012

[4] Stiegel G J, Ramezan M, Hydrogen from coal gasification: An economical pathway to a sustainable energy future, International Journal of Coal Geology 65 (2006) 173– 190

[5] Crnomarkovic N, Repic B, Mladenovic R, Neskovic O, Veljkovic M, Experimental investigation of role of steam in entrained flow coal gasification, Fuel 86 (2007) 194–202

[6] Elliot M A, Chemistry of coal utilization, Secondary supplementary volume, NAS-NRC committee on chemistry of coal, 1981 by Wiley & Sons, Inc.

[7] Li S, Char–slag transition during pulverized coal gasification, PhD Thesis, Chemical Engineering Department, university of Utah, 2010

[8] Kinaef N, A review of mineral matter issue in coal gasification, CCSD (Cooperative research centrefor coal in sustainable development) research report 60, 2006, Australia

[9] Walsh P M, Sarofim A F, Beer J M, Fouling of Convection Heat Exchangers by Lignitic Coal Ash, Energy and Fuels 6:709-715 (1992).

[10] Yang Z, Wang Z, Wu Y, Wang J, Lu J, Li Z, Ni W, Dynamic model for an oxygen-staged slagging entrained-flow gasifier, Energy Fuels 2011, 25, 3646-3656

[11] Song W, Tang L, Flow properties and rheology of slag from coal gasification, engineering research center of large scale reactor engineering and technology, East China University of science and technology, 2010

[12] Duchesne M A, Macchi A, Lu D Y, Hughes R, Artificial neural network model to predict slag viscosity over a broad range of temperatures and slag compositions, Fuel Processing Technology 91 (2010) 831–836

[13] Song W, Tang L, Zhu X, Wu Y, Rong Y, Fusibility and flow properties of coal ash and slag, Fuel 88 (2009) 297–304

[14] Raask E, Mineral impurities in coal combustion, Behavior, Problems and Remedial Measures, Hemisphere Publishing Corporation, New York, 1985.
[15] Wall T F, Mineral matter transformation and ash deposition in pulverized coal combustion, The combustion coal institude, 1992/pp. 1119-1126
[16] Li X, Li G, Cao Z, Xu Sh, Research on Flow Characteristics of Slag Film in a Slag Tapping Gasifier, Energy fuels 2010, 24, 5109-5115
[17] Lingxue K, Jin B, Wen L, Zong-qing B, Zhen-xing G, Effect of lime addition on slag fluidity of coal ash, Journal of Fuel Chemistry and Technology, 2011, 39(6), 407-411
[18] Wei Y, Li H, Honma K, Tanoskai T, Ninomiya Y, Effect of additives on slag properties in an entrained bed gasifier, World of Coal Ash (WOCA) Conference, 2011, Denver, USA
[19] Lu T, Zhang L, Zhang Y, Feng Y, Li H X, Effect of mineral comosition on coal fusion temperature. Journal of Fuel Chemistry and Technology, 2010, 38(2): 23–28.
[20] Yu L J, Huang Z Y, Cheng J, Pan H Y, Zhou J H, Cen K F, Study on the coal ash fusibility during blending coal combustion. Journal of Fuel Chemistry and Technology, 2009, 37(2): 139–144.
[21] Van Dyk J C, Waanders F B, Benson S A, Laumb M L, Hack K, Viscosity predictions of the slag composition of gasified coal, utilizing FactSage equilibrium modeling, Fuel 88 (2009) 67–74
[22] Gupta S, Dubikova M, French D, Sahajwalla V, Effect of CO2 gasification on the transformations of coke minerals at high temperatures, Energy & Fuels 21 (2) (2007) 1052
[23] Skodras G, Sakellaropoulos G P, Mineral matter effects in lignite gasification, fuel process technology 77-78 (2002) 151-158
[24] Bai J, Li W, Li C, Bai Z, Li B, Influence of mineral matter on high temperature gasification of coal char, Journal of Fuel Chemistry and Technology, 2009, 37(2), 134-138

[25] Liu H, Luo C, Toyota M, Kato S, Uemiya S, Kojima T, Tominaga H, Mineral reaction and morphology change during gasification of coal in CO_2 at elevated temperatures, Fuel 82 (2003) 523-530
[26] Matjie R H, French D, Ward C R, Pistorius P C, Li Z, Behavior of coal mineral matter in sintering and slagging of ash during gasification process, Fuel Process Technol. (2011), doi:10.1016/j.fuproc.2011.03.002
[27] Couch G, Understanding of slagging and fouling in PF combustion. IEA Coal Res 1994.
[28] Matsuoka K, Suzuki Y, Eylands K E, Benson S A, Tomita A, CCSEM study of ash forming reactions during lignite gasification, Fuel 85 (2006) 2371–2376
[29] Gupta S K, Wall T F, Creelman R A, Gupta R P, Ash fusion temperatures and the transformations of coal ash particles to slag, Fuel Processing Technology 56 _1998. 33–43
[30] Lin S, Hirato M, Horio M, The characteristics of coal char gasification at around ash melting temperature, Energy & Fuels 8 (1994) 598–606
[31] Montagnaro F, Salatino P, The role of slag formation on late carbon conversion in entrained-flow gasification of coal, Dipartimento di Chimica, UniversitaStudi di Napoli Federico II, Napoli, Italy, 2009
[32] Noda R, Naruse I, Ohtake K, Fundamentals on combustion and gasification behavior of coal particle trapped on molten slag layer. J Chem Eng Jpn 1996;29:235–41.
[33] Zhao X, Zeng C, Mao Y, Li W, Peng Y, Wang T, Eiteneer B, Zamansky V, Fletcher T, The surface characteristics and reactivity of residual carbon in coal gasification slag, Energy Fuels, 2010, 24, 91-94
[34] Costen P G, Locwood F C, Siddique M M, mathematical modeling of ash deposition in pulverized fuel-fired combustors, Proceedings of the Combustion Institute, Volume 28, 2000/pp. 2243–2250
[35] Ghosal S, Ebert J L, Self S A, Chemical composition and size distributions for fly ashes, Fuel Processing Technology 44 (1995) 8 l-94
[36] Brachi P, Montagnaro F, Salatino P, Char-Wall Interaction and Properties of Slag Waste in Entrained-Flow Gasification of Coal, European Combustion Meeting 2011

[37] Naruse I, Kamihashira D, Miyauchi Y, Kato Y, Yamashita T, Tominaga H, Fundamental ash deposition characteristics in pulverized coal reaction under high temperature conditions, Fuel 84 (2005) 405–410

[38] Seggiani M, Bardi A, Vitolo S, Prediction of fly-ash size distribution: a correlation between the char transition radius and coal properties, Fuel 79 (2000) 999–1002

[39] Montagnaro F, Salatino P, Analysis of char–slag interaction and near-wall particle segregation in entrained-flow gasification of coal, Combustion and Flame 157 (2010) 874–883

[40] Wilemski G, Srinivasachar S, Sarofim A F, Modeling of mineral matter redistribution and ash formation in pulverized coal combustion. In: Benson SA, editor. Inorganic transformations and ash Deposition during combustion, New York: Engineering Foundation Press, ASME, 1992.

[41] Barta L E, Toqan M A, Beer J M, Sarofim A F, Prediction of fly-ash size and chemical composition distributions: the random coalescence model. 24th Symp.(Int) on Combustion, The Combustion Institute, 1992. p. 1135–44.

[42] Wall T F, Liu G S, Wu H W, Roberts D G, Benfell K E, Gupta S, Lucas J A, Harris D J, The effects of pressure on coal reactions during pulverised coal combustion and gasification, Progress in Energy and Combustion Science 28 (2002) 405–433.

[43] Yu G, Zhu Q, Chi G, Guo Q, Zhou Z, Study on slag composition and flow property in a bench-scale OMB gasifier, Fuel Processing Technology 2012

[44] Ellis G C, The thermomechanical, electrical conductance and chemical characteristics of coal ash deposits, NERDDP Project No. 1181, Final Report, Vol. 3, SECV R&D Department, Australia, 1989.

[45] Raask E, Sintering characteristics of coal ashes by simultaneous dilatometry–electrical conductance measurements, J. Thermal Anal. 16 _1979. 91.

[46] Bryant G W, Lucas J A, Gupta S K, Wall T F, Use of Thermomechanical Analysis To Quantify the Flux Additions Necessary for Slag Flow in Slagging Gasifiers Fired with Coal, Energy & Fuels 1998, 12, 257-261

[47] Hilliard J E, Quantitative microscopy, in: R.T. DeHoff, F.N. Rhines _Eds., McGraw-Hill, USA, 1968, pp. 45–76.

[48] Ambrosino F, Aprovitola A, Brachi P, Marra F S, Montagnaro F, Salatino P, Char-slag interaction in entrained flow gasifier: modeling of experimental evidences, XXXIV Meeting of the Italian Section of the Combustion Institute

[49] Zhang L, Sato A, Ninomiya Y, CCSEM analysis of ash from combustion of coal added with limestone, Fuel 81 (2002) 1499-1508

[50] Miller S F, Schobert H H, Effect of the Occurrence and Composition of Silicate and Aluminosilicate Compounds on Ash Formation in Pilot-Scale Combustion of Pulverized Coal and Coal-Water Slurry Fuels, Energy Fuels 1994;8:1197–207.

[51] Miller S F, Schobert H H, Effect of the Occurrence and Modes of Incorporation of Alkalis, Alkaline Earth Elements, and Sulfur on Ash Formation in Pilot-Scale Combustion of Beulah Pulverized Coal and Coal-Water Slurry Fuel, Energy Fuels 1994;8:1208–16.

[52] Gupta R, Wall T F, Kajigaya I, Miyamae S, Tsumita Y, Computer controlled scanning electron microscopy of minerals in coal- implications for ash deposition, Prog. Energy Combust.Sci, vol. 24.Pp 523-543, 1998

[53] Ni J, Zhou Z, Yu G, Liang Q, Wang F, Molten slag flow and phase transformation behaviors in a slagging entrained-flow gasifier, Ind. Eng. Chem. Res. 2010, 49, 12302-12310

[54] Hurst H J, Novak F, Patterson J H, Viscosity measurements and empirical predictions for some model gasifier slag, Fuel 78 (1999) 439-444

[55] Patterson J, Hurst H, Quintanar A, Boyd B, Tran H, Evaluation of the slag flow characterization of Australian coals in slagging gasifiers, CCSD (Cooperative research centre for coal in sustainable development) research report, 2001, Australia

[56] Kondrative A, Jak E, Predicting coal ash slag flow characteristics (viscosity model for the Al_2O_3-CaO-FeO-SiO_2 system), Fuel 80 (2011) 1989-2000

[57] Sheng L, Yingli H, Numerical study on slag flow in an entrained-flow gasifier, ASME international Mechanical Engineering Congress and Exposition, Seattle, USA, 2007

[58] Boni, Transformations of inorganic coal constituents in combustion system, DOE Report No. AC22-86PC 90751, 1990.

[59] Shimizu T, Tominaga H, A model of char capture by molten slag surface under high-temperature gasification conditions, Fuel 85 (2006) 170–178.
[60] Li S, Wu Y, Whitty K J, Ash deposition behavior during char-slag transition under simulated gasification condition, Energy & Fuels 24 (2010) 1868–1876.
[61] Li S, Whitty K J, Physical phenomena of char–slag transition in pulverized coal gasification, Fuel Processing Technology 95 (2012) 127–136
[62] Maloney D J, Monazam E R, Casleton K H, Shaddix C R, Evaluation of char combustion models: measurement and analysis of variability in char particle size and density, Proceedings of the Combustion Institute 30 (2005) 2197–2204.
[63] Hurt R H, Dudek D R, Longwell J P, Sarofim A F, The phenomenon of gasification-induced carbon densification and its influence on pore structure evolution, Carbon 26 (1988) 433–449.
[64] Wu H, Wall T, Liu G, Bryant G, Ash liberation from included minerals during combustion of pulverized coal: the relationship with char structure and burnout, Energy & Fuels 13 (1999) 1197–1202.
[65] Hoy H R, Robert A G, Wilkins D M, Behavior of mineral matter in slagging gasification process, J. Inst. Gas Eng., 1965, 5, 444-469
[66] Barroso J, Ballester J, Pina A, Study of coal ash deposition in an entrained flow reactor: Assessment of traditional and alternative slagging indices, Fuel Processing Technology 88 (2007) 865–876
[67] Hutchings I S, West S S, Williamson J, An assessment of coal-ash slagging propensity using an entrained-flow reactor, in: L. Baxter, R. DeSollar (Eds.), Applications of Advanced Technology to Ash-Related Problems in Boiler. Proceedings of the Engineering Foundation Conference. Waterville Valley, New Hampshire., July, 1621, 1995, pp. 201–222.
[68] Rushdi A, Sharma A, Gupta R, An experimental study of the effect of coal blending on ash deposition, Fuel 83 (2004) 495–506
[69] Scott D H, Ash Behavior during Combustion and Gasification, IEA Coal Research, London, 1999.

[70] Li S, Whitty K J, Investigation of Coal Char−Slag Transition during Oxidation: Effect of Temperature and Residual Carbon, Energy Fuels 23 (2009) 1998–2005

[71] Shannon G N, Rozelle P L, Pisupati S V, Sridhar S, Conditions for entrainment into a FeO_x containing slag for a carbon-containing particle in an entrained coal gasifier, Fuel Processing Technology 89 (2008) 1379–1385

[72] Yong S Z, Gazzino M, Ghoniem A, Modeling the slag layer in solid fuel gasification and combustion – Formulation and sensitivity analysis, Fuel 92 (2012) 162–170

[73] Mueller C, Selenius M, Theis M, Skrifvars B J, Backman R, Hupa M, Tran H, Deposition behavior of molten alkali-rich fly ashes—development of a sub-model for CFD applications, Proceedings of the Combustion Institute 30 (2005) 2991–2998

[74] Ni J, Yu G, Guo Q, Zhou Z, Wang F, Sub-model for Predicting Slag Deposition Formation in Slagging Gasification Systems, Energy Fuels 2011, 25, 1004–1009

[75] Seggiani M, Modeling and simulation of time varying slag flow in a Prenflo entrained-flow gasifier, Fuel 77 (1998) 1611-1621

[76] Sheng L, Yingli H, Numerical study on slag flow in an entrained-flow gasifier, ASME international Mechanical Engineering Congress and Exposition, Seattle, USA, 2007

[77] Li B, Brink A, Hupa M, CFD investigation of slagging on a super-heater tube in a kraft recovery boiler, Fuel Process. Technol. (2011), doi:10.1016/j.fuproc.2011.08.007

CFD applications, Proceedings of the Combustion Institute 30 (2005) 2991–2998

[78] Yong S Z, Ghoniem A, Modeling the slag layer in solid fuel gasification and combustion- Tow-way coupling with CFD, Fuel 97 (2012) 457-466

[79] Tominaga H, Tamashita T, Ando T, Asahiro N, Simulator development of entrained flow coal gasifiers at high temperature & high pressure atmosphere. IFRF Combust J 2000, Article No 200004

[80] Sun B, Liu Y, Chen X, Zhou Q, Su M, Dynamic modeling and simulation of shell gasifier in IGCC, Fuel Processing Technology 92 (2011) 1418-1425

[81] Du M, Hao Y, Numerical Simulation of Ash Deposition in Entrained-flow Gasifier, School of Energy and Environment Southeast University Nanjing, China, 2009 IEEE

[82] Lin W, Liang Q, Yu G, Liu H, Gong X, Numerical modeling for non-steady thermal stress analysis of slag layer in a membrane wall entrained-flow gasifier, Fuel 90 (2011) 2396–2403
[83] Chen L, Yong S Z, Ghoniem A F, Modeling the slag behavior in three dimensional CFD simulation of a vertically-oriented oxy-coal combustor, Fuel Processing Technology 112 (2013) 106–117
[84] Chen L, Ghoniem A F, Development of a three-dimensional computational slag flow model for coal combustion and gasification, Fuel 113 (2013) 357–366

Chapter 3

[[1] Luan C, You C, Zhang D, An experimental investigation into the characteristics and deposition mechanism of high-viscosity coal ash. Fuel 119 (2014) 14–20
[2] Zbogar A, Frandsen F, Jensen P A, Glarborg P, Shedding of ash deposits. Prog Energy Combust Sci 2009;35:31–56.
[3] Gupta S, Gupta R, Bryant G, Wall T, Watanabe S, Kiga T, Characterization of ash deposition and heat transfer behavior of coals during combustion in a pilot-scale facility and full-scale utility. Energy Fuels 2009; 23:2570–5.
[4] Yang Z, Wang Z, Wu Y, Wang J, Lu J, Li Z, Ni W, Dynamic model for an oxygen-staged slagging entrained-flow gasifier, Energy Fuels 2011, 25, 3646-3656
[5] Song W, Tang L, Zhu X, Wu Y, Zhu Z, Koyama S, Flow properties and rheology of slag from coal gasification, Fuel 89 (2010) 1709–1715
[6] Richards G H, Slater P N, Harb J N, Simulation of ash deposit growth in a pulverized coal-fired pilot scale reactor. Energy Fuels 1993;7:774–81.
[7] Arvelakis S, Folkedahl B, Dam-Johansen K, Hurley J, Studying the melting behavior of coal, biomass, and coal/biomass ash using viscosity and heated stage XRD data. Energy Fuels 2006;20:1329–40.
[8] Liu Y, Wu M, Qian J, Predicting coal ash fusion temperature based on its chemical composition using ACO-BP neural network. ThermochimActa 2007;454:64–8.
[9] Yin C, Luo Z, Ni M, Cen K, Predicting coal ash fusion temperature with a back-propagation neural network model. Fuel 1998;77:1777–82.

[10] Wall T, Creelman R, Gupta R, Gupta S, Coin C, Lowe A, Coal ash fusion temperatures-new characterization techniques, and implications for slagging and fouling. Prog Energy Combust Sci 1998;24:345–53.
[11] Winegartner E, Rhodes B, An empirical study of the relation of chemical properties to ash fusion temperatures. J Eng Power 1975;97:395.
[12] Skodras G, Sakellaropoulos G P, Mineral matter effects in lignite gasification, fuel process technology 77-78 (2002) 151-158
[13] Winegartner E, Coal fouling and slagging parameters. New York: American Society of Mechanical Engineers; 1974.
[14] Browning G, Bryant G, Hurst H, Lucas J, Wall T, An empirical method for the prediction of coal ash slag viscosity. Energy Fuels 2003;17:731–7.
[15] Jung B, Schobert H H, Improved prediction of coal ash slag viscosity by thermodynamic modeling of liquid-phase composition. Energy Fuels 1992;6:387–98.
[16] Raask E, Mineral impurities in coal combustion, Behavior, Problems and Remedial Measures, Hemisphere Publishing Corporation, New York, 1985.
[17] Song W, Tang L, Zhu X, Wu Y, Rong Y, Fusibility and flow properties of coal ash and slag, Fuel 88 (2009) 297–304
[18] Wei Y, Li H, Honma K, Tanoskai T, Ninomiya Y, Effect of additives on slag properties in an entrained bed gasifier, World of Coal Ash (WOCA) Conference, 2011, Denver, USA
[19] Ling-xue K, Jin B, Wen L, Zong-qing B, Zhen-xing G, Effect of lime addition on slag fluidity of coal ash, J Fuel ChemTechnol, 2011, 39(6), 407-411
[20] Lu T, Zhang L, Zhang Y, Feng Y, Li H X, Effect of mineral composition on coal fusion temperature. Journal of Fuel Chemistry and Technology, 2010, 38(2): 23–28.
[21] Duchesne M, Macchi A, Lu D, Hughes R, Artificial neural network model to predict slag viscosity over a broad range of temperatures and slag compositions, Fuel Processing Technology 91 (2010) 831–836
[22] Gupta S, Dubikova M, French D, Sahajwalla V, Effect of CO_2 gasification on the transformations of coke minerals at high temperatures, Energy & Fuels 21 (2) (2007) 1052

[23] Losurdo M, Spliethoff H, Kiel J, Ash deposition modeling using a visco-elastic approach, Fuel 102 (2012) 145–155

[24] Brachi P, Montagnaro F, Salatino P, Char-Wall Interaction and Properties of Slag Waste in Entrained-Flow Gasification of Coal, European Combustion Meeting 2011

[25] Li S, Whitty K J, Investigation of Coal Char−Slag Transition during Oxidation: Effect of Temperature and Residual Carbon, Energy Fuels 23 (2009) 1998–2005

[26] Rushdi A, Gupta R, Sharma A, Holcombe D, Mechanistic prediction of ash deposition in a pilot-scale test facility, Fuel 84 (2005) 1246–1258

[27] Mueller C, Selenius M, Theis M, Skrifvars B J, Backman R, Hupa M, Tran H, Deposition behavior of molten alkali-rich fly ashes—development of a submodel for CFD applications, Proceedings of the Combustion Institute 30 (2005) 2991–2998

[28] Shannon G N, Rozelle P L, Pisupati V, Sridhar S, Conditions for entrainment into a FeOx containing slag for a carbon-containing particle in an entrained coal gasifier, Fuel Processing Technology 89 (2008) 1379–1385

[29] Ni J, Yu G, Guo Q, Zhou Z, Wang F, Sub-model for predicting slag deposition formation in slagging gasification systems, Energy Fuels 2011, 25, 1004–1009

[30] Montagnaro F, Salatino P, The role of slag formation on late carbon conversion in entrained-flow gasification of coal, Dipartimento di Chimica, Universita Studi di Napoli Federico II, Napoli, Italy, 2009

[31] Montagnaro F, Salatino P, Analysis of char–slag interaction and near-wall particle segregation in entrained-flow gasification of coal, Combustion and Flame 157 (2010) 874–883

[32] Yong S Z, Gazzino M, Ghoniem A, Modeling the slag layer in solid fuel gasification and combustion – Formulation and sensitivity analysis, Fuel 92 (2012) 162–170

[33] Shimizu T, Tominag H, A model of char capture by molten slag surface under high temperature gasification conditions, Fuel 85 (2006) 170–178

[34] Wall T F, Liu G S, Wu H W, Roberts D G, Benfell K E, Gupta S, Lucas J A, Harris D J, The effects of pressure on coal reactions during pulverized coal combustion and gasification, Progress in Energy and Combustion Science 28 (2002) 405–433.

[35] Yu G, Zhu Q, Chi G, Guo Q, Zhou Z, Study on slag composition and flow property in a bench-scale OMB gasifier, Fuel Processing Technology 2012
[36] Costen P G, Locwood F C, Siddique M.M, Mathematical modeling of ash deposition in pulverized fuel-fired combustors, Proceedings of the Combustion Institute, Volume 28, 2000/pp. 2243–2250
[37] Chen L, Yong S Z, Ghoniem A F, Modeling the slag behavior in three dimensional CFD simulation of a vertically-oriented oxy-coal combustor, Fuel Processing Technology 112 (2013) 106–117
[38] Ni J, Liang Q, Zhou Z, Dai Z, Yu G, Numerical and experimental investigations on gas–particle flow behaviors of the Opposed Multi-Burner Gasifier. Energy Conversion and Management 50 (2009) 3035–3044
[39] Li Z, Zeng L, Zhao G, Shen S, Zhang F, Particle sticking behavior near the throat of a low-NOx axial-swirl coal burner. Applied Energy 88 (2011) 650–658
[40] Barroso J, Ballester J, Pina A, Study of coal ash deposition in an entrained flow reactor: Assessment of traditional and alternative slagging indices. Fuel Processing Technology 88 (2007) 865–876
[41] Duchesne M, Hall A, Hughes R, McCalden D, Anthony E, Macchi A, Fate of inorganic matter in entrained-flow slagging gasifiers: Fuel characterization. Fuel Processing Technology 118 (2014) 208–217
[42] Kreutzkam B, Wieland C, Spliethoff H, Improved numerical prediction of ash formation and deposition using a novel developed char fragmentation model. Fuel 98 (2012) 103–110
[43] Weber R, Mancini M, Schaffel-Mancini N, Kupka T, On predicting the ash behavior using Computational Fluid Dynamics. Fuel Processing Technology 105 (2013) 113–128
[44] Lin S, Hirato M, Horio M, The characteristics of coal char gasification at around ash melting temperature. Energy & Fuels 8 (1994) 598–606
[45] Degereji M U, Ingham D B, Ma L, Pourkashanian M, Williams A, Prediction of ash slagging propensity in a pulverized coal combustion furnace, Fuel 101 (2012) 171–178
[46] Vejahati F, Entrained-flow gasification of oil sand coke, PhD thesis, Department of Chemical and Materials Engineering, University of Alberta, Spring 2012

Chapter 4

[1] Yang Z, Wang Z, Wu Y, Wang J, Lu J, Li Z, Ni W, Dynamic model for an oxygen-staged slagging entrained-flow gasifier, Energy Fuels 2011, 25, 3646-3656

[2] Song W, Tang L, Zhu X, Wu Y, Zhu Z, Koyama S, Flow properties and rheology of slag from coal gasification, Fuel 89 (2010) 1709–1715

[3] Zbogar A, Frandsen F, Jensen P A, Glarborg P, Shedding of ash deposits. Prog Energy Combust Sci 2009;35:31–56.

[4] Luan C, You C, Zhang D, An experimental investigation into the characteristics and deposition mechanism of high-viscosity coal ash. Fuel 119 (2014) 14–20

[5] Gupta S, Gupta R, Bryant G, Wall T, Watanabe S, Kiga T, Characterization of ash deposition and heat transfer behavior of coals during combustion in a pilot-scale facility and full-scale utility. Energy Fuels 2009; 23:2570–5.

[6] Erickson T A, Allan S E, Mccollor D P, Hurley J P, Kangb S G, Bakerb J E, Modeling of fouling and slagging in coal fired utility boilers. Fuel Process Technol 1995;44:155-71

[7] Balakrishnan S, Modeling and simulation of fly ash deposition on boiler heat-transfer surfaces and its mitigation strategies for Indian coals, Doctor of Philosophy thesis, Indian institute of technology-Madras, 2014

[8] Tominaga H, Yamashita T, Ando T, Asahiro N, IFRF combustion journal, article number 200004 2000.

[9] Walsh P M, Styre A N, Loehden D O, Monroe L S, Beer J M, Sarofim A F, Deposition of bituminous coal ash on an isolated heat exchanger tube: Effects of coal properties on deposit growth. Prog Energy Comb Sci 1990; 16:327–46.

[10] Winegartner E, Coal fouling and slagging parameters. New York: American Society of Mechanical Engineers; 1974.

[11] Ling-xue K, Jin B, Wen L, Zong-qing B, Zhen-xing G, Effect of lime addition on slag fluidity of coal ash, J Fuel ChemTechnol, 2011, 39(6), 407-411

[12] Browning G, Bryant G, Hurst H, Lucas J, Wall T, An empirical method for the prediction of coal ash slag viscosity. Energy Fuels 2003;17:731–7.

[13] Raask E, Mineral impurities in coal combustion, Behavior, Problems and Remedial Measures, Hemisphere Publishing Corporation, New York, 1985.
[14] Richards G H, Slater P N, Harb J N, Simulation of ash deposit growth in a pulverized coal-fired pilot scale reactor. Energy Fuels 1993;7:774–81.
[15] Yin C, Luo Z, Ni M, Cen K, Predicting coal ash fusion temperature with a back-propagation neural network model. Fuel 1998;77:1777–82.
[16] Skodras G, Sakellaropoulos G P, Mineral matter effects in lignite gasification, fuel process technology 77-78 (2002) 151-158
[17] Lu T, Zhang L, Zhang Y, Feng Y, Li H.X, Effect of mineral composition on coal fusion temperature. Journal of Fuel Chemistry and Technology, 2010, 38(2): 23–28.
[18]Wei Y, Li H, Honma K, Tanoskai T, Ninomiya Y, Effect of additives on slag properties in an entrained bed gasifier, World of Coal Ash (WOCA) Conference, 2011, Denver, USA
[19] Winegartner E, Rhodes B, An empirical study of the relation of chemical properties to ash fusion temperatures. J Eng Power 1975;97:395.
[20] Arvelakis S, Folkedahl B, Dam-Johansen K, Hurley J, Studying the melting behavior of coal, biomass, and coal/biomass ash using viscosity and heated stage XRD data. Energy Fuels 2006;20:1329–40.
[21] Wall T, Creelman R, Gupta R, Gupta S, Coin C, Lowe A, Coal ash fusion temperatures—new characterization techniques, and implications for slagging and fouling. Prog Energy Combust Sci 1998;24:345–53.
[22] Jung B, Schobert H H, Improved prediction of coal ash slag viscosity by thermodynamic modeling of liquid-phase composition. Energy Fuels 1992;6:387–98.
[23] Liu Y, Wu M, Qian J, Predicting coal ash fusion temperature based on its chemical composition using ACO-BP neural network. ThermochimActa 2007;454:64–8.
[24] Song W, Tang L, Zhu X, Wu Y, Rong Y, Fusibility and flow properties of coal ash and slag, Fuel 88 (2009) 297–304
[25] Gupta S, Dubikova M, French D, Sahajwalla V, Effect of CO_2 gasification on the transformations of coke minerals at high temperatures, Energy & Fuels 21 (2) (2007) 1052

[26] Duchesne M, Macchi A, Lu D, Hughes R, Artificial neural network model to predict slag viscosity over a broad range of temperatures and slag compositions, Fuel Processing Technology 91 (2010) 831–836
[27] Brachi P, Montagnaro F, Salatino P, Char-Wall Interaction and Properties of Slag Waste in Entrained-Flow Gasification of Coal, European Combustion Meeting 2011
[28] Losurdo M, Spliethoff H, Kiel J, Ash deposition modeling using a visco-elastic approach, Fuel 102 (2012) 145–155
[29] Rushdi A, Gupta R, Sharma A, Holcombe D, Mechanistic prediction of ash deposition in a pilot-scale test facility, Fuel 84 (2005) 1246–1258
[30] Li S, Whitty K J, Investigation of Coal Char−Slag Transition during Oxidation: Effect of Temperature and Residual Carbon, Energy Fuels 23 (2009) 1998–2005
[31] Degereji M U, Ingham D B, Ma L, Pourkashanian M, Williams A, Prediction of ash slagging propensity in a pulverized coal combustion furnace, Fuel 101 (2012) 171–178
[32] Mueller C, Selenius M, Theis M, Skrifvars B J, Backman R, Hupa M, Tran H, Deposition behavior of molten alkali-rich fly ashes—development of a sub-model for CFD applications, Proceedings of the Combustion Institute 30 (2005) 2991–2998
[33] Costen P G, Locwood F C, Siddique M M, Mathematical modeling of ash deposition in pulverized fuel-fired combustors, Proceedings of the Combustion Institute, Volume 28, 2000/pp. 2243–2250
[34] Yong S Z, Gazzino M, Ghoniem A, Modeling the slag layer in solid fuel gasification and combustion – Formulation and sensitivity analysis, Fuel 92 (2012) 162–170
[35] Yu G, Zhu Q, Chi G, Guo Q, Zhou Z, Study on slag composition and flow property in a bench-scale OMB gasifier, Fuel Processing Technology 2012
[36] Shimizu T, Tominag H, A model of char capture by molten slag surface under high temperature gasification conditions, Fuel 85 (2006) 170–178
[37] Wall T F, Liu G S, Wu H W, Roberts D G, Benfell K E, Gupta S, Lucas J A, Harris D J, The effects of pressure on coal reactions during pulverized coal combustion and gasification, Progress in Energy and Combustion Science 28 (2002) 405–433.

[38] Montagnaro F, Salatino P, The role of slag formation on late carbon conversion in entrained-flow gasification of coal, Dipartimento di Chimica, UniversitaStudi di Napoli Federico II, Napoli, Italy, 2009
[39] Montagnaro F, Salatino P, Analysis of char–slag interaction and near-wall particle segregation in entrained-flow gasification of coal, Combustion and Flame 157 (2010) 874–883
[40] Shannon G N, Rozelle P L, Pisupati V, Sridhar S, Conditions for entrainment into a FeOx containing slag for a carbon-containing particle in an entrained coal gasifier, Fuel Processing Technology 89 (2008) 1379–1385
[41] Mao T, Kuhn DSC, Tran H, Laboratory study of carryover deposition in Kraft recovery boilers. J Pulp Pap Sci 1997;23:565-70
[42] Kim H Y, Chun J H, The recoiling of liquid droplets upon collision with the solid surfaces. Phys Fluids 2001;13:643-59
[43] Fukaj J, Shiiba Y, Yamamoto T, Miyatake O, Poulikakos D, Megaridis CM, Wetting effects on the spreading of a liquid droplet colliding with a flat surface: Experiment and modeling. Phys Fluids 1995;7:236.
[44] Ni J, Yu G, Guo Q, Zhou Z, Wang F, Sub-model for predicting slag deposition formation in slagging gasification systems, Energy Fuels 2011, 25, 1004–1009
[45] Barroso J, Ballester J, Pina A, Study of coal ash deposition in an entrained flow reactor: Assessment of traditional and alternative slagging indices, Fuel Processing Technology 88 (2007) 865–876
[46] Li Z, Zeng L, Zhao G, Shen S, Zhang F, Particle sticking behavior near the throat of a low-NOx axial-swirl coal burner, Applied Energy 88 (2011) 650–658
[47] Chen L, Yong S Z, Ghoniem A F, Modeling the slag behavior in three dimensional CFD simulation of a vertically-oriented oxy-coal combustor, Fuel Processing Technology 112 (2013) 106–117
[48] Ni J, Liang Q, Zhou Z, Dai Z, Yu G, Numerical and experimental investigations on gas–particle flow behaviors of the Opposed Multi-Burner Gasifier, Energy Conversion and Management 50 (2009) 3035–3044

[49] Duchesne M, Hall A, Hughes R, McCalden D, Anthony E , Macchi A, Fate of inorganic matter in entrained-flow slagging gasifiers: Fuel characterization, Fuel Processing Technology 118 (2014) 208–217
[50] Naseri M, Effect of Particle Impact Velocity on Carryover Deposition, Master of Applied Science Thesis, University of Toronto 2000
[51] Weber R, Mancini M, Schaffel-Mancini N, Kupka T, On predicting the ash behavior using Computational Fluid Dynamics, Fuel Processing Technology 105 (2013) 113–128
[52] Vejahati F, Entrained-flow gasification of oil sand coke, PhD thesis, Department of Chemical and Materials Engineering, University of Alberta, Spring 2012

Chapter 5

[1] Gupta S, Gupta R, Bryant G, Wall T, Watanabe S, Kiga T, Characterization of ash deposition and heat transfer behavior of coals during combustion in a pilot-scale facility and full-scale utility. Energy Fuels 2009; 23:2570–5.
[2] Song W, Tang L, Zhu X, Wu Y, Zhu Z, Koyama S, Flow properties and rheology of slag from coal gasification, Fuel 89 (2010) 1709–1715
[3] Luan C, You C, Zhang D, An experimental investigation into the characteristics and deposition mechanism of high-viscosity coal ash. Fuel 119 (2014) 14–20
[4] Zbogar A, Frandsen F, Jensen P A, Glarborg P, Shedding of ash deposits. Prog Energy Combust Sci 2009;35:31–56.
[5] Yang Z, Wang Z, Wu Y, Wang J, Lu J, Li Z, Ni W, Dynamic model for an oxygen-staged slagging entrained-flow gasifier, Energy Fuels 2011, 25, 3646-3656
[6] Seggiani M, Modeling and simulation of time varying slag flow in a Prenflo entrained-flow gasifier, PII: S0016-2361(98)00075-1
[7] Yong S Z, Gazzino M, Ghoniem A, Modeling the slag layer in solid fuel gasification and combustion – Formulation and sensitivity analysis, Fuel 92 (2012) 162–170
[8] Yong S Z, Ghoniem A, Modeling the slag layer in solid fuel gasification and combustion – Two-way coupling with CFD, Fuel 97 (2012) 457–466

[9] Chen. L, Yong S Z, Ghoniem A F, Modeling the slag behavior in three dimensional CFD simulation of a vertically-oriented oxy-coal combustor, Fuel Processing Technology 112 (2013) 106–117

[10] Chen L, Ghoniem A F, Development of a three-dimensional computational slag flow model for coal combustion and gasification, Fuel 113 (2013) 357–366

[11] Chen C, Horio M, Kojima T, Use of numerical modeling in design and scale up of entrained flow coal gasifier, Fuel 80 (20010 1513-1523

[12] Wen C Y, Chaung T Z, Entrainment Coal Gasification Modeling, Ind. Eng. Chem. Process Des. Dev., 1979, 18 (4), pp 684–695

[13] Govind R, Shah J, Modeling and simulation of an entrained flow coal gasifier, AIChE J., 30 (1), 79-92 (1984).

[14] Liu S, Hao Y, Numerical study on slag flow in an entrained-flow gasifier, ASME Conf Proc 2007;2007:793–800.

[15] Ni J, Zhou Z, Yu G, Liang Q, Wang F, Molten slag flow and phase transformation behaviors in a slagging entrained-flow coal gasifier. Ind Eng Chem Res 2010;49:12302–10.

[16] Montagnaro F, Salatino P, Analysis of char–slag interaction and near-wall particle segregation in entrained-flow gasification of coal, Combustion and Flame 157 (2010) 874–883

[17] Noda R, Naruse I, Ohtake K, Fundamentals on combustion and gasification behavior of coal particle trapped on molten slag layer. J Chem Eng Jpn 1996;29:235–41.

[18] Wang X H, Zhao D Q, He L B, Jiang L Q, He Q, Chen Y, Modeling of a coal-fired slagging combustor: development of a slag sub-model. Combustion and Flame 2007;149:249–260.

[19] Ambrosino F, Wall effects in particle-laden flows, PhD thesis in Chemical Engineering, Universita' Degli Studi Di Napoli "FEDERICO II", November 2011

[20] Losurdo M, Spliethoff H, Kiel J, Ash deposition modeling using a visco-elastic approach, Fuel 102 (2012) 145–155

[21] Ai W, Kuhlman J.M, Simulation of Coal Ash Particle Deposition Experiments, Energy Fuels 2011, 25, 708-718.

[22] Montagnaro F, Salatino P, The role of slag formation on late carbon conversion in entrained-flow gasification of coal, Dipartimento di Chimica, UniversitaStudi di Napoli Federico II, Napoli, Italy, 2009
[23] Nakod P, Orsino S, Walavalkar A, Sami M, Development and validation of a volatile break-up approach for gasification simulations, 38th International Technical Conference on Clean Coal and Fuel Systems, June 2-6, 2013
[24] Shimizu T, Tominag H, A model of char capture by molten slag surface under high temperature gasification conditions, Fuel 85 (2006) 170–178
[25] Shannon G N, Rozelle P L, Pisupati V, Sridhar S, Conditions for entrainment into a FeOx containing slag for a carbon-containing particle in an entrained coal gasifier, Fuel Processing Technology 89 (2008) 1379–1385
[26] Mueller C, Selenius M, Theis M, Skrifvars B J, Backman R, Hupa M, Tran H, Deposition behavior of molten alkali-rich fly ashes—development of a sub-model for CFD applications, Proceedings of the Combustion Institute 30 (2005) 2991–2998
[27] Ni J, Yu G, Guo Q, Zhou Z, Wang F, Sub-model for predicting slag deposition formation in slagging gasification systems, Energy Fuels 2011, 25, 1004–1009
[28] Li S, Wu Y, Whitty K J, Ash deposition behaviour during char–slag transition under simulated gasification conditions, Energy & Fuels 24 (2010) 1868–1876.
[29] Li S, Whitty K J, Investigation of Coal Char−Slag Transition during Oxidation: Effect of Temperature and Residual Carbon, Energy Fuels 23 (2009) 1998-2005
[30] Duchesne M A, Bronschb A M, Hughes R W, Masset P J, Slag viscosity modeling toolbox, fuel.2012.03.010
[31] Mills K C, Rhine J M, The measurement and estimation of the physical properties of slags formed during coal gasification: 1. Properties relevant to fluid flow. Fuel 1989;68:193–200.
[32] Mills K C, Rhine J M, The measurement and estimation of the physical properties of slags formed during coal gasification: 2. Properties relevant to heat transfer. Fuel 1989;68:904–10.

[33] Duchesne M, Hall A, Hughes R, McCalden D, Anthony E, Macchi A, Fate of inorganic matter in entrained-flow slagging gasifiers: Fuel characterization. Fuel Processing Technology 118 (2014) 208–217

[34] Vejahati F, Entrained-flow gasification of oil sand coke, PhD thesis, Department of Chemical and Materials Engineering, University of Alberta, Spring 2012

[35] Hosseini S, Gupta R, Inorganic Matter Behavior during Coal Gasification: Effect of Operating Conditions and Particle Trajectory on Ash Deposition and Slag Formation, Energy Fuels 2015, 29, 1503−1519

[36] ANSYS Fluent User's Guide, Release 15.0, November 13

[37] Silaen A, Wang T, Effect of turbulence and devolatilization models on coal gasification simulation in an entrained-flow gasifier, International Journal of Heat and Mass Transfer 53 (2010) 2074–2091

Appendix B

[1] Kapitza P L, Collected papers of Kapitza 1938-1964, Pergamon Press, New York, 1965 2, 662-709.

[2] Bird R B, Stewart W E, Lightfoot E N, Transport Phenomena. Wiley, 1960. New York. 3-179.

[3] Padmanamban A, Film Thickness Measurements in Falling Annular Films, Master of Science thesis, University of Saskatchewan Saskatoon, 2006

Appendix C

[1] Yan L, Gupta R, Wall T, Kerrison K, Computer-controlled scanning electron microscopy (CCSEM) and image analysis of coal, research report 21, Cooperative Research Centre for black coal utilization, University of Newcastle, March 2001

[2] Duchesne M A, Slagging in entrained-flow gasifiers, PhD thesis, Department of Chemical and Biological Engineering, Faculty of Engineering, University of Ottawa, 2012

Appendix D

[1] Ram L C, Tripathi P S M, Mishra S P, Mossbauer spectroscopic studies on the transformations of iron-bearing minerals during combustion of coals: Correlation with fouling and slagging, Fuel Processing Technology 42 (1995) 47-60

[2] Persson M, Investigations of Slag Properties and Reactions, PhD thesis, KTH School of Industrial Engineering and Management, Division of Materials Process Science, Royal Institute of Technology, 2007

[3] Wei Y, Li H, Yamada N, Sato A, Ninomiya Y, Honma K, Tanosaki T, A microscopic study of the precipitation of metallic iron in slag from iron-rich coal during high temperature gasification, Fuel 103 (2013) 101–110

[4] Qi X, Guo X, Xue L, Zheng C, Effect of iron on Shenfu coal char structure and its influence on gasification reactivity, Journal of Analytical and Applied Pyrolysis 110 (2014) 401–407

[5] Dai B Q, Wu X, Girolamo A D, Cashion J, Zhang L, Inhibition of lignite ash slagging and fouling upon the use of a silica-based additive in an industrial pulverized coal-fired boiler: Part 2. Speciation of iron in ash deposits and separation of magnetite and ferrite, Fuel 139 (2015) 733–745

[6] Zhang Z, Wu X, Zhou T, Chen Y, Hou N, Piao G, Kobayashi N, Itaya Y, Mori S, The effect of iron-bearing mineral melting behavior on ash deposition during coal combustion, Proceedings of the Combustion Institute 33 (2011) 2853–2861

[7] Carey R C, Measurement and significance of the flow properties of coal ash and slag, 1964. Bureau Mines Bull., 618.

[8] Hinckley C C, Smith G V, Twardowska H, Saporoschenko M, Shileyt R H, Griffent R A, Mossbauer studies of iron in Lurgi gasification ashes and power plant fly and bottom ash, Fuel, 1980, Vol 59

[9] Kondratiev A, Jak E, A quasi-chemical viscosity model for fully liquid slags in the Al_2O_3 –CaO–FeO–SiO_2 system, Metall Mater Trans B 2005;36:623–38.

[10] Min D J, Fruehan R J, Rate of Reduction of FeO in Slag by Fe-C Drops, Metallurgical transactions B, Volume 23B, February (1992) 29-37

[11] Raask E, Mineral impurities in coal combustion, Behavior, Problems and Remedial Measures, Hemisphere Publishing Corporation, New York, 1985.
[12] Namkung H, Xu L, Shin W C, Kang T J, Kim H T, Study on deposition tendency of coal ash under various gasification environments through DTF, Fuel 117 (2014) 1274–1280
[13] Khadilkar A B, Rozelle P L, Pisupati V S, A study on initiation of ash agglomeration in fluidized-bed gasification systems, Fuel 152 (2015) 48–57
[14] McLennan A R, Bryant G W, Stanmore B R, Wall T F, Ash formation mechanisms during pf combustion in reducing conditions. Energy Fuels 2000;14:150–9.
[15] Li F, Li Z, Huang J, Fang Y, Understanding mineral behaviors during anthracite fluidized-bed gasification based on slag characteristics, Applied Energy 131 (2014) 279–287
[16] Marinov V, Marinov S P, Lazarov L, Stefanova M, Ash agglomeration during fluidized bed gasification of high sulfur content lignites, Fuel Processing Technology, 31 (1992) 181-191
[17] Datta S, Sarkar P, Chavan P D, Saha S, Sahu G, Sinha A K, Saxena V K, Agglomeration behavior of high ash Indian coals in fluidized bed gasification pilot plant, Applied Thermal Engineering (2015), doi: 10.1016/j.applthermaleng.2015.04.046.
[18] Mason D M, The behavior of iron-sulfur species in fluidized-bed gasification on coal, Fuel Processing Technology, 30 (1992) 215-226
[19] Wu X, Zhang Z, Chen Y, Zhou T, Fan J, Piao G, Kobayashi N, Mori S, Itaya Y, Main mineral melting behavior and mineral reaction mechanism at molecular level of blended coal ash under gasification condition, Fuel Processing Technology 91 (2010) 1591–1600
[20] Brooker D, Oh M S, Iron sulfide deposition during coal gasification, Fuel Processing Technology 44 (1995) 181-190

Appendix A: Gasification setup information and sample preparation

1. Setup information

Gasification experiments were performed in an electrically heated vertical drop tube furnace. Gasification reactions were taken place in a cylindrical ceramic tubes located inside the furnace. For temperatures up to 1500°C Mullite tube was used and for higher temperatures alumina tube was used. Alumina can tolerate higher temperature, but, it is fragile and more sensitive to the external shocks. Ceramic tube inside the furnace is shown in Figure1.

Figure 1: Ceramic tube inside the electrically heated furnace

The dimensions of the tube are 63.5mm ID and 1530mm total height. 4 rows of elements are used in 3 levels inside the furnace. 8 elements in one row at the top, 16 elements in two rows in the middle and 8 elements in one row at the bottom are used. The configuration of the elements is shown in Figure 2.

Figure 2: Heating elements of the furnace

The temperature of the furnace during gasification process was controlled by three PID controllers located at the top, middle and bottom sections of the furnace. The control board of the setup is shown in Figure 3. Based on the safe operating procedure (SOP), the maximum allowable gas temperature in the furnace was 1650°C. There is a safety set point controller for temperature on the control board and when the temperature goes higher than the set value, the system automatically shutdown.

The main part of the feeder includes a screw feeder connected to a hopper and a rod as shown in Figure 4. Walls of hopper are vibrating in order to inhibit the bridging of the fine particles to produce a uniform flow of the particles into the furnace. Nitrogen transfers and entrains the coal particles into the drop tube furnace. The nitrogen line is connected to both hopper header and the tip of stirring rod to prevent from particle flow blockage by nitrogen pressure. Due to the high temperature inside the furnace, there might be reverse flow inside the feeding line. In order to be sure about the appropriate flow direction of the particles, there is a glass part at the joint point of the particles and nitrogen flow line as shown in Figure 5 to make visible the flow of entrained particles. Nitrogen and air were preheated by passing around steam generator and an inline heater. The residence time of the particles inside the drop tube furnace could be adjusted by the total gas flow rate. Feeder must be volumetrically calibrated for each fuel (depending on the type and size). Gasification products passes through an air cooled collection probe. After collection probe a cyclone was used to separate and collect large solid particles (including char, ash and slag droplets) from the flue gas. After cyclone a bag filter is used to separate the particles smaller than few macrons in size. The downstream parts of the setup are shown in Figure 6.

Figure 3: Control board of gasification setup

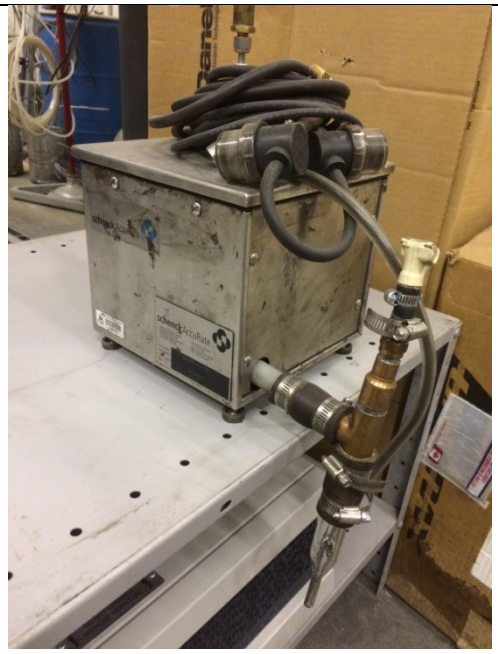

Figure 4: Coal feeder

Figure 5: Glass section of feeder

Feeding probe consists of two concentric tubes to carry coal and gasifying agents. Three different feed injector probes were tested and two were selected to perform gasification experiments. In feeding probes C4 and C3, the tip of the quarter inch coal carrier tube is designed with 4 holes of 3mm and 3 holes of 4mm respectively and these coal carrier tubes are located in an open ended half inch tube which transports gasifying agents. The configuration of this kind of feeder probe are shown in Figure 7.

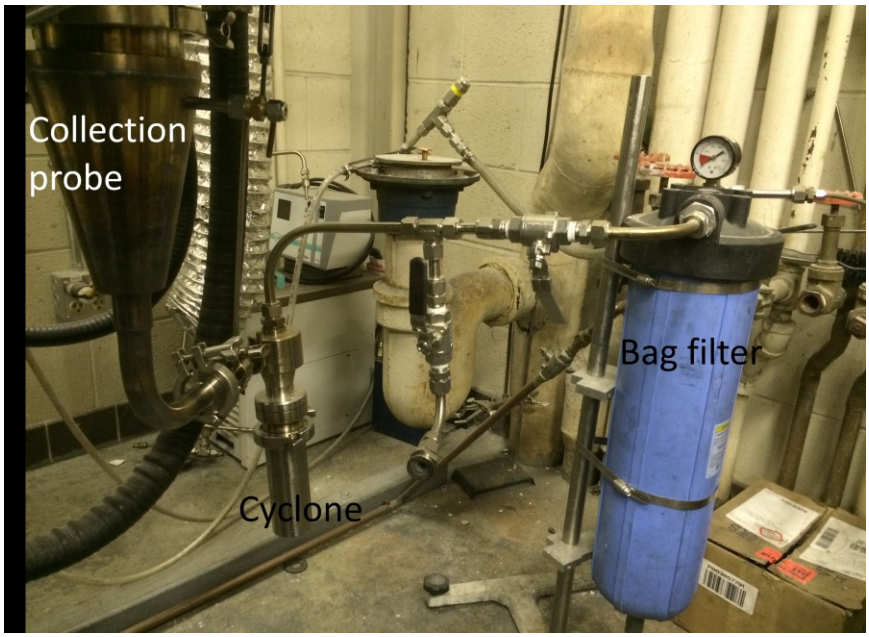

Figure 6: Downstream parts of the gasification setup

In the second type of the feeding probe, which is called A8, the quarter inch coal carrier tube is open-ended which is located inside the gasifying agent transporter tube. The tip of the half inch gasifying agent transporter tube was designed with eight holes at the edge with diameter of 2mm. Figure 8 shows the parts of this feeding probe.

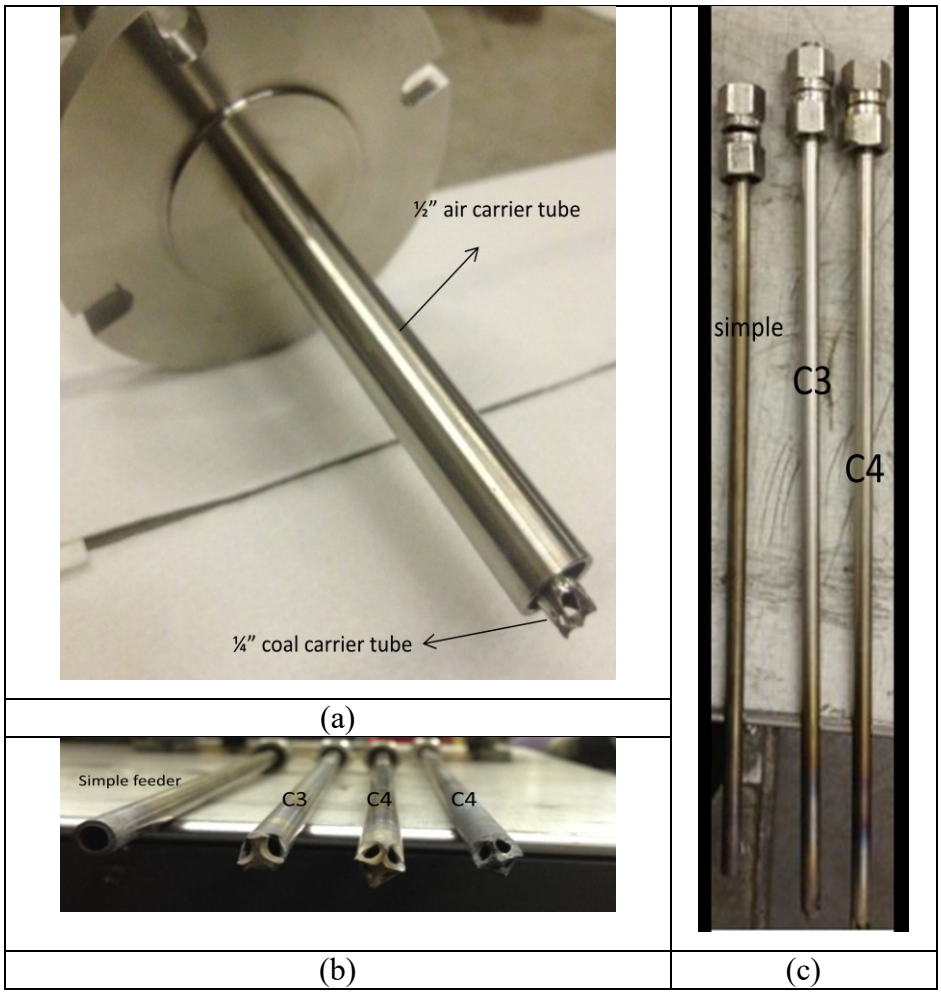

Figure 7: Configuration of feeder C4 and C3 (a) coal carrier tube inside gasifying agent carrier tube of feeder C4 (b,c) coal carrier tubes

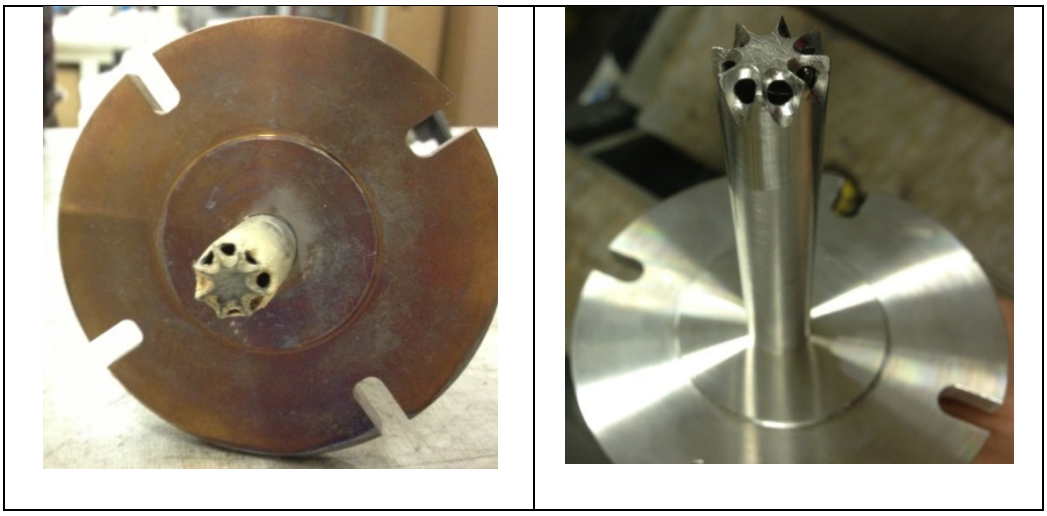

Figure8: Configuration of feeder A8

2. Feed preparation

Two types of Canadian coal were used in the experiments. For each coal type two size ranges were used. Smaller size is 28-53 microns and bigger size included coarser particles in the range of 150-212µm. The raw coal particles were grinned using ball mill grinder shown in Figure 9. Then the grinded coal was dried and sieved to separate particles in each specific size ranges. Figure 10 shows the sieves shaker.

Figure 9: Ball mill grinder

To collect deposition samples, a cylindrical collector probe with a cone plate at the end was used. The probe was made of Kawool paper. After cutting the paper required for each specific configuration, the alumina cement was used to make the desired structure such as cylindrical shape or cone shape. Then the whole structure was soaked in the hardener solution to be strong enough to tolerate high temperatures and to be handled easily while inserting in and removing out of the furnace. The hardening process of the probes was done by soaking them into the hardener solution and drying them several times (once a day during a week).

Figure 10: Sieve shaker

Appendix B: Analytical calculation of slag layer flowing down the wall of furnace

Based on the Reynolds number of the slag layer and the properties of the liquid slag, it can be concluded that liquid slag layer is laminar flow. However at small Reynolds numbers some waves could be observed in the liquid layer falling by gravity and the falling film might not be smooth [1], but, usually the turbulent regime is recognizable above a Reynolds number of 250 [2].

In order to have analytical solution for the laminar flow on the wall of cylindrical furnace, Navier-Stokes equation must be solved. In this regard slag layer is assumed to be an annular film flow. Based on Figure 1, a liquid layer with thickness of δ flows inside a vertical tube with internal radius of R_w is considered with assumptions of incompressible, fully developed, and laminar flow only in the z direction in steady state condition. The axial component of the Navier-Stokes equations in cylindrical coordinates as momentum balance of the liquid layer is as follows [3]:

$$\rho\left[\frac{\partial u_z}{\partial t}+u_r\frac{\partial u_z}{\partial r}+\frac{u_\theta}{r}\frac{\partial u_z}{\partial \theta}+u_z\frac{\partial u_z}{\partial z}\right]=-\frac{\partial P}{\partial z}+\rho g_z+\mu\left[\frac{1}{r}\frac{\partial}{\partial r}\left(r\frac{\partial u_z}{\partial r}\right)+\frac{1}{r^2}\frac{\partial^2 u_z}{\partial \theta^2}+\frac{\partial^2 u_z}{\partial z^2}\right] \quad (1)$$

The continuity equation as the mass balance of the liquid layer is as follows [3]:

$$\frac{1}{r}\frac{\partial}{\partial r}(ru_r)+\frac{1}{r}\frac{\partial}{\partial \theta}(u_\theta)+\frac{\partial}{\partial z}(u_z)=0 \quad (2)$$

r, Θ and z are cylindrical coordinates and t is time. ρ and μ are density and viscosity, P is the pressure and g is the gravity acceleration. By assuming axisymmetric flow, there will not be any flow or changes in Θ direction, therefore, in above equation $u_\theta = 0$ and $\partial/\partial\theta = 0$. Also assuming fully developed flow and constant pressure results in $\frac{\partial}{\partial z} = 0$ and $\frac{\partial P}{\partial z} = 0$ respectively, and finally the momentum equation can be derived as follows [3]:

$$\rho\left[\frac{\partial u_z}{\partial t}+u_r\frac{\partial u_z}{\partial r}\right]=\rho g_z+\mu\left[\frac{1}{r}\frac{\partial}{\partial r}\left(r\frac{\partial u_z}{\partial r}\right)\right] \quad (3)$$

With above assumption, the continuity equation results in $u_r=0$, therefore the momentum equation will be:

$$\rho\left[\frac{\partial u_z}{\partial t}\right]=\rho g_z+\mu\left[\frac{1}{r}\frac{\partial}{\partial r}\left(r\frac{\partial u_z}{\partial r}\right)\right] \quad (4)$$

This equation in steady state condition is:

$$\frac{1}{r}\frac{d}{dr}\left(r\frac{du_z}{dr}\right)=-\frac{\rho g_z}{\mu} \quad (5)$$

Integrating this equation respect to r gives:

$$r\frac{du_z}{dr}=\left(-\frac{\rho g_z}{\mu}\right)\frac{r^2}{2}+C_1 \quad (6)$$

The boundary conditions of the system are as follows [3]:

$u_z=0$ at $r=R_w$ (no slip condition on the wall surface)

$\frac{\partial u_z}{\partial r}=0$ at $r=r_i$ (no shear at gas-liquid interface)

Applying these boundary conditions, the following expression results for the fluid velocity in z direction [3]:

$$u_z=\frac{\rho g_z}{2\mu}\left((R_w-\delta)^2\ln\frac{r}{R_w}+\left(\frac{R_w^2-r^2}{2}\right)\right) \quad (7)$$

By integrating the liquid layer velocity in z direction and on the layer cross section area, the equation for mass flow rate of the liquid film layer can be achieved as below [3]:

$$\dot{m}_l=\int_{\delta}^{R_w}2\rho\pi r u_z dr \quad (8)$$

$$\dot{m}_l=\frac{\pi\rho^2 g_z}{8\mu}\left[-4R_w^2(R_w-\delta)^2+R_w^4-4(R_w-\delta)^4\ln\left(\frac{R_w-\delta}{R_w}\right)+3(R_w-\delta)^4\right] \quad (9)$$

Equation 9 can be used based on the properties of the slag layer (density and viscosity) and ash deposition as the inlet mass flow rate of the liquid film layer. Based on the experimental viscosity measurement for ash content of the coal used in Chapter 5, the information in Table 1 is prepared.

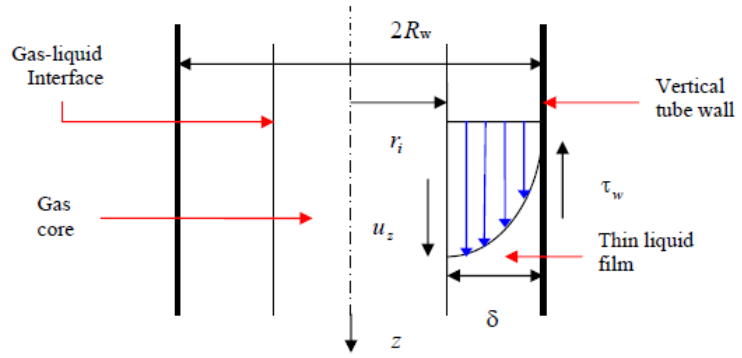

Figure 1: Velocity profile for a laminar fully developed liquid film [1]

Deposition in row (1) obtained at 1450°C and if there is a temperature profile inside the furnace, the thickness at each point is calculated based on equation 9. It means that for the deposition at 1450°C, if we assume that the temperature is constant within the furnace, the slag layer thickness in steady state condition is 1.19mm.

Table1: Calculation slag layer thickness for different conditions

		Deposition Obtained	T(°C)	1450	1400	1350	1300	1250	1200
			μ(Pa.s)	4.16	5.76	8.55	14.3	29.1	91.7
(1)	$\dot{m}_l$ =7.1gr/h	1450°C	δ(mm)	1.19	1.32	1.51	1.80	2.30	3.41
(2)	$\dot{m}_l$ =6.2gr/h	1350°C	δ(mm)	1.13	1.27	1.45	1.72	2.19	3.25
(3)	$\dot{m}_l$ =4.8gr/h	1250°C	δ(mm)	1.04	1.16	1.33	1.58	2.01	2.98

Now, the required slag build-up to reach the steady state condition of the slag layer on the wall can be calculated. The required mass of the slag build up can be calculated by the equation below:

$$M = \rho V = \rho \pi D \delta L \qquad (10)$$

In above equation, δ is the slag layer thickness, D is the diameter of the furnace and L is the length of the furnace. Based on this equation, the required amount of ash deposition

to make enough build up for temperature of 1450°C is 1016.5 gr. Based on ash deposition rate for this condition, the time required to reach steady state condition is:

$$t = \frac{M}{\dot{m}_l} = 143.17\ hr$$

However, due to the non-axisymetric behavior of the ash deposition and slag flow in real condition, probably the whole surface of the wall will not be covered by slag and slag flows down on the wall through some paths with higher thickness than the predicted values.

References

[1] Kapitza P L, Collected papers of Kapitza 1938-1964, Pergamon Press, New York, 1965 2, 662-709.

[2] Bird R B, Stewart W E, Lightfoot E N, Transport Phenomena. Wiley, 1960. New York. 3-179.

[3] Padmanamban A, Film Thickness Measurements in Falling Annular Films, Master of Science thesis, University of Saskatchewan Saskatoon, 2006

Appendix C: CCSEM Analysis

CCSEM analysis of the fuels F1 and F2 were performed in CANMET using a Hitachi 3400N VP-SEM with Oxford Instruments Si(Li) Pentafet Plus 10 mm2 detector [2]. Samples preparation was performed by mounting them in carnauba wax. Then, the samples were carbon coated to reduce the possible charging during the characterization process. Combination of the wax mount glue and epoxy blank helped to decrease the possible structural deformation under the beam. The operations were performed under vacuum condition while samples were exposed to nitrogen before and after characterization process [2]. During CCSEM analysis, the backscatter detector is of great importance for elemental contrast in the image which helps the processor software to recognize the type of association of the inorganic particles with organic material. The process of BSE Imaging and further related analyses, were done at 20 kV. X-ray acquisition for elemental analysis was performed using Oxford INCA Feature software [2]. Imaging analysis was done three times with different magnification for each sample. In the first image analysis with magnification of 500x, 10,000 particles were processed collecting particles in size range of 0.89 μm to 5 μm. Second imaging was performed with magnification of 200x to collect particles in size range of 5 μm to 30 μm over the same area. The last imaging was done with magnification of 75x to process particles larger than 30 μm [2]. During the image processing in each step, the software determined the longest chord of each recognized particle and then EDX acquisition was performed with rate of 5 seconds per particle exactly at the center of each particle based on the

length of chord. By adjusting the grey level ranges before each analysis, the carbonaceous part of each particles were recognized from inorganic part [2].

Table1: Mineral Phase Classification Definition with the BYU CCSEM Technique [1]

Classification No	Mineral/Chemical categories	Compositional criteria (Relative elemental wt %)	Density (g/cm^3)
1	Quartz	Al≤5, Si≥80	2.65
2	$Fe_2O_3/FeCO_3$	Mg≤5, Al≤5, Si≤10, S≤5, Fe≥80	5.30
3*	Aluminosilicate	Al≥15, Si≥15, K≤5, Ca≤5, Fe≤5, Al+Si≥80	2.65
4*	Ca-Al-Silicate	Al≥10, Si≥10, S≤10, K<Ca, Fe<Ca, Ca≥5 Ca+Al+Si≥80	2.65
5*	Fe-Al-Silicate	Al≥10, Si≥10, S≤5, K<Fe, Ca<Fe, Fe≥5 Fe+Al+Si≥80	2.80
6*	K-Al-Silicate	Al≥10, Si≥10, Ca<K, Fe<K, K≥5 Fe+Al+Si≥80	2.60
7	Ankerite	S≤15, Mg<Fe, Ca≥20, Fe≥20, Fe+Ca+Mg≥80	3.00
8*	Pyrite	Ca≤10, Fe≥10, Fe≤40, S≥40, Fe+S≥80	4.60
9*	Gypsum	Si≤10, S≥20, Ca≥20, Ca+S≥80, Ti+Ba≤12	2.50
10*	Barite	Ca≤5, Fe≤10, S≥20, Ba+S+Ti≥80	4.50
11	Gypsum/ Barite	Fe≤5, Ca≥5, Ba≥5, Ti≥5, S≥20, Ca+Ba+S+Ti≥80	3.50
12*	Apatite	P≥20, Ca≥20, Ca+P≥80	3.20
13*	Ca-silicate	Al≤10, S≤10, Si≥20, Ca≥14, Ca+Si≥80	3.09
14	Gypsum/Al-Si	Al≥5, Si≥5, S≥5, Ca≥5, Al+Si+Ca+S≥80	2.60
15*	Ca-Aluminate	Si≤10, S≤10, Al≥20, Ca+Al≥80	2.80
16**	Spinel	Ca≤5, Si≤5, Al≥5, Mg+Al+Fe≥80	2.65
17	Alumina	Al≥80	4.00
18*	Calcite/CaO	S≤10, Mg≤5, P≤15, Si≤5, Ti≤5, Ba≤5, Ca≥80	2.80
19	Rutile	S≤5, Ti+Ba≥80	2.40
20*	Dolomite	Mg≥10, Ca≥10, Ca+Mg≥80	2.86
21**	$FeS/FeSO_4$	Fe+S≥80	5.30
22*	Ca-Al-P	Ca≥20, P≥20, Ca+P+Al≥80	2.80
23*	Ca-rich	65≤Ca≤80	2.60
24	Si-rich	65≤Si≤80	2.65
25	Unclassified	-	2.70
*	Different definition compared to those of MTI and ATC CCSEM systems		
**	Not Defined in the other two CCSEM systems		

Using grey-level analysis, all the particles below a certain grey level were categorized to be coal or carbonaceous material and the rest were categorized to be in specific inorganic class based on the results of EDX elemental analysis. Quantification was performed using the base Oxford factors [2].

The initial results of CCSEM analysis gives the diameter, type of association with coal matrix (include or exclude nature) and elemental composition of each particle. In order to get useful statistical results, a criterion must be applied to have the mass of each particle. In this regard the type of each particle and related density is required. In order to calculate the density of the particles, the mineral phase classification definition presented in Table1 is used. By combining the criterion presented in Table 1 and the initial raw results of CCSEM, the type of each detected particle was determined considering its association and mass. The calculated results are presented in Tables 2 to 4.

CCSEM results for fuel F1

Total number of inorganic particle: 3340

Number of included: 1217

Number of excluded: 2123

Weight percent of included: 33.05%

Weight percent of excluded: 66.95%

Area percent of included: 33.87%

Area percent of excluded: 66.13%

Table2: Inorganic elemental analysis of F1 as overall, included and excluded

	Na	Mg	Al	Si	P	S	Cl	K	Ca	Ti	Fe
Total	0.465	0.272	18.467	67.656	0.018	0.836	0.004	2.185	1.735	0.299	8.057
included	0.210	0.277	19.173	73.046	0.020	0.814	0.000	1.013	1.830	0.559	3.056
excluded	0.591	0.269	18.119	64.996	0.016	0.846	0.005	2.763	1.688	0.170	10.525

CCSEM results for fuel F2

Total number of inorganic particle: 3355

Number of included: 2087

Number of excluded: 1268

Weight percent of included: 46.94%

Weight percent of excluded: 53.06%

Area percent of included: 48.89%

Area percent of excluded: 51.11%

Table3: Inorganic elemental analysis of F2 as overall, included and excluded

	Na	Mg	Al	Si	P	S	Cl	K	Ca	Ti	Fe	Mo
Total	0.451	0.325	16.798	51.901	1.056	6.390	0.01	0.266	13.483	0.431	8.377	0.450
included	0.648	0.479	17.740	44.538	1.337	6.684	0.021	0.213	22.654	0.275	4.478	0.803
excluded	0.278	0.189	15.966	58.415	0.808	6.129	0	0.312	5.368	0.569	11.828	0.137

Comparison the fuels

In the experimental results presented in chapter 3, the different behavior of the inorganic deposition of these two fuels is reported. For explanation that behavior, CCSEM results were used. As discussed in chapter 3, inorganic content, inorganic association, iron and calcium are thought to be the main reasons of different behavior of fuels. A summarized comparison of the main desired CCSEM analysis results for F1 and F2 are presented in table4.

Table4: CCSEM results comparison for F1 and F2

	F1-GC					F2-BD				
	Weight%	Number of particles	Area %	Fe	Ca	Weight%	Number of particles	Area%	Fe	Ca
Total		3340		8.06	1.74		3355		8.38	13.48
Included	33.05	1217(36.4)	33.87	3.06	1.83	46.94	2087(62.2)	48.89	4.48	22.65
Excluded	66.95	2123(63.6)	66.13	10.53	1.69	53.06	1268 (37.8)	51.11	11.83	5.37

References

[1] Yan L, Gupta R, Wall T, Kerrison K, Computer-controlled scanning electron microscopy (CCSEM) and image analysis of coal, research report 21, Cooperative Research Centre for black coal utilization, University of Newcastle, March 2001

[2] Duchesne M A, Slagging in entrained-flow gasifiers, PhD thesis, Department of Chemical and Biological Engineering, Faculty of Engineering, University of Ottawa, 2012

Appendix D: Various states of iron-bearing inorganic matters at different conditions during gasification

1. Introduction

By increasing utilization of coal as a cheap and widely available source of energy, application of various coal types even with high ash content (as high as 55%) is inevitable and consequently the mineral matter related problems such as environmental issues, corrosion, erosion and fouling of the reactor and downstream equipment are of crucial importance during the operation. Highly reducing conditions during gasification process, can cause some metal species (initially presented in the structure of compounds materials) to be reduced to their elemental state and then get embedded in the slag matrix resulting in the release of heavy metals which might finally result in serious threat to the ecological system. Among various inorganic matters in coal, iron-bearing minerals as major components (including illite, pyrite, siderite, ankerite and szomolnokite) are proved to have strong affect on the fouling and slagging behavior of coal. Iron might show different effects. It has been reported that gasification process with iron catalysis generates much more product gas than that of un-catalyzed. The reason is thought to be iron particles prevent from graphitization of carbon during pyrolysis [1-4].

Iron is one of the most important heterovalent species observed in almost all types of coal inorganic residue during utilization process and might be observed in many different states depending on the operating conditions of the reactor. It is widely accepted that precipitation of iron in metallic state inside the melted deposits is essentially governed by the reaction environment (mainly degree of oxidizing or reducing atmosphere) and the

operating temperature. Under a highly reducing condition such as in the oxygen-blown gasifiers, iron-bearing inorganic matters are reduced (which might be partially or fully reduction to metallic iron based on oxygen concentration) and finally might results in many issues while discharging and future handling of the residues. Generated slag in this kind of gasifiers, usually has a obviously recognizable iron containing phase. Also, it is proved that slag has a broad range of properties (physical properties such as density and viscosity and chemical properties related to the phase equilibrium) under different gaseous atmosphere [3]. In combustion or gasification process, iron-bearing inorganic matters especially in reduced states such as pyrrhotite and FeO–FeS eutectics have effective role to initiate slagging [5]. Various states of iron existence (Fe, Fe^{2+} or Fe^{3+}) determine the degree of the deposition sintering of inorganic matters. Wustite (FeO), almandite ($3FeO.Al_2O_3.3SiO_2$) and fayalite are the major iron containing compounds which usually initiates sintering under reducing condition during coal utilization processes [6]. The proportion of iron in Fe^{2+} state increases at higher temperatures and lower oxygen concentration [7]. Hinckley et al. [8] reported the existence of higher ferrous state in comparison with ferric state in the ash produced during gasification process. The relative proportions of various states of iron might give information about the history experienced by the inorganic species such as the temperatures of ash formation. Local change in the slag composition (especially the effect of FeO_x content) is a crucial aspect to consider in the safe operation of the slagging gasifiers [2]. If the iron content in the fully melted phase of $FeO–Al_2O_3–SiO_2$ system reduces from 70 to 35 wt%, the viscosity of the liquid deposition layer increases about 20 times and essentially reduces the stickiness of the mixture. Consequently, the particles are less probable to

stick and therefore might be carried by flue gas to the colder sections of the reactor. In this case iron has enough time to be solidified as spinel [9].

Persson [2] used a Confocal Scanning Laser Microscopy (CSLM) to analyze the reaction between carbon particles in contact with hematite containing deposits under different environments. He performed experiments at different temperature using deposits with different FeO_x content and found out that the particle size decrease was more rapid at higher FeO_x content and at higher temperature. To be sure about the effect of atmosphere, he performed an experiment at 1300˚C with an anthracite particle under inert atmosphere using pure argon and observed no interaction. The results showed that the reaction of anthracite in oxygen containing atmosphere increased by increasing temperature.

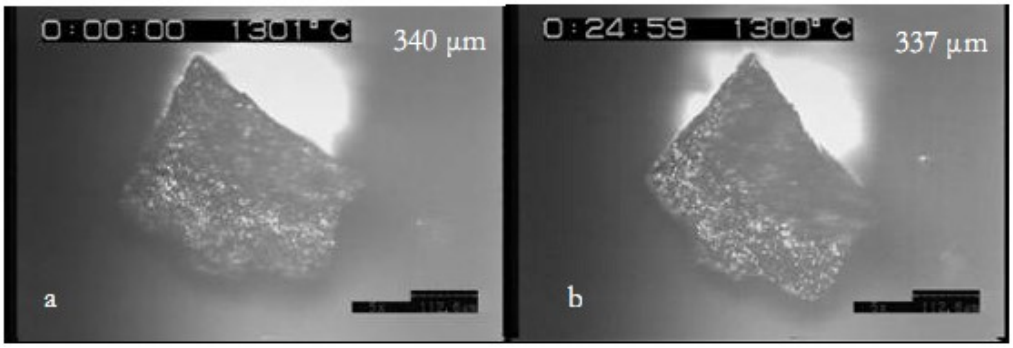

Figure 1: Appearance of anthracite particle in contact with slag at 1300 °C in argon atmosphere [2].

Wei et al. [3] performed experimental analysis on the ash melting behavior and iron deposition tendency under different CO_2 and H_2 containing atmosphere. Figure 2(a) shows BSE images of the slag samples melted in a gas atmosphere of H_2/CO_2 = 50/50. Based on this figure, there is no clear changes in the slag compositional structure at 1300 °C (slag is not fully melted at this temperature). Slag will be completely melted by increasing the temperature to 1500 °C. Figure 2(b) shows BSE images of the slag sample which was formed under highly reducing environment at higher temperature. The bright

spherical particles observed in this image are mostly composed of iron (based on EDX results for elemental investigation). Based on this figure, iron particles exist only on the surface of slag and there is no sign of iron participation into the bulk of deposition [3].

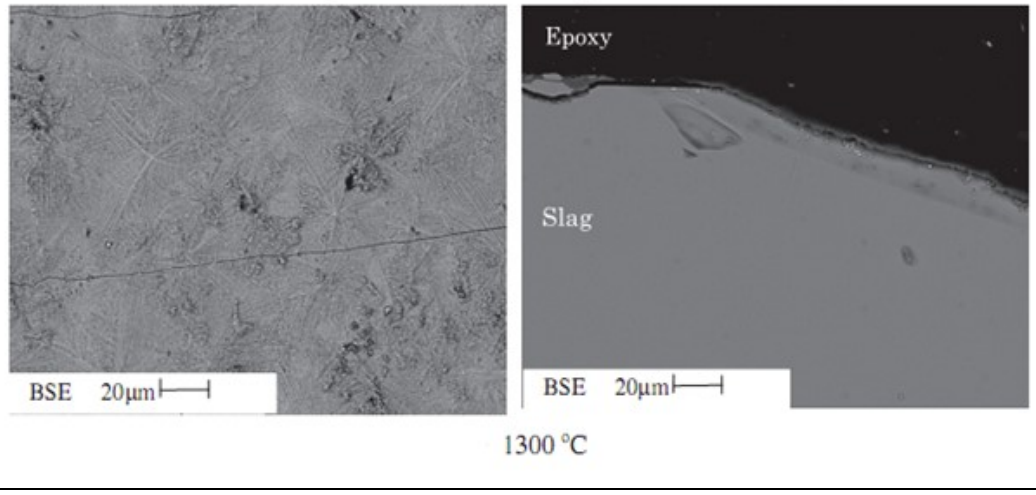

Fig 2: (a) Backscattered electron (BSE) images of slag pellets at inlet gas CO2/H2 = 50/50 (V%) (b) BSE images of slag pellets at inlet gas CO2/H2 = 10/90 (V%) [3].

Wei et al. [3] reported the formation of numerous big iron particles on the surface of slag at 1400 °C. These particles then stick to each other to make up almost the whole surface. Based on their observations, small particles are formed only near the surface and there is not any particle precipitation in the bulk, but, at higher temperature small particles were

observed all over the bulk of the sample. Under strongly reducing atmosphere, due to the precipitation of metallic iron (which has very high melting point), bulk of slag become heterogeneous and uniform liquid will not be observed at temperature as high as 1550 °C. Under moderate reducing environment slag is usually homogeneous which melts completely at 1550 °C with a uniform Fe content all over the bulk of slag. The Fe content in the bulk of slag under mildly reducing conditions is higher than that of the strongly reducing atmosphere. In the systems with considerable amount of iron, reaching to equilibrium is highly related to the diffusivity of Fe^{2+} and oxygen inside the bulk of slag [3].

Local composition of deposit is another affecting parameter on the existing states of iron in the depositions during gasification process. It has been reported that sulfur content has a significant influence on the reduction rate of iron especially in ferrous state [10]. Ferrous iron can react with carbon trapped inside the slag generally based on the reaction below:

$$FeO + C \rightarrow Fe + CO \qquad (1)$$

2. Concentration of iron at different sections on the surface of slag layer

Experimental results of the inorganic deposition in chapter 3, showed that working with F1 (the information about fuels F1 and F2 is presented in chapter3) and using different feeders, the surface of the inorganic deposition and slag layer in the top section were highly covered with iron. BSE images of the deposition and slag layer as shown in Figure 3, proved the presence of very high concentration of iron on the surface of slag. The same concentration of iron was not observed in BSE images of the inside section of slag layer.

In addition, analysis of the slag droplets falling down from the bottom hole of the collector probes showed that the composition of slag droplet is close to the bulk ash composition. Figure 3 shows the deposit material collected at various locations. The different colors and characteristics of the surface and bulk of the slag layer can be seen in Figures 4 and 5. Based on these observations, there is a question about the reason of existence of high iron concentration in the top section of the furnace and the fate of iron in this area.

The importance of the species concentration in the bulk of slag is their effect on the physical properties which affect the flow behavior. Iron oxide in reduced state (FeO), works as network modifier and breaks the network of alumina silicate and consequently reduces the viscosity. Therefore, higher concentration of this component in the slag layer increases the flow of the slag and reduces the thickness of the deposit layer on the wall of furnace. But, existing most of iron oxide on the surface of slag increases the stickiness of the surface which leads to more trapped particles. Large numbers of captured particles in combination with the high viscosity of the bulk of slag result in the higher deposition thickness.

Wei et al. [3] observed bright areas of iron in the BSE images of the deposition in strongly reducing atmosphere only on the surface of the slag samples. But, it must be noticed that there is a difference between the depositions of the two studies. Wei et al. [3] made ash pellet from ahs residue and then put a pellet with approximately uniform composition inside a furnace. But, the samples used in this study are collected depositions from the wall of the furnace in which the difference in the composition is due to the different stickiness and transport mechanisms of various inorganic particles.

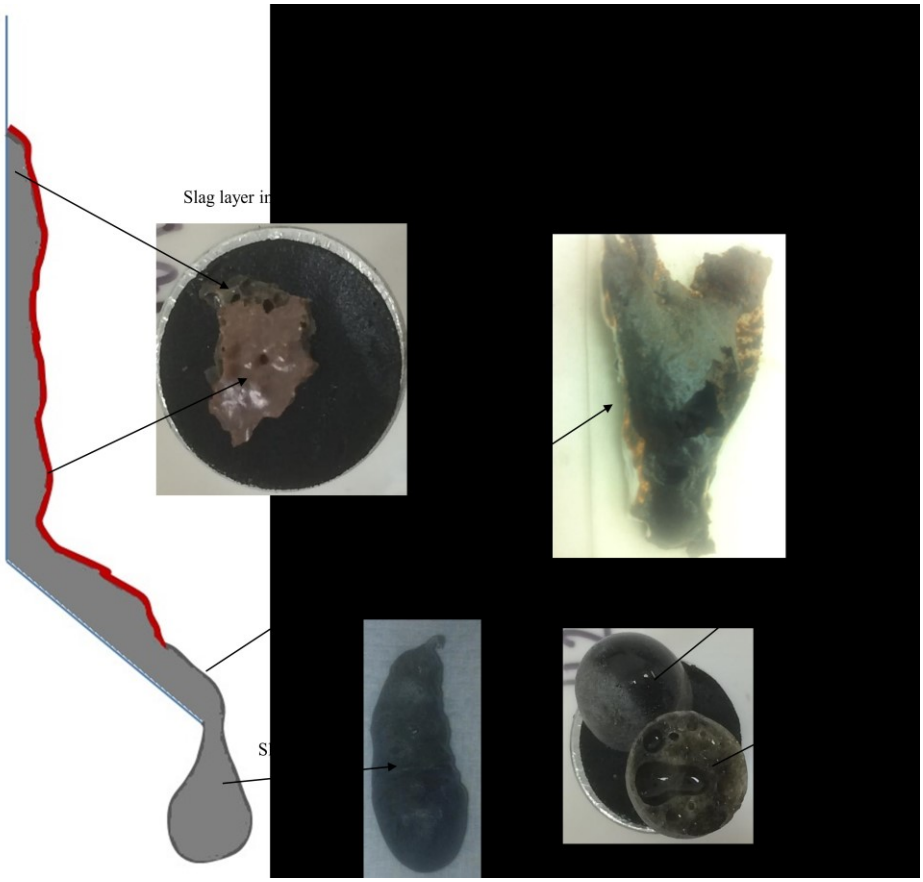

Figure 3: Falling slag layer with various surface characteristics at different levels

BSE images of the slag layer further downstream on the wall, shows that iron concentration is lower as slag moves toward the bottom of the furnace. High stickiness of the iron-bearing inorganic matters at reducing condition, help them to stick in the upper sections as soon as they impact the surface. Based on a hypothesis, as the slag layer moves downward on the wall, the iron on the surface of slag might react with some gaseous species in the atmosphere. In order to test this hypothesis, some pieces of the slag layer were put under reducing and inert environments inside the gasifier in ceramic crucibles. CO and H_2 as dominant species during gasification process make the gas phase a strongly reducing environment. Therefore, to provide reducing environment, the slag samples were put inside the furnace while doing coal gasification process. To have inert

atmosphere nitrogen has been used. The crucible was held using a stainless steel plate from the top of furnace. The characteristics of the furnace are explained in chapters 3-5. Figure 8 shows the crucible installed on the steel plate with some pieces of slag in it.

Figure 4: Difference in surface and cross section area of the slag layer in top section of furnace

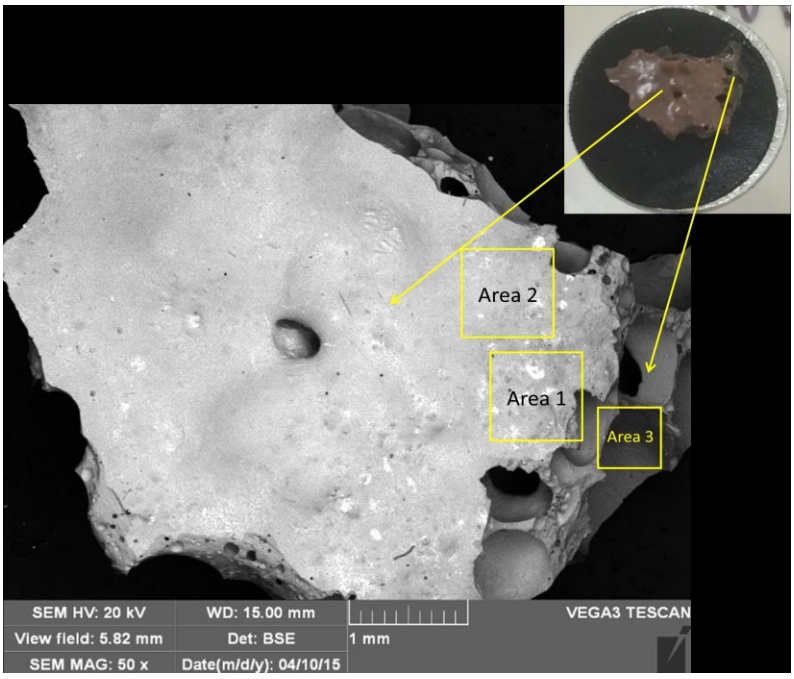

Figure 5: BSE image of the surface and bulk of slag layer

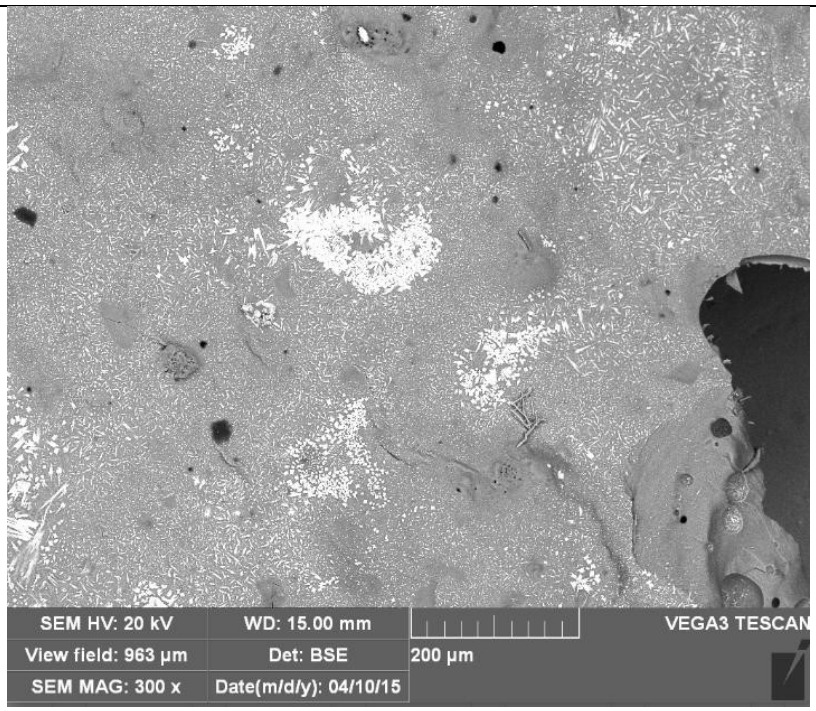

(a)

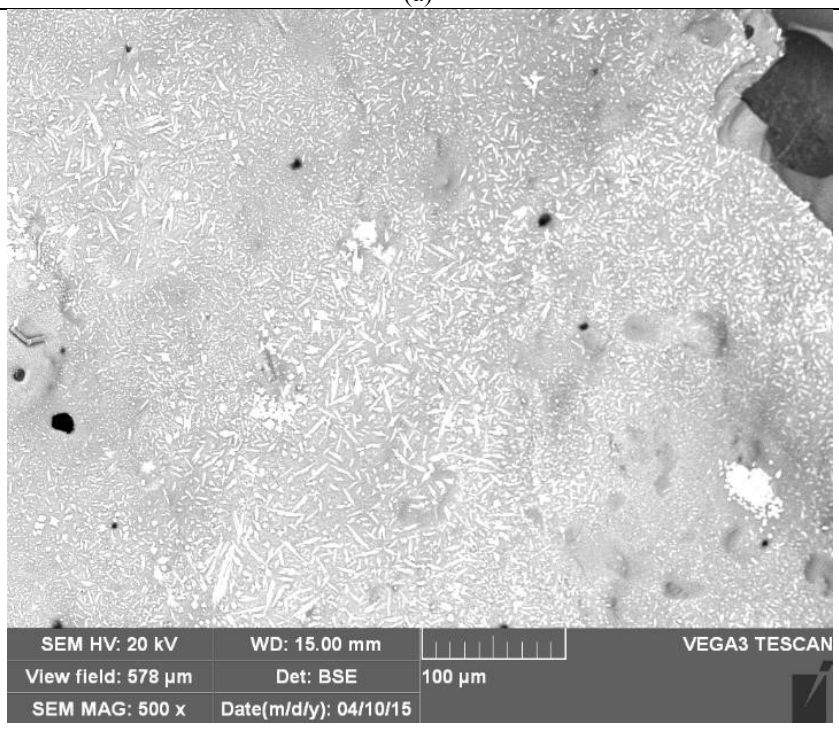

(b)

Figure 6: BSE image of area 1 and 2 of Figure 5, surface of slag layer (a) Area 1 (b) Area 2

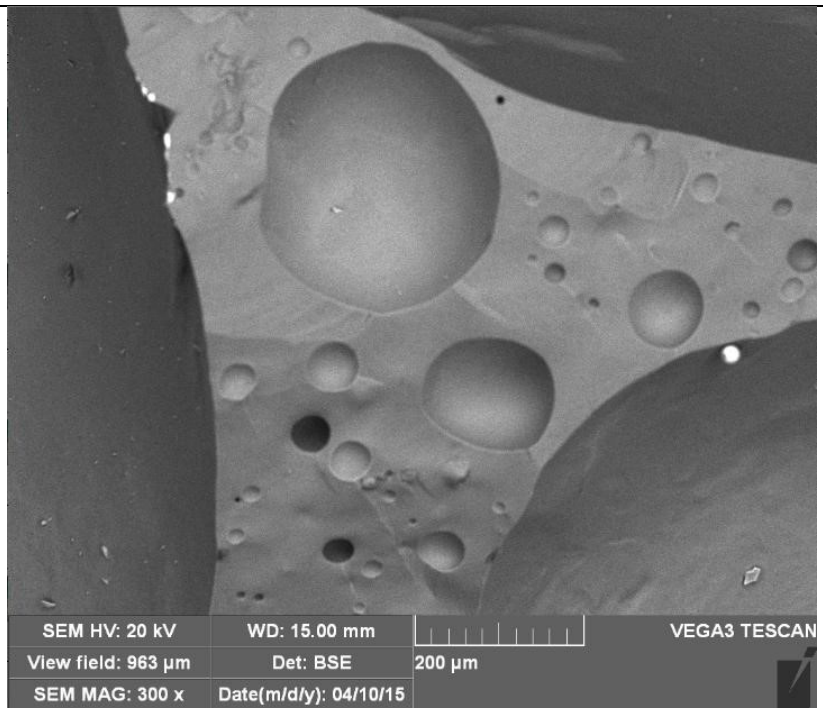

(a)

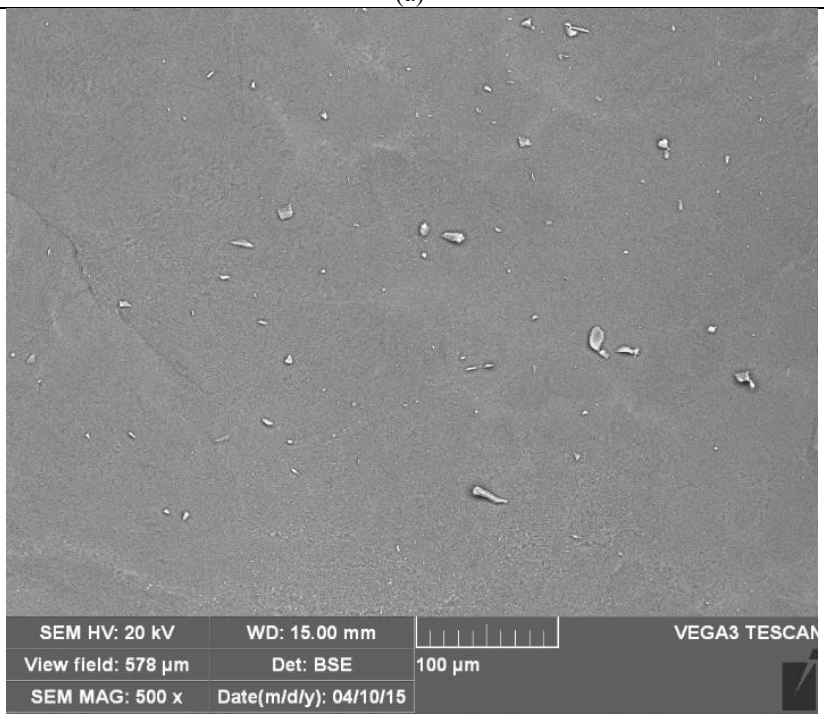

(b)

Figure 7: BSE image of area 3 of Figure 5, bulk of slag layer

Figure 8: The crucible installed on the steel plate with some pieces of iron covered slag

The slag pieces were tested under gasification conditions and inert atmosphere (pure nitrogen) and then the surface of each piece was analyzed with BSE/EDX.

(a) (b)

Figure 9: Comparison of the difference of the surface of slag samples before and after being in gasification environment

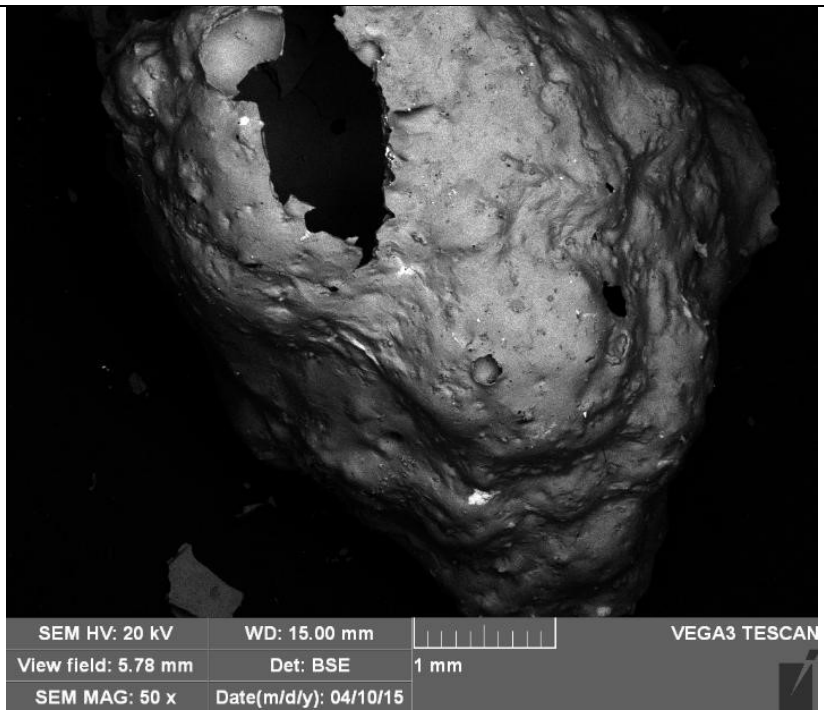

(a)

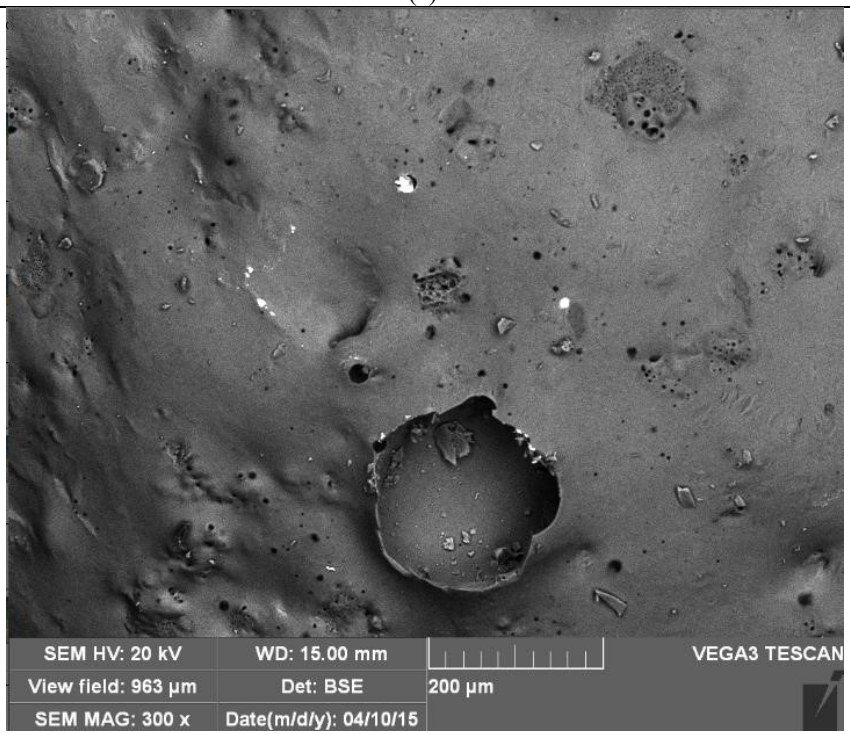

(b)

Figure 10: Slag surface under gasification condition, 1300°C, 15 minutes

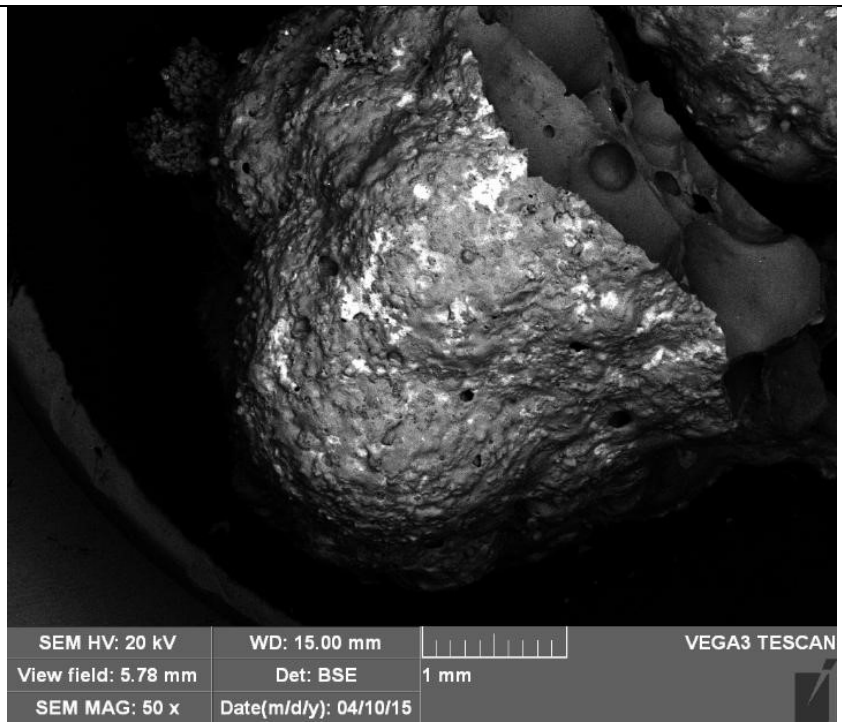

(a)

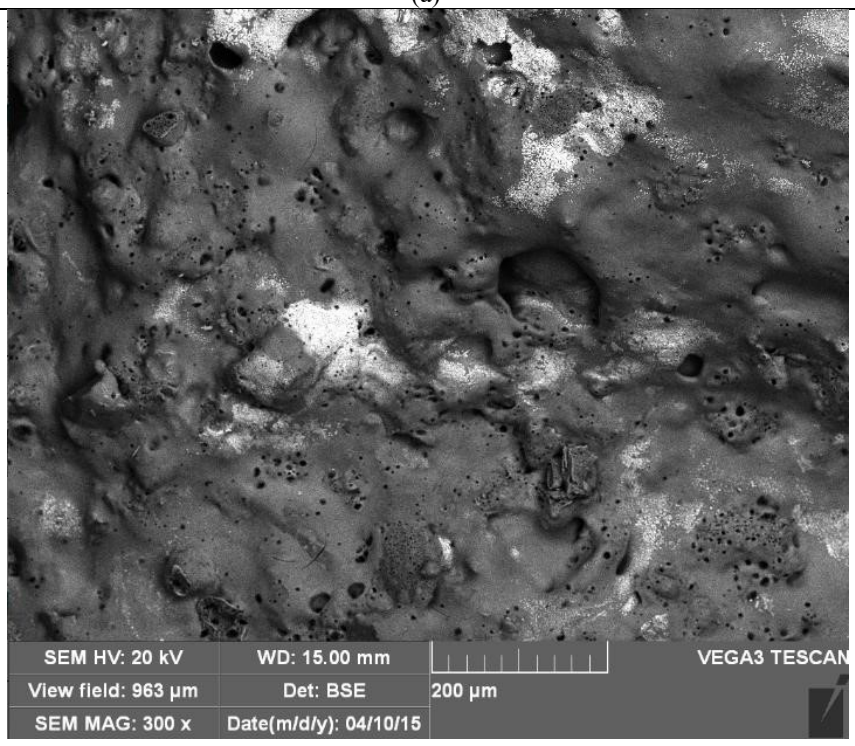

(b)

Figure 11: Slag surface under gasification condition, 1300°C, 3 minutes

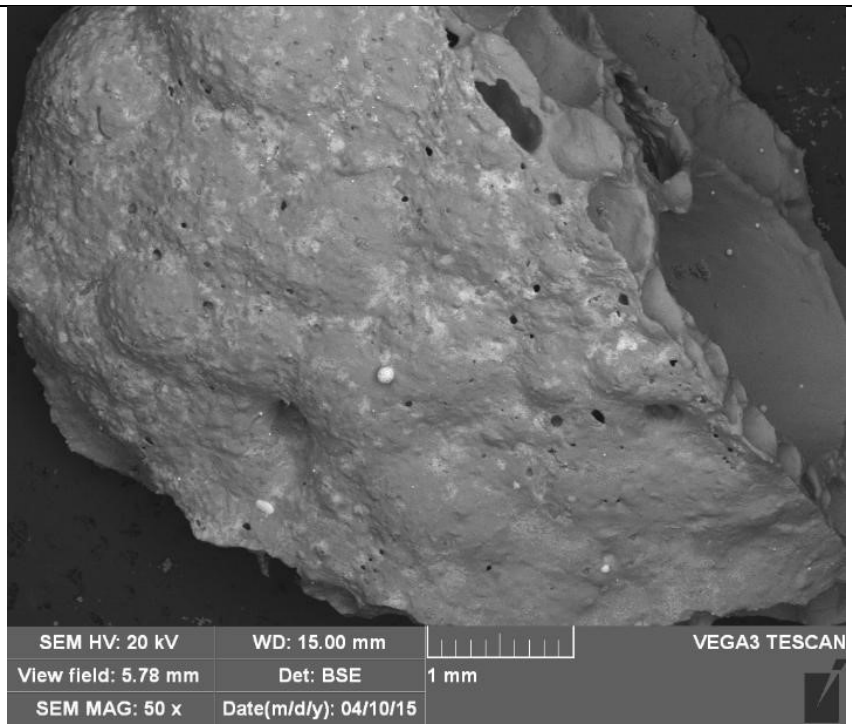

(a)

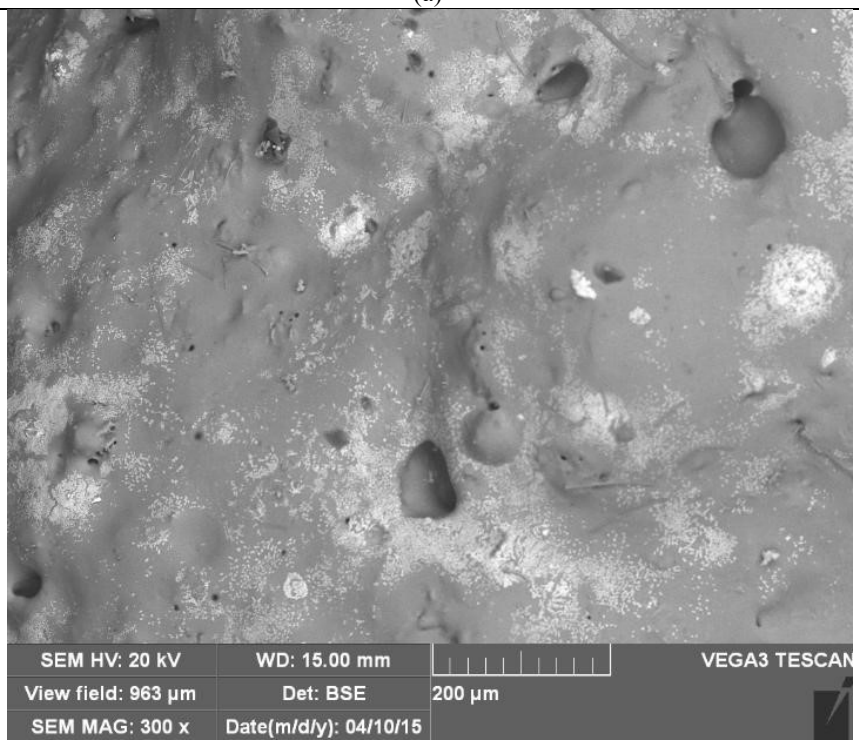

(b)

Figure 12: Slag surface in inert atmosphere (nitrogen), 1300°C, 15 minutes

Figure 9 shows the surface of the slag samples at different conditions. As shown in this figure, the color of the surface of slag after being under gasification conditions changed. This observation reveals that the surface material of these pieces must have changed due to interaction with the gaseous species existing in the atmosphere or inorganic species in slag layer. BSE images of these pieces are presented in figure 10. Comparison of figures 10 and 11 shows that by increasing the residence time of slag pieces, iron concentration decreases. In addition, comparison figures 10 and 12 shows that under inert atmosphere the iron concentration does not change that much. All these observations reveal that iron on the surface of the slag layer can reacts with gaseous species and this could explain the differences of the iron concentrations at different locations on the wall and in the slag droplets. One of the possible reactions might be the reaction of carbon monoxide (CO) with FeO to produce iron pentacarbonyl ($Fe(CO)_5$). Iron pentacarbonyl ($Fe(CO)_5$) is one of the most volatile species of iron and is not stable at high temperatures and therefore, transforms to other species as the gas phase moves toward the end of the furnace.

BSE images show qualitatively that there is a change in the inorganic matters on the surface of the slag while being under different conditions. Performing these experiments with thermogravimetric (TGA) analysis connected to GC could be highly beneficial in this regard for quantitative analysis. It is possible to put slag samples (highly covered with iron on the surface) under specific atmosphere (such as CO, CO_2, H_2 and N_2) and at specific temperature and measure the weight changes and the outlet gas composition as a function of time. The weight loss of the sample as a function of time would give information about the possibility of the reactions at different atmospheres and

temperatures and might also result in the determination of the kinetic parameters for the possible reactions between various species.

Iron concentration profile through slag layer thickness (radial direction), might be related to the restricted solubility of iron in slag. There is a limit in the solubility of each inorganic species (such as iron) in a mixture of inorganic matter like slag layer. Based on this fact, it can be inferred that for each ash composition, there is a limit for iron (FeO) solubility in the ash mixture. In this regard, the difference between FeO solubility limit and the amount of iron oxide present in the ash is used as an adhesion index I_{AD} [11]:

$$I_{AD} = FeO_{SOL} - FeO_A \qquad (2)$$

In case of using coal type with iron-rich ashes, especially during gasification process, it is highly possible that the FeO content exceeds the limit of solubility of FeO in the glassy bulk of slag (containing mainly alumino silicate inorganic matters) and having low melting point species on the surface of these kind of deposits, a strong sticky connection can easily develop at the interface of slag with any other surface. A negative or small positive value of I_{AD} signifies that the inorganic residue potentially can be extremely adhesive. Iron solubility can explain why all the iron particles on the surface of the deposits are not able to dissolve into the slag layer to make a uniform concentration of iron through the whole thickness [11].

Another reason might be related to the state of iron under reducing conditions. Metal iron in fully reduced state under strongly reducing conditions, has high melting point. In order to have a uniform concentration of the solid particles in the liquid slag, the diffusivity of the particles must be high enough. But, considering the high viscosity of the liquid slag

layer resulted from the ash content of F1 and downward flow of slag on the vertical wall, the transfer of the solid particles in radial direction is extremely low.

3. Inorganic matters agglomeration during coal gasification

In chapter 3 it is reported that iron and calcium are the main components determining the deposition on fuels F1 and F2. But, the existing states of these species in these fuels are different in various sections of the furnace. Formation of the big agglomerates (containing calcium-bearing aluminosilicate mixture acting as glue to make the particles to stick to each other) was observed in many occasions working with F2.

Small inorganic particles containing low melting point compound under reducing conditions during coal gasification process is thought to be the trigger of the initiation of the deposit formation. The fouling phenomenon is highly related to the alkali mineral content such as Ca and Mg bearing inorganic matters. Usually there would be higher amount of deposition using fuels with higher alkali contents and at higher operating temperature [12]. Khadilkar et al. [13] reported that particles which are rich in iron and calcium phases melt at very low temperatures, but, presence of iron in hematite state usually hinders the liquid generation. They reported the liquid formation temperature of the calcium and iron-bearing phases as presented in Table 1.

In early stage of the gasification process while oxidization of the iron containing minerals such as pyrite or marcasite, some eutectic compounds such as FeS-FeO can be formed which is stable in reducing condition and therefore will not alter easily and consequently many iron containing element might be observed as FeS-FeO compound in the inorganic

residue deposition at low temperature [14]. Pyrite decomposes to pyrrhotite and then produces molten FeO–FeS which results in the increase of the low-melting-point eutectics of hercynite and anorthite. Interaction of high reactive small particles of SiO_2, Al_2O_3, and CaO causes formation of spherical gehlenite ($Ca_2Al_2SiO_7$), which as a low-melting-point eutectic might initiates agglomeration [15, 16].

Table 1: Equilibrium liquid phases possible around particles with calcium and iron phases [13]

Components forming liquid	Liquid formation temperature in °C
$CaSO_4$-CaS	850
FeS-FeO	924
Fe-FeS	988
Fe_2O_3-SiO_2-Al_2O_3	1073
FeO- Al_2O_3-SiO_2 (47-12.5-40.3)	1073
CaO-FeO-SiO_2 (17-46-37)	1093
CaO-FeO-SiO_2 (11.5-43-45)	1105
FeO-Fe_2O_3-CaO-SiO_2 (41.76-1.15-9.77-47.32)	1105
CaO-FeO	1133
FeO-Fe_2O_3-SiO_2	1147
CaO-SiO_2-Al_2O_3	1170

Agglomeration of the mineral particles is a phenomenon which affects the size distribution of the particles and consequently affects the deposition behavior of inorganic matters. The degree of agglomeration is proved to be a function of the inorganic composition of the fuel and also the type and degree of the association of inorganic matters within coal matrix. By gradual consumption of the carbon content of the char particles, the mineral matters come into contact with each other to form large ash agglomerates. It is accepted that pyrrhotite and wustite are the main initiator of the agglomerates. Another phenomenon affecting size distribution is char fragmentation, which restricts the extent of agglomeration of the inorganic matters. The main parameters in agglomerate formation are localized heat, large compositional variation, presence of iron in reduced state (Fe^{2+}), ash loading/iron loading factors. Fayalite (Fe_2SiO_4) is one of

the main compounds affecting ash agglomeration. It has been reported that during the process of coal gasification, Fe^{2+} is present in most of ash particle agglomerates but Fe^{3+} is usually absent. Steam is another affecting factor in agglomeration that by absorption energy and reducing local heat prevents from formation of hot spot and therefore minimizes the tendency of agglomerate formation. Agglomeration may reduce the residence time of the particles by formation of high density big particles which are so heavy and fall down to the bottom of the gasifier [12, 16, 17]. This fact limits the growth of the agglomerates; however, Marinov et al. [16] reported that there is no limit in the growth of agglomerates working with lignite coal. They identified β-pyrrhotite (FeS) and wustite (FeO) in the deposit and agglomerates using X-ray analysis and reported that the FeS-FeO eutectic had been the main reason for particles agglomeration in the pilot plant. They also studied the form of sulphur in different deposition as presented in Table 2.

Table 2: The sulphur forms in different samples [16]

Sample	Ash	Sulphur			
		Total	As pyrite	As sulphide	As sulphate
Raw coal	35.7	5.9	1.6	-	2.1
slag	85.2	1.4	-	0.5	0.8
Hard agglomerate	99.9	1.2	-	0.8	0.3

Depending on the various parameters such as mechanical design of the gasifier, operating condition, degree of association of various species, particle size and residence time, fluid flow hydrodynamic, localized heat concentration, heterogeneity of chemical constituents, etc. agglomeration might be observed even at temperatures lower than AFT of the ash content of the coal. Ternary phase diagram (for SiO_2-Al_2O_3-FeO system or SiO_2-Al_2O_3-CaO system) can be used to explain the formation of low temperature agglomerates. Based on the phase diagram presented in Figure 13, eutectic formation might be observed at a temperature even as low as 1088°C which is much lower than the AFT of most of the

ashes. However, the most significant component responsible for lowering the eutectic temperature is iron bearing phases, but, high concentration of CaO has numerously been reported to result in the formation of low temperature eutectic by producing anorthite ($Al_2O_3.SiO_2.2CaO$) [17].

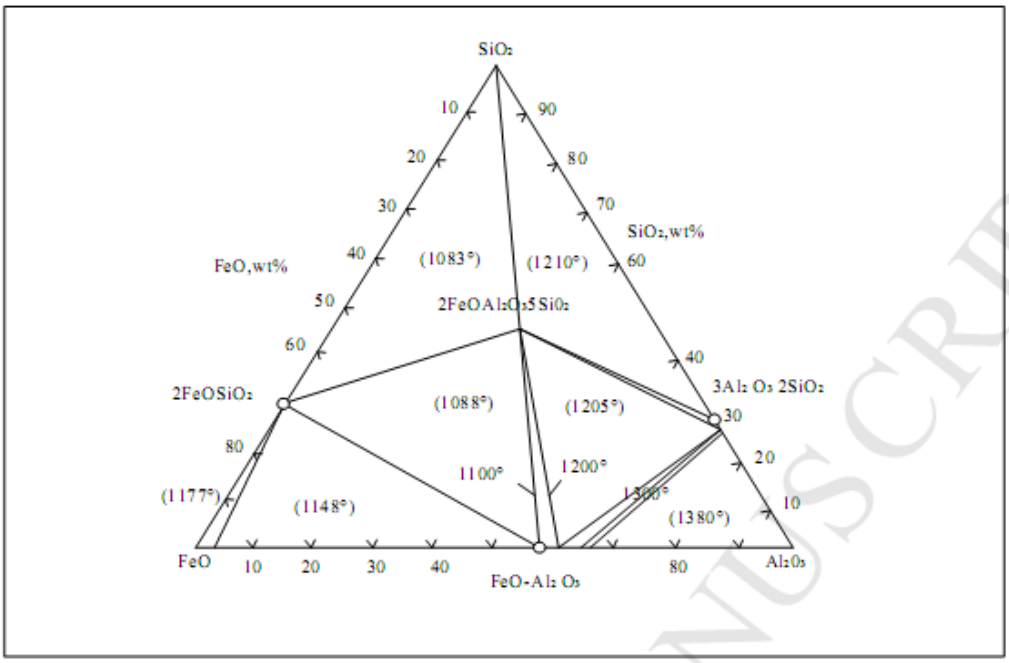

Figure 13: Ternary phase diagram depicting $FeO.Al_2O_3.SiO_2$ system [17]

Ferrous sulfide and ferrous aluminosilicate is found to be the connecting material between ash particles within the agglomerative matrix reported in several studies. Study the phase diagram, helps to understand the iron from pyrite produce the low-melting eutectic most possibly by reacting with quartz and other siliceous minerals [18].

4. Effect of iron loading on inorganic deposition

In Chapter 3 it is reported that although the calcium content of F1 is much lower than F2 and the viscosity of the slag resulted from F1 is much higher than F2, but, the amount of

the deposition of F1 is higher. The indices based only on the ash composition cannot be a reliable reference for ash deposition tendency. If the iron and calcium content in the ash of a coal are very high, but, the ash fraction of coal is low, then the iron and calcium loading on the target surface will be low and the amount of the deposition might be lower in comparison with another coal which has higher iron and calcium loading (due to high ash content), but has lower iron and calcium composition (weight fraction) in ash. In this case, based on the AFT analysis of the ash, the first coal is predicted to result in more deposition but in practice the deposition is lower compared with the coal with higher ATF. Therefore, ash loading and iron loading are other factors which must be considered beside ash composition in inorganic deposition studies. High iron loading can result in an essential and great rise in the local concentration of iron oxide (in reduced state during gasification) as precursor for other particles to be trapped by producing sticky capturing surface [17].

5. Inorganic matter transformation

An accurate characterization of the iron-bearing minerals and other ash constituents in coal is highly precious to predict the deposition tendency and characteristics, pathway of the transformations of the inorganic matters during utilization process and track the complicated reaction mechanisms between the inorganic matters. Among various techniques for characterization of iron-bearing minerals, Mössbauer spectroscopy has been reported to have great advantages over other methods and is being widely used with increasing attention everyday as a robust technique due to its accuracy, high

sensitivity and non-destructive characteristics [1]. Figure 14 shows the iron-bearing phases identification in raw coal and ash by Mossbauer spectroscopy.

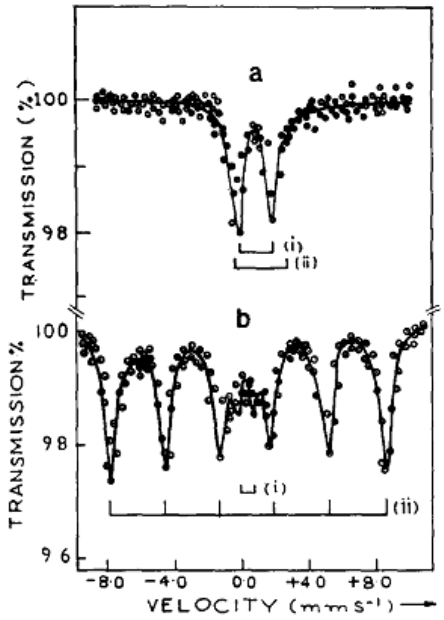

Figure 14: Room temperature Mössbauer spectra of (a) Lodna coal, and (b) its ash obtained at 800°C in air [1].

The Mössbauer spectra of raw coals usually include two peaks showing the existence of Fe^{2+}-illite and pyrite [FeS_2] and in some cases the association of marcasite with pyrite is reported. Pyrite usually is a major phase in association with clay minerals. Iron may also be present as carbonate minerals such as siderite [$FeCO_3$] and ankerite [$Ca(Fe\ Mg)(CO_3)_2$] [1]. After utilization process iron might be present in various phases such as Fe^{3+}-glass silicate, Haematite(α-Fe_2O_3), Fe^{3+}-mullite, Fe^{2+}-mullite and Goethite(α-FeOOH). The presence of each phase is dependant to the condition at which the phase is formed. For instance, at higher temperatures magnetite and at lower temperatures hematite are stable states of iron [1]. Pyrite usually exist as excluded mineral in coal and starts to decompose into pyrrhotite at about 530 °C and then oxidize to molten FeO–FeS

at about 1080 °C. Siderite starts to decompose into wüstite (FeO) at about 1370 °C. FeO–FeS and wüstite exist under reducing condition but will convert to magnetite (Fe_3O_4) and hematite (Fe_2O_3) under oxidizing condition [1]. Dai et al. [4] used Mössbauer spectroscopy in combination with quantitative XRD and SEM-EDX to analyze the iron bearing minerals and their transformation. They reported that the inherent pyrite (mostly existing inside the carbonaceous matrix of coal) initially reduces into FeS–FeO which consequently interact with alumina-silicates to form low molting point eutectic with liquid temperatures in range of 1070 °C for FeO–$CaAl_2SiO_8$–SiO_2 to 1177 °C for FeO–Fe_2SiO_4. This temperature range is essentially lower than the flame temperature in combustion zone and the melting temperature of the pure iron oxides in different states (FeO (1377 °C), Fe_2O_3 (1565 °C) and Fe_3O_4 (1597 °C)) [4].

In the temperature range between 1000 °C to 1200 °C the calcium containing minerals like anhydrite can react with mullite and produce low-melting phases such as anorthite and gehlenite. The main mineral reactions during heating under gasificaiotn condition are shown as below [19]:

$$hematite(Fe_2O_3) \xrightarrow{\sim 1173\ K} FeO + O_2\ (reducing\ condition) \quad (3)$$

$$anhydrite(CaSO_4) \xrightarrow{>1273\ K} CaO + SO_3 \quad (4)$$

$$mullite(3Al_2O_3.2SiO_2) + CaO \xrightarrow{\sim 1403\ K} anorthite\ (CaO.Al_2O_3.2SiO_2) \quad (5)$$

$$anorthite\ (CaO.Al_2O_3.2SiO_2) + CaO \rightarrow gehlenite\ (2CaO.Al_2O_3.2SiO_2) \quad (6)$$

$$quartz(SiO_2) + CaO \rightarrow wollastonite(CaO.SiO_2) \quad (7)$$

$$wollastonite(CaO.SiO_2) + 2CaO \rightarrow Alite(3CaO.SiO_2) \quad (8)$$

$$quartz(SiO_2) + FeO \xrightarrow{1173\sim1273\ K} clinoferroilite\ (FeO.SiO_2) \quad (9)$$

$$clinoferroilite\ (FeO.SiO_2) + FeO \xrightarrow{1173\sim1273\ K} fayalite\ (2FeO.SiO_2) \quad (10)$$

$$mullite\ (3Al_2O_3.2SiO_2) + 3FeO \xrightarrow{1273\sim1473\ K} fayalite\ (2FeO.SiO_2) + hercynite\ (FeO.Al_2O_3) \quad (11)$$

$$anorthite\ (CaO.Al_2O_3.2SiO_2) + 6FeO \xrightarrow{1273\sim1473\ K} fayalite\ (2FeO.SiO_2) + hercynite\ (FeO.Al_2O_3) + almandite\ (3FeO.Al_2O_3.3SiO_2) \quad (12)$$

Among these reactions, the mineral reaction (5) is the most affecting one as it converts mullite (MP=2133 K) to anorthite (MP=1826 K).

6. Formation of iron sulfide layer on the surface of ash particles

In chapter 3, formation of iron sulfide layer on the surface of ash particles has been reported which was observed in case of F2 much more than F1. Figure 15 and 16 show iron sulfide on the surface of ash particles for F2. The EDX analysis of the specified areas in Figure 15 is presented in Table 3.

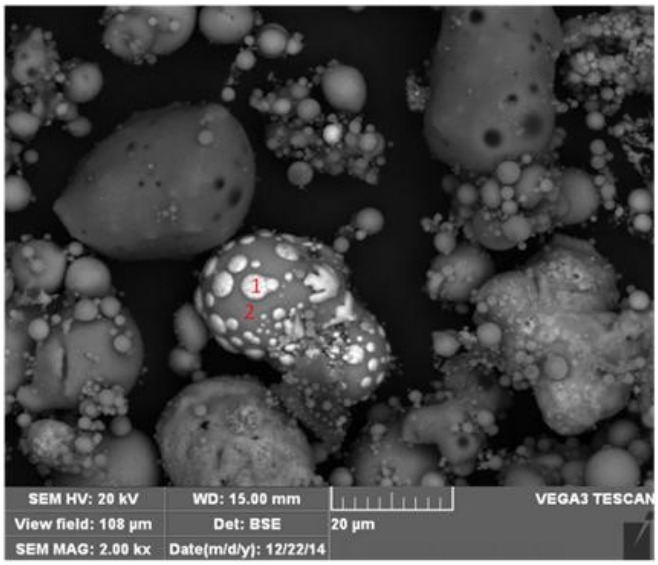

Figure 15: Iron sulfide layer on ash particle in residue of F2, T:1200°C, A:5L/min, N2:1L/min

Table 3: EDX results of the areas specified in Figure 15

	Al	Si	Ca	Fe	S	Na	Mg	Ti	P
Point 1	0.9	1.3	1.0	82.1	14.7	0.0	0.0	0	0
Point 2	17.5	29.7	25.1	18.9	1.5	1.7	3.4	1.9	0.3

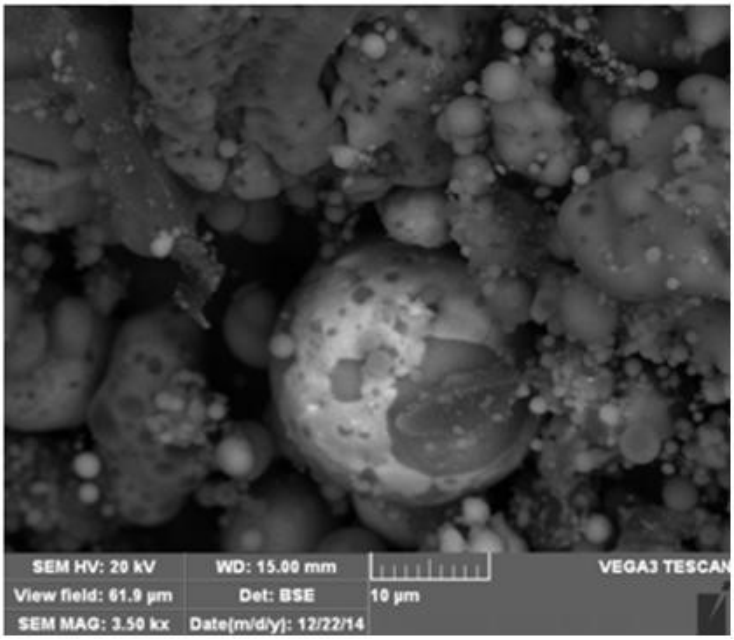

Figure 16: Iron sulfide layer on ash particle in residue of F2, T:1200°C, A:5L/min, N2:5L/min

Iron sulfide is one the lowest melting inorganic phases which might form in considerable amount on the outer surface of the ash particles. Analysis of agglomerates showed that the bonding material that forces other ash particles to stick together is usually contains iron sulfide. Mason et al. [18] reported that decomposition of pyrite generated a melted phase spreading on the surface of ash particles. Brooker et al. [20] observed enriched iron sulfide around many fly ash particles. They reported that the source of sulfide could be from vapor condensation, reaction between iron containing inorganic species and H_2S in the gas. Although they could not determine the real source, but, they noted layers of iron sulfide encapsulating fly ash particles within the deposit which signifies that vapor or fume deposition of iron sulfide might be happened. However, at temperatures in range of 1300 to 1500°C which is normal temperature range of the gasification process, iron sulfide is not predicted to exist as vapor phase. The main mechanisms of the formation of

iron sulfide are formation of FeS during gasification (due to transformation of pyrite), formation of FeS from vapor phase condensation (due to the reaction between condensed volatile iron species and H_2S) and formation of FeS from iron in the glass during cooling (due to the reaction between iron content of the ash residue and H_2S) [20]. In reducing atmosphere the reaction between different iron containing compounds and H_2S might result in FeS formation as below:

$$FeO + H_sS \rightleftharpoons FeS + H_2O \quad (13)$$

$$Fe_2SiO_4 + H_2S \rightleftharpoons 2FeS + SiO_2 + H_2O \quad (14)$$

Figures 17-28 show the BSE images of the ash residue of fuels F1 and F2 at different temperatures and atmosphere. Based on these BSE images, it might be inferred qualitatively that iron sulfide layer formation on the ash particles collected in the cyclone is more dependant to the ash composition and atmosphere rather than to the temperature. Comparison these images shows that iron sulfide layer formation in case of F2 was observed more than F1 which is due to the higher sulfur content of F2 in comparison with F1. By increasing concentration of oxygen in the atmosphere, the presence of iron sulfide will be lower due to oxidation of iron (in this case most of the bright spots in BSE images are iron oxide). Working with F2 and operating at 10L/min of air at 1450°C, iron sulfide was observed in very low occasions.

During any coal utilization process, under mild or strong oxidizing environment in the low temperature region, pyrite combustion happens and SO_2 might be released at the same time based on the equation below [1]:

$$2FeS_2 + 7O_2 \rightarrow Fe_2(SO_4)_3 + SO_2 \quad (15)$$

Release of SO_2 might result in the ash particle rupture as has been observed in many occasions in case of F2 at high oxygen concentration as shown in Figure 28(a).

Further investigations especially quantitative analysis regarding the phenomena of iron sulfide formation would be very beneficial as it affects the fate of iron and influences the stickiness of the particles and the wall and consequently has essential effect on the total amount of the depositions.

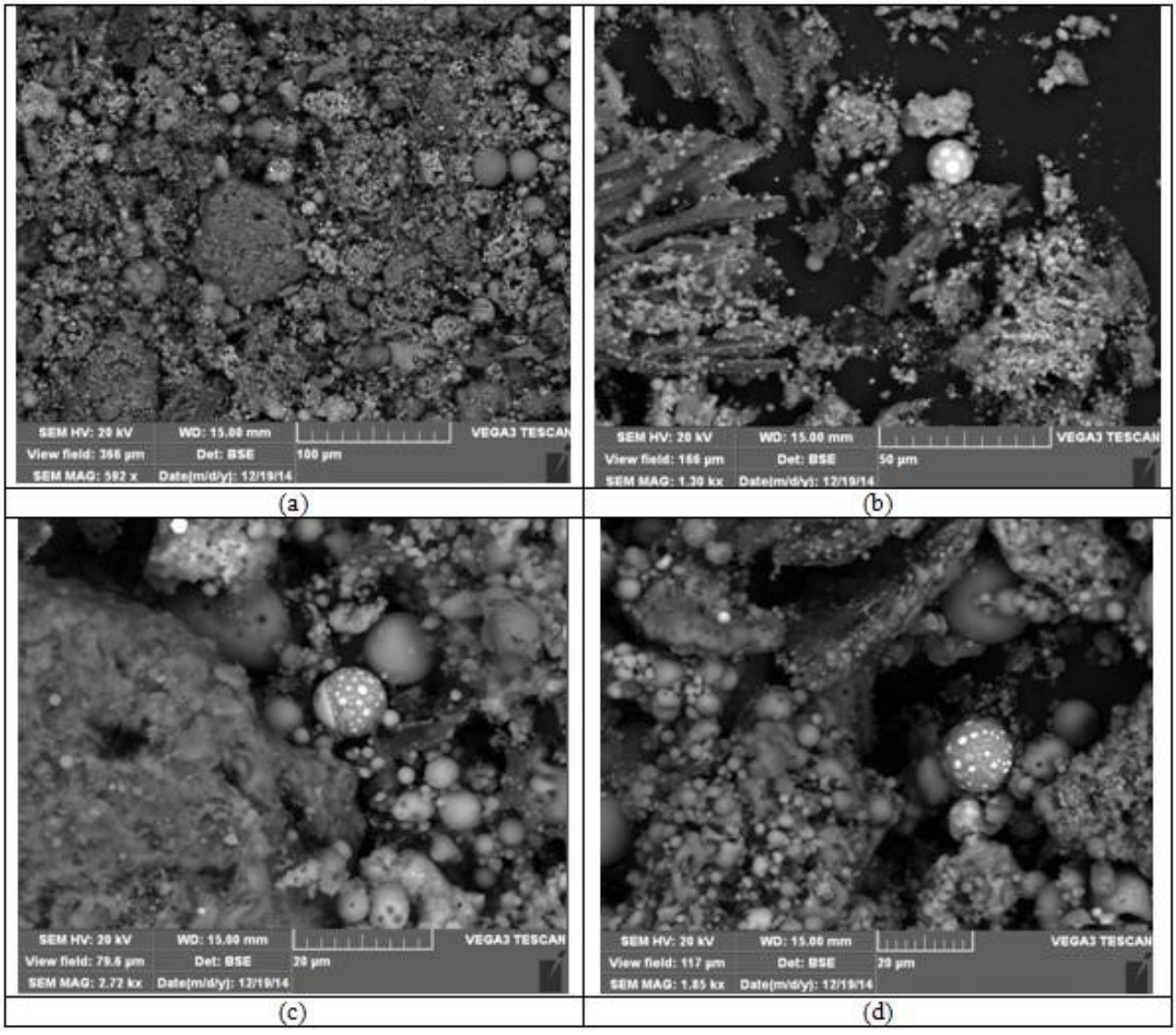

Figure 17: Ash residue of F2, T: 1200°C, Air: 5L/min, N2: 1L/min

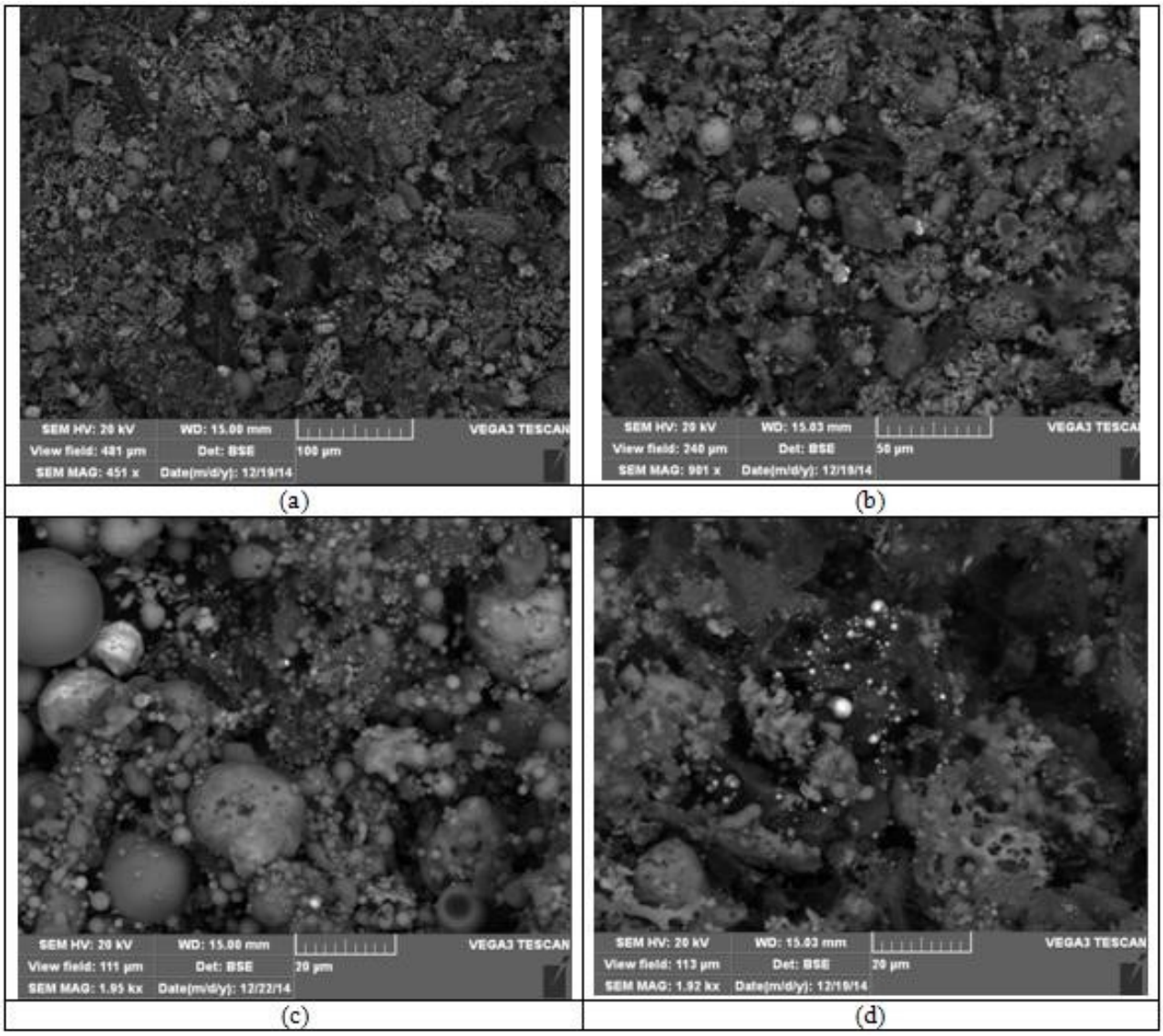

Figure 18: Ash residue of F2, T: 1200°C, Air: 5L/min, N2: 5L/min

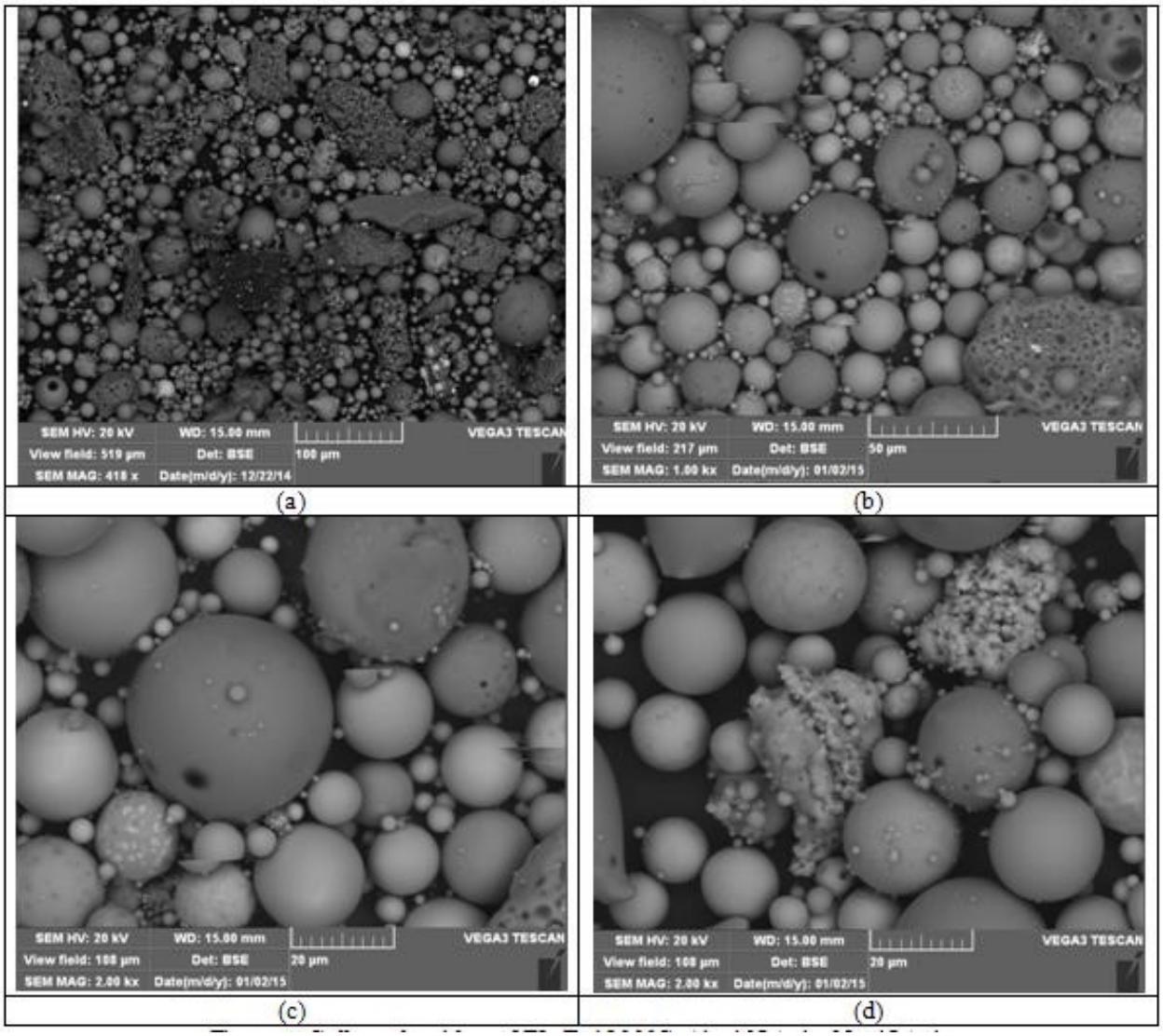

Figure 19: Ash residue of F2, T: 1200°C, Air: 10L/min, N2: 1L/min

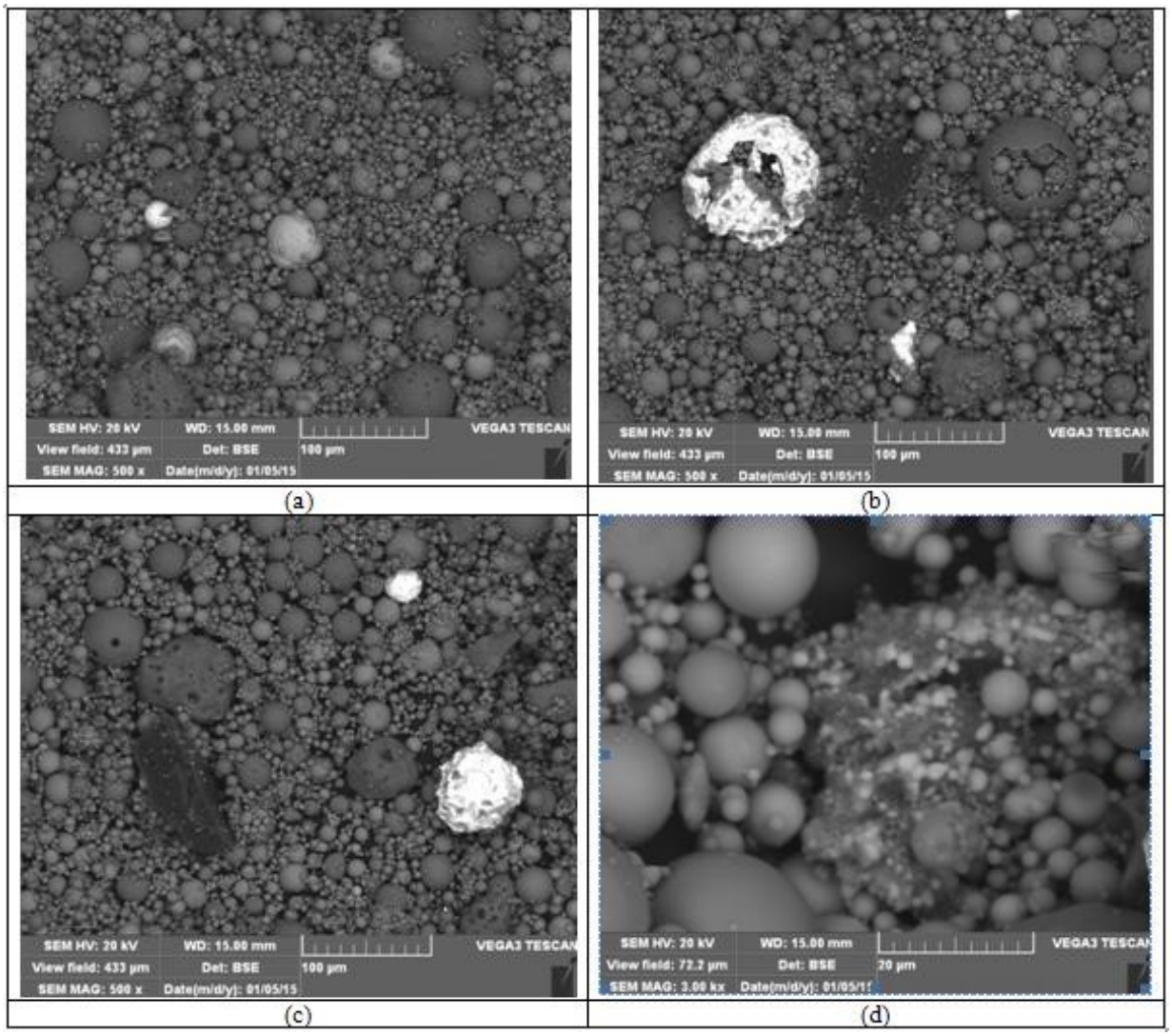

Figure 20: Ash residue of F2, T: 1450°C, Air: 5L/min, N2: 1L/min

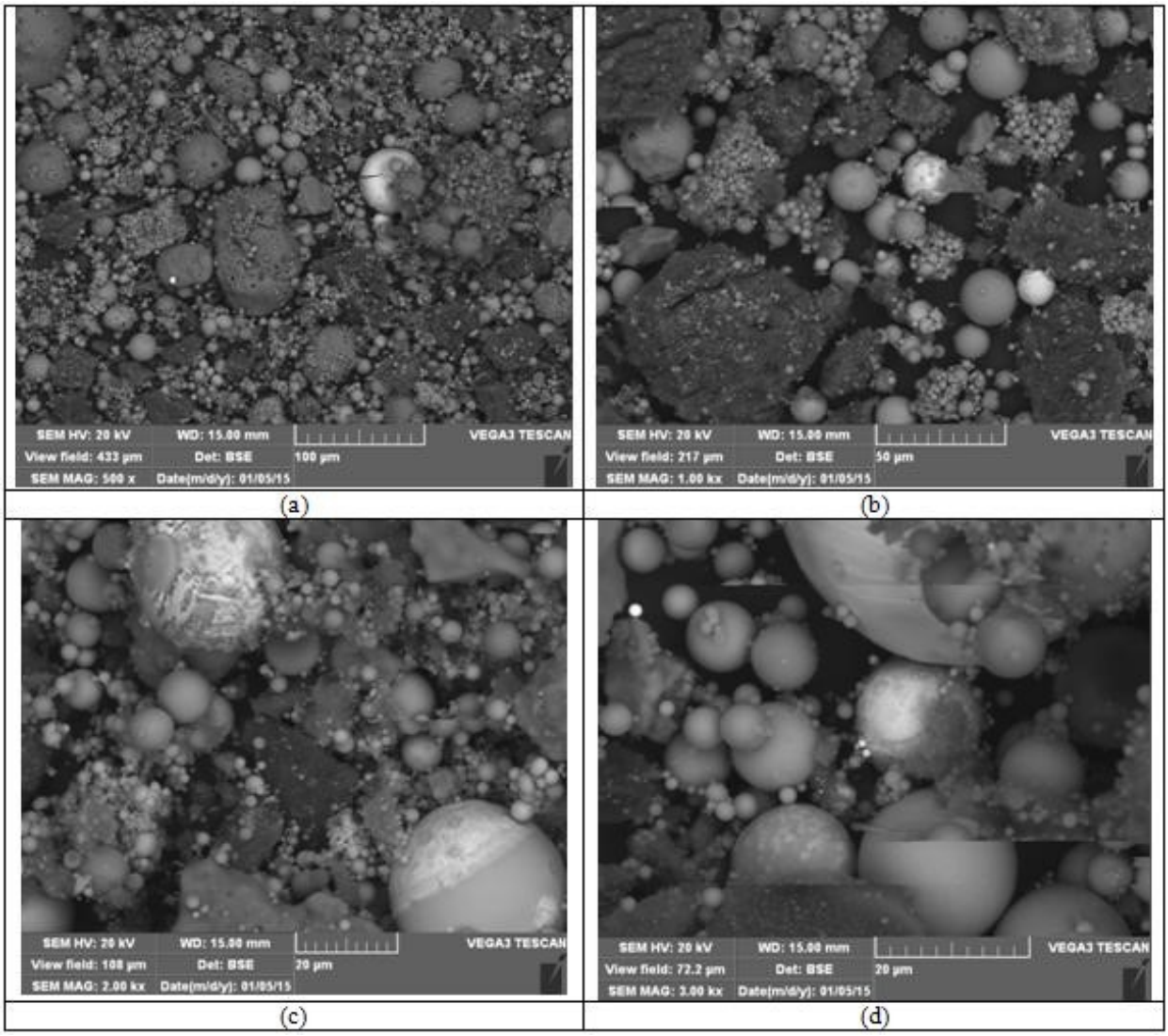

Figure 21: Ash residue of F2, T: 1450°C, Air: 5L/min, N2: 5L/min

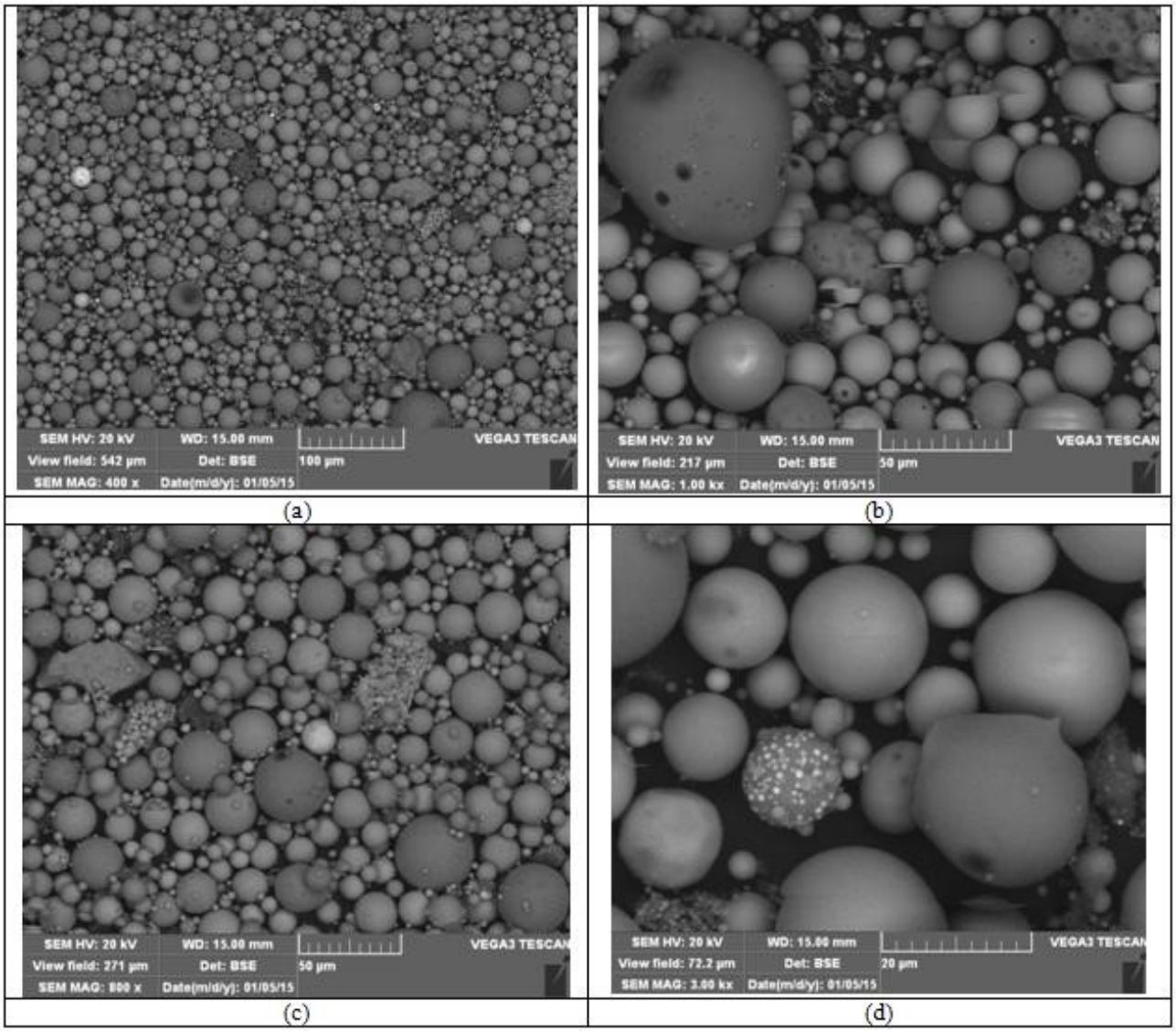

Figure 22: Ash residue of F2, T: 1450°C, Air: 10L/min, N2: 1L/min

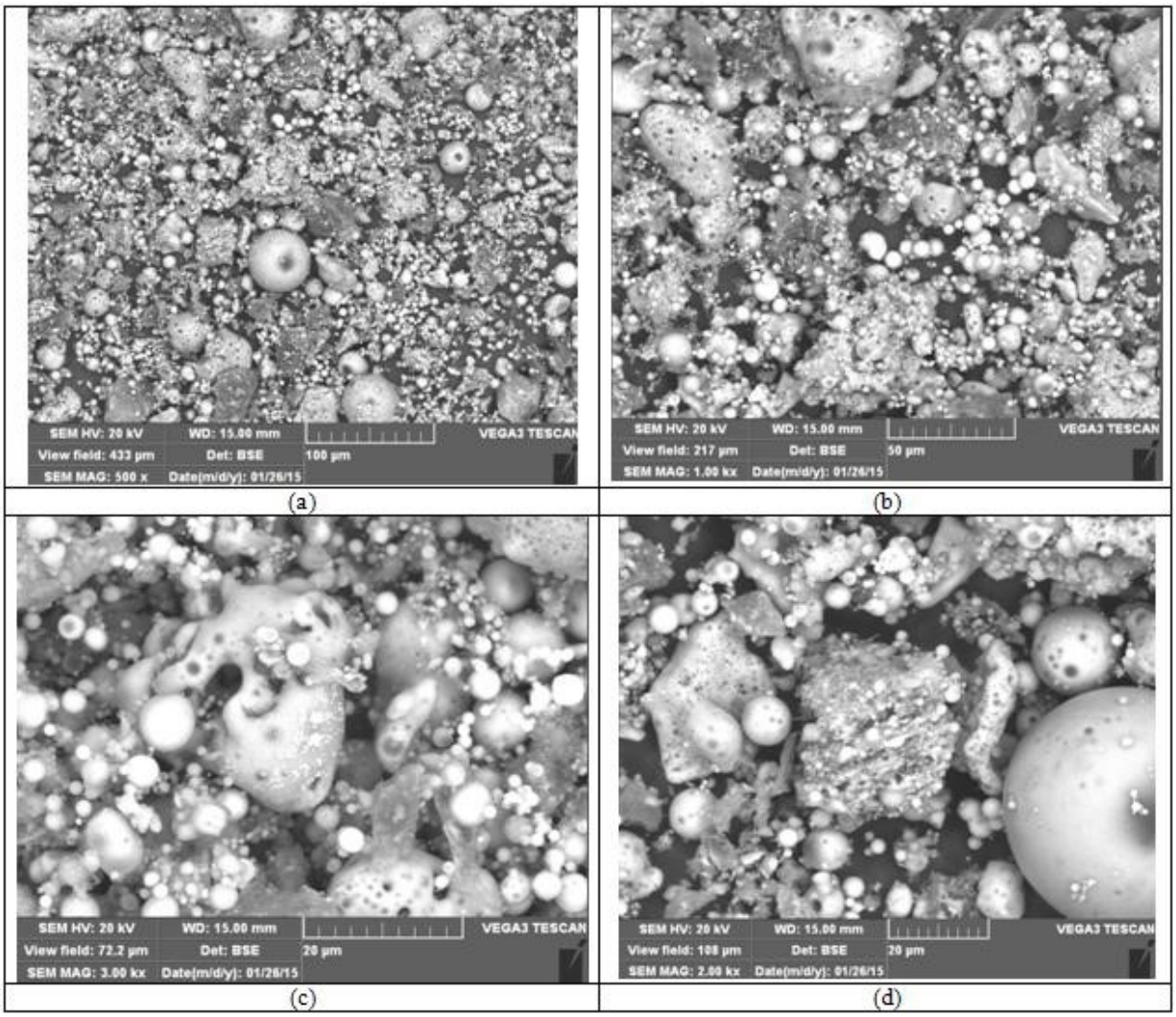

Figure 23: Ash residue of F1, T: 1200°C, Air: 5L/min, N2: 1L/min

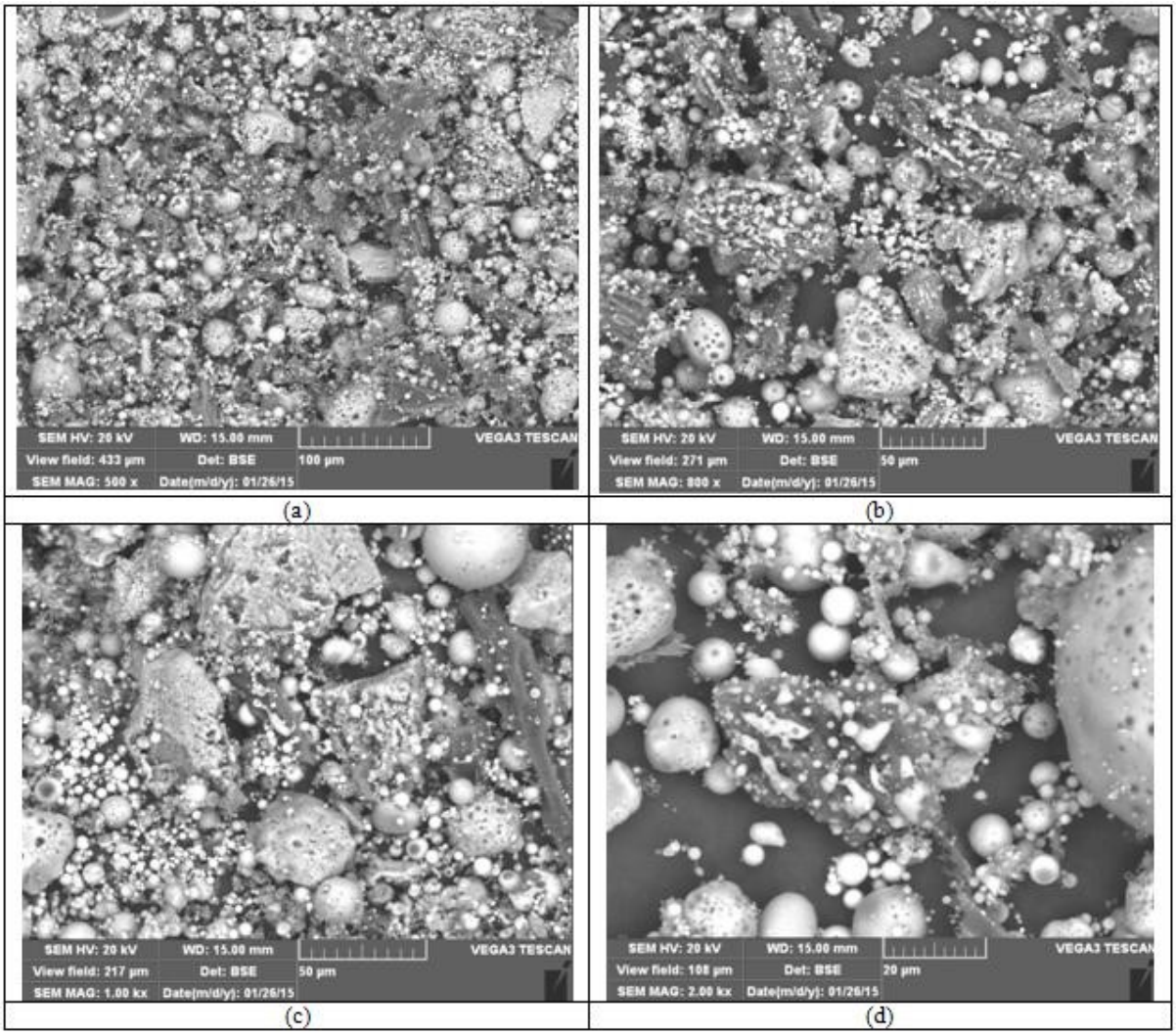

Figure 24: Ash residue of F1, T: 1200°C, Air: 5L/min, N2: 5L/min

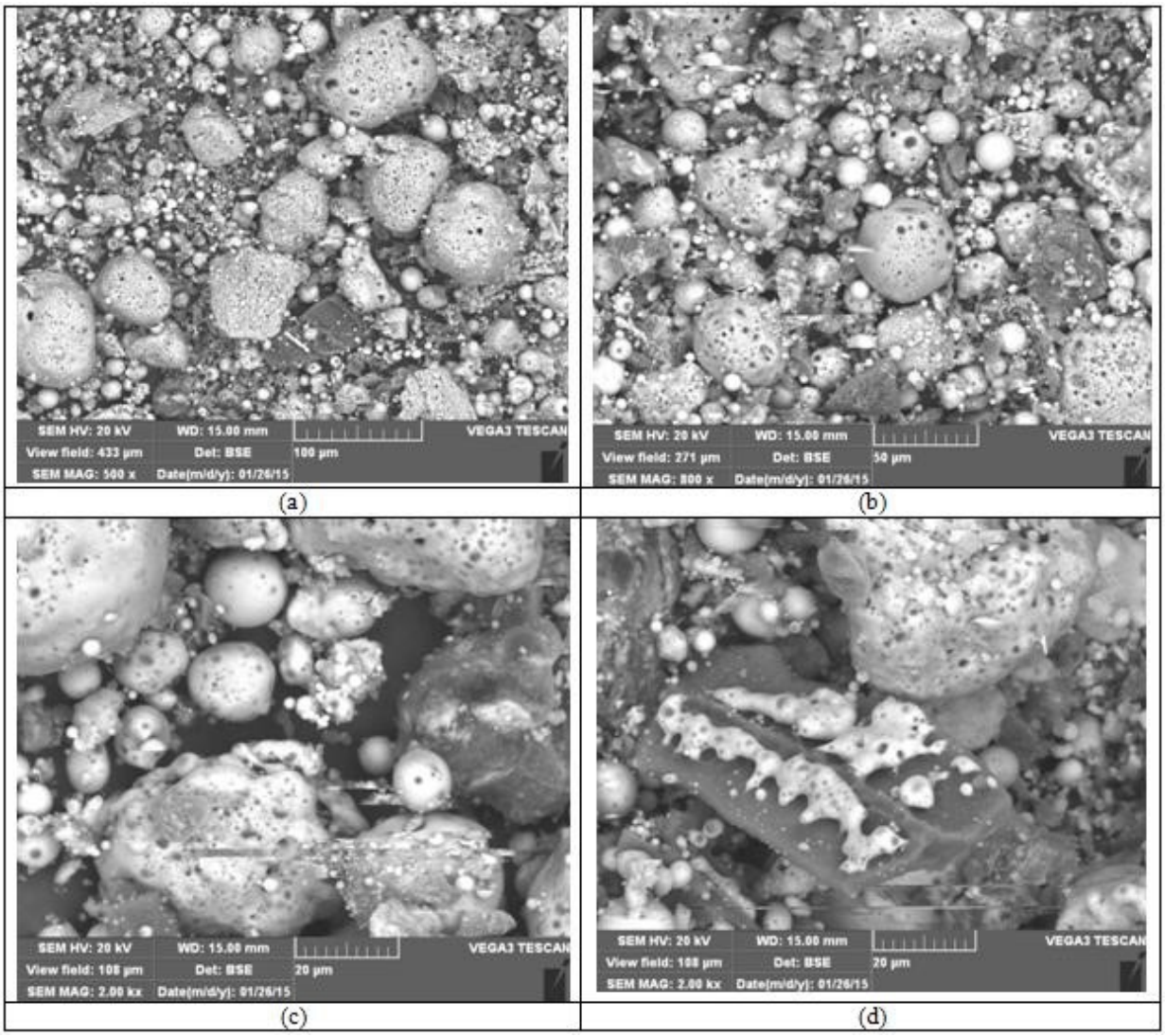

Figure 25: Ash residue of F1, T: 1200°C, Air: 10L/min, N2: 1L/min

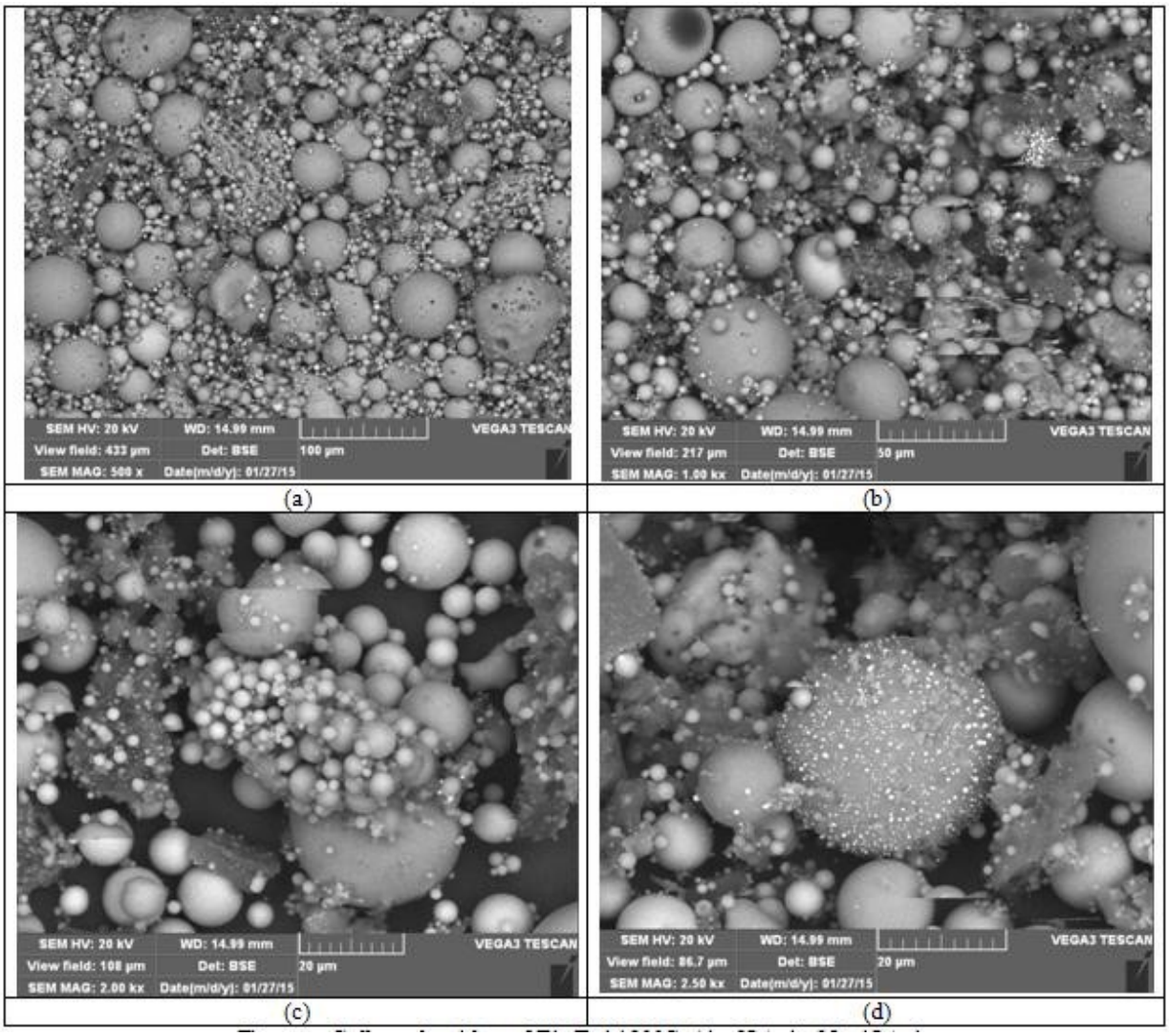

Figure 26: Ash residue of F1, T: 1450°C, Air: 5L/min, N2: 1L/min

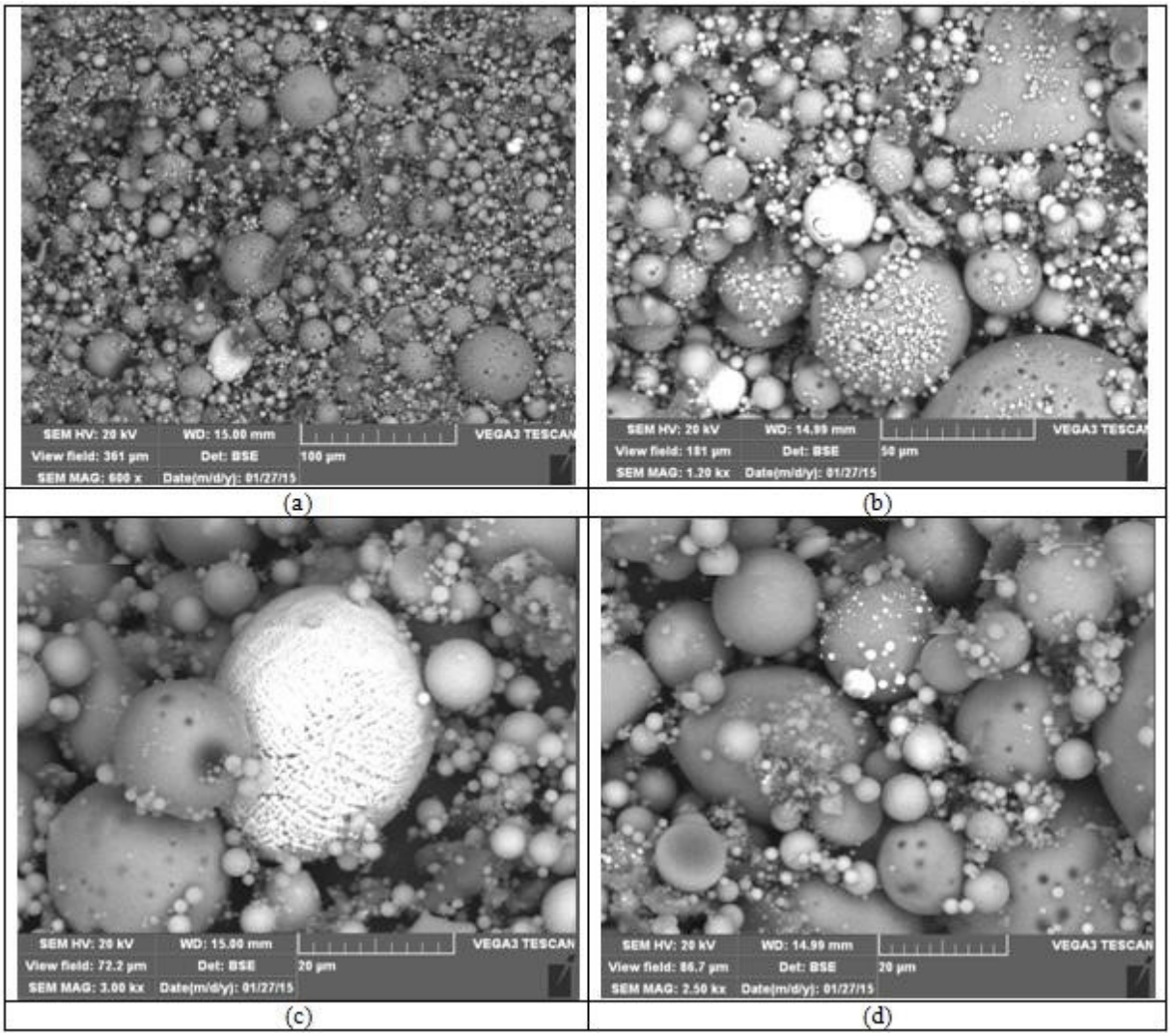

Figure 27: Ash residue of F1, T: 1450°C, Air: 5L/min, N2: 5L/min

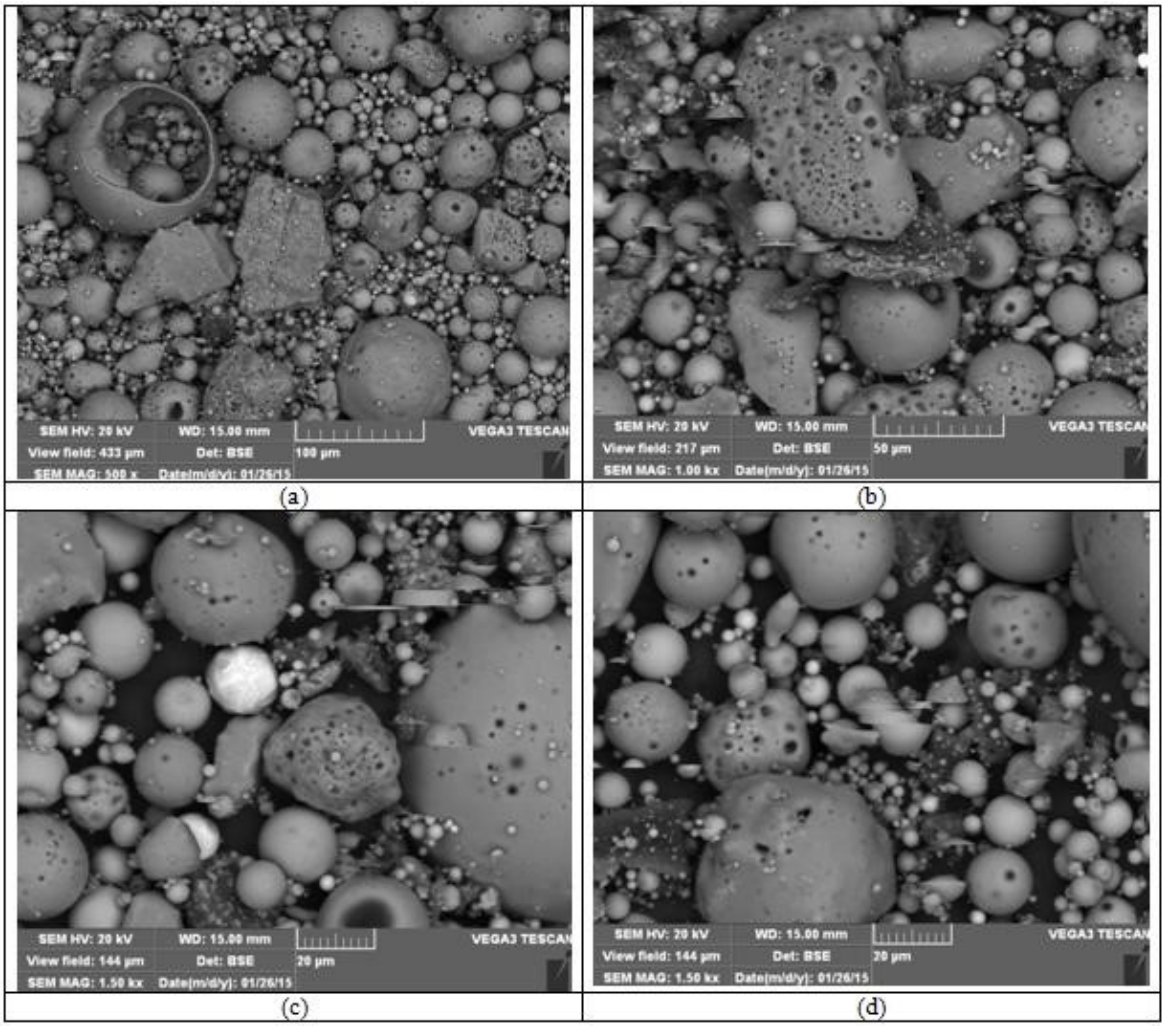

Figure 28: Ash residue of F1, T: 1450°C, Air: 10L/min, N2: 1L/min

References

[1] Ram L C, Tripathi P S M, Mishra S P, Mossbauer spectroscopic studies on the transformations of iron-bearing minerals during combustion of coals: Correlation with fouling and slagging, Fuel Processing Technology 42 (1995) 47-60

[2] Persson M, Investigations of Slag Properties and Reactions, PhD thesis, KTH School of Industrial Engineering and Management, Division of Materials Process Science, Royal Institute of Technology, 2007

[3] Wei Y, Li H, Yamada N, Sato A, Ninomiya Y, Honma K, Tanosaki T, A microscopic study of the precipitation of metallic iron in slag from iron-rich coal during high temperature gasification, Fuel 103 (2013) 101–110

[4] Qi X, Guo X, Xue L, Zheng C, Effect of iron on Shenfu coal char structure and its influence on gasification reactivity, Journal of Analytical and Applied Pyrolysis 110 (2014) 401–407

[5] Dai B Q, Wu X, Girolamo A D, Cashion J, Zhang L, Inhibition of lignite ash slagging and fouling upon the use of a silica-based additive in an industrial pulverized coal-fired boiler: Part 2. Speciation of iron in ash deposits and separation of magnetite and ferrite, Fuel 139 (2015) 733–745

[6] Zhang Z, Wu X, Zhou T, Chen Y, Hou N, Piao G, Kobayashi N, Itaya Y, Mori S, The effect of iron-bearing mineral melting behavior on ash deposition during coal combustion, Proceedings of the Combustion Institute 33 (2011) 2853–2861

[7] Carey R C, Measurement and significance of the flow properties of coal ash and slag, 1964. Bureau Mines Bull., 618.

[8] Hinckley C C, Smith G V, Twardowska H, Saporoschenko M, Shileyt R H, Griffent R A, Mossbauer studies of iron in Lurgi gasification ashes and power plant fly and bottom ash, Fuel, 1980, Vol 59

[9] Kondratiev A, Jak E, A quasi-chemical viscosity model for fully liquid slags in the Al_2O_3 –CaO–FeO–SiO_2 system, Metall Mater Trans B 2005;36:623–38.

[10] Min D J, Fruehan R J, Rate of Reduction of FeO in Slag by Fe-C Drops, Metallurgical transactions B, Volume 23B, February (1992) 29-37

[11] Raask E, Mineral impurities in coal combustion, Behavior, Problems and Remedial Measures, Hemisphere Publishing Corporation, New York, 1985.
[12] Namkung H, Xu L, Shin W C, Kang T J, Kim H T, Study on deposition tendency of coal ash under various gasification environments through DTF, Fuel 117 (2014) 1274–1280
[13] Khadilkar A B, Rozelle P L, Pisupati V S, A study on initiation of ash agglomeration in fluidized-bed gasification systems, Fuel 152 (2015) 48–57
[14] McLennan A R, Bryant G W, Stanmore B R, Wall T F, Ash formation mechanisms during pf combustion in reducing conditions. Energy Fuels 2000;14:150–9.
[15] Li F, Li Z, Huang J, Fang Y, Understanding mineral behaviors during anthracite fluidized-bed gasification based on slag characteristics, Applied Energy 131 (2014) 279–287
[16] Marinov V, Marinov S P, Lazarov L, Stefanova M, Ash agglomeration during fluidized bed gasification of high sulfur content lignites, Fuel Processing Technology, 31 (1992) 181-191
[17] Datta S, Sarkar P, Chavan P D, Saha S, Sahu G, Sinha A K, Saxena V K, Agglomeration behavior of high ash Indian coals in fluidized bed gasification pilot plant, Applied Thermal Engineering (2015), doi: 10.1016/j.applthermaleng.2015.04.046.
[18] Mason D M, The behavior of iron-sulfur species in fluidized-bed gasification on coal, Fuel Processing Technology, 30 (1992) 215-226
[19] Wu X, Zhang Z, Chen Y, Zhou T, Fan J, Piao G, Kobayashi N, Mori S, Itaya Y, Main mineral melting behavior and mineral reaction mechanism at molecular level of blended coal ash under gasification condition, Fuel Processing Technology 91 (2010) 1591–1600
[20] Brooker D, Oh M S, Iron sulfide deposition during coal gasification, Fuel Processing Technology 44 (1995) 181-190